AD_____

Award Number: DAMD17-94-C-4069

TITLE: Services to Operate and Maintain a Microwave Research Laboratory

PRINCIPAL INVESTIGATOR: Yahya Akyel, Ph.D.

CONTRACTING ORGANIZATION: McKesson Bioservices
Rockville, Maryland 20850

REPORT DATE: May 1999

TYPE OF REPORT: Final

PREPARED FOR: U.S. Army Medical Research and Materiel Command
Fort Detrick, Maryland 21702-5012

DISTRIBUTION STATEMENT: Approved for Public Release;
Distribution Unlimited

The views, opinions and/or findings contained in this report are those of the author(s) and should not be construed as an official Department of the Army position, policy or decision unless so designated by other documentation.

DTIC QUALITY INSPECTED 4

19990902 065

REPORT DOCUMENTATION PAGE

Form Approved
OMB No. 0704-0188

Public reporting burden for this collection of information is estimated to average 1 hour per response, including the time for reviewing instructions, searching existing data sources, gathering and maintaining the data needed, and completing and reviewing the collection of information. Send comments regarding this burden estimate or any other aspect of this collection of information, including suggestions for reducing this burden, to Washington Headquarters Services, Directorate for Information Operations and Reports, 1215 Jefferson Davis Highway, Suite 1204, Arlington, VA 22202-4302, and to the Office of Management and Budget, Paperwork Reduction Project (0704-0188), Washington, DC 20503.

1. AGENCY USE ONLY *(Leave blank)*	2. REPORT DATE	3. REPORT TYPE AND DATES COVERED
	May 1999	Final (31 May 94 - 20 May 99)

4. TITLE AND SUBTITLE
Services to Operate and Maintain a Microwave Research Laboratory

5. FUNDING NUMBERS
DAMD17-94-C-4069

6. AUTHOR(S)
Yahya Akyel, Ph.D.

7. PERFORMING ORGANIZATION NAME(S) AND ADDRESS(ES)
McKesson Bioservices
Rockville, Maryland 20850

8. PERFORMING ORGANIZATION REPORT NUMBER

9. SPONSORING / MONITORING AGENCY NAME(S) AND ADDRESS(ES)
U.S. Army Medical Research and Materiel Command
Fort Detrick, Maryland 21702-5012

10. SPONSORING / MONITORING AGENCY REPORT NUMBER

11. SUPPLEMENTARY NOTES

12a. DISTRIBUTION / AVAILABILITY STATEMENT
Approved for Public Release; Distribution Unlimited

12b. DISTRIBUTION CODE

13. ABSTRACT *(Maximum 200 words)*

Based on the growing concerns for the health and safety of military personnel and civilians exposed to radiofrequency radiation a series of research investigating behavioral, biological, cardiovascular, and retinal effects of high power pulsed microwaves, ultra wideband (UWB), and millimeter waves were accomplished. It has been determined that ultra wideband electromagnetic pulses produce changes in nociception and activity in mice. Furthermore, ultra wideband induced hypotension in rats. On the other hand, UWB does not effect UV-induced recombination and mutagenesis in Yeast. Intense flashes of light were observed in sodium bicarbonate and hydrogen peroxide solutions when they were exposed to pulsed microwave radiation and the responses was greatly enhanced by a microwave-absorbing, biosynthesized polymer, diazoluminomelanin. Rhesus monkeys exposed to 1.25 GHz high peak power microwaves at adose level of 4 W/kg SAR at the retinal level, produced no evidence of degenerative changes and electroretinogram depression in these animals. Details and accomplishments of the research program and a list of publications are presented in this report.

14. SUBJECT TERMS
High power pulsed microwaves, ultrawide band microwave fields, millimeter waves, dosimetry, retinal effects, ocular effects, cardiovascular effects, cellular effects, neurotoxins

15. NUMBER OF PAGES
175

16. PRICE CODE

17. SECURITY CLASSIFICATION OF REPORT	18. SECURITY CLASSIFICATION OF THIS PAGE	19. SECURITY CLASSIFICATION OF ABSTRACT	20. LIMITATION OF ABSTRACT
Unclassified	Unclassified	Unclassified	Unlimited

FOREWORD

Opinions, interpretations, conclusions and recommendations are those of the author and are not necessarily endorsed by the U.S. Army.

4.A Where copyrighted material is quoted, permission has been obtained to use such material.

4.A Where material from documents designated for limited distribution is quoted, permission has been obtained to use the material.

4.A Citations of commercial organizations and trade names in this report do not constitute an official Department of Army endorsement or approval of the products or services of these organizations.

____ In conducting research using animals, the investigator(s) adhered to the "Guide for the Care and Use of Laboratory Animals," prepared by the Committee on Care and use of Laboratory Animals of the Institute of Laboratory Resources, national Research Council (NIH Publication No. 86-23, Revised 1985).

____ For the protection of human subjects, the investigator(s) adhered to policies of applicable Federal Law 45 CFR 46.

____ In conducting research utilizing recombinant DNA technology, the investigator(s) adhered to current guidelines promulgated by the National Institutes of Health.

____ In the conduct of research utilizing recombinant DNA, the investigator(s) adhered to the NIH Guidelines for Research Involving Recombinant DNA Molecules.

4.A In the conduct of research involving hazardous organisms, the investigator(s) adhered to the CDC-NIH Guide for Biosafety in Microbiological and Biomedical Laboratories.

YAMA ADAMS 6.18.99

PI - Signature Date

TABLE OF CONTENTS

INTRODUCTION

The following report summarizes the performance of McKessonHBOC BioServices (MBS) staff at the Walter reed Army Institute of Research, US Army Medical Research Detachment, Microwave Bioeffects Branch at Brooks Air Force Base, Texas under the contract DAMD17-94-C-4069.

MBS has a nine year contract with the US Army Medical Research and Acquisition Activity (USAMRAA) to operate and maintain Microwave Bioeffects Branch, a Government-owned Contractor-operated (GOCO) facility. A report summarizing the base three years of this contract (May 20, 1994 - May 21, 1997) was previously filed with the US Army Medical Research and Materiel Command, Fort Detrick, Maryland on June 20, 1997. The present report reflects the efforts of the MBS staff during the first option years (May 21, 1997 - May 20, 1999) of the aforementioned contract.

Based on the guidance provided in the contract and the guidance provided by the Contracting Officer's Representative (COR) Mr. Bruce Stuck, MBS staff concentrated its research efforts in the following areas:

- Conduct research to assess the effects of high peak power radio frequency radiation (RFR) on the health and safety of military personnel,
- Complete the ocular effects of L-Band radiation protocol and provide a report summarizing all the ocular effects data obtained and the implications to current Army exposure limits and soldier performance,
- Conduct research on the biological hazards of ultra wide band (UWB) radiation on analgesia and the cardiovascular systems,
- Complete analysis of millimeter wavelength exposure on neuronal and cellular functions, finalize and publish results, and
- Conduct a series of research studies exploring potential of neurotoxic effects of RFR exposure after a satisfactory external science review.

BODY OF REPORT

- **The effects of high peak power radio frequency radiation (RFR) on the health and safety of military personnel**

The US Army Dismounted Battlespace Battle Lab (DBBL) ACT II Advanced Membrane Transducer (AMT) Antenna was developed for the US Army to provide increased flexibility while operating in urban environment. It was intended to be attached directly to vehicles, radio systems or worn by the soldiers. The Microwave Bioeffects Branch was asked to evaluate the health and safety of this antenna and provide a technical assessment. After a series of tests were conducted to determine if the radio frequency radiation from the antenna conforms to the permissible exposure limits as defined in DoD instructions. A detailed report was presented to Mr. Bruce Stuck, COR concluding that even though the AMT antenna was found to produce large electric fields close to the antenna surface, the specific absorption rate was found to be lower than those prescribed in the safety guidelines. The induced currents in the ankle and wrist was found to be within the safety limits. The report also included specific recommendations regarding the use of this device, when worn by a soldier. A copy of this detailed report can be found in the Volume II of this Final Report.

In a series of experiment intense flashes of light were observed in a sodium bicarbonate and hydrogen peroxide solutions when they were exposed to pulsed microwave radiation, and the response was greatly enhanced by a microwave-absorbing, biosynthesized polymer, diazoluminomelamin. The Branch's FPS-7B radar transmitter operating at 1.25 GHz induced the effect only when appropriate chemical interaction was present. This phenomenon involved acoustic wave generation, bubble formation, pulsed luminescence, ionized gas ejection, and electrical discharge. This type of use of pulsed microwave radiation to generate highly focused energy deposition opens up the possibility of a variety of biomedical applications, including targeting killing of microbes or eukaryotic cells.

In a different experiment, the interbeat interval duration in spontaneously-beating pieces of the atrial wall of the frog heart was used as an endpoint to study biological effects of brief trains of extremely high power microwave pulses. The interbeat interval duration decreased after brief train of extremely high power microwave pulses is attributed to microwave heating.

A method of precise measurement of local heating and the amount of microwave energy absorbed locally in a medium has been proposed and verified for peak specific absorption rates of up to 400 kW/g. Finite-difference time-domain (FDTD) modeling is widely used to estimate local SAR and its distribution in complex biological subjects. However, FDTD predictions could seldom be verified experimentally due to limitations of thermometry methods. A few available artifact-free devices, such as fluoroptic thermometers, tend to be slow and noisy and in many applications their fiber optic probes are too big. Termistors and thermocouples may produce artifacts and usually are avoided though little is known about the actual impact of these artifacts.

MBS staff has analyzed the performance of a microthermocouple in most unfavorable conditions (extremely high peak power microwave pulses) and proved that it can be reliably used for precise measurements of local microwave heating and local SAR. The proposed method of local dosimetry using microthermocouple can be employed to verify FDTD predictions in animal and human models, including cellular phone safety studies.

Relevant Publications / Presentations

Kiel, J. L., Seaman, R. L. Mathur, S. P., Parker, J. E., Wright, J. R., Alls, J L., and Morales, P. J. (1999). Pulsed microwave induced light, sound, and electrical discharge enhanced by a biopolymer. *Bioelectromagnetics,* 20, 216 - 223.

Kiel, J. L., Mason, P. A., Alls, J. L., Morales, P., and Seaman, R. L. (1998). A mechanism of single-pulse radio frequency radiation interaction with biological molecules. *Twentieth Annual Meeting of the Bioelectromagnetic Society*, June 7 - 11, Florida.

Kiel, J., Parker, J., Alls, J., Morales, P., Seaman, R., Mathur, S., and Wright, J. (1997). Pulsed microwave radiation induction of electrosonoluminescence. *Fourth Annual Michaelson Research Conference*, August 15-18, Canandaigua, NY.

Pakhomov, A. G., Mathur, S. P., Akyel, Y., and Murphy, M. R. (1998). High resolution microwave dosimetry in lossy media. NATO Advanced Research Workshop, October 12-16, Slovenia.

Pakhomov, A. G., Belt, M. L., Cox, D. D., Mathur, S., Akyel, Y., and Murphy, M. R. (1998). Immediate effects of extremely high power microwave pulses on the beating rhythm in isolated frog heart auricle. *Twentieth Annual Meeting of the Bioelectromagnetic Society*, June 7 - 11, Florida.

Pakhomov, A. G. Mathur, S. P., Akyel, Y., and Kiel, J. L. (1998). Direct microdosimetry in media exposed to extremely high peak power microwaves. *Twentieth Annual Meeting of the Bioelectromagnetic Society*, June 7 - 11, Florida.

Pakhomov, A. G., Mathur, S. P., and Murphy, M. R. (1998). Dose dependencies in bioeffects of extremely high peak power microwave pulses. *World Health Organization (WHO) Annual Meeting*, 18-22 March, Moscow, Russia.

- **The ocular effects of L-Band radiation**

Generally, microwave-induced alteration of biological endpoints other than behavioral disruption requires specific absorption rates (SARs) greater than the 4 W/kg threshold known to disrupt ongoing behaviors. The eye is one of the critical organs which can potentially be injured by microwave and RF radiation exposure and has been an extensively studied organ regarding the injurious action of microwave radiation. To date, most microwave eye research has concentrated on damage to the lens in the form of lenticular opacities (cataracts). Most investigators assumed that the lens is more susceptible to microwave induced damage than other parts of the eye due to its lack of vascular system. It was believed that the lack of vascular system prevented adequate heat loss, thus exaggerating the temperature rise in the lens.

Due to the potential importance of microwave ocular hazards in relation to health and safety of soldiers, sailors, airmen, and the general public, an ocular study using rhesus monkeys was requested by the TERP. The objective of the research was to identify the presence or the absence of high peak power microwave induced retinal injuries by studying changes in fundus photographs, angiography, electroretinalgrams, and histopathology of monkeys exposed to 1.25 GHz pulsed microwave at 0,4,8 and 20W/kg retinal SAR. The following special considerations were incorporated in the experimental design:

- Extensive densitometry and dosimetry were performed prior to experimentation.
- Extensive pre-exposure screenings were used to assure the retinal normality prior to the acceptance of experimental subjects into the study.
- Pre-exposure baselines were used for individual control.
- Data obtained in the exposed monkeys were further compared to those of sham-exposed monkeys.
- Ketamine restraint and general anesthesia were not used during the exposure.
- A minimum of a 72 hour recovery period was mandatory between pre-screenings and beginning of the repeated exposures.
- Exposures were randomized.
- All investigators except one (code keeper) were blind to the experimental treatments.

All these procedures were necessary to assure data quality and to avoid introducing unidentified confounding factors and unintentional biases by the investigators.

The following summarizes the Tri-Services research efforts on the retinal effects of 1.25 GHz high peak power microwave exposure in monkeys. Fundus photography, retinal angiograms and electroretinograms (ERG) were used prior to exposure to screen for normal ocular structure and function of the monkeys' eyes, and after exposure as endpoints of the experiment. Histopathology of the retina was also used as an endpoint. Nineteen monkeys were randomized to receive sham exposure or pulsed microwave exposures. Microwaves were delivered cranially at 4, 8, or 20 W/kg average retinal specific absorption rates (R-SAR). The pulse characteristics was 1.04 MW (≈1.30 MW/kg peak SAR), 5.59 μs pulse width at 0, 0.59, 1.18 and 2.79 Hz pulse repetition rates. The exposure regimen was 4 hours per day and 3 days per weeks for 3 weeks, a total of 9 exposures. The following preliminary results and conclusions are a synopsis of data in 17 monkeys. The pre-exposure and post-exposure fundus pictures and angiograms were all within normal limits. The response of cone photoreceptor to light flash was enhanced (Fig. 1) in monkeys exposed at 8 or 20 W/kg R-SAR but not in monkeys exposed at 4 W/kg R-SAR (Fig. 2). Retinal histopathology revealed enhanced glycogen storage in photoreceptors which was distributed evenly among sham (2/5), 8 W/kg (3/3) and 20 W/kg (2/5) exposed monkeys with exception of the 4 W/kg (0/4) exposed monkeys. Further quantitative index of the glycogen storage in photoreceptors is being analyzed. Supranormal cone photoreceptor b-wave was R-SAR dependent, and may be an early indicator of mild injury. However, no evidence of histopathological changes were seen in these animals. Thus, we

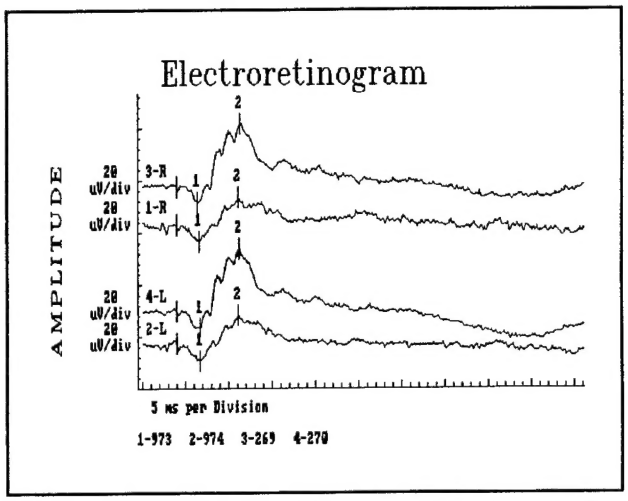

Fig. 1. An example of Post-Exposure Enhancement of Photopic b-wave Amplitude. Trace 1,2= pre-exposure, Trace 3,4= post-expousre, R= right eye, L= left eye.

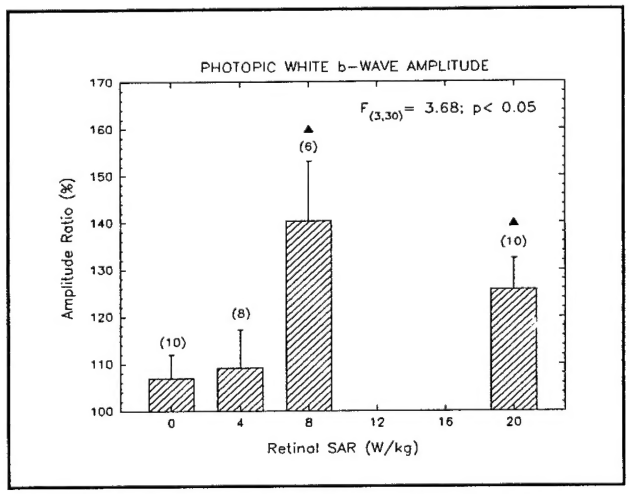

Fig. 2.Enhancement of the ERG Photopic b-wave Amplitude. Error bar= S.E., arrow head= p< 0.05 from shams.

concluded that retinal injury is very unlikely at 4 W/kg, and functional changes that occur at higher R-SAR are probably reversible because of lack of histopathologic correlates.

Relevant Publications / Presentations

D'Andrea, J. A., Ziriax, J, Lu, S-T., Mathur, S., and Merritt, J. H. (1997). Rhesus monkey vision after exposure to high peak power microwave pulses. *Department of Defense Electromagnetic Environmental Effects (E3) Program Review*. 10-14 March, Everett, WA.

D'Andrea, J. A., Ziriax, J, Lu, S-T., Mathur, S., Merritt, J. H., Johnson, M, Lutty, G., Zwick, H., and Stuck, B. (1997). Rhesus monkey vision after exposure to high peak power microwave pulses. *The Second World Congress for Electricity and Magnetism in Biology and Medicine*, June 8 - 13, Bologna, Italy.

Lu, S-T. (1999). Retinal effects of high peak power microwaves in rhesus monkeys. *Tri Service Report*; US Army Medical Research Detachment, Naval Health Research Center Detachment, US Air Force Research Laboratory, Brooks AFB, Texas.

Lu, S-T., Mathur, S. P., Stuck, B., Zwick, H., D'Andrea, J. A., Ziriax, J. M., Merritt, J. H., Lutty, G., McLeod, S., and Johnson, M. (1998). Retinal effects of high peak power L-band microwaves in monkeys. *Twentieth Annual Meeting of the Bioelectromagnetic Society*, June 7 - 11, Florida.

The copies of the above references can be found in Volume II of this Final report.

♦ **The biological hazards of ultra wide band (UWB) radiation on analgesia, the cardiovascular and other cellular systems,**

The aim of this research was to evaluate the cardiovascular effects of Ultra-Wide Band (UWB) pulses, a new modality in radar technology. Forty-five male Wistar-Kyoto (WKY) rats were used in three experiments. The peak electric field of the unipolar UWB pulses was 85 to 95 kV/m (≈1.92 to 2.39 kW/cm^2) with 160 to 200 ps risetime and 0.91 to 1.02 ns pulse width. The exposure was performed in a GTEM cell with various pulse repetition rates. For comparison, equivalent power density was calculated from peak electric field, pulse width, repetition rate and wave impedence (377 ohms). The pulse repetition rates were 0 Hz (sham), 500 Hz (≈1.15 mW/cm^2) and 1,000 Hz (≈1.95 mW/cm^2) in experiment I; 0 Hz (sham), 125 Hz (≈0.28 mW/cm^2) and 250 Hz (≈0.61 mW/cm^2) in experiment II, and 0 Hz (sham), 500 Hz (≈0.96 W/cm^2) and 1,000 Hz (≈1.28 mW/cm^2) in experiment III. Exposure duration was 6 minutes. A non-invasive tail cuff sphygmonanometer with photoelectric sensor was used to measure heart rate, systolic, mean, and diastolic arterial pressures in unanesthetized rats. These cardiovascular endpoints were obtained as pre-exposure baseline, and 0.75 h, 24 h, 72 h, 1 wk, 2 wk, 3 wk and 4 wk after exposure. Each individual rat served as its own control. The data presented were expressed as changes from the pre-exposure baseline level. Bradycardia (decreased heart rate) was noted in one group of animals only (experiment III, 500 Hz, 0.96 mW/cm^2). Delayed reduction in arterial pressures was noted in rats exposed to UWB pulses at 0.96, 1.15, 1.28, and 1.95 mW/cm^2 but not in rats exposed at 0.28 or 0.61 mW/cm^2 (Figs. 3, 4, 5). Pre-exposure baselines of 6 additional rats (a total of 51 rats, 297 measurements) were

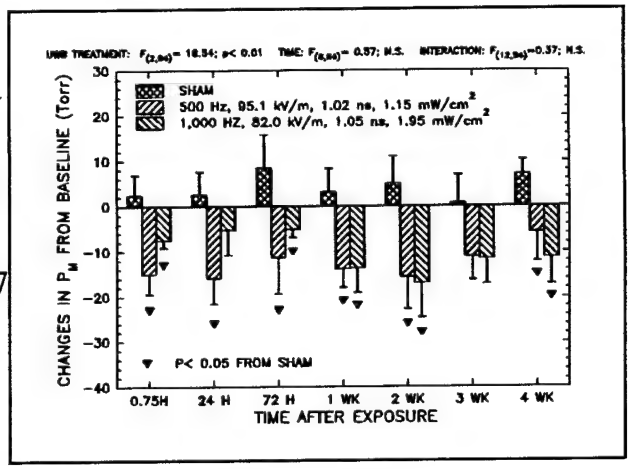

Fig. 3. EXP. I

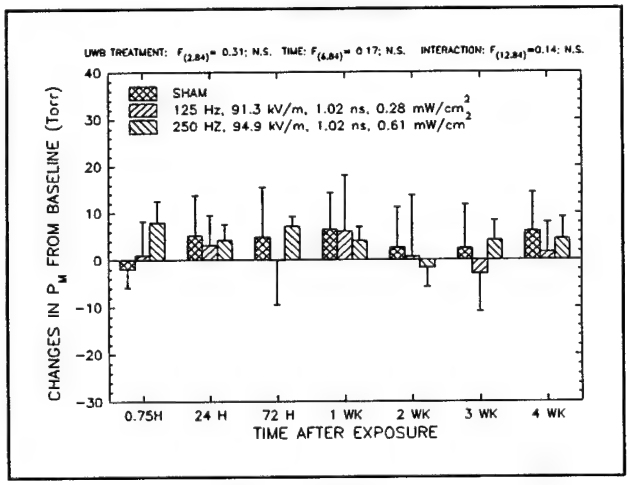

Fig. 4. EXP. II

included to determine the normal range of systolic arterial pressure. These data was used to determine the physiological status of animals according to a clinically accepted practice for defining normality/abnormality status. In this laboratory, the borderline systolic hypotension [< (mean - 1 S.D.)] was a systolic arterial pressure lower than 127.4 torr and systolic hypotension was a systolic arterial pressure [< (mean - 2 S.D.)] lower than 109.8 torr in WKY rats. The probability of borderline hypotension and hypotension were determined from all the systolic arterial pressure records (n= 81 to 94) in rats (5 rats in each group) between 1 and 3 weeks after treatment. It was apparent that rats exposed to UWB pulses at averaged power density higher than 0.96 mW/cm^2 had increased probability of becoming borderline hypotensive and hypotensive (Fig. 6). It can be concluded that UWB pulses possess a hypotensive effect in rats. The UWB induced hypotension is dose-dependent, robust, persistent and replicable. The threshold for UWB induced hypotension was lower than 1 mW/cm^2 average equivalent power density and 100 kV/m peak electric field.

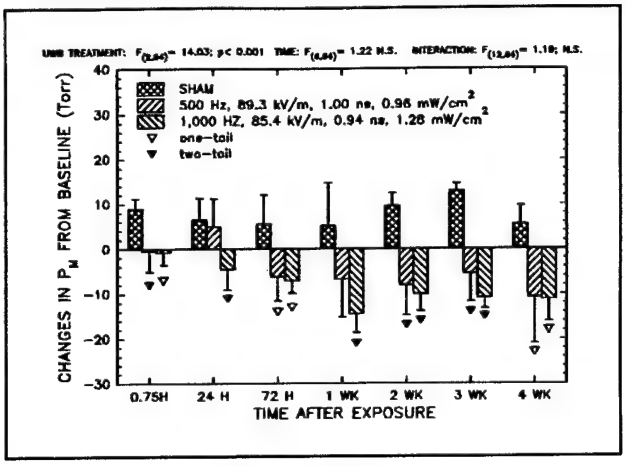

Fig. 5. EXP. III

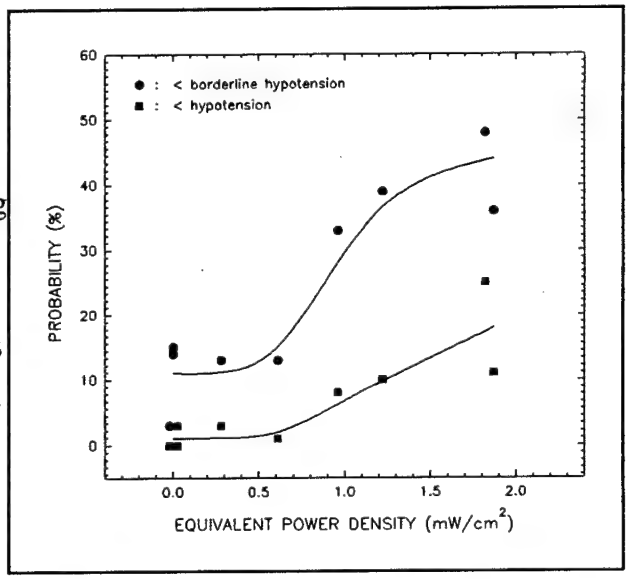

Fig. 6. Dose-Response Characteritics of the UWB Induced Systolic Hypotension.

In another experiment, mice were exposed to UWB electromagnetic pulses averaging 99-105 kV/m peak amplitude, 0.97-1.03 ns duration, and 155-174 ps rise time, after intraperitoneal administration of saline or morphine sulfate. They were then tested for thermal nociception on a hot surface and for spontaneous activity. Analysis of results showed no effect of UWB pulses on nociception and activity measures in CF-1 mice after 15-, 30-, or 45-min exposure to pulses at 600/s or after 30-min exposure to UWB pulses at 60/s. This result indicated lack of effect of the UWB pulses used in these experiments on nervous system components, including endogenous

opioids, involved in these behaviors.

In a related experiment executed in our laboratories no evidence for excess genotoxocity was found in peripheral blood or bone marrow cells of mice exposed to UWB.

Also, when cell samples of the yeast were exposed to 100 J/m^2 of 254 nm ultraviolet (UV) radiation followed by a 30 min treatment with UWB pulses. The effect of exposure was evaluated from the colony-forming ability of the cells on complete and selective media and the number of aberrant colonies. This experiment established no effect of UWB exposure on the UV-induced reciprocal and non-reciprocal recombination, mutagenesis, or cell survival.

Relevant Publications / Presentations

Lu, S-T., Mathur, S. P., Akyel, Y., and Lee, J. C. (1999). Ultra-wideband electromagnetic pulses induced hypotension in rats. *Physiology and Behavior*, 65, 753-761.

Lu, S-T., Mathur, S. P., and Akyel, Y. (1998). Dose-response characteristics of an UWB-induced hypotension in rats. *Twentieth Annual Meeting of the Bioelectromagnetic Society*, June 7 - 11, Florida.

Jauchem, J. R., Seaman, R. L., Lehnert, H. M., Mathur, S. P., Ryan, K. L., and Frei, M. R. (1998). Exposures of rats to ultra-wideband electromagnetic pulses: Lack of effects on heart rate and blood pressure. *Twentieth Annual Meeting of the Bioelectromagnetic Society*, June 7 - 11, Florida.

Pakhomova, O. N., Belt, M. L., Mathur, S. P., Lee, J. C., and Akyel, Y. (1998). Ultra-wide band electromagnetic radiation does not effect UV-induced recombination and mutagenesis in yeast. *Bioelectromagnetics*, 19, 128-130.

Seaman, R. L., Belt, M. L., Doyle, J. M., and Mathur, S. P. (1998). Ultra-wideband electromagnetic pulses and morphine-induced changes in nociception and activity in mice. *Physiology and Behavior*. 65, (2), 263-270.

Seaman, R. L., Belt, M. L., Doyle, J. M., and Mathur, S. P. (1998). Ultra-wideband pulses

counteract hyperactivity but not reduced nociception induced by NOS inhibitor L-Name in CF-1 mice. *Twentieth Annual Meeting of the Bioelectromagnetic Society*, June 7 - 11, Florida.

Vijayalaxmi, Seaman, R. L., Belt, M. L., Doyle, J. M., Mathur, S. P., and Prihoda, T. J. (1999). Frequency of micronuclei in the blood and bone marrow cells of mice exposed to ultra-wideband electromagnetic radiation. *International Journal of Radiation Biology*, 75 (1), 115-120.

The copies of the above articles can be found in the Volume II of this Final Report.

- **Millimeter wavelength exposure on neuronal and cellular functions**

Dr. Andrei Pakhomov executed a series of experiments to study the effects of millimeter wave (MMW) radiation. In order to establish whether MMW irradiation alters conduction in a polysynaptic pathway from dorsal root afferent fibers to efferents of the respective ventral root, effects of 41.34 GHz MMWs were studied in the isolated frog spinal cord preparation. After isolating and placement of the cord in the exposure bath, the cord was simulated with single supramaximal pulses every 30 s. Experiments began after 30-160 min of stabilization and lasted for 65 min, without any changes or interruptions of the stimulation routine. He concluded that the effect of even a short MMW irradiation is not limited to changes taking place during this irradiation. The aftereffect of the first MMW exposure was not detectable by physiological indices, but manifested itself as a change in the sensitivity to the second exposure. Moreover, this aftereffect could be either a decrease or an increase in the sensitivity of the preparation, depending on whether the preparation responded to the first exposure or not.

In another series of experiment, effects of short-term exposure to millimeter waves on the compound action potential (CAP) conduction were studied in an isolated frog sciatic nerve preparation. The low rate of stimulation did not alter the functional state of the nerve, and the amplitude, latency, and peak latency of CAPs could stay virtually stable for hours. The effects observed under irradiation at higher field intensity of 2-3 mW/cm^2 were a subtle and transient reduction of CAP latency and peak latency along with a rise of the test CAP amplitude.

Dr. Pakhomov published an important milestone review paper in 1998. In this paper he reviewed the current state and implications of research on biological effects of millimeter waves. This paper analyzed general trends in the area and reviewed the most significant publications, proceedings from cell-free systems, dosimetry, and spectroscopy issues through cultured cells and isolated organs to animals and humans. The studies reviewed demonstrated effects of low-intensity MMW on cell growth and proliferation, activity of enzymes, state of cell genetic apparatus, function of excitable membranes, peripheral receptors, and other biological systems. This long over due paper also outlines some problems and uncertainties in the MMW research area, identifies tasks for future studies, and discusses possible implications for development of exposure safety criteria and guidelines.

Relevant Publications / Presentations:

Pakhomov, A. G., Mathur, S. P., Akyel, Y., and Murphy, M. R. (1998). High resolution microwave dosimetry in lossy media. NATO Advanced Research Workshop, October 12-16, Slovenia.

Pakhomov, A. G., Belt, M. L., Cox, D. D., Mathur, S., Akyel, Y., and Murphy, M. R. (1998). Immediate effects of extremely high power microwave pulses on the beating rhythm in isolated frog heart auricle. *Twentieth Annual Meeting of the Bioelectromagnetic Society*, June 7 - 11, Florida.

Pakhomov, A. G., Akyel, Y., Pakhomova, O. N., Stuck, B. E., and Murphy, M. R. (1998). Current state and implications of research on biological effects of millimeter waves: A review of the literature. *Bioelectromagnetics*, 19, 393-413.

Pakhomov, A. G., Prol, H. K., and Akyel, Y. (1998). A pilot study of the millimeter-wavelength radiation effect on synaptic transmission. *Electro-magnetobiology*, 17, (2), 115-125.

Pakhomov, A. and Akyel, Y. (1997). Nonthermal physiological effects to microwave exposure. *The 33rd International Congress of Physiological Sciences*, June 30- July 5, St. Petersburg, Russia.

Pakhomov, A. G., Prol, H. K., Mathur, S. P., Akyel, Y., and Campbell, C. B. G. (1997). Search for frequency-specific effects of millimeter-wave radiation on isolated nerve function. *Bioelectromagnetics*, 18, 324-334.

The copies of the above articles can be found in the Volume II of this Final Report.

- **A series of research studies exploring potential of neurotoxic effects of RFR exposure. A satisfactory external science review will be required for each study protocol before the study is initiated.**

Upon the recommendation of the U.S. Army Medical Research and Material Command and COR Mr. Bruce Stuck, MBS staff submitted proposals for a Neurotoxin Exposure Treatment Research Program. These proposed projects are:

- **Role of glutamergic and GABAergic systems in neurotoxic effects of microwave.** This project is designed to understand the cellular mechanisms that underlie microwave effects on the central nervous system and to develop predictive models for microwave radiation effects. The research is driven by a clear hypothesis about the possible role of microwaves in neurodegenerative diseases. Evidence that pulsed microwaves increase agonist binding to glutamate receptors and decrease binding to GABA receptors suggests a possible neurotoxic mechanism. This project plans to study the effects of extremely high powered microwave pulses on activation of the excitatory glutamate system and suppression of the inhibitory GABA system.

- **Animal behavior testing for modification of the central nervous system by electromagnetic fields of military relevance.** This project will develop and test a toxin induced neurodegeneration model. It should help determine the dependence of harmful behavioral effects on microwave exposure and indicate possible neurotoxic effects in humans. The experiments on drug induced neurodegeneration will help to determine if nitric oxide plays a role in the mechanism of these changes. The strengths of this project are the plausible rationale and the diverse set of endpoints. The rodent model of 3-nitropropionic acid neurotoxicity is well developed.

- **Behavioral modalities to study potential toxic military threat agents.** This research protocol involves a range of endpoints from simple sensory functions to higher mental processes, such as learning and memory, in rats. Memory impairment will be studied with various maze tasks; physical endurance will be measured with treadmill performance; and behavioral despair will use Porsolt's swimming task, a recent animal model for depression. These studies should provide information on the effects of high power microwaves on the behavioral and cognitive performance of rats. This information will, in turn, help

determine the potential for neurotoxic effects in humans.

The American Institute of Biological Sciences (AIBS) conducted a two day peer review session at the Microwave Bioeffects Branch on December 2-3, 1998, upon the request of the Army Operational Medicine Research Program. The four scientist peer review panel concluded that the proposed research plans are clearly relevant to the objectives of the Army's program. Furthermore, the panel commented favorably on the "highly motivated operation struggling to do its best with limited resources." The AIBS panel recommended the restoration of full funding and staffing of the program.

MBS fully understands the needs of the Neurotoxin Exposure Treatment Research Program, and is dedicated to accomplish the objectives of the above approved proposals. A copy of the AIBS peer review panel report can be found in Volume II of this Final Report.

MAJOR ACCOMPLISHMENTS

McKessonHBOC BioServices' understanding of technical issues and insight into scientific principles have been the keystone of success for the Microwave Bioeffects Branch's research program. Due to MBS staff efforts in planning and managing the research program, and the dedication and the enthusiasm of the staff members, the scientific productivity of the program has risen dramatically despite drastic budget cuts. During the last two years the US Army's program continued to be a well-respected member of the Tri-Service Directed Energy Bioeffects Program at Brooks AFB. A summary list of our major accomplishments during the last two years of the contract is as follows:

- Besides two major technical reports, MBS staff presented and published two dozen scientific papers. Eleven of these papers are published in peer-reviewed scientific journals or books. A list of Branch's publications is presented at the end of this report. Volume II of this report contains copies of these publications.

- A very positive peer review of the Neurotoxin Exposure Treatment Research Program of the MBB is provided by the American Institute of Biological Sciences (AIBS). Volume II of this report contains a copy of the peer review.

- A technical report investigating the safety of army personnel from exposure to radio frequency radiation from the Advanced Membrane Transducer Antenna is prepared and presented to Mr. Bruce Stuck (COR). A copy of this report can be found in Volume II of this report.

- A major cornerstone Tri-Service report investigating retinal effects of high power microwaves in rhesus monkeys is prepared under the leadership of MBS staff. A copy of this report can be found in Volume II of this report.

- Various dielectric measurements of brain tissue were accomplished.

- A new microdosimetry method is developed to study the lossy media exposed to extremely high power microwave pulses.

- Frequency-specific mmWave effects on nerve conduction were studied and a review paper summarizing the biological effects of mmWaves was published.

- Two major health studies investigating the effects of UWB on analgesia, activity level, and cardiovascular system were accomplished.

- Significant steps were taken in UWB field characterization and system improvement.

CONCLUSIONS

During the last two years of the contract MBS employees proved that they were determined to provide, under the general guidance of the COR and appropriate WRAIR Program Managers, high quality scientific products. Despite significant decreases in funding and number of staff the Microwave Bioeffects Branch stayed highly productive and continued to support the US Army's needs. We were able to publish and/or present 24 scientific articles over the last two years. This is an excellent proof of the productivity and the dedication of the McKessonHBOC staff. Our staff do realize that the research efforts of the US Army in high power microwave fields have little precedence and are considered innovative and pioneering.

In the next two option years, MBS researchers will focus on the approved Neurotoxin research protocols. We will conduct a series of at least three major studies exploring the potential of neurotoxic effects of radio frequency radiation exposure. Furthermore, MBS will continue to conduct research on the biological effects of ultra wideband radiation on the cardiovascular and other cellular systems. We will produce data to be used to set the guidelines for safe exposure criteria for this new modality as promulgated by the Tri Service Electromagnetic Radiation Panel (TERP). As recommended by the AIBS we will improve existing connections with scientists at the University of Texas and other scientists in the immediate area.

MBS is dedicated to continue to promote the success of the Walter Reed Army Institute of Research and be the world leader in military relevant biomedical research. We will help WRAIR to ensure that the soldiers will have the best possible knowledge and protection against environmental electromagnetic threats.

PERSONNEL

The following McKessonHBOC BioServices personnel served under the present contract:

♦ Dr. Yahya Akyel	Program Manager / Behavioral Psychologist
♦ Dr. Shin-Tsu Lu	Radiation Biologist / Veterinarian
♦ Dr. Andrei Pakhomov	Electrophysiologist
♦ Dr. Olga Pakhomova	Cellular Biologist
♦ Dr. Ronald Seaman	Biomedical Engineer / Physiologist
♦ Dr. Satnam Mathur	Electrical Engineer / Antenna Design
♦ Dr. Jian Bao	Physicist
♦ Ms. Lori Allen	Administrative Assistant / Safety Officer
♦ Ms. Joanne Doyle	Biomedical Technician
♦ Mr. Bryan Wohlfeld	Biomedical Technician
♦ Mr. Kenneth Prol	Biomedical Engineer
♦ Mr. Duane Cox	Electronic Technician / Machinist
♦ Mr. Jonathan Lee	Electrical Engineer / Computer Support

MICROWAVE BIOEFFECTS BRANCH
PRESENTATIONS / PUBLICATIONS LIST
(MAY 1997 - MAY 1999)

Bao., J-Z. (1997). Picosecond domain electromagnetic pulse measurements in an exposure facility: An error compensation routine using deconvolution techniques. *Review of Scientific Instruments*, 68 (5), 2221 - 2227.

Bao, J-Z., Lee, J. C., Belt, M. E., Cox, D. D., Mathur, S. P., and Lu, S-T. (1997). Error correction in transient electromagnetic field measurements using deconvolution techniques. *Ultra-wideband, Short-Pulse Electromagnetics* 3, Plenum Press, New York.

Bao, J-Z., Lu, S-T., and Hurt, W. D. (1997). Complex dielectric measurements and analysis of brain tissues in the radio and microwave frequencies. *IEEE Transactions on Microwave Theory and Techniques*, 45 (10), 1730 - 1741.

D'Andrea, J. A., Ziriax, J, Lu, S-T., Mathur, S., and Merritt, J. H. (1997). Rhesus monkey vision after exposure to high peak power microwave pulses. *Department of Defense Electromagnetic Environmental Effects (E3) Program Review*. 10-14 March, Everett, WA.

D'Andrea, J. A., Ziriax, J, Lu, S-T., Mathur, S., Merritt, J. H., Johnson, M, Lutty, G., Zwick, H., and Stuck, B. (1997). Rhesus monkey vision after exposure to high peak power microwave pulses. *The Second World Congress for Electricity and Magnetism in Biology and Medicine*, June 8 - 13, Bologna, Italy.

Jauchem, J. R., Seaman, R. L., Lehnert, H. M., Mathur, S. P., Ryan, K. L., and Frei, M. R. (1998). Exposures of rats to ultra-wideband electromagnetic pulses: Lack of effects on heart rate and blood pressure. *Twentieth Annual Meeting of the Bioelectromagnetic Society*, June 7 - 11, Florida.

Kiel, J. L., Seaman, R. L. Mathur, S. P., Parker, J. E., Wright, J. R., Alls, J L., and Morales, P. J. (1999). Pulsed microwave induced light, sound, and electrical discharge enhanced by a

biopolymer. *Bioelectromagnetics,* 20, 216 - 223.

Kiel, J. L., Mason, P. A., Alls, J. L., Morales, P., and Seaman, R. L. (1998). A mechanism of single-pulse radio frequency radiation interaction with biological molecules. *Twentieth Annual Meeting of the Bioelectromagnetic Society*, June 7 - 11, Florida.

Kiel, J., Parker, J., Alls, J., Morales, P., Seaman, R., Mathur, S., and Wright, J. (1997). Pulsed microwave radiation induction of electrosonoluminescence. *Fourth Annual Michaelson Research Conference*, August 15-18, Canandaigua, NY.

Lu, S-T., Mathur, S. P., Akyel, Y., and Lee, J. C. (1999). Ultrawide-band electromagnetic pulses induced hypotension in rats. *Physiology and Behavior*, 65, 753-761.

Lu, S-T., Mathur, S. P., and Akyel, Y. (1998). Dose-response characteristics of an UWB-induced hypotension in rats. *Twentieth Annual Meeting of the Bioelectromagnetic Society*, June 7 - 11, Florida.

Lu, S-T., Mathur, S. P., Stuck, B., Zwick, H., D'Andrea, J. A., Ziriax, J. M., Merritt, J. H., Lutty, G., McLeod, S., and Johnson, M. (1998). Retinal effects of high peak power L-band microwaves in monkeys. *Twentieth Annual Meeting of the Bioelectromagnetic Society*, June 7 - 11, Florida.

Pakhomov, A. G., Mathur, S. P., Akyel, Y., and Murphy, M. R. (1998). High resolution microwave dosimetry in lossy media. NATO Advanced Research Workshop, October 12-16, Slovenia.

Pakhomov, A. G., Belt, M. L., Cox, D. D., Mathur, S., Akyel, Y., and Murphy, M. R. (1998). Immediate effects of extremely high power microwave pulses on the beating rhythm in isolated frog heart auricle. *Twentieth Annual Meeting of the Bioelectromagnetic Society*, June 7 - 11, Florida.

Pakhomov, A. G. Mathur, S. P., Akyel, Y., and Kiel, J. L. (1998). Direct microdosimetry in media exposed to extremely high peak power microwaves. *Twentieth Annual Meeting of the Bioelectromagnetic Society*, June 7 - 11, Florida.

Pakhomov, A. G., Mathur, S. P., and Murphy, M. R. (1998). Dose dependencies in bioeffects of extremely high peak power microwave pulses. *World Health Organization (WHO) Annual Meeting*, 18-22 March, Moscow, Russia.

Pakhomov, A. G., Akyel, Y., Pakhomova, O. N., Stuck, B. E., and Murphy, M. R. (1998). Current state and implications of research on biological effects of millimeter waves: A review of the literature. *Bioelectromagnetics*, 19, 393-413.

Pakhomov, A. G., Prol, H. K., and Akyel, Y. (1998). A pilot study of the millimeter-wavelength radiation effect on synaptic transmission. *Electro-magnetobiology*, 17, (2), 115-125.

Pakhomov, A. and Akyel, Y. (1997). Nonthermal physiological effects to microwave exposure. *The 33rd International Congress of Physiological Sciences*, June 30- July 5, St. Petersburg, Russia.

Pakhomov, A. G., Prol, H. K., Mathur, S. P., Akyel, Y., and Campbell, C. B. G. (1997). Search for frequency-specific effects of millimeter-wave radiation on isolated nerve function. *Bioelectromagnetics*, 18, 324-334.

Pakhomova, O. N., Belt, M. L., Mathur, S. P., Lee, J. C., and Akyel, Y. (1998). Ultra-wide band electromagnetic radiation does not effect UV-induced recombination and mutagenesis in yeast. *Bioelectromagnetics*, 19, 128-130.

Seaman, R. L., Belt, M. L., Doyle, J. M., and Mathur, S. P. (1998). Ultra-wideband electromagnetic pulses and morphine-induced changes in nociception and activity in mice. *Physiology and Behavior*. 65, (2), 263-270.

Seaman, R. L., Belt, M. L., Doyle, J. M., and Mathur, S. P. (1998). Ultra-wideband pulses counteract hyperactivity but not reduced nociception induced by NOS inhibitor L-Name in CF-1 mice. *Twentieth Annual Meeting of the Bioelectromagnetic Society*, June 7 - 11, Florida.

Vijayalaxmi, Seaman, R. L., Belt, M. L., Doyle, J. M., Mathur, S. P., and Prihoda, T. J. (1999). Frequency of micronuclei in the blood and bone marrow cells of mice exposed to ultra-

wideband electromagnetic radiation. *International Journal of Radiation Biology*, 75 (1), 115-120.

Physiology & Behavior, Vol. 65, Nos. 4/5, pp. 753–761, 1999
© 1999 Elsevier Science Inc.
Printed in the USA. All rights reserved
0031-9384/99 $–see front matter

ELSEVIER

PII S0031-9384(98)00214-5

Ultrawide-Band Electromagnetic Pulses Induced Hypotension in Rats

SHIN-TSU LU,[1] SATNAM P. MATHUR, YAHYA AKYEL AND JONATHAN C. LEE

McKesson BioServices, U.S. Army Medical Research Detachment, Microwave Bioeffects Branch, 8308 Hawks Road, Building 1168, Brooks Air Force Base, TX 78235

Received 17 December 1997; Accepted 17 July 1998

LU, S.-T., S. P. MATHUR, Y. AKYEL AND J. C. LEE. *Ultrawide-band electromagnetic pulses induced hypotension in rats.* PHYSIOL BEHAV **65**(4/5) 753–761, 1999.—The ultrawide-band (UWB) electromagnetic pulses are used as a new modality in radar technology. Biological effects of extremely high peak E-field, fast rise time, ultrashort pulse width, and ultrawide band have not been investigated heretofore due to the lack of animal exposure facilities. A new biological effects database is needed to establish personnel protection guidelines for these new type of radiofrequency radiation. Functional indices of the cardiovascular system (heart rate, systolic, mean, and diastolic pressures) were selected to represent biological end points that may be susceptible to the UWB radiation. A noninvasive tail-cuff photoelectric sensor sphygmomanometer was used. Male Wistar–Kyoto rats were subjected to sham exposure, 0.5-kHz (93 kV/m, 180 ps rise time, 1.00 ns pulse width, whole-body averaged specific absorption rate, SAR = 70 mW/kg) or a 1-kHz (85 kV/m, 200 ps rise time, 1.03 ns pulse width, SAR = 121 mW/kg) UWB fields in a tapered parallel plate GTEM cell for 6 min. Cardiovascular functions were evaluated from 45 min to 4 weeks after exposures. Significant decrease in arterial blood pressures (hypotension) was found. In contrast, heart rate was not altered by these exposures. The UWB radiation-induced hypotension was a robust, consistent, and persistent effect. © 1999 Elsevier Science Inc.

Arterial pressure Heart rate Pulsed radiofrequency radiation Ultrawide-band radiation Delayed effects

THE ultrawide-band (UWB) radiofrequency (RF) radiation is a new modality in radar technology. The potential usages of UWB radar are not limited to military application only. At much lower power, an example of civilian UWB radar application is in automobile safety. Devices designed as warning systems for backing up and parking are planned, and expected to be available in the next few years. A commonly used definition accepted by the Defense Advanced Research Project Agency is "Ultrawide band radar is any radar whose fractional bandwidth is greater than 0.25, regardless of the center frequency or the signal time–bandwidth product" (45). The UWB is a radiofrequency signal with an ultrashort pulse width (a few ns) and a very fast rise time (<200 ps). Because of the ultrashort pulse width, the peak electric field of a UWB pulse can be operated in excess of the breakdown voltage without arcing. In fact, systems with peak electric field in excess of hundreds of kV/m are known to exist. Another characteristic is a very low duty cycle of these UWB devices resulting from an ultrashort pulse width.

Radiofrequency personnel protection guidelines usually are promulgated on a time-averaged specific absorption rate or power density. From operational characteristics of the UWB devices with an extremely high peak electric field and very low duty cycle, the energy absorption rate per pulse in humans can be extremely high (temporal peak SAR), but the average specific absorption rate (average SAR) can be very low if a time–average procedure is applied. The ratio of peak to average SARs will be much greater than those of narrowband RF radiation used in the past for evaluation of the biological effects of pulsed RF radiation. Concerns on UWB radiation safety issues have been voiced (1). However, the experimental database on UWB safety issues is very limited (41,48). Therefore, there is a need for additional toxicological testing to address the safety of UWB radiation.

Interests in the cardiovascular effects of RF radiation can be traced back to as early as the 1940s (37), and it has continued until today. Specifically, cardiovascular effects of RF radiation include human studies with emphasis on changes in regional blood flow for diathermy, epidemiology, and case report, studies in experimental animals such as cardiac injuries caused by intense RF exposure, cardiovascular adjustments to localized "low-level" RF exposure, changes in arte-

[1]To whom requests for reprints should be addressed. E-mail: shin-tsu.lu@aloer.brooks.af.mil

rial pressure, and heart rate by moderate RF exposure. The effect of RF radiation on heart rate can be further divided into tachycardia, bradycardia, cardiac pacing, effects on isolated cardiac tissue in vitro and the RF interference of the implanted cardiac pacemaker. This database forms a foundation for a comparative analysis between narrow-band RF and UWB radiations. However, the majority of these studies are acute experiments employing a short-term (acute) exposure and studying cardiovascular end points in a short period of time, for example, during or immediately after RF exposure, and usually under anesthesia. Three studies used a long-term (chronic) RF exposure, but cardiovascular functions were not their main emphasis; instead, they were embedded in a battery of end points (8,10,46).

Two types of chronic cardiovascular effects have been observed. They are the cardiovascular effect of a chronic exposure and the delayed effect of an acute exposure. The chronic effect is represented by a biphasic (hypertension→normotension→hypotension) or a monophasic (hypotension) arterial response in rats chronically exposed to RF radiation (37). The delayed effects are from case reports (13,49) indicating the presence of delayed hypertension in conjunction with anxiety attacks, which was termed "atypical post-traumatic syndrome," months after an accidental exposure to RF fields. This delayed vascular response has never been confirmed experimentally. In the present experiment, heart rate and blood pressure in awake rats were evaluated periodically with a tail-cuff photoelectric sphygmomanometer from 45 min to 4 weeks after acute UWB exposures.

MATERIALS AND METHODS

General Description of the Experimental Procedure

Fifteen male Wistar–Kyoto (WKY) rats aged between 71 and 89 days were used at the beginning of the experiment. They were obtained at 56 days of age from a commercial source (Charles River, Portage, MI). They were maintained in the vivarium at 21–23°C ambient temperature, 100% conditioned fresh air for more than 10 exchanges per hour, and a 12 L–12 D (lights on 0600–1800 h) light cycle. Tap water and feed (Purina Rodent Diet 5008, Ralston Purina Co., St. Louis, MO) were available ad lib. After a 10-day quarantine period, they were acclimated to a test holder (IITC Life Science, Woodland Hills, CA, model 81) 1 h daily for 3 days. Preexposure baseline of the heart rate and arterial pressures (systolic, mean, and diastolic) were determined 1–2 days after the holder acclimation. Three to 4 days later, they were individually subjected to sham exposure, low UWB, or high UWB exposure for 6 min between 0900 and 1000 h in an exposure holder maintained at 23–25°C. On the exposure day, average body weight was 250 ± 4 g (n = 15, SE). Immediately after exposure, the rat was transferred to the test holder for heart rate and blood pressure measurements. Postexposure heart rate and blood pressures were determined at 45 min, 24 h, 72 h, 1, 2, 3, and 4 weeks after exposure. Four to six determinations were obtained at each time point, and the average value was used to represent the cardiovascular endpoints at that time point. Fifteen animals were divided randomly into three groups of five rats each for sham exposure, "low" UWB and "high" UWB exposures. Each rat was assigned randomly to receive one of the three treatments in five experimental cycles. The UWB-exposed rats were always accompanied by at least one sham-exposed animal such that the time-related experimental error caused by different experimental cycles or animal shipments could be minimized.

Photoelectric Sphygmomanometer

An indirect tail-cuff arterial pressure measurement system without external preheating in awake rats was first introduced by Yen et al. (51). Validation of pressure markers (systolic and mean arterial pressures), and theoretical analysis of this indirect method based on a photoelectric sensor have been performed by various investigators (4,36,50). For the present experiment, a commercial system (IITC Life Sci., Woodland Hills, CA) was used. The system was composed of a pulse amplifier (IITC model 29), tail-cuff photoelectric sensor assembly (IITC model B-60, 5/8" cuff), smaller bore tubing (Tygon, 1.6 mm i.d., 0.8-mm wall thickness for connecting tail-cuff, pressure amplifier, pressurizing bulb, and pressure gauge) and animal holder (IITC model 81). Outputs of the pressure transducer and pulse sensor from the pulse amplifier were split evenly. One set of outputs was monitored continuously with a digital oscilloscope (Tektronix 2430 A, Tektronix, Inc., Wilsonville, OR). The other set of outputs was converted to a digital signal and recorded using a strip chart program (AYSTANT+, Asyst Software Technology, Rochester, NY) by a computer (Hewlett–Packard Vectra, Hewlett Packard, Greenley, CO) at 50 Hz data acquisition rate. The recorded data was imported into a graphics program (SigmaPlot 4.1, Jandel Scientific Softwares, San Rafael, CA) and viewed graphically and digitally. A custom-made microenvironment chamber was fabricated from acrylic tubes (28 cm long, 12 and 14 cm i.d., 3.2-mm wall thickness). Plastic tubing (Tygon, 6.4 mm i.d., 1.6-mm wall thickness, from Cole Palmer, Vernon Hills, IL) was wrapped around the smaller acrylic tube with tubing wall touching each other to form a coil 18 cm in length. The larger acrylic tube was used as an outer wall. Both ends of the Tygon tubing were connected to the pump inlet and outlet port of a precision circulator water bath (Neslab RTE-110, Neslab Instruments, Portsmouth, NH) providing an microenvironment within the inner acrylic tube between 26.5 and 27.5°C to prevent sudden temperature surges. The microenvironment chamber was monitored continuously with a thermistor temperature probe (Yellow Springs 405 air temperature probe, Yellow Springs Instrument, Yellow Springs, OH) and a digital thermistor bridge (Cole Palmer 08502-12, Cole Palmer, Vernon Hills, IL). The pressure amplifier output was set at 1.00 volt per Torr (mmHg). Light intensity and photosensor output amplifier were adjusted to provide a tail-pulse signal at no more than 5 volts at the maximum oscillation. Pressure amplifier output was calibrated daily against a certified sphygomomanometer before use. The same tail-cuff-photoelectric sensor assembly was used throughout the entire experiment.

Cardiovascular Parameter Measurement

Rats were transported from the vivarium to the laboratory in the morning. They were allowed to sit quietly in their own cage for at least 30 min before being transferred to the test holder. The rat and test holder were then inserted into the microenvironment chamber. Heating in the microenvironment chamber caused by animal body heat was offset by adjusting the waterbath temperature. After 20 min in the microenvironment chamber, the rat tail was passed through the tail cuff. The tail-cuff/photoelectric sensor was then attached to the test holder. by this time, characteristic tail pulses could be detected if the tail cuff was inflated to 40–60 Torr (mmHg). When the presence of tail pulses was ascertained, tail cuff was quickly inflated to 200–220 Torr until tail pulses disappeared. The cuff was then deflated immediately afterwards at approximately 2 Torr per heart beat for 25.6 s. Systolic pressure (P_s)

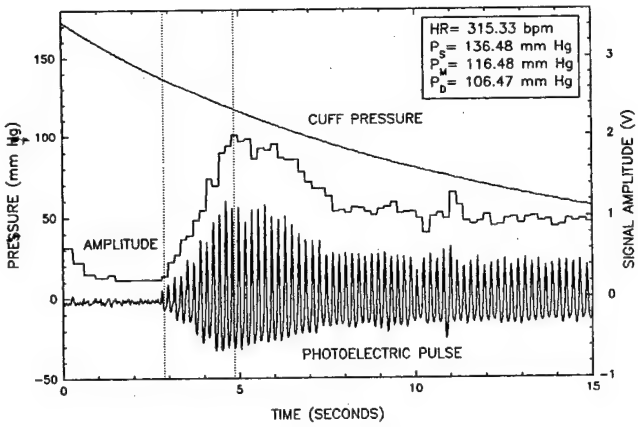

FIG. 1. An example of the indirect arterial pressure measurement in the rat.

was determined during the deflation cycle as the corresponding cuff pressure at the reappearance of the tail pulse while mean pressure (P_m) was the cuff pressure when amplitude of the tail pulse reached a maximum. Diastolic pressure (P_d) was calculated by $P_d = (P_m \times 3 - P_s)/2$ (42). Heart rate was determined from the average of pulse-to-pulse intervals for at least 60 beats. An example of this deflation cycle is shown in Fig. 1. The arterial pressure/heart rate measurement was repeated for four to six times separated by a 5-min interval between determinations to avoid the collapse of the tail artery during measurement.

UWB Exposure

The UWB exposure system was originally designed and built at the Sandia National Laboratories (Albuquerque, NM). The UWB pulses were generated by a spark gap pulse generator and transmitted into a GTEM cell (Gigahertz Transverse Electromagnetic cell, a flared rectangular coaxial transmission line) (Fig. 2). The rise time and pulse width were 180 ps and 1.00 ns, respectively, when the system was operated at 500 Hz, and they were 200 ps and 1.03 ns when operated at 1,000 Hz. The pulsed electric field was measured with a EG&G (Wellesley, MA) D-dot sensor (model ACD-1R) (33). Outputs of the D-dot sensors were measured with a 4.5-GHz bandwidth Tektronix SCD5000 transient sampling scope. A transfer function was used for data compensation of the pulsed electric field. The transfer function was based on deconvolution technique of a standard pulse generated by a Picosecond Pulse Laboratories 4050 B picosecond step generator with 5100 pulse forming network. The corrected D-dot values were converted into E field intensity (2). For UWB exposures, the rat was placed in an exposure holder fabricated from an acrylic tube (6.5-cm i.d., 3.2-mm wall thickness, 28 cm long, 6.4 × 50-mm slots separated by 19 mm for ventilation) and polyethylene endcaps. No metallic parts was used, and this holder was used to align the animal position to UWB fields. The long axis of the tube, i.e., the major axis of the animal was placed in parallel with magnetic vector on the ground plane at 72.7 cm from the source end of GTEM cell. The animal was isolated from the ground plane by placing the exposure holder 4.2 cm from the ground plane on an acrylic stand. After transferring the animal into the GTEM cell, a 5-min equilibration period was given before exposure. Three exposure protocols were used: sham exposure, low-UWB and high-UWB exposures for 6 min. During the sham exposure, all UWB exposure conditions were maintained except trigger pulses were never generated to cause discharge across the spark gap. Table 1 lists pertinent pulse parameters used. Figure 3 shows the pulse characteristics operated at 500 Hz (low-UWB) and 1,000 Hz (high-UWB) repetition rate.

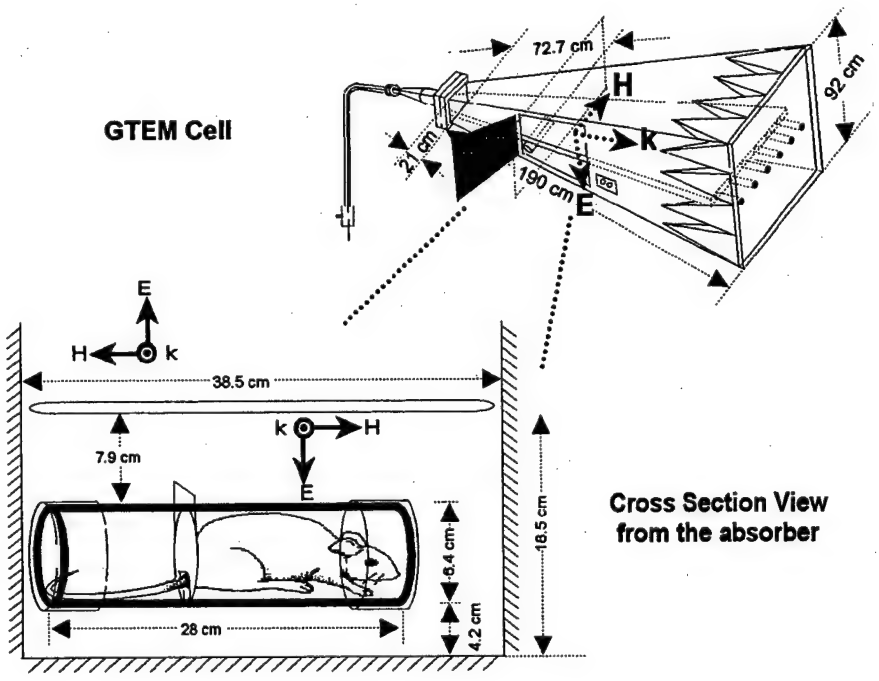

FIG. 2. The UWB exosure system for rats.

TABLE 1
CHARACTERISTICS OF THE UWB PULSES

Pulse Parameters	Sham	Low UWB*	High UWB*
Risetime	—	180 ± 7 ps	200 ± 5 ps
Pulse width	—	1.00 ± 0.004 ns	1.03 ± 0.02 ns
Peak E field intensity	0 kV/m	93.0 ± 5.0 kV/m	84.6 ± 4.0 kV/m
Pulse repetition rate	0 Hz	500 Hz	1,000 Hz
Average power density	0 mW/cm2	1.15 mW/cm^2	1.96 mW/cm^2
Total radiant exposure	0 J/cm2	0.41 J/cm^2	0.70 J/cm^2
Highest frequency†	—	2.78 GHz	2.50 GHz
Medium frequency†	—	0.50 GHz	0.49 GHz
Lowest frequency†	—	0.09 GHz	0.10 GHz
Fractional bandwidth†	—	187%	185%

*Mean ± SD, obtained in five exposures.

†Estimated according to Foster (14). Ultrawide band radar is a radar whose fractional bandwidth is greater than 25%, regardless of the center frequency or the signal time-bandwidth product (45). The fractional bandwidth of these pulses was wider than the minimum required to qualify as UWB radar.

Data Analysis

The present experiment utilized a factorial design with repeated observations. The time after exposure was designated as "blocks" ($r = 7$), UWB treatments ($t = 3$) as treatments and five observations ($s = 5$) were included. Therefore, the present experiment was a $7 \times 3 \times 5$ experiment which contained 105 experimental units. For each experimental unit, the average of four to six measurements was used. To limit the individual variation, the use of individual control was incorporated prior to the commencement of the experiment. Therefore, the end points were changes from the preexposure baseline in each individual rat. Postexposure heart rate and blood pressure data were the magnitude of change from the preexposure baseline of the same rat under study. An analytic method based on an analysis of variance with multiway classification and multiple observations was used. The sources of variation were identified, and the variance and degree of freedom (df) were computed. These various variances associated with the present experiment were total (experimental units, df = $rst - 1 = 104$), time after exposure (df = $r - 1 = 6$), UWB treatments (df = $t - 1 = 2$), interaction [df = $(r - 1)(t - 1) = 12$] and error [df = $rt(s - 1) = 84$]. Dunnett's test was used for post hoc analysis when a significant UWB treatment effect was found. Null hypothesis was rejected at the 0.05 level.

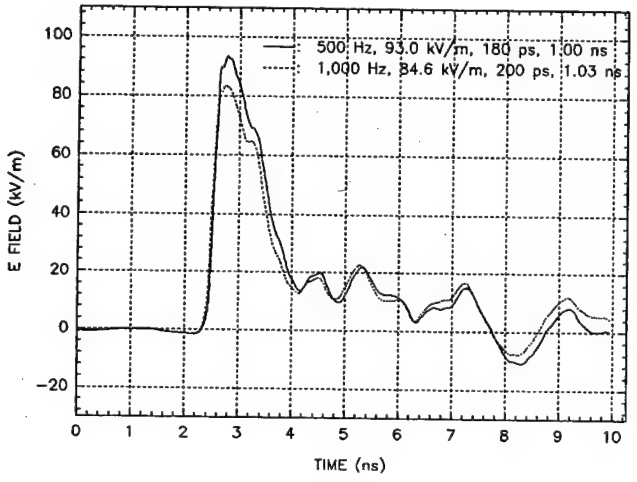

FIG. 3. The UWB pules operated at 500 and 1,000 Hz repetition rate.

RESULTS

Body Weight

Body weight of animals is shown in Fig. 4. Data are body weight before exposure, 24 h, 72 h, 1 week, 2, 3, and 4 weeks after exposure. Other than an initial insignificant weight loss in sham and 500 Hz exposed rats, weight gains were similar among these three groups of animals.

Preexposure Baseline

Figure 5 shows the preexposure baseline. Average heart rate ranged between 332 and 351 beats per minutes (bpm). The ranges in systolic, mean, and diastolic pressures were 146.1 to 147.7, 120.1 to 123.6, and 107.2 to 112.1 Torr, respectively. Difference among groups in any of the preexposure baseline was not found.

Heart Rate

Figure 6 shows the changes in heart rate from the preexposure baseline. Heart rate usually decreased from the preexposure baseline irrespective of UWB treatments. The UWB treatments, time after exposure and interaction between UWB treatments and time after exposure were not significantly different in this study.

Systolic Pressure

Systolic pressure of the sham-exposed rats had a tendency to increase (Fig. 7). In contrast, the systolic pressure was consistently lower than the preexposure baseline in rats exposed to 500 or 1,000 Hz UWB fields. UWB treatments were the only significant factor noted, $F(2,84) = 16.62$, $p < 0.001$. Time after exposure, $F(6, 84) = 1.00$, NS, and interaction between UWB treatments and time after exposure, $F(12,84) = 0.75$, NS, were not statistically significant. The largest changes from the respective preexposure baseline were +13.65 Torr at 4 weeks after sham exposure, −23.0 Torr at 2 weeks after exposure to 500 Hz and −22.8 Torr at 2 weeks after exposure to 1,000 Hz UWB. Post hoc analysis revealed that decreased sys-

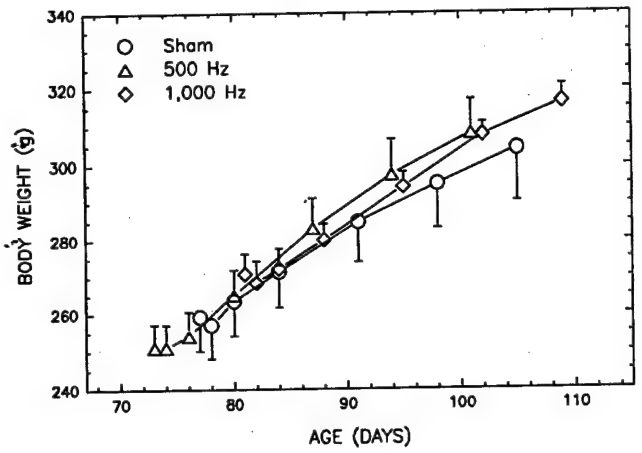

FIG. 4. Body weight of WKY rats exposed to UWB. Data shown are preexposure, 24 h, 72 h, 1 week, 2 weeks, 3 weeks, and 4 weeks after exposure.

tolic pressure occurred at 45 min, 24 h, 1, 2, and 4 weeks after exposure but not at 72 h, and 3 weeks after exposure in the 500 Hz exposed rats. In the 1,000 Hz exposed rats, significant decreases in systolic pressure occurred at 45 min, 1, 2, and 4 weeks after exposure but not at 24 h, 72 h, and 3 weeks after exposure. In comparison to the systolic pressure in sham-exposed rats, the most intense systolic hypotension occurred at 2 weeks after exposure. The magnitude of systolic pressure decrease from the sham-exposed group was 34.9 Torr in the 500 Hz group, and 34.7 Torr in the 1,000 Hz group.

Mean Arterial Pressure

Changes in mean arterial pressure were similar to changes in systolic pressure (Fig. 8). Mean arterial pressure had a tendency to increase from the preexposure baseline in sham-exposed rats while decreased mean arterial pressure was noted in rats exposed to 500 and 1,000 Hz UWB. Results of the factorial analysis of variance revealed that UWB treatments, $F(2,84) = 18.55$, $p < 0.001$, was statistically significant, but the times after exposure, $F(6,84) = 0.57$, NS was not. Interaction between UWB treatments and time after exposure was statistically insignificant, $F(12,84) = 0.37$, NS. The largest

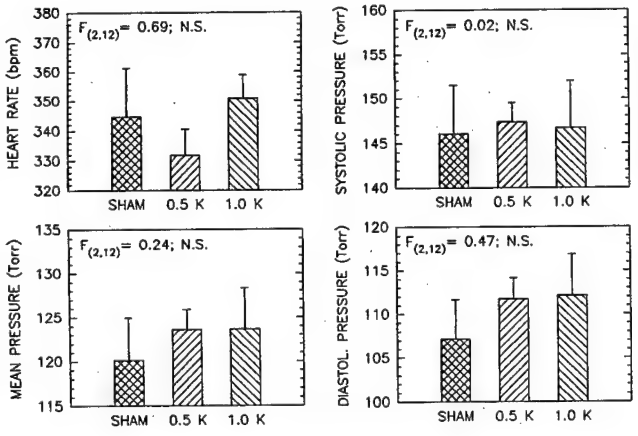

FIG. 5. Preexposure cardiovascular baseline.

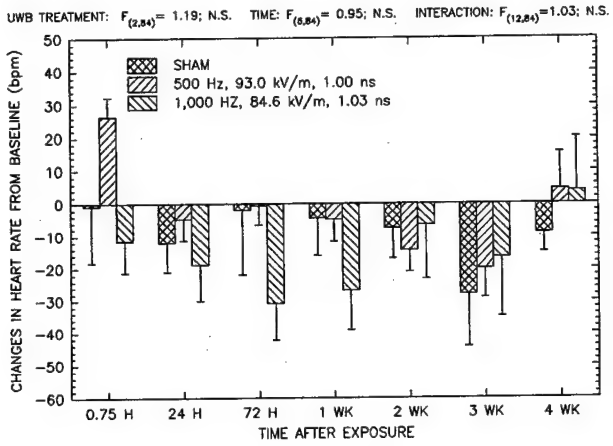

FIG. 6. Heart rates in UWB-exposed rats.

changes from their respective baseline were +8.5 Torr at 72 h after sham exposure, −15.9 Torr at 24 h after 500 Hz, and −16.9 Torr at 2 weeks after 1,000 Hz UWB exposure. In comparison to sham-exposed rats, significant lower mean arterial pressure was noted in 500 Hz-exposed rats at all times after exposure except at 3 weeks after exposure, and in 1,000 Hz-exposed rats at all time except at 24 h and 3 weeks after exposure. The largest magnitude of hypotension was 20.6 Torr in 500 Hz and 21.89 Torr in 1,000 Hz-exposed groups. Both of these occurred at 2 weeks after exposure.

Diastolic Pressure

Although systolic and mean arterial pressures can be determined with a photoelectric sphygmomanometer in rats, the diastolic pressure can only be estimated because a characteristic pulse marker is not available for identifying the diastolic pressure reliably during the deflection cycle. It is known that the mean arterial pressure is equal to the sum of diastolic pressure and 1/3 of the pulse pressure (difference between systolic and diastolic pressures) (42). Therefore, the diastolic pressure can be estimated from the systolic and mean arterial pressures. Changes in diastolic pressure were similar to systolic and mean arterial pressure (Fig. 9). In comparison to the pre-

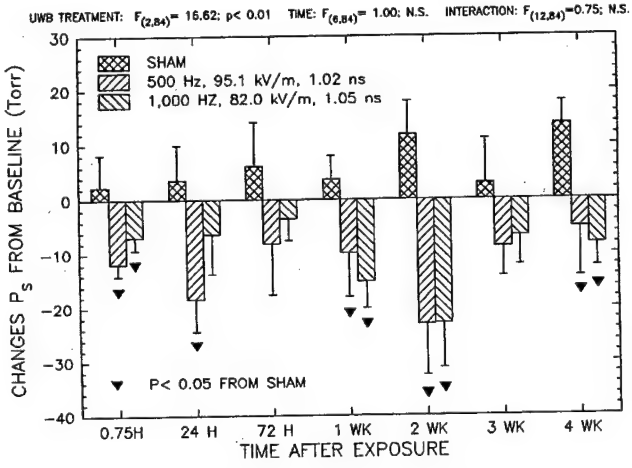

FIG. 7. UWB-induced systolic hypotension in WKY rats.

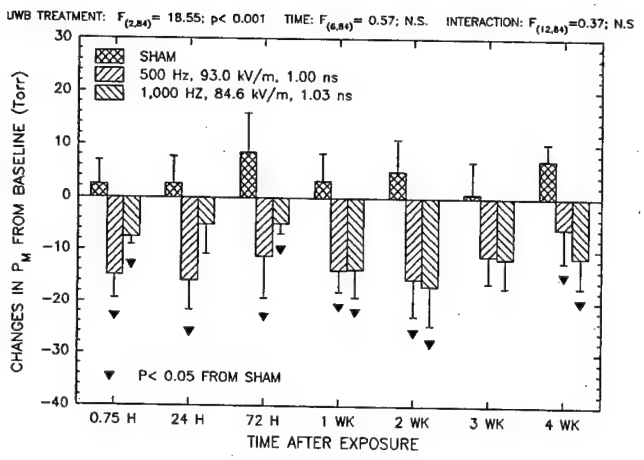

FIG. 8. UWB-induced decreases in mean arterial pressure in WKY rats.

exposure baseline, change in sham-exposed rats was primarily an increase in diastolic pressure, while decreases were noted in rats exposed to 500 or 1,000 Hz UWB. The largest change from baseline was +9.6 Torr at 72 h after sham exposure, −16.6 Torr at 45 min after exposure to 500 Hz, and −14.0 Torr at 3 weeks after exposure to 1,000 Hz UWB. Again, the UWB treatments were statistically significant, $F(2,84) = 16.30$, $p < 0.001$, but the time after exposure, $F(6,84) = 0.46$, NS, and the interaction between UWB treatments and time after exposure, $F(12,84) = 0.37$, NS were not. Diastolic hypotension was found in four of the six sampling points, i.e., at 45 min, 24 h, 72 h, 1, and 3 weeks but not at two and four weeks after exposure, in rats exposed to 500 Hz UWB. Rats exposed to 1,000 Hz UWB had a lower diastolic pressure than sham-exposed rats in five of the six postexposure sampling points. Diastolic hypotension was not noted in rats at 24 h after exposure to 1,000 Hz UWB. In comparison to sham exposure, the largest magnitude of changes in diastolic pressure was −22.5 Torr at 1 week after 500 Hz and −16.7 Torr at 4 weeks after 1,000 Hz.

DISCUSSION

The observation of a delayed, robust, and persistent decrease in arterial pressures (delayed hypotension) without

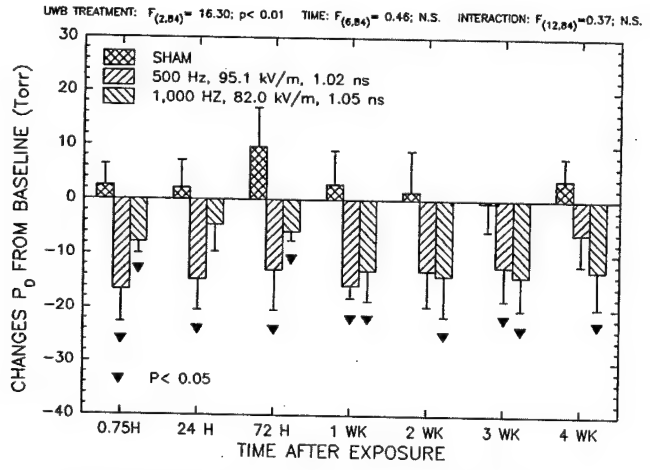

FIG. 9. UWB-induced diastolic hypotension in WKY rats.

changes in the heart rate in rats subjected to an acute UWB exposure is uncommon, no matter what the cause is. The heart rate is known to covary with blood pressure, or to be more susceptible than the blood pressure to RF perturbation (37). As indicated in the introduction, the anticipated UWB-induced change in the cardiovascular function, if any, was hypothesized to be hypertension (increased arterial pressure) as part of "atypical post-traumatic syndrome," which included emotional lability, irritability, headaches, insomnia, and delayed hypertension. In addition, the cardiovascular effect of UWB radiation appears to be different from the effect induced by conventional RF radiation. Results of a recent series of experiments (15–18,23–30) on thermogenic effects of RF radiation on cardiovascular functions also supported the concept that susceptibilities of the heart rate and arterial pressure to thermogenic RF radiations were different.

Jauchem and Frei (15–18,23–30) evaluated the cardiovascular responses of rats exposed to discrete narrow-band microwave radiation at 1.2 (30), 1.2–1.8/1.2–1.4 (26), 2.45 (17,23, 27), 2.8 (16,24,28), 5.6 (17,29), 9.3 (15), and 25 GHz (18). Except in one experiment (26), these investigators utilized ketamine-anesthetized rats as the experimental model. Their experimental design involved a comparison of cardiovascular end points, mean arterial pressure, and heart rate, in microwave exposed rats when their rectal temperature reached 38.5 and 39.5°C during the course of microwave exposure. Occasionally, the cardiovascular end points were the time sequential data in a lethal exposure. The whole-body average SAR used in these experiments ranged between 6 and 16.8 W/kg. Because ketamine-anesthetized rats could not maintain a rectal temperature at 38.5 and 39.5°C, sham-exposure data was not presented in these experiments. Thermal tachycardia and thermal hypertension were usually concluded. In contrast, the specific aims of the present experiment were to study the late cardiovascular sequelae of UWB exposure in unanesthetized rats without confounding factors such as postsurgical complications and anesthesia. In addition, the magnitude of response of each individual rat was adjusted with its own preexposure baseline in the present experiment. Furthermore, the cardiovascular responses studied in the present experiment were compared to the end points obtained from sham-exposed rats. Because of these differences in experimental approaches, it is difficult to compare the results obtained in these two laboratories. Lacking a comparable experiment on RF-induced delayed cardiovascular effects, the uniqueness of the UWB-induced delayed hypotension cannot be ascertained at the present time.

Arterial pressure is determined by the cardiac output and total peripheral resistance. Based on hemodynamics principles, the cause of a decrease in arterial pressure in the absence of heart rate alteration (therefore, no change in cardiac output) is a decrease in total peripheral resistance. Rats are known to possess a baroreceptor reflex mechanism, which serves to maintain a constant arterial pressure by increasing heart rate (therefore, cardiac output) if arterial pressure decreases or by decreasing the heart rate if arterial pressure increases (31). The absence of compensation by baroreceptor reflexes can result from baroreceptor reset, alterations in autonomic outflows or alterations in adrenergic receptors. The exact mechanism of the UWB-delayed hypotension is not known.

The Committee on Care and Use of Spontaneous Hypertensive Rats has recommended the use of an indirect blood (arterial) pressure measurement method for determining the arterial pressure in rats (22). Indirect arterial pressure measurement requires restraint. Restraint is a known psychogenic/

emotional stress. It is known to cause tachycardia and hypertension through sympathetic arousal in animals (3,5,38,40). The WKY rats used in the present experiment were acclimated to the holder to prevent novelty stress. Successful acclimation to novelty stress was indicated by the absence of reluctance to be placed in holder, absence of defecation and urination, and the reduction in number of restless episodes during the 1-h period in the holder. A recent study (5) has shown that the peak tachycardia response to restraint was not affected after 10 acclimation sessions. Acclimation, however, did accelerate the return of the tachycardia to baseline. Interpretation of results in the present study should include the possibility that the method of indirect blood pressure measurement is a "stress test" rather than a test procedure for the basal/resting cardiovascular functions. It is possible that demonstration of the UWB-induced hypotension requires additional "stimuli" associated with the indirect blood pressure measurement procedure.

Genetic predisposition appears to be an important factor in animal's response to stress. Sudakov (44) used a 30-h continuous restraint to differentiate three types of cardiovascular changes to restraint: resistant, adaptive, and sensitive. More than 50% of Wistar rats that did not exhibit heart rate and arterial pressure responses to the prolonged restraint were classified as resistant. Forty to 65% of Wistar, Vegh, August, and mixed strains that exhibited initial hypertension or hypotension followed by a return almost to the initial level at the end of 30-h restraint, were classified as adaptive. Approximately 30% of August and Vegh rats were classified as sensitive; they perished during the 30-h restraint bearing ECG T-wave changes and myocardial infarction. Genetic predisposition was also considered to be an important factor in the basal/resting cardiovascular functions, and the magnitude of cardiovascular responses to various emotional stresses (3,6,32,35, 44). The WKY rats appeared to be adaptive because the cardiovascular indices were different from those of Wistar rats, their parent strain, which is classified as resistant.

It has been reported that responses of heart rate and arterial pressures reached a plateau and remained reasonably constant after 10 min in the restrainer (3). In addition, studies in several animal species including rats demonstrated that arterial pressure and heart rate were characterized by a large spontaneous variability in an unanesthetized state (12). To limit the spontaneous variation and genetic predisposition, we have instituted strenuous measurement controls such as sources of animals, strain of rats, ambient temperature (26.5–27.5°C), time of day (0900–1200 h), duration in the test holder (between 20 and 60 min), and interval between testing (5 min). These controls were used to maintain a consistent level of stimulus during indirect arterial pressure measurement procedure. In addition, the average value of multiple measurements was used to represent the cardiovascular functions at each datum point for each animal to minimize sampling errors.

The heart rate and arterial pressure data obtained in rats bearing chronic arterial cannula (direct blood pressure measurement) in their home cages were accepted as stress-free measurements. Representative data for heart rate ranged between 279 ± 10 (mean ± SE, $n = 5$) and 345 ± 9 ($n = 6$) bpm and mean arterial pressure between 115 ± 3 ($n = 7$) and 122 ± 4 ($n = 6$) Torr in male adult cannulated WKY rats by various investigators (6,35,40). The ranges of the preexposure cardiovascular baseline of the present experiment were 332 ± 9 ($n = 5$) to 351 ± 8 ($n = 5$) bpm for heart rate and 120 ± 5 ($n = 5$) to 124 ± 5 ($n = 5$) Torr for mean arterial pressure. Therefore, these baseline values in the present study compared well to other reported ranges in the literature.

A decrease in blood pressure may not be a hypotension if the blood pressure is within the normal ranges of the species under study. The mean arterial pressures of the UWB-induced hypotension at the lowest point were 108 ± 7 ($n = 5$, 500 Hz) and 107 ± 8 ($n = 5$, 1,000 Hz) which qualify these values in the range of true hypotension instead of a decrease in arterial pressure in WKY rats. On the other hand, the range of stress-free mean arterial pressure of Wistar rats, the parent strain of WKY rats, was between 97 ± 2 ($n = 6$) and 112 ± 3 ($n = 10$) Torr (36,47). The stress-free mean arterial pressure of the Sprague–Dawley rats was also lower than that of WKY rats. The range reported were 85 ± 5 ($n = 4$) to 115 ± 3 ($n = 12$) Torr (3,12,20,43). The UWB-induced changes in arterial pressure in the present experiment was a mild form of hypotension in the WKY rats and should be asymptomatic if the mean arterial pressures of various strains of rats are considered.

In comparison to studies using narrow-band RF, the averaged exposure intensity of the present UWB exposure is relatively low—1.15 and 1.96 mW/cm^2. Conventional dosimetry methods, such as thermometry and calorimetry, lack of sensitivity to determine the specific absorption rate (SAR) from exposure to these low intensities. Equipment, instrumentation and techniques for measuring the internal electric field are not available. To estimate the whole-body average SAR, the relative power spectrum was computed from the padded data file, from 10 ns to 100 ns for a 10 MHz resolution of the UWB pulse by Mathcad's Maximum Entropy Method in the Numerical Recipes Function Pack. It appeared that the majority of power was below 200 MHz (Fig. 10, power spectrum, dashed line). The relative power (RP) spectrum was then convolved with the SAR vs. Frequency curve (11) in a spheroidal model of a medium rat for H polarization (Fig. 10, SAR, dotted line), also at 10 MHz intervals from 10 MHz to 10 GHz. The convoluted curve (Fig. 10, SAR × RP, solid line) represented the absorption spectrum of a rat exposed to the UWB pulse used in the present experiment. Ninety % of the spectrum power was between 10 MHz and 1.08 GHz. The maximum value of the absorption for a single discrete frequency was at 90 MHz, which indicated that SAR was less than 1.3 mW/kg/mW/cm^2 according to the value presented in the SAR curve. Integration of the convolved curve (SAR × RP) and normalized by the area under the RP curve yielded a whole-body SAR at 61.7 mW/kg/mW/cm^2 for the high UWB pulse. Analysis of the low UWB pulse (500 Hz) yielded a similar result in relative power spectrum, absorption spectrum, and whole-body SAR (60.9 mW/kg/mW/cm^2). For the 1,000 Hz group, total absorption in 6 min was, therefore, in the order of 43.5 J/kg or less, which is incapable of inducing any significant temperature increase in the animal. The mechanism of the UWB-induced hypotension is not known.

A widely known effect specific to pulsed microwave radiation with high peak power in the induced auditory sensation elicited by microwave pulses. This effect has been the subject of several reviews (7,34,39). It is generally accepted that the pulsed microwave-induced audible sound is generated from a thermoelastic expansion of cranial tissue and launches an acoustic wave that is detected by hair cells in the cochlea. For pulsed microwave with pulse width shorter than 30 μs, the microwave-induced auditory threshold was independent of temporal peak power density (or temporal peak specific absorption) and it is entirely dependent on the energy density of the microwave pulse or specific absorption (SA) per pulse. The auditory threshold SA per pulse has been determined in human volunteers, cat (19) and rats (9), 16, 10, to 12 and 0.9 to

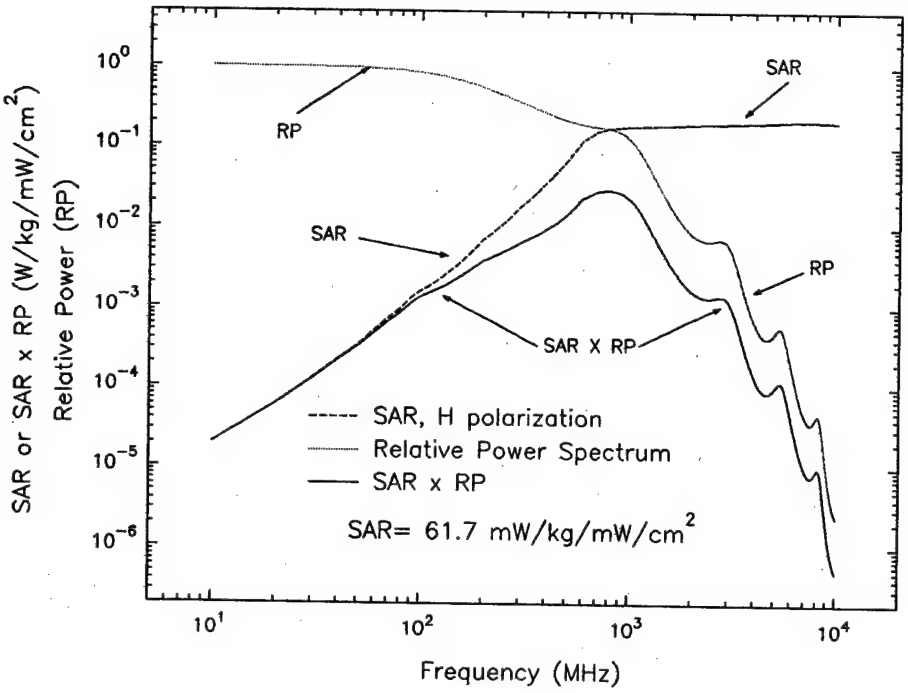

FIG. 10. Power spectrum and absorption spectrum of the UWB pulse.

1.8 mJ/kg, respectively. The temporal peak SAR of the high UWB pulse used in the present experiment was 2.09 kW/kg (duty cycle $\approx 10^{-6}$). Due to an extremely short pulse (pulse width = 1.03 ns), the SA per pulse from the high UWB pulses was around 2.15 μJ/kg, which was three orders of magnitude lower than the known auditory threshold in rats. Therefore, the UWB-induced delayed hypotension was not a sequela of an audiogenic effect.

The estimated threshold SAR (0.002 W/kg, high UWB pulse) for UWB-induced hypotension in rats was 200 times less than 0.4 W/kg, the basis for the IEEE C95.1-1991 safety standard in a controlled environment (21). The threshold peak electric field of the UWB pulses was less than the allowable peak electric field (100 kV/m) used in this standard. Hypotension is known to possess adverse health implications. The UWB-induced hypotension is a recent finding that has not been addressed during the promulgation of personnel protection guidelines. Further research on effect replication and dose–response characteristics are highly recommended.

ACKNOWLEDGEMENTS

This work was supported by the U.S. Army Medical Research and Matériel Command under the contract No. DAMD17-94-C-4069 with McKesson BioServices. The authors acknowledge the contributions of Jian-Zhong Bao for providing a transfer function for field measurement, Pamela J. Henry for technical assistance, D. Duane Cox for fabrication of the microenvironment chambers, and Bruce E. Stuck for valuable suggestions during the preparation of the manuscript. In conducting this research, the investigators adhered to the "Guide for the Care and Use of Laboratory Animals" and policies of the Walter Reed Army Institute of Research and U.S. Air Force Armstrong Laboratory. Disclaimer: The views, opinions and/or findings contained in this report are those of the authors and should not be construed as an official Department of the Army position, policy, and decision.

REFERENCES

1. Albanese, R.; Blaschak, J.; Median, R.; Penn, J.: Ultrashort electromagnetic signals: Biophysical questions, safety issues, and medical opportunities. Aviat. Space Environ. Med. 65:A116–A120; 1994.
2. Bao, J.-Z.; Lee, J. C.; Lu, S.-T.; Seaman, R. L.; Akyel, Y.: Analysis of ultra-wide-band pulses in a GTEM cell. In: Brandt, H. E., ed. Intense microwave pulses III, Proc. Spie 2557. Danvers: International Society for Optical Engineering; 1995:237–248.
3. Barron, B. A.; Van Loon, G. R.: Role of sympathoadrenomedullary system in cardiovascular response to stress in rats. J. Autonomi. Ner. Syst. 28:179–188; 1989.
4. Bunag, R. D.; Butterfield, J. B.: Tail-cuff blood pressure measurement without external preheating in awake rats. Hypertension 4:898–903; 1982.
5. Chen, X.; Herbert, J.: Regional changes in c-*fos* expression in the basal forebrain and brainstem during adaptation to repeated stress: Correlations with cardiovascular, hypothermic and endocrine responses. Neuroscience 64:675–685; 1995.
6. Chiueh, C. C.; Kopin, I. J.: Hyperresponsivity of spontaneously hypertensive rat to indirect measurement of blood pressure. Am. J. Physiol. H690–H695; 1978.
7. Chou, C. K.; Guy, A. W.; Galambos, R.: Auditory perception of radio-frequency electromagnetic fields. J. Acoust. Soc. Am. 71:1321–1334; 1982.
8. Chou, C.-K.; Guy, A. W.; Kunz, L. L.; Johnson, R. B.; Crowley, J. J.; Krupp, J. H.: Long-term, low-level microwave irradiation of rats. Bioelectromagnetics 13:469–496; 1992.
9. Chou, C.-K., Yee, K.-C.; Guy, A. W.: Auditory response in rats exposed to 2,450 MHz electromagnetic fields. Bioelectromagnetics 6:323–326; 1985.
10. D'Andrea, J. A.; Gandhi, O. P.; Lords, J. L.; Durney, C. H.; Astle, L.; Stensaas, L. J.; Schoenberg, A. A.: Physiological and behavioral effects of prolonged exposure to 915-MHz microwaves. J. Microwave Power 15:123–135; 1980.
11. Durney, C. H.; Massoudi, H.; Iskander, M. F.: Radiofrequency radiation dosimetry handbook, 4th ed. Brooks AFB: USAF

School of Aerospace Medicine Aerospace Medical Division (USAFSAM-TR-85-73) 1985:617.
12. Ferrari, A. U.; Dafffonchio, A.; Albergati, F.; Mancia, G.: Inverse relationship between heart rate and blood pressure variabilities in rats. Hypertension 10:533–537; 1987.
13. Foreman, S.; Holmes, C.; McManamon, V.; Wedding, W.: Psychological symptoms and intermittent hypertension following acute microwave exposure. J. Occupat. Med. 24:932–934; 1982.
14. Foster, P. R.: Antennas and UWB signals. In: Taylor, J. D., ed. Introduction to ultra-wideband radar systems. Boca Raton, FL: CRC Press; 1995:237–248.
15. Frei, M. R.; Jauchem, J. R.: Thermoregulatory response of rats exposed to 9.3-GHz microwave: A comparison of E and H orientation. Physiol Chem. Phys. Med. NMR 24:1–10; 1992.
16. Frei, M.; Jauchem, J.; Heinmets, F.: Physiological effects of 2.8 GHz radiofrequency radiation: A comparison of pulsed and continuous-wave radiation. J. Microwave Power 23:85–93; 1988.
17. Frei, M. R.; Jauchem, J. R.; Price, D. R.; Padilla, J. M.: Field orientation effects during 5.6-GHz radiofrequency irradiation of rats. Aviat. Space Environ. Med. 61:1125–1129; 1990.
18. Frei, M. R.; Ryan, K. L.; Berger, R. E.; Jauchem, J. R.: Sustained 35-GHz radiofrequency irradiation induces circulatory failume. Shock 4:289–293; 1995.
19. Guy, A. W.; Chou C. K.; Lin, J. C.: Microwave-induced acoustic effects in mammalian auditory systems and physical materials. Ann. NY Acad. Sci. 247:194–218; 1975.
20. Houdi, A. A.; Dowell, R. T.; Diana, J. N.: Cardiovascular responses to cigarette smoke exposure in restrained conscious rats. J. Pharmacol. Exp. Ther. 275:646–653; 1995.
21. Institute of Electrical and Electronics Engineers: IEEE C95.1 Standard for safety levels with respect to human exposure to radio frequency electromagnetic fields, 3 kHz to 300 GHz. New York: Institute of Electrical and Electronics Engineers; 1992.
22. Institute of Laboratory Resources: Committee on care and use of spontaneously hypertensive (SHR) rats. Spontaneously hypertensive (SHR) rats: Guidelines for breeding care and use, vol 19. Washington, DC: ILAR News; Natl. Acad. Sci.–Natl. Res. Council, 1976:G1–G20.
23. Jauchem, J. R.; Chang, K. S.; Frei, M. R.: Tolazoline decreases survival time during microwave-induced lethal heat stress in anesthetized rats. Proc. Soc. Exp. Biol. Med. 211:236–243; 1996.
24. Jauchem, J. R.; Frei, M. R.: Cardiovascular changes in unanesthetized and ketamine-anesthetized Sprague–Dawley rats exposed to 2.8-GHz radiofrequency radiation. Lab. Anim. Sci. 41:70–75; 1991.
25. Jauchem, J. R.; Frie, M. R.: Cardiorespiratory changes during microwave-induced lethal heat stress and β-adrenergic blockage. J. Appl. Physiol. 77:434–440; 1994.
26. Jauchem, J. R.; Frei, M. R.: High-peak power microwave pulses: Effects on heart rate and blood pressure in unanesthetized rats. Aviat. Space Environ. Med. 66:992–997; 1995.
27. Jauchem, J. R.; Frei, M. R.; Chang, K. H.; Berger, R. E.: Microwave-induced lethal heat stress: Effect of phentolamine, prazosin and metoprodol. Methods Find. Exp. Clin. Pharmacol. 17:241–248; 1995.
28. Jauchem, J. R.; Frei, M. R.; Heinmets, F.: Thermal bradycardia during radiofrequency irradiation. Physiol. Chem. Phys. Med. NMR 15:429–434; 1983.
29. Jauchem, J. R.; Frei, M. R.; Heinmets, F.: Heart rate changes due to 5.6 GHz radiofrequency radiation: Relation to average power density. Proc. Soc. Exp. Biol. Med. 177:383–387; 1984.
30. Jauchem, J. R.; Frei, M. R.; Padilla, J. M.: Thermal and physiologic responses in 1200-MHz radiofrequency radiation: Difference between exposure in E and H orientation. Proc. Soc. Exp. Biol. Med. 194:358–363; 1990.
31. Kirchheim, A. R.: Systemic arterial baroreceptor reflexes. Physiol. Rev. 56:100–176; 1976.
32. Lawer, J. E.; Barker, G. F.; Hubbard, J. W.; Schaub, R. G.: Effect of stress on blood pressure and cardiac pathology in rats with borderline hypertension. Hypertension 3:496–505; 1981.
33. Lee, J.; Bao, J.-Z.; Lu, S.-T.; Seaman, R. L.: An ultra-wide-band exposure system for studying biological effects. In: Abstract book of the seventeenth annual meeting of the bioelectromagnetics society. Fredrick: Bioelectromagnetics Society, Fredrick; 1995:160.
34. Lin, J. C.: Microwave auditory effects and applications. Springfield, IL: Charles C. Thomas; 1978.
35. Ludin, S.; Ricksten, S.-E.; Thoren, P.: Interaction between "mental stress" and baroreceptor reflexes concerning effects on heart rate, mean arterial pressure and renal sympathetic activity in conscious spontaneously hypertensive rats. Acta. Physiol. Scand. 120:273–281; 1984.
36. Mauck, G. W.; Smith, C. R.; Geddes, L. A.; Bourland, J. D.: The meaning of the point of maximum oscillations in cuff pressure in the indirect measurement of blood pressure—Part II. J. Biomech. Eng. 102:28–33; 1980.
37. Michaelson, S. M.; Lin, J. C.: Cardiovascular effects. In: Michaelson, S. M.; Lin, J. C., eds. Biological effects and health implications of radiofrequency radiation. New York: Plenum Press; 1987: 451–488.
38. Nagasaka, T.; Hirata, K.; Shibata, H.; Sugano, Y.: Metabolic and cardiovascular changes during physical restraint in rats. Jpn. J. Physiol. 30:799–803; 1980.
39. NCRP Report 86: Perception of RFEM fields. In: Biological effects and exposure criteria for radiofrequency fields. Bethesda, MD: National Research Council on Radiation Protection and Measurements; 1986:175–180.
40. Sakaguchi, A.; LeDoux, J. E.; Reis, D. J.: Sympathetic nerves and adrenal medulla: Contributions to cardiovascular-conditioned emotional responses in spontaneous hypertensive rats. Hypertension 5:728–738; 1983.
41. Sherry, C. J.; Blick, D. W.; Walters, T. W.; Brown, G. C.; Murph, M. R.: Lack of behavioral effects in non-human primates after exposure to ultrawideband electromagnetic radiation on the microwave frequency range. Radiat. Res. 143:93–97; 1995.
42. Sodeman, W. A., Jr.; Sodeman, W. A.: Systemic arterial pressure. In: Pathological physiology. Philadelphia, PA: W. B. Saunders Co.; 1974:177–205.
43. Sparrow, M. G.; Roggendorf, H.; Vogel, W. H.: Effect of ethanol on heart rate and blood pressure in nonstressed and stressed rats. Life Sci. 40:2551–2559; 1987.
44. Sudakov, K. V.: Organization of cardiovascular functions under experimental emotional stress. J. Autonom. Nerv. Syst. 4:165–180; 1981.
45. Taylor, J. D.: Ultra-wideband radar overview. In: Taylor, J. D., ed. Introduction to ultra-wideband radar systems. Boca Raton, FL: CRC Press; 1995:1–10.
46. Toler, J.; Popovic, V.; Bonasera, S.; Popovic, P.; Honeycutt, C.; Sgoutas, D.: Long-term study of 435 MHz radio-frequency radiation on blood-borne end points in cannulated rats, Part II: Methods, results and summary. J. Microwave Power 23:105–136; 1988.
47. Van Den Berg, D. T. W. M.; De Jong, W.; De Kloet, E. R.: Mineralocorticoid antagonist inhibits stress-induced blood pressure response after repeated daily warming. Am. J. Physiol. 267:E921–E9926; 1994.
48. Walters, T. J.; Mason, P. A.; Sherry, C. J.; Steffen, C.; Merritt, J. H.: No detectable bioeffects following acute exposure to high peak power ultra-wide band electromagnetic radiation in rats. Aviat. Space Environ. Med. 66:562–567; 1995.
49. Williams, R.; Webb, T.: Exposure to radiofrequency radiation from an aircraft radar unit. Aviat. Space Environ. Med. 51:1243–1244; 1980.
50. Yamakoshi, K.-I.; Kamiya, A.: Noninvasive measurement of arterial blood pressure and elastic properties using photoelectric plethysmography technique. Med. Prog. Technol. 12:123–143; 1987.
51. Yen, T. T.; Powell, C. E.; Pearson, D. V.: An indirect method of measuring the blood pressure of rats without heating. In: Spontaneous hypertension: Its pathogenesis and complications. Bethesda, MD: U.S. Public Health Service (DHEW Publication No. 77-1179); 1977:486–490.

Bioelectromagnetics 19:393–413 (1998)

Review Article

Current State and Implications of Research on Biological Effects of Millimeter Waves: A Review of the Literature

Andrei G. Pakhomov,[1]* Yahya Akyel,[1] Olga N. Pakhomova,[1] Bruce E. Stuck,[2] and Michael R. Murphy[3]

[1]McKesson BioServices, Brooks Air Force Base, San Antonio, Texas
[2]U.S. Army Medical Research Detachment of the Walter Reed Army Institute of Research, Brooks Air Force Base, San Antonio, Texas
[3]Directed Energy Bioeffects Division, Human Effectiveness Directorate, Air Force Research Laboratory, Brooks Air Force Base, San Antonio, Texas

In recent years, research into biological and medical effects of millimeter waves (MMW) has expanded greatly. This paper analyzes general trends in the area and briefly reviews the most significant publications, proceeding from cell-free systems, dosimetry, and spectroscopy issues through cultured cells and isolated organs to animals and humans. The studies reviewed demonstrate effects of low-intensity MMW (10 mW/cm^2 and less) on cell growth and proliferation, activity of enzymes, state of cell genetic apparatus, function of excitable membranes, peripheral receptors, and other biological systems. In animals and humans, local MMW exposure stimulated tissue repair and regeneration, alleviated stress reactions, and facilitated recovery in a wide range of diseases (MMW therapy). Many reported MMW effects could not be readily explained by temperature changes during irradiation. The paper outlines some problems and uncertainties in the MMW research area, identifies tasks for future studies, and discusses possible implications for development of exposure safety criteria and guidelines. Bioelectromagnetics 19:393–413, 1998. © 1998 Wiley-Liss, Inc.

Key words: electromagnetic fields; bioeffects; mm wave band; millimeter waves, review

INTRODUCTION

The term "millimeter waves" (MMW) refers to extremely high-frequency (30–300 GHz) electromagnetic oscillations. Coherent oscillations of this range are virtually absent from the natural electromagnetic environment. This absence might have had important consequences. First, living organisms could not have developed adaptation to MMW during the course of evolution on Earth. Second, some specific features of MMW radiation and the absence of external "noise" might have made this band convenient for communications within and between living cells [Golant, 1989; Betzky, 1992]. These arguments, although not adequately proven, are often used to explain the high sensitivity to MMW of biological subjects. Indeed, MMW have been reported to produce a variety of bioeffects, many of which are quite unexpected from a radiation penetrating less than 1 mm into biological tissues. A number of theoretical models have been set forth to explain peculiarities and primary mechanisms of MMW biological action [Fröhlich 1980, 1988; Golant, 1989; Grundler and Kaiser, 1992; Belyaev et al., 1993a; Kaiser, 1995].

One of the most remarkable events in contempo-

Contract grant sponsor: U.S. Army Medical Research and Materiel Command; Contract grant sponsor: U.S. Air Force Armstrong Laboratory; Contract grant number: U.S. Army contract DAMD17-94-C-4069 (to McKesson BioServices).

*Correspondence to: Andrei G. Pakhomov, USA-MCMR, McKesson BioServices, 8308 Hawks Road, Building 1168, Brooks Air Force Base, San Antonio, TX 78235-5324. E-mail: andrei.pakhomov@aloer.brooks.af.mil

Received for review 21 October 1997; final revision received 30 January 1998

© 1998 Wiley-Liss, Inc.

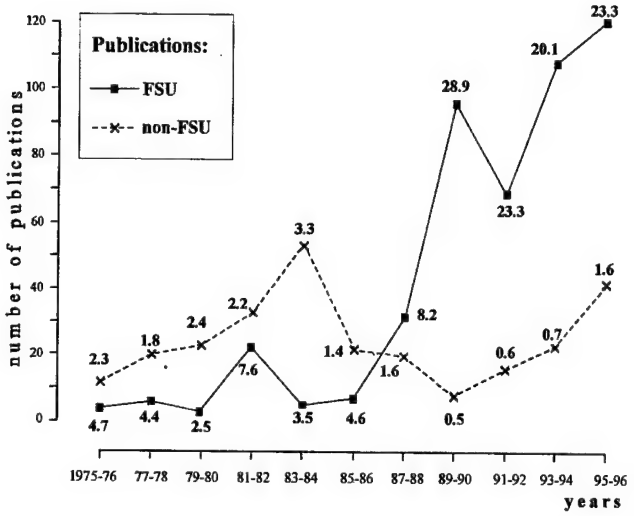

Fig. 1. Absolute numbers and percentages of publications on topics related to biological action of millimeter waves vs. years of publication. The graph is based on counts of citations in the EMF Database version 3.0, 1997. Studies by the former Soviet Union (FSU) scientists and by all other (non-FSU) were counted separately. Vertical scale is the number of published MMW studies per 2-year time intervals (abscissa). Numbers next to the datapoints indicate the weight (%) of MMW studies in the FSU and non-FSU bioelectromagnetic research (i.e., the percentage of MMW studies relative to the total number of studies included in the EMF database for the respective time periods).

rary electromagnetic biology is a surge in interest in MMW biological and medical effects in the countries of the former Soviet Union (FSU). A striking difference in the FSU and "non-FSU" research activity in this area can be seen from counts of related publications. For example, the EMF Database[1] version 3.0 (1997) lists a total of 463 FSU publications on MMW-related topics, and only 261 such publications from the rest of the world. Although these numbers should not be taken as exact (the Database includes most but certainly not all relevant citations), the situation in general is portrayed correctly and is particularly explicit in a historic perspective (Fig. 1). The non-FSU production reached its peak of 52 papers (including meeting abstracts) in 1983–1984, when MMW titles were 3.3% of all non-FSU publications in the bioelectromagnetics area. Then it gradually declined to only seven papers (0.5%) in 1989–1990. Concurrently, MMW research in the FSU expanded greatly: Both the count of publications (up to 120 in 1995–1996) and their portion in the FSU bioelectromagnetic research (20 to 30%) far exceeded these numbers for non-FSU publications.

Aside from the number of studies, there are important qualitative differences. Western (non-FSU) research was largely driven by concerns for public safety. However, safety issues occupy a relatively small portion of the FSU research, whereas far more studies are related to medical applications of MMW. Over 50 diseases and conditions have been claimed to be successfully treated with MMW alone or in combination with other means. Lebedeva and Betskii [1995] have reported more than a thousand MMW therapy centers in the FSU and over 3 million people who received this therapy. Naturally, the extensive medical use of MMW has stimulated basic research as well.

Nowadays, MMW technologies are increasingly being used in practical applications (e.g., wireless communication, traffic and military radar systems), making it imperative that bioeffects data be available for health hazard evaluation and restoring the interest to MMW biological research in the West. The number of non-FSU publications on this topic is again increasing. A specialized MMW session appeared at the 1996 meeting of the Bioelectromagnetics Society and the 1997 Second World Congress on Electricity and Magnetism in Biology and Medicine, and the first Infrared Lasers and MMW Workshop was held at Brooks Air Force Base, Texas in 1997. Unfortunately, the FSU research, a rich source of MMW bioeffects data, is not readily available in the West and is scarcely known by Western scientists.

The present paper is intended to fill in this gap by reviewing recent research in the MMW field, from molecules and cells to MMW therapy. We have analyzed over 300 original FSU publications and about 50 non-FSU papers and selected those which appeared more interesting and credible. This review is primarily focused on experimental and clinical findings reported during the last decade. Therefore, it includes only a few essential citations of earlier publications and does not cover such topics as theoretical modeling of possible interaction mechanisms. Interested readers should see other reviews for additional information [Fröchlich, 1980, 1988 (ed.); Gandhi, 1983; Grundler, 1983; Postow and Swicord, 1986; Belyaev, 1992].

PHYSICOCHEMICAL EFFECTS, MMW ABSORPTION, AND SPECTROSCOPY

A number of independent studies have shown specific MMW effects in the absence of living subjects,

[1]The EMF Database is produced by Information Ventures, Inc. (Philadelphia, PA) and covers topics related to biological effects of electromagnetic fields, from DC to submillimeter wavelengths. The Database contains over 20,000 citations of relevant publications from various sources, including peer-reviewed journals, books, proceedings, and meeting abstracts. Available citations are assimilated in the Database without any preselection based on the language, affiliation of the authors, or relevance to a particular EMF frequency range.

i.e., in solutions of biomolecules and even in pure water. Fesenko and Gluvstein [1995] analyzed MMW effects on periodic voltage oscillations during discharge of a water capacitor. The capacitor, which was a distilled water sample in a 1-mm capillary, was charged by 18 V, 1-ms-wide unipolar rectangular pulses. The capacitor discharged within 500–600 ms after a pulse. The discharge curve contained periodic voltage oscillations reaching 10–15 mV. The Fourier spectrum of these oscillations included two strong peaks, at 5.25 and 46.8 Hz, and these peaks did not change during at least 2 h of experimentation. The water sample was exposed at 36 GHz from an open-ended waveguide (7.2 × 3.4 mm cross-section). Irradiation at 50 μW output power greatly reduced the 46.8 Hz peak in 1 min and virtually eliminated it in 10 min; the 5.25 Hz peak shifted to 6.75 Hz. These changes showed little or no recovery within 2–60 min after cessation of a 10-min exposure. Irradiation at 5 mW output power produced similar changes, but, unexpectedly, was far less effective: the changes developed more slowly, and the original peaks were restored more quickly. Mechanisms of the phenomenon itself, its anomalous power sensitivity, and the long-lasting "memory" of water were not understood. The authors suggested that MMW-induced changes in water properties could underlie biological effects.

Direct MMW effects on pure water properties were also observed by holographic interferometry [Berezhinskii et al., 1993; Litvinov et al., 1994]. Refraction of light in fluid was determined from the width and number of interference bands formed by a He-Ne laser beam (630 nm) passing through the fluid and a referent beam. Irradiation of distilled water at 10 mW output power for 5–7 min caused no effect at 41.5 GHz, but decreased the number of the interference bands from 6 to 5 at 51.5 GHz; the distance between the bands increased 1.2 times. These changes developed faster and were more profound in a 2% human blood plasma solution. The effect reached saturation in 6–7 min and was completely reversible. Both theoretical calculations and direct measurements established that maximal MMW heating was about 1 °C. MMW-induced changes in the light refraction coefficient were almost an order of magnitude greater than produced by conventional heating by 1 °C and, therefore, were attributed to a specific effect of MMW.

Other properties of blood plasma, such as dielectric permittivity and absorption coefficient, could be altered by MMW irradiation as well [Belyakov et al., 1989]. Changes of only 0.05–0.5% in these parameters were measured but were well beyond the limits of the method used (0.01%). The sensitivity of plasma samples to particular radiation wavelengths strongly varied from one blood donor to another.

Khizhnyak and Ziskin [1996] analyzed peculiarities of MMW heating and convection phenomena in water solutions. Besides the most expected reaction (gradual temperature rise), irradiation could induce either temperature oscillations and a decrease in average temperature or a biphasic response in which the temperature initially rises and then decreases. These anomalous effects resulted from convective processes, i.e., the formation of a toroidal vortex. When the vortex became stable, the temperature decreased after the initial rise phase, although the irradiation was constantly maintained. The local temperature could decrease with increasing power density, and, in biological systems, this would appear as an effect opposite to heating. Probably, this phenomena could explain some of reported "nonthermal" MMW effects. If irradiation continued for a long time (30–40 min), the convection phenomena disappeared and could not be reintroduced, even after restoration of the initial temperature. This observation suggested that some irreversible process had occurred in the liquid, which resembles findings of the water "memory" cited above.

The supposed role of water as a primary target for MMW radiation motivated Zavizion et al. [1994] and Kudryashova et al. [1995] to study how MMW absorption at the wavelengths of 2.0, 5.84, and 7.12 mm is affected by the presence of other substances, namely α-amino acids (0.25–2.5 mol/l). Because MMW absorption by amino acid molecules is negligible, the absorption of solutions in most cases decreased proportionally to the amino acid concentration. This difference in absorption by pure water and solutions, called "absorption deficit," increased with increasing length of the hydrophobic radical in a series of homologous amino acids (glycine, alanine, GABA, valine). Paradoxically, the absorption deficit was negative for sarcosine at 5.84 mm and 7.12 mm and for glycine at all the wavelengths, meaning that these two amino acids can increase MMW absorption by water molecules.

A detailed theoretical analysis of MMW absorption in flat structures with high water content was performed by Ryakovskaya and Shtemler [1983]. The authors produced dependencies of the specific absorption rate (SAR) on the radiation frequency, temperature, thickness of the absorptive medium, and presence of dielectric layer(s) above and/or underneath. This work modeled most common biological setups, such as irradiation of cell suspensions in Petri dishes, cuvettes, etc. The wavelength in the medium, reflection coefficients, depth of penetration, and SAR at the surface of a semi-infinite absorptive medium were calculated for wavelengths from 1 to 10 mm, using 1-mm steps. For exam-

ple, the depth of penetration for 1- and 10-mm wavelengths at 20 °C equals 0.195 mm and 0.56 mm, respectively, and the respective surface SARs are 79.4 and 15.5 mW/cm^3 per 1 mW/cm^2. Exposure through a thin dielectric layer (e.g., bottom of a Petri dish) may decrease reflection and further increase SAR by up to 2.5 times. SAR in thin absorptive films (0.1–0.01 mm) increases greatly and may exceed SAR at the surface of a semi-infinite medium more than 10-fold. Furthermore, presence of a dielectric above or below the thin absorptive film may increase SAR in the film by as much as 20-fold. Apparently, the possibility of reaching very high SAR levels and of local heating cannot be underestimated, even for the incident power levels that are often regarded as nonthermal (0.1–1 mW/cm^2).

MMW EFFECTS AT SUBCELLULAR, CELLULAR, AND TISSUE LEVELS

Growth Rate Effects

Debates about resonance growth rate effects of MMW have been going on for over 20 years, and this problem was widely discussed in earlier reviews. In brief, Grundler and coauthors [1977, 1982, 1988] reported that the growth rate of the yeast *Saccharomyces cerevisiae* may be either increased by up to 15% or decreased by up to 29% by certain frequencies of MMW within a 41.8–42.0 GHz band. The effect was established by different methods, both in suspended cells and in monolayer. According to recent observations [Grundler and Kaiser, 1992], an effect of about the same magnitude is produced by field intensities from 5 pW/cm^2 to 10 mW/cm^2 (8 kHz modulation). The width of the resonance peaks increased with the intensity from about 5 MHz to 12–15 MHz over the above intensity range. However, thorough independent attempts to replicate these findings were not successful [Furia et al., 1986; Gos et al., 1997], suggesting that these MMW effects could be dependent on (or even produced by) some as yet unidentified and uncontrolled conditions.

Dardanoni and coauthors [1985] observed frequency- and modulation-dependent effects on the growth of yeast *Candida albicans.* MMW modulated at 1 kHz reduced the growth rate by about 15% at 72 GHz, but not at 71.8 or 72.2 GHz. A 3-h continuous wave (CW) irradiation at 72 GHz had the opposite effect, i.e., the growth rate increased by about 25% over the sham-irradiated control. Remarkable variability of the results was noted, which could be a result of cell subpopulations with different sensitivity.

Golant and coauthors [1994] reported that a marked synchronicity of periodic fluctuations in the growth rate and bud formation in the culture of *S. cerevisiae* can be induced by 0.03 mW/cm^2, 46 GHz irradiation for 50 min. This effect was claimed to persist for over 20 cell generations. Periodicity of bud formation was observed in control samples as well, but it was less pronounced and had a different time duration (60 min vs. 80 min after MMW exposure).

Synchronizing effects of MMW were also observed in higher plant specimens (Shestopalova et al., 1995). Barley seeds were exposed for 20 min at 0.1 mW/cm^2 (61.5 GHz), and then the exposed and control seeds (150 seeds per group) were put into an incubator for sprouting. The incubator was maintained at either 28 °C or 8 °C. Cytologic examination established that the degree of synchronization of cell division in MMW-exposed sprouts increased by 36% (28 °C) and 50% (8 °C) over the respective control plants.

Levina et al. [1989] studied MMW effects on the development of a protozoan *Spirostum sp.* cell population. The population was begun in a saline medium with beer yeast (550 mg/l) as food by adding of 5–6 protozoan cells/ml. The culture was exposed once for 30 min at 1.5 mW/cm^2 (7.1-mm wavelength), between days 2 and 11 of growth. Unexposed cultures grew exponentially up to a density of 100 cells/ml on day 11, then rapidly died without reaching stationary phase, obviously due to poisoning by waste products. Exposures on days 2, 4, or 7 caused the populations to enter the stationary phase on or around day 9. Exposures on day 9 or 11 postponed the population death by 5 days, and the final cell content increased to 115–135 cells/ml on day 14. Irradiation on day 2 also increased the proliferation rate, and by day 7 the cell density was nearly twice as high as in control samples. In another series of experiments, the population began with an initial concentration of 1-2 protozoan cells/ml and stabilized in 8–10 days at 12–13 cells/ml. In these cultures, MMW exposure suppressed proliferation, and the final cell density was only 6–10 cells/ml. This study indicated that irradiation affects the population's own growth control mechanisms and that the effect depends on the stage and other particulars of the population development.

Exposure for 30 min at 2.2 mW/cm^2, 7.1-mm wavelength enhanced the growth of a blue-green algae *Spirulina platensis* by 50% [Tambiev et al., 1989], whereas 8.34-mm wavelength produced no changes compared with sham control. The alga growth rate more than doubled when a 30-min irradiation at 7.1 mm was immediately followed by exposure to high-peak power microwave pulses (15 pulses, 10-ns pulse width, 6-min pause, 3-cm wavelength, 200 kW/cm^2 peak incident power density). Concurrently, photosynthetic oxygen evolution increased about 1.5 times. The

observed stimulatory effects are of considerable promise in biotechnology, in which *S. platensis* is used for production of food protein and biologically active compounds.

Other publications by the same authors [Tambiev and Kirikova, 1992] and independent investigators [Rebrova, 1992; Shub et al., 1995] presented MMW effects on the growth rate of several species of bacteria, Cyanobacteria, algae, yeasts, and higher plants (fennel, lettuce, tomato). For example, in the yeasts *S. cerevisiae* and *S. carlsbergensis* MMW shortened the phases of culture growth 2.3–6.0 times and could increase the biomass production rate by up to 253%. Effects on *Escherichia coli* growth could be either stimulatory or inhibitory, depending on the wavelength (6.0- to 6.7-mm band, $\leq$ 1 mW/cm^2 for 30 min). However, all three papers were summaries of the authors' multiyear experiences with studying these and other MMW effects and did not provide enough detail for full evaluation or possible replication.

Chromosome Alterations and Genetic Effects of MMW

Absence of mutagenic or recombinagenic effects of MMW radiation was clearly demonstrated in the late 1970s [Dardalhon et al., 1979, 1981], and later investigations were consistent with this conclusion. At the same time, a number of studies indicated that MMW could affect the fine chromosome structure and function, cell tolerance to standard mutagens, and lesion repairs.

Best known is the recent work by Belyaev and coauthors [1993a, b, 1994, 1996], who discovered sharp frequency resonances by using an anomalous viscosity time dependence (AVTD) technique. This technique is supposed to reflect fine changes in DNA conformation and DNA-protein bonds. At a resonance frequency, biological changes could be produced by field intensities as low as 10^{-19} W/cm^2. The magnitude of changes gradually increased with the field intensity and reached a plateau between 10^{-17} and 10^{-8} W/cm^2, depending on cell density in exposed samples. Resonance peaks for *E. coli* cells were found at 51.76 and 41.34 GHz; these values decreased in strains with increased haploid genome length. These results pointed to the chromosomal DNA as a target for resonance interaction between living cells and MMW. The width of the resonances increased from units to tens of megahertz by increasing the incident power, and this dependence is in notable agreement with the one reported for cell growth rate effects [Grundler and Kaiser, 1992].

However, the AVTD test is not a conventional technique in cell biology. Interpretation of AVTD data is uncertain and functional consequences of AVTD changes have not yet been convincingly defined. A discussion is continuing as to whether super-low radiation intensities in these studies were measured correctly [Osepchuk and Petersen, 1997a, 1997b; and a reply by Belyaev et al., 1997]. Supposedly, some power at a harmonic frequency might be transmitted to the sample despite large attenuation at the fundamental frequency. Whether this was the case or not, consistent observations of resonance effects represent an important finding, which requires understanding and independent replication.

MMW-induced visible changes in giant chromosomes of salivary glands of the midge *Acricotopus lucidus* [Kremer et al., 1988]. A certain puff, the Balbiani ring BR1 in the chromosome II, reduced in size after irradiation at 67.2 $\pm$ 0.1 GHz or 68.2 $\pm$ 0.1 GHz (5 mW/cm^2), and this effect seemed to be unrelated to heating. Numerous alterations in the giant chromosome morphology were also independently found in *Chironomus plumosus* (Diptera) after a 15-min exposure at 1 mW/cm^2 [Brill' et al., 1993].

Exposure of ultraviolet (UV)-treated *E. coli* culture to MMW at 61 $\pm$ 2.1 GHz, 1 mW/cm^2 increased cell survival [Rojavin and Ziskin, 1995]. The most likely mechanism of this effect was either direct or indirect activation of the dark repair system. No survival effects were found if the sequence of exposures was reversed, i.e., when UV irradiation was performed immediately after a 10- to 30-min MMW exposure.

Genetic effects of 61.02-61.42 GHz radiations were studied in the D7 strain of the yeast *S. cerevisiae* [Pakhomova et al., 1997]. MMW exposures lasted for 30 min at 0.13 mW/cm^2, and were followed in 60 min by a 100 J/m^2 dose of 254 nm UV radiation. Compared with the parallel control, the MMW pretreatment did not affect cell survival or the rate of reverse mutations, but significantly increased the incidence of gene conversions. Sham-exposed samples showed no differences from respective parallel control groups. The data suggested that MMW did not alter the UV-induced mutagenesis, but might facilitate UV-induced recombinagenic processes. A thermal mechanism for this effect was improbable, but could not be ruled out entirely.

Excitable Tissues and Membranes

Along with the genetic apparatus, the cell membrane is another site suspected to be a primary target for MMW radiation. Many of the works discussed below established profound MMW effects; however, only a few attempts have been made to replicate them.

Brovkovich et al. [1991] reported that 61 GHz, 4 mW/cm^2 radiation significantly activates the Ca^{++} pump in the sarcoplasmic reticulum (SR) of skeletal and heart muscles of the rat. The rate of Ca^{++} uptake

by SR membranes was measured by an ion-selective electrode in an ATP-containing medium. An intermittent MMW treatment (5-min exposure, 15-min pause, 3 cycles) of skeletal muscle SR increased the rate of Ca^{++} uptake by 23%, and this increased level was retained for 1 h after the exposure. Uninterrupted MMW irradiation had no effect in 10 min, but increased Ca^{++} uptake by 27% in 20 min; and the effect reached maximum (48%) in 40 min. In heart muscle SR, even a 5-min exposure enhanced Ca^{++} uptake by 18%.

Geletyuk and coauthors [1995] used patch-clamp (inside-out mode) to study 42.25 GHz radiation effects on single Ca^{++}-activated K^+ channels in cultured kidney cells (Vero). Exposure for 20–30 min at 0.1 mW/cm^2, CW, greatly modified the activation characteristics of the channels, particularly the open state probability. The field increased the activity of channels with a low initial activity and inhibited channels with initially high activity. In a subsequent study [Fesenko et al., 1995], these effects were reproduced without direct irradiation of the membrane, just by applying bathing solution pre-exposed for 30 min at 2 mW/cm^2, 42.25 GHz. Irradiation of the solution did not alter its pH or Ca^{++} concentration, and the nature of the MMW-introduced channel-modifying properties of the solution is not understood. The solution retained its biological efficacy for at least 10-20 min after cessation of the exposure.

Kataev and coauthors [1993] used a voltage clamp to study membrane currents in giant alga cells (*Nitellopsis obtusa*, Characea). Irradiation for 30–60 min at 41 GHz, 5 mW/cm^2 suppressed the chloride current to zero with no recovery for 10–14 h. Marked inhibitory effects were also found at 50 and 71 GHz, whereas most of other frequencies tested in the 38–78 GHz range enhanced the chloride current up to 200–400% (49, 70, 76 GHz). This activation was reversible, and recovery to the initial value took 30–40 min. Moreover, "activating" frequencies could restore the chloride current after its complete and normally irreversible suppression by "inhibitory" frequencies. MMW heating did not exceed 1 °C, and neither activating nor inhibitory effects were related to or could be explained by it. Calcium current also changed during irradiation, but this effect was not frequency dependent and could be adequately explained by heating. The authors noted that algae collected in the fall of 1990 and stored over the winter had entirely lost MMW sensitivity by February 1991.

Experiments with artificial bilayer membranes and snail neurons did not reveal any frequency-specific effects of MMW [Alekseev and Ziskin, 1995; Alekseev et al., 1997]. The capacitance of artificial membranes, ionic channel currents, and the transport of tetraphenylboron anions changed proportionally to MMW heating, regardless of the frequency (53–78 GHz range) or modulation used. Irradiation of snail neurons at 75 GHz (600–4200 W/kg) produced biphasic alterations of their firing rate, which were similar to those caused by equivalent conventional heating.

Burachas and Mascoliunas [1989] studied MMW effects on the compound action potential (CAP) in isolated frog sciatic nerve. CAP decreased exponentially and fell 10-fold within 50-110 min of exposure at 77.7 GHz, 10 mW/cm^2. CAP restored entirely soon after the exposure, but the nerve became far more sensitive to MMW: CAP suppression due to the next exposures became increasingly steep and finally took only 10–15 min. This sensitized state persisted for at least 16 h. In addition to this "slow" response, switching the field on increased CAP amplitude instantly by 5–7%, and switching it off caused the opposite reaction. These effects were found in "winter" frogs, but weakened and finally disappeared in spring.

A different effect in the isolated frog nerve was described by Chernyakov and coauthors [1989]. The exposures lasted for 2-3 h, either with a regular frequency change by 1 GHz every 8–9 min or with a random frequency change every 1-4 min (53–78 GHz band, 0.1-0.2 mW/cm^2). The latter regimen induced an abrupt CAP "rearrangement" in 11 of 12 exposed preparations: the position, magnitude, and polarity of CAP peaks (the initial CAP was polyphasic) drastically changed in an unforeseeable manner. The other exposure regimen altered the amplitude and duration of late CAP components in 30-40 min. The authors supposed that MMW increased CAP conduction velocity in fast nerve fibers and decreased it in slow fibers.

Neither of these effects on CAP conduction was observed by Pakhomov et al. [1997a]. Irradiation for 10–60 min, either at various constant frequencies or with a stepwise frequency change did not alter CAP at 0.2–1 mW/cm^2. At 2.0–2.8 mW/cm^2, it produced minor changes, which were independent from the frequency and matched the effect of heating. At the same time, a different MMW effect was revealed using a high-rate nerve stimulation test. MMW attenuated the stimulation-induced CAP decrease in a frequency-dependent manner. The effect reached maximum at 41.34 GHz [Pakhomov, 1997b], and at this frequency the magnitude of changes was the same (20–25%) at 0.02, 0.1, and 2.6 mW/cm^2 [Pakhomov et al., 1997c]. A 100 MHz deviation from 41.34 GHz (to 41.24 or 41.44 GHz) reduced the effect about twofold, and a 200 MHz deviation eliminated it. The field distribution over the preparation at these frequencies was virtually the same, so different MMW absorption or heating patterns could not account for the frequency specificity

of the effect. Interestingly, the most effective frequency in these experiments happened to be the same as the resonance frequency in the cell genome studies of Belyaev et al. [1993a].

Low-intensity MMW radiation effectively changed membrane functions in striated muscle and cardiac pacemaker cells [Chernyakov et al., 1989]. Exposure at 0.1-0.15 mW/cm^2 for 90 s or less (frequencies between 54 and 78 GHz) decelerated the natural loss of transmembrane potential in myocytes, or even increased it by 5–20 mV. Exposure reduced the overshoot voltage, action potential amplitude, and conduction velocity. This effect was observed in 80% of exposures, with no clear dependence on the radiation frequency. MMW influence on pacemaker activity was analyzed in 990 experiments with 80 tissue strip preparations from the frog heart sinoatrial area. In most cases, irradiation immediately decreased the interspike interval, often in less than 2 s. The maximal effect was reached within 30 s. The changes linearly increased with the incident power increase in the range from 20–30 to 500 μW/cm^2. The frequency dependence of the effect was individual, with at least four maximums in the studied range. Maximal preparation heating after a 2 s exposure at 1 mW/cm^2 was calculated as 0.005 °C. With a physiologic response latency of less than 2 s, this response could not be thermal. Exposure to infrared light (4 to 6 μm wavelength) often evoked the same effects as MMW, but the threshold intensity was hundreds of times greater.

In other experiments described in the same paper, low-intensity MMW synchronized firing of urinary bladder mechanoreceptors, suppressed and altered the T-peak on electrocardiography of in situ exposed myocardium, enhanced respiration, altered membrane calcium binding, and reduced the contractility of cardiomyocytes. Summarizing their results, the authors stated that the dependence of bioeffects upon radiation frequency is not monotonic. Peaks of this dependence are individual and are not fixed at particular frequencies, and they become smoother with increased complexity of physiologic control mechanisms involved.

Other In Vitro Effects

Bulgakova et al. [1996] studied how MMW exposure of *Staphylococcus aureus* affects its sensitivity to antibiotics with different mechanisms of action. Irradiations lasted from 1.5 to 60 min (54 or 42.195 GHz, or 66-78 GHz band with 1 GHz steps, 10 mW/cm^2). MMW heating did not exceed 1.5 °C. Over 1000 experiments with 14 antibiotics were completed. A difference in the growth of exposed cells compared with control cells was most often observed with polypeptide antibiotics, which affect the cell membrane (gramicidin group), but not with inhibitors of cell wall synthesis (penicillin group), of DNA-dependent RNA synthesis (actinomycin D), of the RNA polymerase and RNA synthesis (heliomycin), or protein biosynthesis inhibitors (neomycin, tetracycline, etc.). Irradiation either increased or decreased the antibiotic sensitivity, and the probability of these opposite effects depended on the antibiotic concentration. MMW could induce sensitivity to subbactericidal antibiotic concentrations, which normally would not affect the cell growth. Within studied limits, the effect showed no clear dependence on the radiation intensity or frequency. The data suggested that some membrane processes might be a target for the MMW effect. The authors also noted that MMW treatment can reveal (or even induce) the heterogeneity of the sensitivity of a cell population to certain antibiotics.

Rebrova [1992] reviewed various MMW effects on cell metabolism, synthesis of enzymes, and other processes in unicellular organisms, e.g., frequency-dependent enhancement and suppression of colicin synthesis in *E. coli,* stimulation of synthesis of fibrinolytic enzymes in *Bacillus firmus,* increasing of the contents of peptides, DNA, and RNA in *B. mucilaginous,* and suppression of tolerance to antibiotics in *S. aureus.* The maximal magnitude of MMW-induced changes ranged from 20 to 90%, depending on the wavelength and the initial condition of the strain. In contrast to bacteria, reproduction rate and biosynthetic properties of fungi *Aspergillus sp., Endomyces fibuliger,* and *Dacthilyum dendraides* changed only after repeated exposures (10 times). Certain MMW frequencies increased alpha amylase activity in *A. orizae* by 67% and suppressed glucoamylase by 30%; others had the opposite effect. In yeast species, MMW accelerated maltose fermentation by 73%, whereas synthesis of diacetil and aldehydes decreased by 20%. New biosynthetic culture properties introduced by exposure persisted in at least 100 (*S. carlsbergensis*) and 300 (*S. cerevisiae*) cell generations. The selective stimulation of production of some enzymes and suppression of others is promising for biotechnology.

An unusual "double-resonance" effect of MMW was described by Gapeev et al. [1994]. Spontaneous locomotor activity of the protozoan *Paramecium caudatum* was not affected by irradiation unless both the radiation frequency and modulation were tuned to "resonance" values. These values were 42.25 GHz and 0.0956 Hz, respectively (0.5 duty ratio). At these parameters, the threshold field intensity was about 0.02 mW/cm^2. The effect reached maximum (about 20%) at 0.1 mW/cm^2, and remained at this level at intensities up to 50 mW/cm^2, despite increasing heat production (0.1–0.2 °C at 5 mW/cm^2). CW irradiation

or modulation rates of 16, 8, 1, 0.5, 0.25, or 0.05 Hz produced no effect, regardless of the field intensity or heating. At the resonance modulation frequency, a shift of the carrying frequency to 42.0 or 42.5 GHz eliminated the reaction. No effects were observed with heating of samples by other means, e.g., infrared light modulated at 0.0956 Hz. Locomotor activity changes similar to the MMW effect could be evoked by increasing the level of intracellular calcium, pointing to a possible mechanism of the MMW action. However, reasons for the "double-resonance" dependence of this MMW effect remain unclear.

More reported MMW effects in various in vitro systems are summarized in Table 1.

ANIMAL AND HUMAN STUDIES

MMW Effects on Peripheral Receptors

Abundant evidence for MMW effects in specimens directly exposed in vitro neither explains nor predicts possible effects at the organism level. It is clearly understood that MMW penetration into biological tissues is rather shallow, and any primary response must occur in skin or subcutaneous structures, or at the eye surface. This primary response would then mediate all subsequent reactions by means of neural and/or humoral pathways. The nature of the primary response and consequent events has been a subject of intense speculation [Golant, 1989; Mikhno and Novikov, 1992; Rodshtadt, 1993], but there is little experimental proof. As a matter of fact, the link between cellular and organismal effects is missing and remains the least understood area in the MMW field. However, several studies have suggested that peripheral receptors and afferent nerve signaling could be involved in the whole organism's response to a local MMW exposure.

Akoev et al. [1992] studied the response of electroreceptor Lorencini capsules in anesthetized rays. Spontaneous firing in the afferent nerve fiber from the capsule could be either enhanced or inhibited by MMW irradiation (33–55 GHz, CW). The most sensitive receptors increased their firing rate at intensities of 1–4 mW/cm^2, which produced less than 0.1 °C temperature rise. Intensities of 10 mW/cm^2 and higher could evoke a delayed inhibition of firing, so the response became biphasic. The authors emphasized that what they observed was not merely a bioeffect of MMW, but was indeed a specific response of the receptor.

Chernyakov and coauthors [1989] were able to induce heart rate changes in anesthetized frogs by MMW irradiation of remote skin areas. The latency of the changes was about 1 min. Complete denervation of the heart did not prevent the reaction, but decreased its probability. The data suggested a reflex mechanism of the MMW action, maybe involving certain peripheral receptors.

These data are in agreement with later findings by Potekhina et al. [1992]. Certain frequencies from the 53–78 GHz band (CW) effectively changed the natural heart rate variability in anesthetized rats. The radiation was applied to the upper thoracic vertebrae for 20 min at 10 mW/cm^2 or less. The frequencies of 55 and 73 GHz caused pronounced arrhythmia: the variation coefficient of the R-R interval increased four to five times. Exposure at 61 or 75 GHz had no effect, and other tested frequencies caused intermediate changes. Skin and whole-body temperature of the animals remained unchanged. Similar frequency dependence was observed in additional experiments with 3-h exposures; however, about 25% of experiments were interrupted because of sudden animal death that occurred after 2.5 h of exposure at 51, 61, and 73 GHz. A possible role for receptor structures and neural pathways in the development of the MMW-induced arrhythmia was discussed.

Sazonov et al. [1995] compared alterations of spontaneous afferent firing in the bladder nerve in frogs when the bladder was exposed to infrared radiation and to MMW (42.19 ± 0.15 GHz, 10 mW/cm^2). The infrared intensity was adjusted to produce the same heating as MMW. In control experiments, the firing rate was stable for at least 1–1.5 h, but MMW increased it instantly from 30.9 to 32 spikes/s ($P < .05$) and to 48.3 spikes/s ($P < .01$) by the end of a 20-min exposure. Immediately after cessation of irradiation, the rate fell to 35.8 spikes/s, which was still significantly higher ($P < .05$) than before the treatment. Infrared irradiation did not cause statistically significant changes. This difference was interpreted as a proof of a specific (nonthermal) MMW effect, which might in principle take place in skin receptors as well.

In contrast, infrared light and MMW at equivalent intensities produced similar effects on the firing rate of crayfish stretch receptor [Khramov et al., 1991]. Changes were proportional to the average incident power, regardless of modulation or radiation frequency, and were regarded as merely thermal.

The possibility of modifying the peripheral receptor function by low-intensity MMW has been demonstrated directly by Enin and coauthors [1992]. An electrodynamic mechanostimulator was used to apply mechanical stimuli (50-ms duration, 1 to 2 mm amplitude) to individual skin mechanoreceptors on the sole of the hind limb of anesthetized rats. Responses to the stimuli were recorded from afferent fibers in the isolated and cut peripheral end of the tibial nerve. The sole was exposed to 55, 61, or 73 GHz radiation at

TABLE 1. Other In Vitro Effects of Millimeter Wave Radiation

Citation	End points/findings	Exposure conditions	Details
1	2	3	4
Berzhanskaya et al., 1995	Suppression of bioluminescence of *Photobacterium leiognathi*	36.2 to 55.9 GHz 1.3 to 48.0 μW/cm^2 MMW heating <0.1 °C	The effect reached maximum within 10 min, with a gradual recovery after the cessation of exposure, and could be repeated many times in the same cell culture. The maximal effect (16–18% decrease) was caused by the lower frequencies. At 36.2 GHz, 1.3 and 13 μW/cm^2 intensities produced virtually the same effect.
Mudrick et al., 1995	Changes in the intensity of $BaSO_4$-induced flash of chemoluminescence in the presence of luminol in human leukocytes	42.19, 46.84, or 53.53 GHz 1 mW/cm^2 30 min	The effect depended on the frequency, and the dependence was individual for blood samples from each particular donor. The maximal observed effect was a twofold flash enhancement ($P < 0.01$) at 42.19 GHz.
Gapeev et al., 1996	Inhibition of the luminol-dependent chemoluminescence of neutrophils activated by opsonized zymosan	41.8 to 42.05 GHz 0.15–0.25 mW/cm^2	In the near zone of the irradiator, the effect depended on the radiation frequency in a quasiresonance manner, whereas in the far field it was independent of the frequency.
Logani and Ziskin, 1996	No MMW effect on lipid peroxidation in phosphatidylcholine liposomes	53.6, 61.2, or 78.2 GHz 10, 1, and 500 mW/cm^2, respectively, 30 or 60 min	MMW did not increase the level of lipid peroxidation under any of the experimental conditions (in liposomes loaded or not loaded with melanin, or in the presence or absence of iron (III) adenosine diphosphate).
Roshchupkin et al., 1994, 1996	MMW changed aggregation of thymocytes with erythrocytes in a dose- and frequency-dependent manner	46.12 or 46.19 GHz either: (1) at 0.35 mW/cm^2, 0 to 120 min, or: (2) 0.05 to 0.5 mW/cm^2, 90 min	(1) The threshold was 60 min for both frequencies, increasing the number of aggregates to 115–140% of the parallel control. The effect of 46.12 GHz did not change when the exposure duration was further increased to 90 or 120 min, whereas the effect of 46.19 GHz fell to 80–90%. (2) The threshold was 0.25–0.35 mW/cm^2. The effect of 46.19 GHz stayed at 110–120% at 0.35 and 0.5 mW/cm^2, whereas the effect of 46.12 GHz grew linearly to 170% at 0.5 mW/cm^2.
Shub et al., 1995	Changes in transmisxsivity of R-plasmids in various strains of *E. coli* and *S. aureus*	6.0- to 6.7-mm band, <1 mW/cm^2 60 min	A number of biologically active frequencies affected the transmissivity of R-plasmids, either decreasing or increasing plasmid- and chromosome-dependent resistivity to antibiotics. Irradiation for 60 min had a bacteriostatic effect, which was not related to the activity of the recA-dependent DNA repair. Cells carrying Iα, I*j*, N, and E plasmids appeared to be protected from the antibacterial effect of MMW.
Kazbekov and Vyacheslavov, 1987	No nonthermal effects in prototrophic, thymidine-deficient, and tryptophan-requiring strains of *E. coli* and *B. subtilis*	6- to 7.8-mm wavelengths 5 mW/cm^2	MMW either had no effect on studied parameters (thymine and thymidine uptake, potassium leakage, hydrogen ion release, uptake of DNA, etc.), or produced the same changes as conventional heating by 1–2 °C.

0.75, 2.90, or 7.81 mW/cm^2, respectively. Exposure lasted for 35 min and caused no changes in the skin temperature (0.01 °C accuracy). MMW did not excite mechanoreceptors, but markedly altered the threshold and latency of their response to mechanic stimuli. In some receptors, the threshold gradually increased, up to 180% of the initial value. In others, the threshold initially decreased by 8–12%, recovered within 10 min, and increased to 160% by the 25th min of irradiation. After that, the receptors became completely inactive and no longer responded to mechanical stimuli. The receptor response latency under exposure could fall to 70% or rise to 120%; the changes could also be biphasic. The MMW-induced changes were maximum at 73 GHz, intermediate at 55 GHz, and minimum at 61 GHz, despite that the incident power at 61 GHz was 4-fold greater than at 55 GHz. The authors supposed that sensations reported by patients under MMW therapy (vibration, warmth, numbness, etc.) may result from functional disturbances and blockage of receptors.

The ability of humans to detect weak MMW has also been repeatedly established under double-blind conditions [Lebedeva, 1993, 1995; Kotrovskaia, 1994]. An examinee was situated in an isolated room and had no contact with the experimenter. The outer surface of the hand was exposed 20 times, for 1 min each. Exposures were separated by 1 min intervals and randomized with sham exposures. The start and end of each irradiation and placebo were accompanied by sound clicks. The examinee had to push a button when he felt the field. Neither examinee nor researcher knew the sequence of exposures and sham exposures; correct and incorrect reactions were recorded automatically. Field perception was characterized by the reaction reliability (the percent of MMW exposures detected) and the false alarms level (the percentage of sham exposures erroneously detected). An examinee was regarded as capable of detecting the field if the reaction reliability consistently and statistically significantly exceeded the false alarm level. With different frequencies (37.7, 42.25, 53.57 GHz), intensities (from 5 to 15 mW/cm^2) and bandwidths, the radiation was detected by 30 to 80% of examinees. Interestingly, 37.7 GHz radiation at 15 mW/cm^2 was detected by far fewer people than 42.25 GHz at 5 mW/cm^2. The reaction latency was usually between 40 and 50 s. It was speculated that MMW perception could involve some types of mechanoreceptors and nociceptors.

Teratogenic effects of MMW

The only study of MMW teratogenic effects was performed in *Drosophila* flies by Belyaev et al. [1990]. Embryos of the blastula and gastrula stages (2.5–3 h after laying) and pupas at the stage of imago tissue formation were exposed in a waveguide at 46.35, 46.42, or 46.50 GHz, for 4–4.5 h at 0.1 mW/cm^2, followed by incubation at 25 °C. Irradiation at 46.35 GHz, but not at 46.42 or 46.50 GHz, caused marked effects. Exposure of pupas increased incidence of morphologic abnormalities 2-4.5 times ($P < .05$), but did not influence imago survival. Exposure of embryos decreased survival by about 30% ($P < .05$) and enhanced morphologic abnormalities, but this effect was rather variable. Supposedly, MMW disturbed DNA-protein interactions that determine the realization of the ontogenetic program.

High-Power MMW Effects

Over the past several years, physiologic effects of high levels of MMW radiation have been intensively studied by Frei et al. [1995], Frei and Ryan [1997], and Ryan et al. [1996, 1997]. In ketamine anesthetized rats, exposure to 35 GHz, 75 mW/cm^2 radiation (12–13 W/kg whole body SAR) increased the subcutaneous temperature by 0.25 °C/min and the colonic temperature by 0.08 °C/min. Concurrently with the hyperthermia, mean arterial blood pressure first increased slightly and then fell until the point of death. Hypotension was accompanied by vasodilation in the mesenteric vascular bed, similar to what occurs in heat stroke induced by environmental heating. However, the onset of vasodilation and hypotension occurred at much lower colonic temperatures (< 37.5 °C vs. > 41.5 °C). The lethal effect became irreversible when the mean arterial pressure fell to 75 mm Hg, even if the exposure was discontinued. Most intriguing, pathologic examination of the skin of lethally exposed animals revealed no significant thermal damage or full-thickness burn, and cardiovascular responses did not mimic those observed in traditional burn models. Searching for physiologic mechanisms mediating the hypotensive response, the authors established that nitric oxide, platelet-activating factor, and histamine did not contribute to it. Exposure of rats at 94 GHz at a similar SAR produced a comparable pattern of heating and cardiovascular responses.

Experimental MMW Therapy: Animal Studies

Except those cited above, virtually all animal studies on MMW effects have been related to various issues of MMW therapy, such as stress relief, wound healing, tissue regeneration, and protection from ionizing radiations. Paradoxically, these animal studies are still less numerous and comprehensive than reports on MMW therapy in humans. Many applications of the MMW therapy seem to have never been adequately tested in animal experiments. For example, we counted 38 publications (including meeting abstracts) on vari-

ous clinical aspects of the MMW therapy for peptic ulcers, but could find just one animal study on this subject. It seems that in some cases animal studies did not precede the clinical use of MMW (as one would expect), but were carried out to create experimental justification for already reported clinical data.

Tissue repair and regeneration. Among possible therapeutic applications of MMW, the more plausible and understandable are treatments of surface lesions (wounds, burns, ulcers), which are directly reachable by the radiation. Indeed, this application has gained sound experimental support from several independent works. Other studies have demonstrated that repair of deep tissues (bone and nerve) could also be stimulated by MMW, suggesting that such effects are mediated by activation of the organism's own recovery mechanisms.

Zemskov et al. [1988] studied MMW effects on healing of skin wounds in rabbits. The animals were randomly assigned to four groups; wounds in groups 1 and 2 were kept aseptic, and those in groups 3 and 4 were infected with a pathogenic *Staphylococcus*. The wound surface in groups 1 and 3 was treated with 37 or 46 GHz CW MMW at 1 mW/cm^2 for 30 min, twice a day for 5 days. A horn irradiator was placed 2–5 mm over the wound surface. Rabbits in groups 2 and 4 served as untreated control animals. MMW decreased swelling of wound edges, hyperemia, and infiltration, and rapidly reduced the wound area in the first 24 h; it also stimulated phagocytosis and reduced bacterial contamination. Complete healing of aseptic wounds in the exposed group took 2.9 days less than in the control group. Infected wounds cleaned up and filled with granulation tissue on days 14–16 in the exposed group and only on days 21–23 in the respective control animals.

A similar protocol was used in a double-blind replicative study by Korpan et al. [1994]. Rabbits with 4 × 6 cm cutaneous wounds were randomly divided into four groups of 18 animals each. The wounds of two groups were rendered septic by inoculating them with 10^9 *Staphylococcus* cells. The wound was exposed for 30 min a day (37 GHz CW, 1 mW/cm^2), for 5 days in one aseptic group and for 7 days in a septic one. The horn aperture was 10 cm from the wound surface. The other two groups were sham-irradiated and served as aseptic and septic control groups. In irradiated animals, wound edge swelling and hyperemia subsided faster, and granulation tissue filled the wound earlier. On day 7, for example, the surface area of septic wounds decreased by 19% in the control group, and by 44% in the irradiated group. The mean daily decrease in wound surface area of the irradiated animals was significantly greater than in the control animals: 7.9% vs. 3.2% in the aseptic groups, and 6.3% vs. 2.7% in the septic groups ($P < .05$). Exposures stimulated phagocytic activity of neutrophils and decreased the blood level of circulating immune complexes. Thus, MMW irradiation enhanced both septic and aseptic wound healing and stimulated immune function.

Detlavs et al. [1993, 1994, 1995, 1996] have extensively studied MMW effects on the composition of granulation fibrous tissue (GFT) during early stages of wound healing. Their experiments were performed in rats with incised full-thickness dermal wounds. The injured area was exposed for 30 min daily for 5 days at 10 mW/cm^2 (53.53 or 42.19 GHz CW, or 42.19 GHz with 200 MHz frequency modulation. Control animals underwent the same manipulations, but were sham exposed. GFT samples from the wound were taken for analysis on the 7th day. CW irradiation significantly decreased the GFT contents of glycoproteins (hexosamines, hexoses, and sialic acids), indicating a suppression of the inflammatory process. In contrast, modulated MMW enhanced the inflammation and increased the production of glycoproteins. CW exposure decreased the GFT content of hydroxyproline, which is a marker for total collagen, to 79–85% of the control ($P < .01$), whereas the modulated regimen increased it to 126-133% ($P < .001$). CW radiation at 53.53 GHz usually was more effective than at 42.19 GHz. Both the anti- and proinflammatory effects of MMW could be useful in clinical practice. CW exposure can be recommended for early stages of the wound healing when control of the inflammatory reaction is desirable. Modulated radiation can be used to promote ultimate recovery in slow-healing wounds or in cases of healing deceleration in the late stages of tissue repair.

Ragimov et al. [1991] used MMW to stimulate the repair of an experimentally produced bone defects in rabbits. A hole 6 mm in diameter was drilled in the lower jaw bone, and the wound was sutured. The first exposure for 30 or 60 min was performed the next day, and six more exposures were done over the next 2 weeks. The shaven nape was exposed from a horn (2-cm^2 aperture) placed 3–4 mm from the skin (5.6-mm wavelength, 25 mW output power). Control animals were handled similarly. Five animals from each group were killed every week for morphologic and roentgenographic analysis of bone repair. One week after the operation, the extent of reparative osteogenesis was the same in all the groups. Later on, the regeneration was faster in exposed animals, particularly in the group with 60-min exposures. By the end of the observation period (28 days), the appearance of the traumatic defect in the control group was nearly the same as it was in exposed animals on day 21.

Hence, irradiation shortened the bone repair time by approximately 1 week.

Kolosova and coauthors [1996a] established that MMW treatment could promote regeneration of a damaged peripheral nerve. The sciatic nerve in 40 rats was transected in the thigh region and sutured. Skin over the injury area was irradiated every third day for 10 min with 4-mW/cm^2, 54-GHz radiation for 7 or 20 days; control rats were sham irradiated. Exposures did not change the skin temperature (0.1 °C accuracy). Upon the completion of the treatment course, the nerve was isolated, and the extent of regeneration was assessed electrophysiologically. After the 7-day course, the regeneration distance was 4.8 mm vs. 3.0 mm in the control animals ($P > .05$). After the 20-day course, the effect became statistically significant: the regeneration distance was 18.4 ± 0.4 mm versus 14.0 ± 1.4 mm ($P < .01$). The nerve conduction velocity also significantly increased, whereas the amplitude and duration of the action potential were not affected.

In a continuation study [Kolosova et al., 1996b], the same irradiations were performed for 2 weeks after the injury, and the nerve was isolated for examination in 5 months. Indices of regeneration were the compound action potential amplitude and conduction velocity at different distances (5 to 19 mm) distal from the suture. Both parameters were higher in the exposed animals. For example, 19 mm from the suture, the velocity was 20.4 ± 0.9 m/s vs. 15.5 ± 0.9 m/s in control animals ($P < .05$), and the amplitude was 313 ± 34 μV versus 156 ± 15 μV ($P < .001$). Hence, exposures not only stimulated the growth of nerve fibers, but facilitated their functional maturation as well.

Tumor growth and development. Experiments by Smirnov et al. [1991] were designed to evaluate the possible use of MMW for the treatment of cancer. VMR tumor cells with a high metastasizing activity were inoculated into the tibial muscle of A/SNL line mice at 5×10^5 cells/animal. Exposure for 5 days, 1 h daily (12.5 mW/cm^2, 7.09- to 7.12-mm wavelength, 50 Hz modulation), increased the average life span by 17% compared with sham control cells. The number of visible metastases decreased by more than 50% in lungs, liver, kidney, and adrenal glands, but not in lymph nodes. The authors noted variability of the MMW effect, and in one series exposure even intensified metastasizing.

Chernov et al. [1989] attempted to suppress malignant growth by extremely high peak power nanosecond MMW pulses. Rats were exposed immediately after inoculation with 10, 25, or 50 ($\times 10^3$) Walker tumor cells and received two more exposures during the next 2 days. Each exposure consisted of 43 pulses delivered at 40-s intervals. Two regimens were tested: 8-mm wavelength at 4–5 MW output power, yielding 20 kV/cm E-field level at the skin surface, and 5 mm, 8–10 MW, 30 kV/cm, respectively. The first of these regimens retarded tumor growth 1.5 times and increased the life span by 17–25 days after the inoculations with 10 and 25 ($\times 10^3$) cells the other regimen was less effective. The antitumor effect was presumably mediated by stimulation of immune system, namely the so-called skin-associated lymphoid tissue. Preliminary studies with exposure before tumor inoculation showed that MMW retarded the tumor growth nearly twofold.

Because of concern about possible adverse effects of MMW use in cancer patients, Brill' and Panina [1994] studied the transplantability and growth of a benign tumor (mammary fibroadenoma) in rats. Two tumor pieces were implanted to the right and left sides through a cut in the middle of the abdomen. In 20 of 49 operated animals, tissues in the cut were exposed to MMW (42.0–43.3 GHz band) for 15 min before the implantation, the other animals served as control. In 3 weeks, 39 of 58 tumors (67.3%) resolved in the control group, but only 11 of 40 (27.5%) resolved in the exposed animals ($P < .001$). The percentages of stable and growing unresolved tumors in both the groups were the same. Hence, a single MMW exposure of the implantation area increased tumor transplantability, although did not affect its proliferation.

Stress alleviation and prevention effects. Temur'iants and Chuyan [1992] demonstrated that MMW can alleviate immobilization-induced stress in rats. The authors established that this MMW effect differed in specimens with different characteristic levels of exploratory activity, as evaluated by an open-field testing. In further studies, the open-field testing was always done before stressing and MMW exposures, to divide the population into appropriate groups.

One of these studies [Temur'iants et al., 1993] was performed on 350 animals divided by low (LA), medium (MA), and high (HA) activity. Each activity level was subdivided into five groups; group 1 was cage control, and groups 2–5 were housed for 9 days in individual boxes restricting their motion. Animals in groups 3–5 received daily 30-min MMW exposures of the occipital area, left hip, or right hip, respectively (5.6-mm wavelength, 10 mW/cm^2). Stress severity was quantified by indices of the "nonspecific resistivity" of the organism, which included the lipids and peroxidase contents in neutrophils, and succinate and alpha-2-glycerophosphate dehydrogenases activities in lymphocytes. A typical stress reaction developed in unexposed MA rats: by days 6–9, the contents of lipids and

peroxidase decreased by 21–24%, and the activity of dehydrogenases fell by 36–46%. Occipital or right hip MMW irradiation prevented the stress reaction in MA rats, whereas the left hip exposure was not effective. The immobilization stress was the most pronounced in unexposed HA animals; MMW exposures of the left hip or occipital area prevented stress, whereas exposures of the right hip had little effect. In LA animals, the stress reaction was relatively weak, and all the types of MMW treatment alleviated it.

The next study used 640 albino rats, all with a medium level of locomotor activity [Temur'iants et al., 1994]. The same indices as above were compared in four groups: cage control, hypokinesia without exposures, exposures without hypokinesia, and both. The occipital area was exposed for 30 min/day, 9 days at either 5.6- or 7.1-mm wavelength. Exposures without hypokinesia strongly activated succinate dehydrogenase (up to twofold, $P < .05$). Irradiation at 5.6 mm (but not at 7.1 mm) increased the activities of acid and alkaline phosphatases and glycerophosphate dehydrogenase by 20–30%. Both wavelengths prevented or reversed stress-induced changes, 5.6 mm was more effective. Further experiments with 5.6-mm radiation established that exposures for 15 min/day were less effective than for 30 min/day, and, paradoxically, increasing the exposure duration to 60 min/day eliminated its antistress effect.

A similar exposure technique was independently used by Arzumanov et al. [1994]. The occipital area was exposed at 5.6 mm simultaneously with immobilization of the rat's head for 60 min/day for 10 days. This stressing suppressed feeding and sexual behavior. It also increased the motor activity in a swimming test to the same degree in exposed and unexposed groups. The authors hypothesized that the immobilization stress was too severe and might mask MMW effects, so in the next series rats were immobilized and exposed for only 30 min/day for 9 days. The stress effect was assessed by the electric shock threshold, free-access water consumption, and Vogel's choice test (consumption of water when each attempt to drink is accompanied by an electric shock). Immobilization without exposure decreased threefold the number of attempts to drink in Vogel's test; but, when immobilization was combined with MMW exposures, this index remained the same as in cage control animals. The shock threshold and free-access water consumption were not changed by MMW.

It is interesting to note some parallelism in the above two studies. Using the same exposure procedures, but different protocols and end points, both research groups established that there is an anti-stress effect of a 30-min irradiation, but there is no such effect if the exposure duration is 60 min. The decreased efficacy of a more prolonged MMW irradiation has been observed in some other clinical and experimental studies as well, but this unusual time dependence has not yet been discussed or explained.

Combined MMW and ionizing radiation exposure. Gubkina et al. [1996] researched whether low-intensity MMW can alleviate the effect of X-rays in rats. The abdominal area was shaved and exposed to MMW in a frequency-sweep regimen (38 to 53 GHz) at 7 mW/cm^2 for 23 days, 30 min/day. Control animals not treated by MMW underwent all the same manipulations, including shaving. Exposures to 150 keV X-rays were performed daily during the last 8 days of the MMW course up to a total dose of 24 roentgen. Blood serum and brain tissue samples were collected the next day after the end of exposures. MMW alone did not alter the serum glucose level (6.24 ± 0.79 mM versus 6.53 ± 0.80 mM in control animals); X-ray exposure increased it to 10.37 ± 0.75 mM ($P < .05$), but combining X-rays with MMW prevented this rise (6.81 ± 0.37 mM). MMW decreased the content of the soluble form of the acidic glial fibrillar protein (s-AGFP) 1.5–2 times ($P < .05$) in all analyzed structures of the brain (cerebellum, midbrain, and medulla oblongata) and did not change the content of its fibrillar form (f-AGFP). X-rays decreased the levels of both forms of the protein two to three times. After combined treatment with MMW and X-rays, both s- and f-AGFP levels did not differ from control animals and were significantly ($P < .05$ and $P < .01$) higher than after X-rays only. The authors concluded that MMW alleviated the effect of X-rays at both cellular and organism levels.

Two other studies are of interest, although they are only brief reports that do not contain essential experimental details. Kuzmanova and Ivanov [1995] studied changes in the surface electrical charge of erythrocytes after MMW and γ-ray exposures in rats. The shin of the right hind limb was exposed to 5.6-mm radiation for 10 days, 20 min/day at 1.1 mW/cm^2, followed with a 6 Gy whole-body dose of ^{137}Co γ-rays. The surface charge of erythrocytes was assessed from their electrophoretic mobility (EPM) 3, 7, 14, 21, and 30 days after the exposures. The MMW treatment alone had practically no effect, whereas γ-rays alone decreased EPM for the whole period of observation. When γ-irradiation was preceded by MMW, the EPM remained the same as in control animals. The authors concluded that MMW stabilized the membrane structure and increased its resistivity to γ-radiation.

Tsutsaeva et al. [1995] examined MMW-induced survival changes in mice after a lethal dose of X-rays. Irradiation with pulse-modulated MMW at 1 μW/cm^2 continued for 80 or 24 h before X-ray exposure or was

simultaneous with the X-ray exposure. All tested X-ray doses (7, 7.5, and 8 Gy) were 100% lethal with an average life span of 6–8 days; the first fatalities occurred on days 4–6. MMW treatment for 80 h before 7 Gy of X-rays delayed the first deaths until day 14; 50% of the population died within 30 days, and 100% of the animals died by day 96. The MMW treatment for 24 h appeared even more effective: first deaths occurred on day 8, 50% of the animals died within 30 days, but no more fatalities were observed through day 96. Microwave irradiation simultaneously with the X-rays (7 Gy) increased the survival and life span of mice approximately fivefold. The protective effect of 24-h MMW pretreatment decreased with increasing X-ray dose to 7.5 Gy and became insubstantial at 8 Gy.

MMW Therapy: Clinical Studies

The first clinical trials of MMW therapy began in 1977, and today the method has been officially approved by the Russian Ministry of Health and is used widely. As mentioned in the Introduction section, by 1995 over 3 million people have been treated at more than a thousand specialized centers as well as at regular hospitals [Lebedeva and Betskii, 1995].

General issues of the MMW therapy. MMW therapy involves repetitive local exposures of certain body areas with low-intensity MMW. The area(s) to be exposed, the radiation wavelength, and daily duration of procedures are determined by the physician based on the disease and the condition of the particular patient. The radiation intensity is usually regarded as a less important variable. For most diseases, the daily exposure varies from 15 to 60 min, and the therapy lasts for 8–15 days.

Publications on the clinical use of MMW number in the hundreds. Many of them have claimed that MMW monotherapy is more effective (sometimes, far more effective) than conventional methods, such as drug therapy, for a variety of diseases and disorders. In some cases, MMW has helped the patients who had already tried all other known therapies without success and were considered incurable. At the same time, MMW seldom caused any adverse effects or allergies. MMW in combination with drug therapy facilitated favorable effects and/or reduced adverse side effects of drugs. Some authors reported that MMW might be highly effective or not effective at all, contingent on the patient's condition, individual sensitivity to MMW, and parameters of irradiation. A few authors reported that MMW therapy was always less effective than conventional techniques, and we found only one clinical study saying that MMW therapy was not effective at all [Serebriakova and Dovganiuk, 1989].

Diseases reported to be successfully treated with MMW belong to rather diversified groups. The most common applications of MMW are for gastric and duodenal ulcers (about 25% of studies); cardiovascular diseases, including angina pectoris, hypertension, ischemic heart disease, infarction (about 25%); respiratory sicknesses, including tuberculosis, sarcoidosis, bronchitis, asthma (about 15%); and skin diseases, including wounds, trophic ulcers, burns, atopic dermatitis (about 10%). These percentages are approximate, because we could not cover all clinical studies published and because many authors reported treatment of several diseases in one paper (so the sum would be over 100%). Isolated studies claimed successful MMW treatment for asthenia, neuralgia, diabetes mellitus, osteochondrosis, acute viral hepatitis, glomerulonephritis, alcoholism, etc. MMW were also used for alleviation of toxic effects of chemotherapy in cancer patients and in preventive medicine and health resort therapy.

In most cases, physicians use specialized MMW generators, which are produced commercially by the medical equipment industry. These generators operate at average radiation intensities of 10 mW/cm^2 or less in CW or frequency-modulated regimens at certain fixed frequencies or within a wide frequency band. Three models have been reported used more often than all others together: "Yav'-1-7,1" (7.1-mm wavelength, 42.19 GHz) (36%), "Yav'-1-5,6" (5.6 mm, 53.53 GHz) (31%), and "Electronica-KVCh" (4.9 mm, 59–63 GHz band) (10%). Different generators were often used within a single study to compare their therapeutic efficacy; and more often than not, the efficacy was different, depending on the disease and patients' condition. Some authors used in vitro tests to determine which wavelength is more suitable for a particular patient before the onset of the therapy [Novikova et al., 1995]. However, we have been unable to identify references to the original studies that had shown why the frequencies of 42.19, 53.53, and 59–63 GHz (and not others) should be used for therapy.

In about 30% of clinical studies, the radiation is applied to standard acupuncture points or so-called biologically active points. This procedure is often combined with finding the individual "resonance" frequency based on MMW-evoked "sensations" of the patient (a method called "microwave resonance therapy"). In our opinion, this procedure should be regarded as a variety of acupuncture techniques along with electropuncture, acupressure, etc. Assuming the therapeutic efficacy of these techniques, it is no surprise that MMW can be effective as well: irradiation at about 10 mW/cm^2 can also stimulate acupuncture points by subtle heating or thermal "micromassage." Clinical effects of the "MMW-puncture" are nonspe-

cific, meaning that they are similar to those of traditional puncture-based techniques. These effects are determined by the selection of acupuncture points, intensity and duration of their stimulation, rather than by using MMW or other means for the stimulation. Therefore, studies using the MMW-puncture seem to be of greater interest for the acupuncture practice than for the bioelectromagnetic science; such studies will be left beyond the scope of the present review.

Other areas of MMW exposure include sternum and xiphoid process, skin projection of the diseased organ, large joints, and the surface of wounds and ulcers. Once again, we could not identify the studies that originally provided the rationale and experimental proof for the useful nature of MMW exposure of these particular body areas. Except for the surface lesions, the radiation is unable to penetrate to diseased organs. This fact is understood and discussed by many physicians, but no proven explanation of the MMW therapy has been given yet.

Many clinical studies do not conform to conventional quality criteria (double-blind protocol, placebo treatment, adequate statistics, etc.). However, still others do conform and a lot of matching results have been provided by independent groups of investigators. Some clinical data on the MMW efficacy are quite impressive, and a few examples are given below (see a specialized review by Rojavin and Ziskin [1998] for additional detail).

Examples of MMW therapy. Korpan and Saradeth [1995] performed a double-blind controlled trial of MMW therapy for postoperative septic wounds. The study group consisted of 141 patients, 31–83 yr old, with purulent wounds after an abdominal surgery. The wounds were infected mostly with *S. aureus* and *Bacteroides fragilis*. MMW therapy with 1 mW/cm^2, 37 GHz CW radiation was used in 71 patients. Wound surface and adjacent soft tissue were exposed for 30 min/day for 7 days. The remaining 70 patients received placebo therapy from a similar but defective MMW generator (neither patients nor physicians knew it was defective). Radical surgical cleaning of the wounds was performed regularly in both groups. The MMW-treated patients showed 1.8 times more rapid wound clearance (5.6 ± 0.6 vs. 10.2 ± 0.5 days in control subjects), 1.7 times earlier onset of wound granulation (4.9 ± 0.2 vs. 8.7 ± 0.4 days), and 1.8 times earlier onset of epithelization (7.0 ± 0.4 vs. 12.8 ± 0.6 days). The average daily decrease of wound surface area in the treated patients was twice that of the control subjects (7.1% vs. 3.2%). The authors concluded that low intensity MMW seems to be an effective postoperative wound treatment.

Poslavsky et al. [1989] used MMW as a monotherapy in 317 patients with duodenal and gastric ulcers. The ulcer diameter ranged from 0.3 to 3.5 cm, and the disease duration was from several months to more than 10 years. The epigastric area was exposed at 10 mW/cm^2, 5.6-mm wavelength for 30 min daily, excluding weekends, until complete ulcer cicatrization. A comparable control group of 50 patients received conventional drug therapy. The ulcers cicatrized in 95.3% of MMW-treated patients, with mean healing duration of 19.8 ± 0.45 days. The respective control group values were substantially worse, namely 78% and 33.6 ± 1.12 days. The ulcer relapse rate was significantly lower after the MMW therapy.

Megdiatov et al. [1995] evaluated the efficacy of MMW therapy (42.2 GHz, 10 mW/cm^2) in 52 patients with neuralgia. The radiation was applied to areas where branches of the affected trigeminal nerve approach the skin (10 exposures or sham exposures, 15 min each, concurrently with medicinal therapy). Evident clinical improvement (decrease of the incidence and severity of pain attacks) was achieved in 19 of 27 patients treated with MMW, and only in 4 of 25 patients receiving placebo exposures.

Liusov et al. [1995] studied MMW therapy effects in 100 patients with unstable angina pectoris (this is an intermediate condition between stable angina pectoris and infarction, and is characterized by a high risk of myocardial necrosis). The patients were divided into four groups. Group 1 was treated by MMW only (10 exposures of the right shoulder joint for 30 min/day, 7.1 mm); these patients ceased taking any vasodilators and antianginal medicines. In group 2, the same MMW therapy was combined with drugs (beta-adrenergic antagonists, calcium blockers, organic nitrates, etc.). Group 3 received the same drug therapy and placebo exposures, and group 4 received the drug therapy only. The therapy in groups 1 and 2 substantially decreased the rate and severity of angina attacks, making it possible to reduce the amount of nitroglycerin taken. It also decreased blood levels of malonic dialdehyde and dienic conjugates, normalized T-helper and T-suppresser ratios, reduced the diameter of venules, and increased the diameter of arterioles. No significant improvement of the lipid peroxidation system, immune status, or microcirculation was achieved in groups 3 and 4.

Karlov and coauthors [1991] used MMW in a combined therapy for cerebral circulatory disorders. The 79 patients in the study were mostly 50-80 yr old and suffered from hypertensive disease and/or atherosclerosis; 61 patients were hospitalized for acute ischemic cerebral infarction, 13 for a transient disorder of the cerebral circulation, and 5 for circulatory encephalopathy. Patients were divided into two comparable groups. Both groups received the same drug therapy

(hypotensive, anticoagulant, cardiotonic, and other remedies), whereas the first one was also treated with MMW (10 days, 30 min/day, 4.9-mm wavelength). Patients of the second group were sham-exposed under a double-blind protocol. A favorable therapeutic effect was reported in 70% of the patients in group 1 and in 40% in group 2. MMW procedures helped decrease blood pressure, normalize the blood glucose level, and eliminate serum fibrinogen B.

The efficacy of the MMW therapy is often illustrated by individual clinical cases. Naumcheva [1994] described the history of a 54-yr-old male patient, who had two myocardial infarctions within a 2-yr interval. He experienced severe attacks of angina both on exertion and at rest and took up to 80 nitroglycerin tablets a day (0.4 mg). Repeated courses of in- and outpatient treatment with beta-adrenoblockers, nitrates, plasmapheresis, etc. had little effect. Finally, he was hospitalized in a grave condition with a third infarction. Conventional methods were ineffective, so MMW therapy was ordered on day 10 after admission (7.1-mm wavelength, for 30 min/day to the left border of sternum). Cardialgia decreased after two exposures and nighttime pain attacks ceased after seven procedures. The nitroglycerin intake was decreased to 1–2 tablets/day after 12 exposures. After the MMW course, the patient did not have angina attacks for 3–4 days, was able to walk up to 5 km a day, and was discharged in a satisfactory condition. Another man, age 62, was admitted to hospital with a severe macrofocal infarction, collapse, extrasystolia, and acute insufficiency and aneurysm of the left ventricle. Three days of intensive treatment still left the patient in this critical condition. Even the first MMW irradiation of sternum (5.6-mm wavelength, three 10-min exposures with 5-min intervals) had a striking effect: it arrested angina attacks and normalized sleep, and indices of hemodynamics stabilized within 5 days of the MMW therapy. The patient was discharged in a satisfactory condition and later underwent two additional MMW courses as a preventive measure.

Side effects of MMW therapy. As a rule, MMW therapy is well tolerated by patients, and this is regarded as one of its advantages over a drug therapy. Although most investigators reported no negative reactions to MMW, others observed them in up to 26% of patients [Golovacheva, 1995]. The possibility of induction of adverse health effects by a local, low-intensity MMW irradiation is of potential significance for setting health and safety standards and requires special attention.

Kuz'menko [1989] summarized experience with MMW use in 200 patients with cerebrovascular diseases, such as cerebral circulation insufficiency, discirculatory encephalopathy, and cerebral insult consequences. Irradiation of the sinocarotid zone at various frequencies between 58 and 62 GHz, 0.3–1 mW/cm^2, was performed for 20 min/day or less, for 4 to 10 days. MMW therapy facilitated recovery in 56–77% of patients with different pathologies. However, it also caused adverse side effects, including elevation of the blood pressure (nine cases), induction of a diencephalic crisis or paroxysm during irradiation (seven cases), angina attacks (three cases), fever (five cases), and enhancement of menstrual bleeding (six cases). In hypertension patients, MMW usually decreased blood pressure by 10–15 mm Hg, but occasionally increased it by 20-30 mm Hg. The author concluded that MMW can be successfully used in cerebrovascular therapy, but possible complications must be taken into account.

Afanas'eva and Golovacheva [1997] used MMW therapy in 124 patients with stage II essential hypertension (5.6- or 7.1-mm wavelength, CW, 10 mW/cm^2, 10 procedures for 30 min each). Unfavorable autonomous nervous system reactions (whole-body shivering, sweating, heart pains along with skin paling or reddening) were observed in 18 patients (15.5%). In two cases, these reactions developed into hypertensive crises, which had to be arrested by drug injections. In 33 patients (26.6%), MMW-induced fluctuations of the arterial blood pressure and enhanced headaches. A temporary improvement after four to five exposures was followed by an increase in both systolic (by 25 ± 7.0 mm Hg) and diastolic (by 10.0 ± 2.0 mm Hg) blood pressure, which required medicinal correction. General adverse reactions after the entire MMW course (six patients; 4.8%) included sleeplessness or sleep with distressful dreams, weakness, emotional instability, and irritability. These manifestations were not profound and disappeared without further treatment. The authors emphasized that these adverse reactions were not encountered in patients who received placebo exposures.

Gun'ko and Kozshina [1993] tried MMW therapy in 528 patients with various diseases (ulcerative disease, ischemic heart disease, essential hypertension, bronchitis, pneumonia, and others). Exposures at 5.6- or 7.1-mm wavelength lasted from 15 to 60 min/day, from 5 to 18 days. Three patients being treated for rheumatic polyarthritis, psoriasis, and duodenal ulcer (without any concurrent drug therapy) developed urticaria (hives) on the fifth to seventh day of exposures. An itchy rash appeared first in the abdominal and thoracic areas, and soon spread everywhere. Nevertheless, the treatment of the main disease in all these cases was successful. The rash disappeared 2-10 days after the completion of the MMW therapy but reappeared during

the repeated MMW courses. The authors called for more studies of MMW effects on the immune system.

DISCUSSION

In this review, we have found that recent research in the MMW area covers a variety of subjects. Profound MMW effects were established at all biological levels, from cell-free systems through cells, organs, and tissues, to animal and human organisms. Although trying to avoid a general discussion of thermal versus nonthermal mechanisms in this review, we nonetheless must note that many of the reported effects were principally different from those caused by heating, and their dose and frequency dependencies often suggested nonthermal mechanisms. Regardless of the primary mechanism, the possibility of significant bioeffects of a short-term MMW irradiation at intensities at or below current safety standards deserves consideration and further study.

The major question about FSU publications in the MMW area is their reliability. A number of studies cited here were performed at the highest scientific level. Other studies, perhaps the majority of those cited, were flawed, but may still bear valuable information and should not be discarded without proper analysis. For example, free-field dosimetry in the MMW band is a serious technical problem. To our knowledge, no commercially available probes are rated for near-field measurements in the MMW band even in the U.S. Therefore, it is not surprising that many investigators, particularly clinicians, have had to rely on manufacturer-specified field intensities, such as 10 mW/cm^2 for "Yav'-1" therapeutic generator. One may doubt that the field actually was 5, 10, or 15 mW/cm^2, but under no circumstances could it exceed a spatial average of, say, 50 mW/cm^2, which is beyond the generator's capabilities. Thus, whereas the precise exposure parameters may not be known, a range of possible exposure intensities may be estimated. With an understanding of this fact, the experimental data may still be important and usable.

Another widespread shortcoming of clinical studies occurs when MMW therapy is compared with drug therapy, without using a sham-exposed control group. MMW therapy was often reported to be more effective than drugs. This result could be a placebo effect; but if so, one would have to conclude that placebo was more effective than modern drug therapy. This possibility could certainly be true for certain patients and certain disorders, but does not seem feasible for large populations and a wide scale of diseases.

A further source of skepticism about findings made by FSU scientists is that they have not been replicated in the West. Replication is much needed indeed, but it can hardly be anticipated without adequate attempts. To our knowledge, only three laboratories throughout the U.S. (less than 10 scientists total) are currently doing any research on MMW bioeffects, which is by no means sufficient to match the amount and variety of the FSU research. Besides, many cited studies are very recent (1995–1997), so replication has yet to be expected.

With all the diversity of the MMW research and differences in studied subjects and end points, some particulars seem to be common for various situations and MMW effects. Considering these particulars may be critical for replication studies:

(1) Individuals or groups in a population, which would usually be regarded as uniform, may react to MMW in rather different or even opposite ways. For example, Temur'iants et al. [1993, 1994] divided the vivarium population of rats by their open-field activity before performing exposures. Not only the animal's reactions to MMW, but also their reactions to immobilization stress, were very different in animals with low, medium, and high activity levels. Pooling all the data together, as well as neglecting the intrinsic differences in the population, would have inevitably masked MMW effects.

(2) There seem to exist unknown and uncontrolled factors that determine the MMW sensitivity of a specimen or a population. Irradiation could increase antibiotic resistivity in one experiment and decrease it in the next one [Bulgakova et al., 1996]. It increased the beating rate in one isolated heart and decreased it in the other [Chernyakov et al., 1989]. MMW therapy usually decreased blood pressure, but eventually increased it greatly [Kuz'menko, 1989]. As long as these changes exceeded the "noise" level and were not produced by a sham exposure, they can be regarded as MMW effects. Again, pooling all data together, regardless of the direction of changes, could easily mask an MMW effect.

(3) Even robust MMW effects may be well reproducible for a limited time and then disappear. The effects of complete suppression or 200–400% enhancement of chloride transmembrane current in alga cells were far beyond any spontaneous variations and could hardly be confused with any artifact [Kataev et al., 1993]. However, both effects weakened and disappeared by the end of winter without any apparent reason. MMW effects on isolated frog nerve also disappeared in spring [Burachas and Mascoliunas, 1989], suggesting that MMW sensitivity may be somehow related to the base level of metabolism.

4. MMW effects could often be revealed only in subjects that are experiencing some deviation from the

"normal" state. MMW caused little or no reactions in intact animals, but significantly alleviated effects of immobilization, ionizing radiation, etc. Many clinical studies claim that MMW therapy is effective only when one or another kind of pathology is present, whereas in a healthy organism MMW will not produce any reactions. However, this thesis has not been adequately proven.

5. Increased sensitivity and even hypersensitivity of individual specimens to MMW may be real. Depending on the exposure characteristics, especially wavelength, a low-intensity MMW radiation was perceived by 30 to 80% of healthy examinees [Lebedeva, 1993, 1995]. Some clinical studies reported MMW hypersensitivity, which was or was not limited to a certain wavelength [Golovacheva, 1995]. In a study by Afanas'eva and Golovacheva [1997], adverse health reactions to MMW appeared only in women (100%) who had a labile course of angina pectoris (100%), most of whom were in the menopausal period (66.7%). The authors suggested that this category of people is particularly sensitive to MMW.

It is important to note that, even with the variety of bioeffects reported, no studies have provided evidence that a low-intensity MMW radiation represents a health hazard for human beings. Actually, none of the reviewed studies with low-intensity MMW even pursued the evaluation of health risks, although in view of numerous bioeffects and growing usage of MMW technologies this research objective seems very reasonable. Such MMW effects as alterations of cell growth rate and UV light sensitivity, biochemical and antibiotic resistivity changes in pathogenic bacteria, as well as many others, are of potential significance for safety standards. MMW therapy in many cases uses field intensities comparable to or lower than those allowed by current safety standards, but even local and short-term exposures were reported to produce marked effects. It should also be realized that biological effects of a prolonged or chronic MMW exposure of the whole body or a large body area have never been investigated. Safety limits for these types of exposure are based solely on predictions of energy deposition and MMW heating, but in view of recent studies this approach is not necessarily adequate.

The significance of MMW bioeffects for human health, considering both safety limitations and possible clinical applications, should be neither over- nor underestimated. It is, however, an intriguing and potentially important area that needs to be further explored. If this present review draws attention to the MMW research and stimulates new studies, we will consider its goal accomplished.

ACKNOWLEDGMENTS

The work was supported in part by the U.S. Army Medical Research and Materiel Command and the U.S. Air Force Armstrong Laboratory under U.S. Army contract DAMD17-94-C-4069 awarded to McKesson BioServices. The views expressed in this article are those of the authors and should not be construed as reflecting the official policy or position of the Department of the Army, Department of the Air Force, Department of Defense, or the United States Government.

REFERENCES

Afanas'eva TN, Golovacheva TV (1997): Side effects of the EHF-therapy for essential hypertension. Zvenigorod, Russia: 11th Russian Symposium "Millimeter Waves in Medicine and Biology," April, 1997 (Digest of papers). Moscow: IRE RAN, pp 26–28 (in Russian).

Akoev GN, Avelev VD, Semen'kov PG (1992): Perception of the low-level millimeter-range electromagnetic radiation by electroreceptors of the ray. Dokl Akad Nauk 322:791–794 (in Russian).

Alekseev SI, Ziskin MC (1995): Millimeter microwave effect on ion transport across lipid bilayer membranes. Bioelectromagnetics 16:124–131.

Alekseev SI, Ziskin MC, Kochetkova NV, Bolshakov MA (1997): Millimeter waves thermally alter the firing rate of the Lymnaea pacemaker neuron. Bioelectromagnetics 18:89–98.

Arzumanov YuL, Kolotygina RF, Khonichava NM, Tverytskaya IN, Abakumova AA (1994): Animal study of the stress-protective effect of electromagnetic radiation of the extremely-high-frequency range. Millimetrovie Volni v Biologii i Meditcine 3:5–10 (in Russian).

Belyaev IYa (1992): Some biophysical aspects of the genetic effect of low-intensity millimeter waves. Bioelectrochem Bioenerg 27:11–18.

Belyakov EV, Kichaev VA, Poslavskii MV, Starshinina VA, Soboleva ES (1989): Use of blood radiophysical parameters in the extremely high-frequency range for diagnostic purposes. In Devyatkov ND (ed): "Millimeter Waves in Medicine and Biology." Moscow: Radioelectronica, pp 83–88 (in Russian).

Belyaev IYa, Okladnova OV, Izmailov DM, Sheglov VS, Obukhova LK (1990): Differential sensitivity of developmental stages to low-level electromagnetic radiation of extremely ultrahigh frequency. Dokl Akad Nauk SSSR [Ser B Geol Chim Biol] 12:68–70 (in Russian).

Belyaev IYa, Alipov YD, Polunin VA, Shcheglov VS (1993a): Evidence for dependence of resonant frequency of millimeter wave interaction with *Escherichia coli* K12 cells on haploid genome length. Electromagnetobiology 12:39–49.

Belyaev IYa, Shcheglov VS, Alipov YeD, Radko SP (1993b): Regularities of separate and combined effects of circularly polarized millimeter waves on *E. coli* cells at different phases of culture growth. Bioelectrochem Bioenerg 31:49–63.

Belyaev IYa, Alipov YD, Shcheglov VS, Polunin VA, Aizenberg OA (1994): Cooperative response of *Escherichia coli* to the resonance effect of millimeter waves at super low intensity. Electromagnetobiology 13:53–66.

Belyaev IY, Shcheglov VS, Alipov YD, Polunin VA (1996): Resonance effect of millimeter waves in the power range from 10^{-19} to 3×10^{-3} W/cm^2 on *Escherichia coli* cells at different concentrations. Bioelectromagnetics 17:312–321.

Belyaev IYa, Shcheglov VS, Alipov YD, Ushakov VL (1997): Reply to comments of Osepchuk and Petersen. Bioelectromagnetics 18:529–530.

Berezhinskii LI, Gridina NIa, Dovbeshko GI, Lisitsa MP, Litvinov GS (1993): Visualization of the effects of millimeter radiation on blood plasma. Biofizika 38:378–384 (in Russian).

Berzhanskaya LYu, Berzhanskii VN, Beloplotova OYu (1995): Effect of electromagnetic fields on the activity of bioluminescence in bacteria. Biofizika 40:974–977 (in Russian).

Betzky OV (1992): Use of low-intensity electromagnetic millimeter waves in medicine. Millimetrovie Volni v Biologii i Meditcine 1:5–12 (in Russian).

Brill' GE, Panina NP (1994): Effect of millimeter waves on transplantability and growth of tumors. Fizicheskaia Meditzina 4:25 (in Russian).

Brill' GE, Apina OR, Belyanina CI, Panina NP (1993): Effect of low-level extremely high-frequency radiation on the genetic activity of polytene chromosomes of Chironomus plumosus. Fizicheskaia Meditzina 3:69–71 (in Russian).

Brovkovich VM, Kurilo NB, Barishpol'ts VL (1991): Action of millimeter-range electromagnetic radiation on the Ca pump of sarcoplasmic reticulum. Radiobiologiia 31:268–271 (in Russian).

Bulgakova VG, Grushina VA, Orlova TI, Petrykina ZM, Polin AN, Noks PP, Kononenko AA, Rubin AB (1996): Effect of millimeter-band radiation of nonthermal intensity on the sensitivity of *Staphylococcus* to various antibiotics. Biofizika 41:1289–1293 (in Russian).

Burachas G, Mascoliunas R (1989): Suppression of nerve action potential under the effect of millimeter waves. In Devyatkov ND (ed): "Millimeter Waves in Medicine and Biology." Moscow: Radioelectronica, pp 168–175 (in Russian).

Chernov ZS, Faikin VV, Bernashevskii GA (1989): Experimental study of the effect of nanosecond EHF pulses on malignancies. In: Devyatkov ND (ed): "Millimeter Waves in Medicine and Biology." Moscow: Radioelectronica, pp 121–127 (in Russian).

Chernyakov GM, Korochkin VL, Babenko AP, Bigdai EV (1989): Reactions of biological systems of various complexity to the action of low-level EHF radiation. In Devyatkov ND (ed): "Millimeter Waves in Medicine and Biology." Moscow: Radioelectronica, pp 141–167 (in Russian).

Dardalhon M, Averbeck D, Berteaud AJ (1979): Determination of a thermal equivalent of millimeter microwaves in living cells. J Microw Power 14:307–312.

Dardalhon M, Averbeck D, Berteaud AJ (1981): Studies on possible genetic effects of microwaves in prokaryotic and eukaryotic cells. Radiat Environ Biophys 20:37–51.

Dardanoni L, Torregrossa MV, Zanforlin L (1985): Millimeter wave effects on Candida albicans cells. J Bioelectr 4:171–176.

Detlav IE, Shkirmante BK, Dombrovska LE, Pahegle IV, Slutskii LI (1993): Biochemical parameters of developing granulo-fibrous tissue after the effect of an extremely high-frequency electromagnetic field. Millimetrovic Volni v Biologii i Meditcine 2:43–50 (in Russian).

Detlavs I, Dombrovska L, Klavinsh I, Turauska A, Shkirmante BB, Slutskii L (1994): Experimental study of the effect of electromagnetic fields in the early stage of wound healing. Bioelectrochem Bioenerg 35:13–17.

Detlavs I, Dombrovska L, Shkirmante B, Turauska A, Slutskii L (1995): Some biological effects of mm-wave electromagnetic fields on the granulation-fibrous tissue in a healing wound. Moscow, Russia: 10th Russian Symposium "Millimeter Waves in Medicine and Biology," April, 1995 (Digest of papers). Moscow: IRE RAN, pp 117–119 (in Russian).

Detlavs I, Dombrovska L, Turauska A, Shkirmante B, Slutskii L (1996): Experimental study of the effects of radiofrequency electromagnetic fields on animals with soft tissue wounds. Sci Total Environ 180:35–42.

Enin LD, Akoev GN, Potekhina IL, Oleiner VD (1992): Effect of extremely high-frequency electromagnetic radiation on the function of skin sensory endings. Patol Fiziol Eksp Ter 5-6:23–25 (in Russian).

Fesenko EE, Gluvstein AYa (1995): Changes in the state of water induced by radiofrequency electromagnetic fields. FEBS Lett 367:53–55.

Fesenko EE, Geletyuk VI, Kazachenko VN, Chemeris NK (1995): Preliminary microwave irradiation of water solutions changes their channel modifying activity. FEBS Lett 366:49–52.

Frei MR, Ryan KL (1997): Circulatory failure resulting from sustained millimeter wave irradiation. Brooks AFB, TX: Infrared Lasers and Millimeter Waves Workshop "The Links Between Microwaves and Laser Optics," January, 1997.

Frei MR, Ryan KL, Berger RE, Jauchem JR (1995): Sustained 35-GHz radiofrequency irradiation induces circulatory failure. Shock 4:289–293.

Fröhlich H (1980): The biological effects of microwaves and related questions. Adv Electronics Electron Phys 53:85–152.

Fröhlich H (ed) (1988): Biological coherence and response to external stimuli. Berlin: Springer-Verlag, p 265.

Furia L, Hill DW, Gandhi OP (1986): Effect of millimeter-wave irradiation on growth of Saccharomyces cerevisiae. IEEE Trans Biomed Eng 33:993–999.

Gandhi OP (1983): Some basic properties of biological tissues for potential biomedical applications of millimeter-waves. J Microw Power 18:295–304.

Gapeev AB, Chemeris NK, Fesenko EE, Khramov RN (1994): Resonance effects of a low-intensity modulated EHF field. Alteration of the locomotor activity of the protozoa Paramecium caudatum. Biofizika 39:74–82 (in Russian).

Gapeev AB, Safronova VG, Chemeris NK, Fesenko EE (1996): Modification of the activity of murine peritoneal neutrophils by exposure to millimeter waves at close and far distances from the emitter. Biofizika 41:205–219 (in Russian).

Geletyuk VI, Kazachenko VN, Chemeris NK, Fesenko EE (1995): Dual effects of microwaves on single Ca^{2+}-activated K^+ channels in cultured kidney cells Vero. FEBS Lett 359:85–88.

Golant MB (1989): Resonance effect of coherent millimeter-band electromagnetic waves on living organisms. Biofizika 34:1004–1014 (in Russian).

Golant MB, Kuznetsov AP, Boszhanova TP (1994): Mechanisms of synchronization of the yeast cell culture by the action of EHF radiation. Biofizika 39:490–495 (in Russian).

Golovacheva TV (1995): EHF therapy in complex treatment of cardiovascular diseases. Moscow, Russia: 10th Russian Symposium "Millimeter Waves in Medicine and Biology," April, 1995 (Digest of papers). Moscow: IRE RAN, pp 29–31 (in Russian).

Gos P, Eicher B, Kohli J, Heyer W-D (1997): Extremely high frequency electromagnetic fields at low power density do not affect the division of exponential phase Saccharomyces cerevisiae cells. Bioelectromagnetics 18:142–155.

Grundler W (1983): Biological effects of RF and MW energy at molecular and cellular level. In Rindi A, Grandolfo M, Michaelson SM (eds): "Biological Effects and Dosimetry of Nonionizing Radiation. Radiofrequency and Microwave Energies." New York: Plenum Press, pp 299–318.

Grundler W, Kaiser F (1992): Experimental evidence for coherent excitations correlated with growth. Nanobiology 1:163–176.

Grundler W, Keilman F, Froehlich H (1977): Resonant growth rate response of yeast cells irradiated by weak microwaves. Phys Lett 62A:463–466.

Grundler W, Keilman F, Putterlik V, Strube D (1982): Resonant-like

dependence of yeast growth rate on microwave frequencies. Br J Cancer 45:206–208.

Grundler W, Jentzsch U, Keilmann F, Putterlik V (1988): Resonant cellular effects of low intensity microwave. In Fröhlich H (ed): "Biological Coherence and Response to External Stimuli." Berlin: Springer-Verlag, pp 65–85.

Gubkina EA, Kushnir AE, Bereziuk SK, Potapov VA, Lepekhin EA (1996): Effects of low-intensity electromagnetic radiation of extremely high-frequency on the animal organism in combination with whole-body low-dose X-ray irradiation. Radiats Biol Radioecol 36:722–726 (in Russian).

Gun'ko VT, Kozshina NM (1993): Some complications of extremely high-frequency therapy. Millimetrovie Volni v Biologii i Meditcine 2:102–104 (in Russian).

Kaiser F (1995): Coherent oscillations - their role in the interaction of weak ELM-fields with cellular systems. Neural Network World 5:751–762.

Karlov VA, Rodshtat IV, Kalashnikov IuD, Kitaeva LV, Khokhlov IuK (1991): Experience with using extremely high frequency radiotherapy of the millimeter wave range in cerebrovascular disorders. Sov Med 3:20–21 (in Russian).

Kataev AA, Alexandrov AA, Tikhonova LL, Berestovsky GN (1993): Frequency-dependent effects of the electromagnetic millimeter waves on the ion currents in the cell membrane of Nitellopsis: Nonthermal action. Biofizika 38:446–462 (in Russian).

Kazbekov EN, Vyacheslavov LG (1987): Effects of microwave irradiation on some membrane-related processes in bacteria. Gen Physiol Biophys 6:57–64.

Khizhnyak EP, Ziskin MC (1996): Temperature oscillations in liquid media caused by continuous (nonmodulated) millimeter wavelength electromagnetic irradiation. Bioelectromagnetics 17:223–229.

Khramov RN, Sosunov EA, Koltun SV, Ilyasova EN, Lednev VV (1991): Millimeter-wave effects on electric activity of crayfish stretch receptors. Bioelectromagnetics 12:203–214.

Kolosova LI, Akoev GN, Avelev VD, Riabchikova OV, Babu KS (1996a): Effect of low-intensity millimeter wave electromagnetic radiation on regeneration of the sciatic nerve in rats. Bioelectromagnetics 17:44–47.

Kolosova LI, Akoev GN, Riabchikova OV, Avelev VD (1996b): The effect of low-intensity millimeter-range electromagnetic radiation on the functional recovery of the damaged sciatic nerve in rat. Fiziol Zh Im I M Sechenova 82:85–90 (in Russian).

Korpan NN, Saradeth T (1995): Clinical effects of continuous microwave for postoperative septic wound treatment: A double-blind controlled trial. Am J Surg 170:271–276.

Korpan NN, Resch K-L, Kokoschinegg P (1994): Continuous microwave enhances the healing process of septic and aseptic wounds in rabbits. J Surg Res 57:667–671.

Kotrovskaia TI (1994): Sensory reactions evoked by weak electromagnetic stimuli in humans. Millimetrovie Volni v Biologii i Meditcine 3:32–38 (in Russian).

Kremer F, Santo L, Poglitsh A, Koschnitzke C, Behrens H, Genzel L (1988): The influence of low intensity millimetre waves on biological systems. In Fröhlich H (ed): "Biological Coherence and Response to External Stimuli." Berlin: Springer-Verlag, pp 86–101.

Kudryashova VA, Zavizion VA, Khurgin YuV (1995): Effects of stabilization and destruction of water structure by amino acids. Moscow, Russia: 10th Russian Symposium "Millimeter Waves in Medicine and Biology," April, 1995 (Digest of papers). Moscow: IRE RAN, pp 213-215 (in Russian).

Kuzmanova M, Ivanov St (1995): Effect of millimeter waves and gamma-radiation on the surface electrical charge of erythrocyte membranes. In: "Millimeter Waves in Medicine and Biology," Digest of papers of the 10th Russian Symposium with International Participation, 24–26 April, Moscow, Russia, pp 111–112 (in Russian).

Kuz'menko VM (1989): Indications and contraindications to the use of microwave resonance therapy (MRT) in patients with cerebrovascular diseases. Kiev, Ukraine: First All-Union Symposium with International Participation "Fundamental and Applied Aspects of the Use of Millimeter Electromagnetic Radiation in Medicine," May, 1989, pp 272–273 (in Russian).

Lebedeva NN (1993): Sensor and subsensor reactions of a healthy man to peripheral effects of low-intensity millimeter waves. Millimetrovie Volni v Biologii i Meditcine 2:5–23 (in Russian).

Lebedeva NN (1995): Neurophysiological mechanisms of biological effects of peripheral action of low-intensity nonionizing electromagnetic fields in humans. Moscow, Russia: 10th Russian Symposium "Millimeter Waves in Medicine and Biology," April, 1995 (Digest of papers). Moscow: IRE RAN, pp 138–140 (in Russian).

Lebedeva NN, Betskii OV (1995): Application of low intensity millimeter waves in medicine. Boston, MA: 17th Annual Meeting of the Bioelectromagnetics Society, June, 1995, p 14.

Levina MZ, Veselago IA, Belaya TI, Gapochka LD, Mantrova GM, Yakovleva MN (1989): Influence of low-intensity VHF irradiation on growth and development of protozoa cultures. In Deyatkov ND (ed): "Millimeter Waves in Medicine and Biology." Moscow: Radioelectronica, pp 189–195 (in Russian).

Litvinov GS, Gridina NYa, Dovbeshko GI, Berezhinsky LI, Lisitsa MP (1994): Millimeter wave effect on blood plasma solution. Electromagnetobiology 13:167–174.

Liusov VA, Volov NA, Lebedeva AYu, Kudinova MA, Schelkunova IG, Fedulayev YuN (1995): Some mechanisms of the effect of millimeter-range radiation on pathogenesis of unstable angina pectoris. Moscow, Russia: 10th Russian Symposium "Millimeter Waves in Medicine and Biology," April, 1995 (Digest of papers). Moscow: IRE RAN, pp 26–27 (in Russian).

Logani MK, Ziskin MC (1996): Continuous millimeter-wave radiation has no effect on lipid peroxidation in liposomes. Radiat Res 145:231–235.

Megdiatov RS, Vasilenko AM, Arkhipov VV, Kislov VYa, Kolesov VV, Smirnov VF (1995): Use of a "Sharm" therapeutic-diagnostic system in complex therapy of trigeminal nerve neuralgia. Moscow, Russia: 10th Russian Symposium "Millimeter Waves in Medicine and Biology," April, 1995 (Digest of papers). Moscow: IRE RAN, pp 83–84 (in Russian).

Mikhno LE, Novikov SA (1992): The mechanism of the therapeutic action of millimeter electromagnetic waves and their importance in treating cardiovascular diseases (a review of the literature). Vrach Delo 10:14–18 (in Russian).

Mudrick DG, Golant MB, Izvol'skaia VE, Slutzkii EM, Oganezova RA (1995): Chemoluminescence of human blood leukocytes after exposure to a low-intensity extremely-high frequency electromagnetic field. Moscow, Russia: 10th Russian Symposium "Millimeter Waves in Medicine and Biology," April, 1995 (Digest of papers). Moscow: IRE RAN, pp 109–111 (in Russian).

Naumcheva NN (1994): Effect of millimeter waves on ischemic heart disease patients. Millimetrovie Volni v Biologii i Meditcine 3:62–67 (in Russian).

Novikova LN, Kaminskaia GO, Efimova LN (1995): Significance of the functional state of blood phagocytes in the choice of optimal regime of EHF therapy of patients with pulmonary tuberculosis. Probl Tuberk 6:17–20 (in Russian).

Osepchuk JM, Petersen, RC (1997a): Critical reviews of millimeter-wave athermal effect studies relative to microwave engineering principles. Brooks AFB, TX: Infrared Lasers and Millimeter

Waves Workshop "The Links Between Microwaves and Laser Optics," January, 1997.

Osepchuk JM, Petersen, RC (1997b): Comments on "Resonance Effect of Millimeter Waves in the Power Range from 10^{-19} to 3×10^{-3} W/cm2 on *Escherichia coli* Cells at Different Concentrations," Belyaev et al., Bioelectromagnetics, 17:312–321 (1996). Bioelectromagnetics 18:527–528.

Pakhomov AG, Prol HK, Mathur SP, Akyel Y, Campbell CBG (1997a): Search for frequency-specific effects of millimeter-wave radiation on isolated nerve function. Bioelectromagnetics 18:324–334.

Pakhomov AG, Prol HK, Mathur SP, Akyel Y, Campbell CBG (1997b): Frequency-specific effects of millimeter wavelength electromagnetic radiation in isolated nerve. Electromagnetobiology 16:43–57.

Pakhomov AG, Prol HK, Mathur SP, Akyel Y, Campbell CBG (1997c): Role of field intensity in the biological effectiveness of millimeter waves at a resonance frequency. Bioelectrochem Bioenerg 43:27–33.

Pakhomova ON, Pakhomov AG, Akyel Y (1997): Effect of millimeter waves on UV-induced recombination and mutagenesis in yeast. Bioelectrochem Bioenerg 43:227–232.

Poslavsky MV, Korochkin IM, Zdanovich OF (1989): Experience with application of millimeter-range radiation for treatment and prophylactics of stomach and duodenal ulcer. Vopr Kurortol Fizioter Lech Fiz Kult 4:31–36 (in Russian).

Postow E, Swicord ML (1986): Modulated fields and "window" effects. In Polk C, Postow E (eds): "Handbook of Biological Effects of Electromagnetic Fields." Boca Raton, FL: CRC Press, Inc. pp 425–460.

Potekhina IL, Akoyev GN, Yenin LD, Oleyner VD (1992): Effects of low-intensity electromagnetic radiation in the millimeter range on the cardio-vascular system of the white rat. Fiziol Zh 78:35–41 (in Russian).

Ragimov ChR, Ter-Asaturov GP, Golant MB, Rogov KA, Balakireva LZ (1991): Stimulation of reparative osteogenesis by electromagnetic oscillations in the millimeter range in traumatic defects of the lower jaw in experimental animals. Biull Eksp Biol Med 111:436–439 (in Russian).

Rebrova TB (1992): Effect of millimeter-range electromagnetic radiation on the vital activity of microorganisms. Millimetrovie Volni v Biologii i Meditcine 1:37–47 (in Russian).

Rodshtadt IV (1993): Physiological basis for some immune effects of millimeter-range radiation action on skin. Millimetrovie Volni v Biologii i Meditcine 2:24–35 (in Russian).

Rojavin MA, Ziskin MC (1995): Effect of millimeter waves on survival of UVC-exposed *Escherichia coli*. Bioelectromagnetics 16:188–196.

Rojavin MA, Ziskin MC (1998): Medical application of millimetre waves. Q J Med 91:57–66.

Roshchupkin DI, Kramarenko GG, Anosov AK, Golant MB (1994): Changes in the aggregation ability of rabbit thymocytes under the combined effect of UV-radiation and extremely high frequency radiation. Biofizika 39:1046–1050 (in Russian).

Roshchupkin DI, Kramarenko GG, Anosov AK (1996): Effect of extremely high frequency electromagnetic radiation and ultraviolet radiation on aggregation of thymocytes and erythrocytes. Biofizika 41:866–869 (in Russian).

Ryakovskaya ML, Shtemler VM (1983): Absorption of electromagnetic waves of millimeter range in biological preparations with a plane-layer structure. In: Devyatkov ND (ed): "Effect of Nonthermal Action of Millimeter Radiation on Biological Subjects." Moscow: USSR Academy of Sciences, pp 172–181 (in Russian).

Ryan KL, Frei MR, Berger RE, Jauchem JR (1996): Does nitric oxide mediate circulatory failure induced by 35-GHz microwave heating? Shock 6:71–76.

Ryan KL, Frei MR, Jauchem JR (1997): Circulatory failure induced by 35 GHz microwave heating: Effects of chronic nitric oxide synthesis inhibition. Shock 7:70–76.

Sazonov AYu, Zamuraev IN, Lukashin VG (1995): Effect of the extremely high frequency electromagnetic radiation on bush-like receptors of frog bladder. Fiziol Zh Im I M Sechenova 81:46–49 (in Russian).

Serebriakova SN, Dovganiuk AP (1989): The treatment of patient with peptic ulcer using millimeter-range waves. Vopr Kurortol Fizioter Lech Fiz Kult 4:37–38 (in Russian).

Shestopalova NG, Makarenko BI, Golovina LN, Timoshenko YuP, Baeva TI, Vinokurova LV, Miroshnichenko VS (1995): Modification of synchronizing effect of millimeter waves on first mitoses by different temperature regimens of germination. Moscow, Russia: 10th Russian Symposium "Millimeter Waves in Medicine and Biology," April, 1995 (Digest of papers) Moscow: IRE RAN, pp 236–237 (in Russian).

Shub GM, Luniova IO, Denisova SG, Ostrovskii NV (1995): Effects of millimeter waves on bacteria in in vitro and in vivo experiments. Moscow, Russia: 10th Russian Symposium "Millimeter Waves in Medicine and Biology," April, 1995 (Digest of papers). Moscow: IRE RAN, pp 96–97 (in Russian).

Smirnov AIu, Zinovev SV, Bogoliubov VM (1991): An experimental study of the action of weak-intensity superhigh-frequency electromagnetic radiation in the millimeter range on metastasis of malignant neoplasms. Vopr Kurortol Fizioter Lech Fiz Kult 4:23–27 (in Russian).

Tambiev AH, Kirikova NN (1992): Perspectives of the application of millimeter-range electromagnetic radiation in photobiotechnology. Millimetrovie Volni v Biologii i Meditcine 1:48–54 (in Russian).

Tambiev AKh, Kirikova NN, Lapshin OM, Betzkii OV, Novskova TA, Nechaev VM, Petrov IYu (1989): The combined effect of exposure to EMF of millimeter and centimeter wavelength ranges on productivity of microalgae. In Devyatkov ND (ed): "Millimeter Waves in Medicine and Biology." Moscow: Radioelectronica, pp 183–188 (in Russian).

Temur'iants NA, Chuyan EN (1992): Effect of nonthermal microwaves on hypokinetic stress development in rats with different individual features. Millimetrovie Volni v Biologii i Meditcine 1:22–32 (in Russian).

Temur'iants NA, Chuyan EN, Tumaniants EN, Tishna OO, Victorov NV (1993): Dependence of anti-stress effects of millimeter-range electromagnetic fields on localization of the exposed area in rats with different typological features. Millimetrovie Volni v Biologii i Meditcine 2:51–59 (in Russian).

Temur'iants NA, Chuyan EN, Khomiakova OV, Tishkina OO (1994): Dependence of the stress-protective effect of extremely-high-frequency electromagnetic radiation on parameters of irradiation. Millimetrovie Volni v Biologii i Meditcine 3:11–15 (in Russian).

Tsutsaeva AA, Makarenko BI, Beznosenko BI, Gomosov VI, Simonova NYa, Kovalenko LA, Shatilova LE, Tupchienko GS, Nikitash AV, Kudokotseva OV, Rozniak AI, Lisenko NA, Shurda GG (1995): Radioprotective effect of microwave action. Millimeter Waves in Medicine and Biology, Digest of papers of the 10th Russian Symposium with International Participation, 24-26 April, Moscow, Russia, pp 123–124 (in Russian).

Zavizion VA, Kudriashova VA, Khurgin YuI (1994): Effect of alpha-amino acids on the interaction of millimeter-wave radiation with water. Millimetrovie Volni v Biologii i Meditcine 3:46–52 (in Russian).

Zemskov VS, Korpan NN, Khokhlich IaI, Pavlenko VA, Nazarenko LS, Koval'chuk AI, Stefanishin IaI (1988): Effect of millimeter-band low intensity electromagnetic radiation on the course of wound healing. Klin Khir 1:31–33 (in Russian).

Physiology & Behavior, Vol. 65, No. 2, pp. 263–270, 1998
© 1998 Elsevier Science Inc. All rights reserved.
Printed in the U.S.A.
0031-9384/98 $19.00 + .00

ELSEVIER

PII S0031-9384(98)00165-6

Ultra-Wideband Electromagnetic Pulses and Morphine-induced Changes in Nociception and Activity in Mice

RONALD L. SEAMAN,[1] MICHELLE L. BELT, JOANNE M. DOYLE AND SATNAM P. MATHUR

McKesson BioServices and Microwave Bioeffects Branch, U.S. Army Medical Research Detachment, Brooks AFB, TX 78235 USA

Received 17 November 1997; Accepted 15 May 1998

SEAMAN, R. L., M. L. BELT, J. M. DOYLE AND S. P. MATHUR. *Ultra-wideband electromagnetic pulses and morphine-induced changes in nociception and activity in mice.* PHYSIOL BEHAV **65**(2) 263–270, 1998.—Mice were exposed to ultra-wideband (UWB) electromagnetic pulses averaging 99–105 kV/m peak amplitude, 0.97–1.03 ns duration, and 155–174 ps rise time, after intraperitoneal administration of saline or morphine sulfate. They were then tested for thermal nociception on a 50°C surface and for spontaneous locomotor activity and its time profile over 5 min. Analysis of results showed no effect of UWB exposure on nociception and activity measures in CF-1 mice after 15-, 30-, or 45-min exposure to pulses at 600/s or after 30-min exposure to UWB pulses at 60/s. Similarly, no effect was seen in C57BL/6 mice after 30-min exposure to pulses at 60/s or 600/s. Although trends in morphine-modified measures seen with UWB pulse repetition frequency could be expected because of increased levels of low-frequency energy, no significant change was seen in normal or morphine-modified nociception or activity after UWB exposure. This indicated lack of effect of the UWB pulses used in these experiments on nervous system components, including endogenous opioids, involved in these behaviors. © 1998 Elsevier Science Inc.

Ultra-wideband pulses Electromagnetic fields Nociception Analgesia Hyperactivity Hypoactivity Morphine

CONCERN has grown for the health and safety of individuals, including military personnel, exposed to ultra-wideband (UWB) radiation as it is being considered for more and more applications. This form of non-ionizing electromagnetic radiation is most commonly described in terms of electric field pulses. Practical UWB pulses typically have amplitudes of 10–100 kilovolts/meter (kV/m), durations on the order of a few nanoseconds (ns), and rise times of 100–200 picoseconds (ps). The pulses can be produced at repetition frequencies into the megahertz (MHz) range. Each pulse has a broad frequency spectrum that can extend from DC, or 0 Hz, to several gigahertz (GHz)—static to microwave-frequency fields. These characteristics are useful in radar-like imaging and jamming applications (1), and the technology to produce more powerful UWB sources is developing rapidly (4). The few studies of UWB biologic effects report no effect in animal cardiovascular and behavioral endpoints during and after exposure lasting 2 min or less (13,14,35,43). Because of concern for health and safety issues related to UWB pulses, experiments with other endpoints and longer UWB exposures are desired to provide further information on UWB biologic effects.

Effects of electromagnetic fields on opioid and related systems have been observed in a number of laboratories. These fields are too small to elevate tissue temperature to a degree that might cause observed effects. Although effects have been seen for different types of fields and a variety of endpoints (9,21,23), most studies have been on changes in nociception after exposure to low-frequency magnetic fields. In CF-1 mice, a 0.5 Hz rotating magnetic field reduces analgesia (antinociception) induced by morphine (16) and stress (18). Morphine-induced analgesia in these mice is also reduced by 60-Hz magnetic fields (31) and electromagnetic fields used in magnetic resonance imaging (MRI) (32,33). In CD-1 mice, a static magnetic field reduces stress-induced analgesia (6). In Wistar rats, a pulsed magnetic field increases the response threshold to electrical shock (8). Observations of similar effects in an invertebrate model indicate action on basic nervous system components. Analgesic behavior induced in a land snail by opiate agonists is reduced with a 0.5-Hz rotating magnetic field (19), 60 Hz magnetic fields (42), and magnetic resonance imaging fields (32) but is increased with a pulsed magnetic field (39). The 60-Hz fields also cause an analgesia-like antinociception in the snail (20), as does a specific pulsed magnetic field (39,40).

Other studies show that effects of magnetic fields in rodents are not limited to those on nociception. A 0.5-Hz rotating magnetic field attenuates increased spontaneous locomotor activity in C57BL

[1] Requests for reprints should be addressed to Ronald L. Seaman, McKesson BioServices, P.O. Box 35460, Brooks AFB, TX 78235-5460. E-mail: ronald.seaman@aloer.brooks.af.mil

mice induced by morphine (16) and stress (18). Learning of a water-maze task is improved after exposure to a 60-Hz magnetic field in meadow voles (15) and deer mice (22). However, learning by rats is decreased in a 12-arm radial maze after exposure to a 60-Hz magnetic field (24) and in a 4-arm maze between repeated exposures to a pulsed magnetic field (41).

Collectively, the studies on nociception, activity, and learning indicate action on the nervous system by magnetic fields of various frequencies and modulations. Involvement of opioid receptors in these studies has been confirmed by use of opioid agonists and antagonists (17,18,21,22,38,39). Opioid receptors are also involved in changes in brain chemistry caused by 2.45-GHz microwaves (2-s pulses, 500 pulses per s, average 1 mW/cm^2, 0.6 W/kg) (23,25,26), indicating that effects are not solely related to low-frequency magnetic fields. This same microwave exposure also causes retarded learning by rats in a 12-arm radial maze and involves cholinergic and opioid systems (23,27). Analgesia in mice, due in part to opioids, has also been observed after exposure to higher levels of continuous-wave 2.45-GHz microwaves (CW, 20 mW/cm^2, 46 W/kg), which produced an average 1.6°C increase in body temperature (28).

Although repetitive, extremely short UWB pulses are quite different from the sinusoidal and pulsed magnetic fields used in previous work; frequencies used in the earlier work are represented in the broad frequency spectra of the electric and magnetic fields of UWB pulses. This representation indicates that UWB pulses may also be able to modify nociception, activity, and other behaviors. However, the unique characteristics of UWB pulses do not allow direct use of results from earlier studies. As shown by the previous work, tests of nociception and spontaneous locomotor activity provide sensitive and robust assays for effects of electromagnetic fields. Results of the tests are very likely to be indicative of effects on other systems and other behaviors involving opioid receptors, which are widespread in the animal kingdom [e.g., (11,21,36)]. Knowledge of UWB biologic effects, or lack of them, is important for protection of military personnel and other persons and for development of appropriate safety standards. The experiments described here used controlled UWB exposures of two strains of mice to test for effects on endogenous nociception and spontaneous locomotor activity and on morphine-induced changes in the two behaviors to provide knowledge on the biologic effects of UWB pulses.

GENERAL METHODS AND MATERIALS

Animals

Male CF-1/Plus white mice (Charles River Labs, Portage, MI, USA) and male C57BL/6-VAF/Plus black mice (Charles River Labs, Portage, MI, and Raleigh, NC, USA) were used in separate experiments. After a 10-day quarantine period, mice were housed in polycarbonate shoe box cages with ad lib. Purina rodent chow and tap water. The controlled environment of the animal room included temperature of 22 ± 1°C, relative humidity of 50 ± 5%, air flow of 10–15 exchanges per hour, and a 12/12 light/dark cycle. The light period started at either 0500 or 0600 hours, with only one lights-on time for a particular group of animals. All exposures and tests were done 7–10 h after lights on.

Nociception and Activity Tests

Nociception was tested by placing the animal on a metallic surface heated by circulating water, to 49.5–50.5°C across all experiments. The animal was within an upright, open cylinder made of clear plastic with inside diameter of 14.5 cm. In early experiments, latency to licking a front paw and latency to licking a back paw in response to the heated surface were measured by an observer using a stopwatch. To have a more reliable early measure of nociception, front-paw latency was replaced in later experiments by latency to the first response to the heated surface. The first response consisted of lifting, shaking, or licking a paw or jumping. The animal was removed from the hot plate after licking a back paw. If a back paw was not licked after 160 s, the animal was removed and this time was assigned to the latency. If a front-paw lick or other first response did not occur before back-paw licking, the back-paw latency was also assigned to the earlier response.

Spontaneous locomotor activity was tested by placing the animal in a 38.5-cm square arena with 24-cm walls for 5 min with room lights off. Animal movement interrupted light beams crossing the arena, with five beams in each horizontal direction. A computer registered and counted beam interruptions. A count for each minute of the test was recorded.

The order of testing was different in different experiments. The primary measure of interest was tested first: nociception for CF-1 mice and activity for C57BL/6 mice. An animal was returned to its home cage after completion of testing.

UWB Exposure

Exposure to UWB pulses was accomplished with a custom-built giga transverse electromagnetic (GTEM) cell originally constructed by Sandia National Laboratories (Albuquerque, NM, USA). The cell, a tapered two-conductor transmission line with a square cross section, was positioned so that one ground plane wall was horizontal. A modified RG-220 coaxial cable connecting the center conductor of the GTEM cell to a source of high voltage included a spark gap. Ionization of pressurized nitrogen gas in the spark gap resulted in high voltage pulses that led to UWB pulses propagating in the GTEM cell, with the electric field vector directed from the center conductor to the ground conductor. Two four-inch speakers outside the GTEM cell provided broadband noise for auditory masking of UWB system operation. The 74–75 dBA noise consisted of 56 ± 7 dB SPL (mean ± SD) from 50 Hz to 20 kHz (third octave analysis using Brüel & Kjaer sound level meter Type 2230 and 1/3 octave filter set Type 1625).

The UWB pulses in the GTEM cell were monitored during animal exposures using signals from an EG&G ACD(A) D-dot probe mounted in the wall of the cell. The signals were sampled with 0.01-ns resolution by a Tektronix SCD 5000 Transient Digitizer. Each digitized waveform, representing the average of 200 individual pulses, was stored and later processed using a correction algorithm (3) to give pulse electric field versus time. UWB pulses were triggered by an external pulse generator at either 60/s (60 pulses per s) or 600/s. Specific absorption rate (SAR) was estimated to be 3.7 mW/kg for UWB pulses at 60/s and 37 mW/kg for UWB pulses at 600/s [Note: Estimates of whole-body SAR were made by W. D. Hurt (Radiofrequency Radiation Division, Air Force Research laboratory, Brooks AFB) using the power spectrum of the corrected UWB pulse electric field and the frequency-dependent normalized SAR (in W/kg per mW/cm^2) for a prolate spheroidal model of a medium-sized mouse (Durney, C. H.; Massoudi, H.; Iskander, M. F. Radiofrequency radiation dosimetry handbook. Technical Report USAFSAM-TR-85–73. Brooks Air Force Base: USAF School of Aerospace Medicine; 1986). The integral of the product of these two functions in the frequency domain was mulitiplied by the ratio of pulse duration to repetition period (duty cycle) to obtain an SAR value. The average of results for k- and H-polarizations of the animal was used to account for the movement of the animal in the UWB field.]. For sham exposure, all conditions and procedures were the same except that no pulses were triggered (0/s).

Three parameters were used to characterize UWB pulse electric field: peak amplitude, rise time, and duration. These parameters, particularly peak amplitude, were adjusted by changing nitrogen gas pressure to achieve consistency across experiments. Peak amplitude was a nominal 100 kV/m. Rise time was typically less than 200 ps. Half-amplitude duration was a nominal 1 ns. Mean ± SD of each parameter is given for reported experiments.

A holder made from clear plastic was placed in the GTEM cell on the horizontal ground plane for animal exposure to UWB pulses. It consisted of an upright cylinder with 0.32-cm walls and 12.1-cm internal diameter, a floor of four concentric loops of 0.63-cm plastic rod, and a plastic cover. The animal was thus in a circular chamber with a 12.1-cm diameter and a vertical space of 4.6 cm between floor and cover. The floor supported the animal 3.8 cm above the ground plane, a distance sufficient to prevent contact of the animal's tail with the ground plane. Holes in the cylinder below the floor and in the cover allowed air to flow at the animal location. An animal exhibited normal spontaneous behavior while in the well-ventilated holder.

Common Procedures

Animals were first injected intraperitoneally (i.p.) with 0.9% saline or morphine sulfate in saline (1 mg/mL of the salt). An animal to be exposed was then placed in a holder and positioned in the GTEM cell. At the end of exposure, the animal was taken from the GTEM cell and the holder and tested for nociception and spontaneous locomotor activity. A cage control animal was returned to its home cage after injection and was later removed for testing after a period matching the exposure duration in the respective experiment. A cage control animal was thus not exposed to UWB pulses nor did it experience the holder or the GTEM cell. The noise level in the GTEM cell at the location of the animal holder was checked daily with a Realistic 33–2055 sound level meter and adjusted if necessary to 74–75 dBA. Low-frequency magnetic fields were also measured daily with a Dexsil Magnum 310 three-axis digital gaussmeter at three locations: at the home cage in the laboratory, near the GTEM cell, and immediately above the heated surface device. Measured magnetic fields were 0.08–1.72 mG, 0.04–2.80 mG, 0.04–0.88 mG at the respective locations, with similar results using the 60 Hz and 40–310 Hz filters of the meter.

Analysis of Results

Two-way ANOVA was performed separately on front-paw or first-response latency, back-paw latency, and total activity count with morphine and UWB as factors. ANOVA was also performed on the time profile of activity count with repeated measures on time. This was a three-way test with morphine, UWB, and time as factors in experiments with saline controls and a two-way test with UWB and time as factors in experiments without saline. Significant effects in ANOVAs were further investigated using pair-wise comparisons with Newman–Keuls testing. The difference between cage and sham conditions for each measure was tested with a Student's *t*-test with Bonferroni correction. When only two conditions were to be tested, a Student's *t*-test was used. Statistical tests were performed using GB-STAT software (Dynamic Microsystems, Silver Spring, MD, USA). The significance level was 0.05 in all tests.

EXPERIMENTS WITH WHITE MICE

In the initial experiment with white mice only nociception was measured. The experiment was patterned after experiments showing effects of magnetic fields on stress- and morphine-induced analgesia (16,17,18,31) by choices of strain of mouse, nociception test, and 30-min exposure. A lower dose of morphine (7.5 vs. 10 mg/kg) was used in an attempt to minimize the number of animals reaching the maximum allowed time on the heated surface. Two UWB pulse repetition frequencies were used: 60/s and 600/s. The lower frequency was chosen to maximize energy at 60 Hz, an effective frequency in previous magnetic-field studies. The higher frequency was the greatest repetition frequency available for the UWB pulses during a 30-min exposure, providing a maximum UWB "dose" in terms of number of pulses delivered.

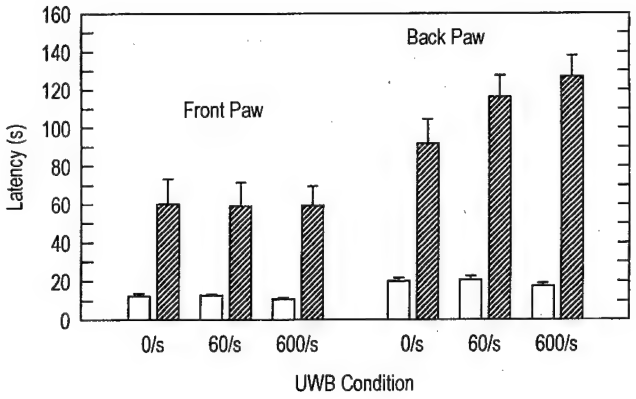

FIG. 1. Latencies (mean + SEM) to front-paw licking and back-paw licking on the heated surface for CF-1 mice injected with saline (open bars) or 7.5 mg/kg morphine sulfate (shaded bars) and exposed to UWB pulses at 0/s (sham), 60/s, or 600/s for 30 min. Measures are from the same animals with $n = 20$ for each of the six groups.

METHODS

Male CF-1 mice housed three to five per cage weighed 32–50 g and were 10–12 weeks of age when used. Animals were assigned in sequence to one of eight morphine/UWB conditions, with all conditions being delivered randomly in a block before their next delivery. The three UWB conditions consisted of UWB pulses at 0/s (sham), 60/s, and 600/s with exposure duration of 30 min. A cage control condition was also included (see common procedures above). The morphine conditions were 0 mg/kg (saline) and 7.5 mg/kg morphine sulfate. Front paw-licking and back paw-licking latencies were measured on the 50°C surface in twenty animals for each morphine/UWB condition, resulting in twenty blocks of the conditions, with each animal used only once. Measured UWB pulse parameters were 105.0 ± 5.5 kV/m peak amplitude, 0.97 ± 0.02 ns duration, and 165.0 ± 6.3 ps rise time for 60/s. Corresponding values were 100.1 ± 6.1 kV/m, 0.97 ± 0.02 ns, and 167.9 ± 10.5 ps for 600/s.

RESULTS AND DISCUSSION

Latencies to licking front paw and back paw for the white mice are shown in Fig. 1. For each measure, mean latency for saline was nearly the same across UWB conditions, 10.8–12.3 s for front-paw licking and 17.5–20.5 s for back-paw licking. Morphine clearly induced analgesia, increasing each latency by several-fold over the respective saline-control value for each UWB condition. Respective sham and cage mean latencies were not different for saline for either latency or for morphine for back-paw latency. Mean sham latency was longer than mean cage latency for front-paw latency for morphine, indicating some effect of being placed in the animal holder and/or the GTEM cell. Mean front-paw latency was 58.9–

60.3 s for morphine across UWB conditions. ANOVA (2 × 3) indicated no significant effect of morphine-UWB interaction or UWB [$F(2, 114)<1$] but a significant main effect of morphine [$F(1, 114) = 47.94$, $p < 0.0001$]. Mean back-paw latency was 91.9–126.8 s for morphine. Despite the increase in mean back-paw latency with higher UWB pulse repetition frequency, morphine-UWB interaction was not significant [$F(2, 114) = 2.49$, $p = 0.087$], as was the UWB main effect [$F(2, 114) = 2.02$, $p = 0.137$]. But, as for front-paw latency, a significant main effect of morphine was indicated [$F(1, 114) = 178.72$, $p < 0.0001$]. Respective Newman–Keuls comparisons revealed a strong effect of morphine to increase each latency for each UWB condition. Results of this initial experiment with white mice showed the expected effect of morphine to increase response latencies but no effect of 30-min exposure to UWB pulses at 60/s or 600/s on either latency.

Additional Experiments

Three additional experiments were performed with white mice. These experiments were similar to the initial one but differed in the duration of exposure to UWB pulses and the addition of spontaneous locomotor activity measurement after latency measurements on the 50°C surface. Animal size and age as well as UWB pulse parameters were quite similar to those in the initial experiment.

In two experiments, animals were injected with morphine and exposed to UWB pulses at either 0/s (sham) or 600/s. The 30-min UWB exposure in the first experiment had no significant effect on first-response latency [$t(38) = 0.0084$, $p = 0.993$] or back-paw latency [$t(38) = 1.15$, $p = 0.257$]. For activity, no significant effect of UWB [$F(1, 38) = 2.36$, $p = 0.132$] or UWB-time interaction [$F(4, 152) < 1$] was found. A decline of activity counts with minute of test for both UWB conditions was reflected in a significant main effect of time [$F(4, 152) = 11.56$, $p < 0.0001$]. Similar results were obtained using a 45-min exposure in the second experiment, except that a slower decline in activity with minute of test after UWB exposure than after sham exposure was reflected in a significant UWB-time interaction [$F(4, 152) = 3.53$, $p = 0.0087$].

In another experiment, animals were injected with morphine or saline and exposed to UWB pulses at either 0/s (sham) or 600/s for 15 min. Morphine-induced analgesia was reflected in significant main effects of morphine on first-response latency [$F(1, 76) = 29.05$, $p < 0.0001$] and back-paw latency [$F(1, 76) = 109.05$, $p < 0.0001$]. However, the main effects of UWB and morphine-UWB interaction were not significant [$F(1, 76)<1$ or $F(1, 76) = 1.82$, $p = 0.181$]. Morphine had a significant effect to decrease activity [$F(1, 76) = 9.27$, $p < 0.0032$]. But UWB and morphine-UWB interaction, as well as UWB and morphine interactions with time, did not significantly influence activity [$F(1,76)<1$ or $F(4,304)<1$]. A decline of activity with minute of test, common to all conditions, was reflected in a significant main effect of time [$F(4, 304) = 22.51$, $p < 0.0001$].

The results of the three additional experiments were consistent with the results of the initial experiment with white mice. For exposure durations of 15, 30, and 45 min, UWB did not have a significant effect on post-exposure measures of response latencies on the heated surface or spontaneous locomotor activity. A significant effect of time on activity reflected the decline in counts during the 5-min activity test after each exposure duration. A significant effect of morphine was seen for each latency and on activity after 15-min exposure.

EXPERIMENT WITH BLACK MICE

In another early experiment, activity was measured in black mice. The experiment was patterned after experiments showing effects of magnetic fields on stress- and morphine-induced hyperactivity (16,18) by choices of mouse strain, 30-min exposure, and morphine dose. A testing period of activity longer than the previously used 1 min was used because morphine-induced increases could not be detected during 1-min tests in preliminary experiments. The two UWB pulse repetition frequencies used, 60/s and 600/s, were chosen for the same reasons as for the initial experiment with white mice. Nociception testing was included to gather information on additional endpoints.

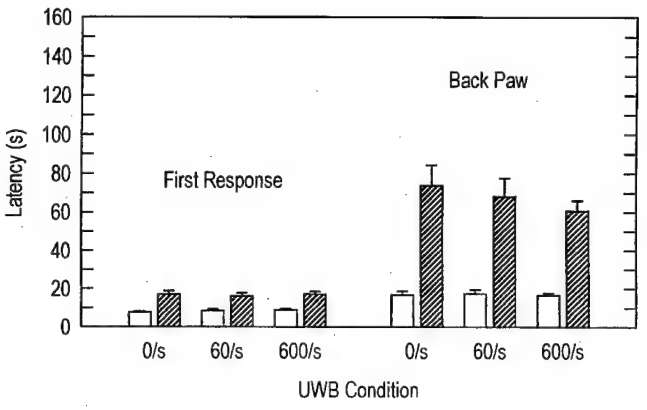

FIG. 2. Latencies (mean + SEM) to first response and back-paw licking on the heated surface for C57BL/6 mice injected with saline (open bars) or 10 mg/kg morphine sulfate (shaded bars) and exposed to UWB pulses at 0/s (sham), 60/s, or 600/s for 30 min. Measures are from the same animals with $n = 20$ for each of the six groups for first response. For back paw, $n = 20$ for saline-600/s and morphine-0/s groups and $n = 19$ for the other four groups.

Methods

Male C57BL/6 mice housed one to three per cage weighed 22–30 g and were 8–17 weeks of age when used. An animal was housed singly if aggressive home-cage behavior was detected. As in the initial experiment with white mice, animals were assigned in sequence to one of eight morphine/UWB conditions, with all conditions delivered randomly in a block before their next delivery. The three UWB conditions consisted of UWB pulses at 0/s (sham), 60/s, and 600/s, with exposure duration of 30 min. A cage condition was also included (see common procedures above). The morphine conditions were 0 mg/kg (saline) and 10 mg/kg morphine sulfate. Twenty animals were tested for each morphine/UWB condition, resulting in 20 blocks of the conditions, with each animal used only once. Activity in the arena was measured and then first-response and back paw-licking latencies were measured on the 50°C surface. Due to technical problems, only 19 data were available for back-paw latency for saline-0/s, saline-60/s, morphine-60/s, and morphine-600/s conditions and for activity by minute of test for saline-60/s and saline-600/s conditions. Measured UWB pulse parameters were 104.6 ± 3.7 kV/m peak amplitude, 1.03 ± 0.03 ns duration, and 165.8 ± 4.1 ps rise time for 60/s. Corresponding values were 99.0 ± 2.2 kV/m, 1.03 ± 0.03 ns, and 164.9 ± 5.4 ps for 600/s.

RESULTS AND DISCUSSION

Latencies to first response and back-paw licking for the black mice are shown in Fig. 2. For each measure, mean latencies for saline were similar across UWB conditions, 7.7–9.0 s for first response and 16.6–17.4 s for back-paw licking. Analgesia was indicated by increases in each latency with morphine, first-

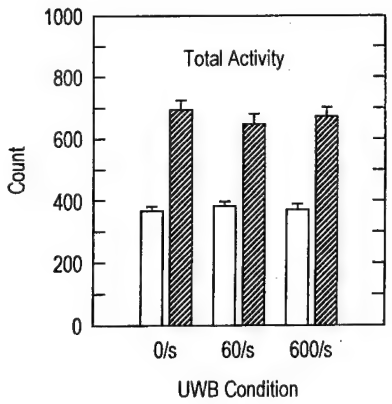

FIG. 3. Total activity count (mean + SEM) for C57BL/6 mice injected with saline (open bars) or 10 mg/kg morphine sulfate (shaded bars) and exposed to UWB pulses at 0/s (sham), 60/s, or 600/s for 30 min. Measures are from the same animals as in Fig. 2 with $n = 20$ for each of the six groups.

response approximately doubling and back-paw licking increasing three- to fourfold. Respective sham and cage latencies were not different for saline or morphine for either latency. First-response mean latencies were 16.3–17.9 s for morphine across UWB conditions. ANOVA (2×3) indicated no significant effect of morphine-UWB interaction or UWB [$F(2, 114) < 1$] but a significant main effect of morphine [$F(1, 114) = 58.95$, $p < 0.0001$]. For back-paw latency, mean latencies were 91.9–126.8 s for morphine, decreasing with greater UWB-pulse repetition frequency. However, ANOVA indicated no significant effect of morphine-UWB interaction or UWB [$F(2, 110) < 1$]. As for first-response latency, a significant main effect of morphine was indicated [$F(1, 110) = 96.02$, $p < 0.0001$]. Respective Newman–Keuls comparisons showed a significant, strong effect of morphine to increase each latency measure for each UWB condition.

Total activity count is shown in Fig. 3. Mean activity count was similar across UWB conditions: 368–372 for saline and 649–695 for morphine. Respective cage and sham mean activity counts were not different. ANOVA (2×3) indicated no significant effect of morphine-UWB interaction or UWB [$F(2, 114) < 1$], but, as for latencies, a significant main effect was indicated for morphine [$F(1, 114) = 227.39$, $p < 0.0001$]. Newman–Keuls comparisons showed the same results as for latencies—a strong, significant effect of morphine to increase the mean count for each UWB condition.

Activity count by minute of test is shown in Fig. 4. Mean activity declined with time for saline conditions but increased and reached a plateau for morphine conditions. The respective change was similar for all UWB conditions. Respective cage and sham mean activity counts were not different for each minute of test. ANOVA ($2 \times 3 \times 5$, repeated measures) indicated significant effects of morphine-time interaction [$F(4, 456) = 71.35$, $p < 0.0001$], morphine [$F(1, 114) = 230.58$, $p < 0.0001$], and time [$F(4, 456) = 11.01$, $p < 0.0001$]. The significant interaction reflected the difference in activity time profile between morphine conditions evident in Fig. 4. No significant effect was indicated for morphine-UWB interaction or UWB [$F(2, 114) < 1$]; UWB-time interaction [$F(8, 456) = 1.65$, $p = 0.109$]; or morphine-UWB-time interaction [$F(8, 456) = 1.59$, $p = 0.125$]. Respective Newman–Keuls comparisons showed that mean counts during each minute of test were significantly different between saline and morphine conditions for each UWB condition.

Results of this experiment with black mice showed the expected effects of morphine to cause analgesia and hyperactivity. However, analysis indicated a lack of effect of UWB pulses at 60/s and 600/s for 30 min on nociception as well as on spontaneous locomotor activity. The nociception results were consistent with a preliminary experiment in which no effect of 30-min UWB exposure was seen on latencies to front-paw and back-paw licking.

GENERAL DISCUSSION

The effect of morphine was clearly seen in each experiment and was reflected in respective significant main effects. Morphine increased both latency measures on the heated surface for both CF-1 and C57BL/6 mice (Figs. 1 and 2) as expected from the known analgesic action of morphine in these strains (5,10,16,17). Under the same test conditions and with similar morphine doses, latency increases were more pronounced for CF-1 mice than for C57BL/6 mice. Overall, the effects of morphine on nociception were quite similar to those seen in previous work.

Morphine effects on activity measures were also similar to

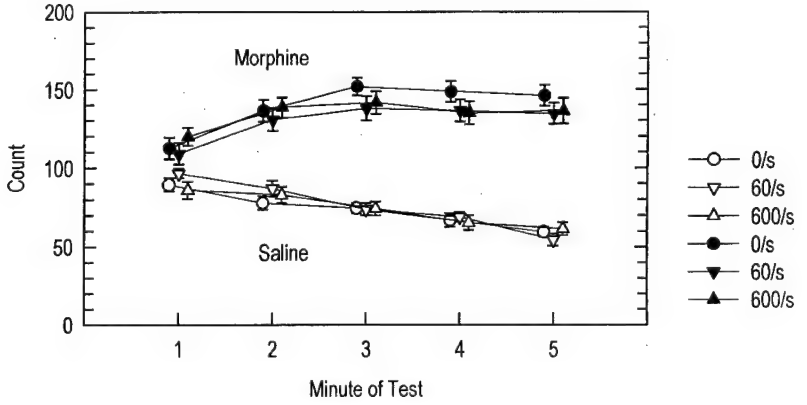

FIG. 4. Activity count (mean ± SEM) by minute of test for C57BL/6 mice injected with saline or 10 mg/kg morphine sulfate and exposed to UWB pulses at 0/s (sham), 60/s, or 600/s for 30 min. Data correspond to total activities in Fig. 3 but with $n = 19$ for saline-60/s and saline-600/s groups.

those seen in previous work. The increased spontaneous locomotor activity in C57BL/6 mice with morphine (Fig. 3) was consistent with previous findings for this and other strains in tests of various durations (7,16,18,29,44). The corresponding change in the activity time profile (Fig. 4) was similar to increases in C57BL/6J mice 30 min after morphine injection (2,5,30). The decreases in the activity measure for CF-1 mice seen 30 min after 7.5 mg/kg morphine was opposite to the increases seen in this strain for similar and higher morphine doses in longer tests (29,44). However, the decrease was consistent with initial periods of hypoactivity after morphine injection seen in various mouse strains (7,34,37). The hypoactivity could explain the small net changes in CF-1 activity after morphine sulfate injection in 4-h and 90-min tests (29,44). The measurements in this study at 15–45 min postinjection could have well occurred during such an initial or early period of hypoactivity. The decline in activity with time for CF-1 mice supported this pattern of activity. The consistency of morphine effects on nociception and spontaneous locomotor activity with respect to previous work assured reliable bases for testing possible modification by UWB pulses.

No significant effect of UWB exposure was found on nociception in these experiments. This was the case for function without morphine and for morphine-induced changes in nociception. However, some trends in nociception occurred with UWB exposure. Mean latency to back-paw licking in CF-1 mice tended to increase with UWB exposure. The increase was larger for higher UWB pulse repetition frequency for 30-min exposure (Fig. 1). The trend of increased latency was opposite to the effect of static and low-frequency magnetic fields and MRI fields to decrease analgesia (6,16,18,31–33). However, the trend was in the same direction as the effect of pulsed magnetic fields to induce analgesia and increase opiate-mediated analgesia (8,39,40). On the other hand, mean back-paw latency in C57BL/6 mice with morphine tended to decrease with repetition frequency (Fig. 2), consistent with the findings for decreased analgesia after exposure to magnetic fields that were not pulsed.

Similarly, no significant effect of UWB exposure was found on spontaneous locomotor activity. As for nociception, this was the case for normal activity and for morphine-induced changes in activity. However, some trends in activity also occurred with UWB exposure. The CF-1 mice tended to be more active after all durations of UWB exposure to pulses at 600/s. For 15-min UWB exposure, the effect was to counteract a decrease in activity due to morphine. For 45-min exposure, the effect was to change the shape of the activity time profile, reflected in a significant interaction between UWB exposure and minute of test. In C57BL/6 mice, the trend was for the morphine-increased activity to decrease weakly with UWB exposure (Figs. 3 and 4), opposite to the trend in CF-1 mice but in the same direction as the change caused by low-frequency magnetic fields (16).

The lack of significant effect of UWB pulses is consistent with results of UWB studies with behavioral and cardiovascular endpoints and 2-min or shorter exposures. Performance on an equilibrium platform was not changed in monkeys after 2-min exposure to 250 kV/m, 5–10 ns pulses at 60/s (35). No change in a functional observational battery was seen in rats after exposure with the same parameters (43). Tests included home cage and open field behaviors as well as motor activity and grip strength. Heart rate and blood pressure were not changed in anesthetized rats by exposure to single and 2-min trains of 0.5-s bursts of 19–21 kV/m, 6-ns pulses at 1000/s (13) or by 2-min exposure to 87–104 kV/m, 1-ns pulses at 50/s, 500/s, and 1000/s (14). However, awake rats exposed for 6 min to 1 ns pulses at 93 kV/m at 500/s or 85 kV/m at 1000/s exhibited hypotension without a change in heart rate for up to 4 weeks after exposure (S. T. Lu, personal communication 1998).

In this study, delivered UWB pulses were similar in amplitude, duration, and rise time across experiments, even between the 60/s and 600/s repetition frequencies. The similarity assured that animals received exposures to UWB pulses that differed only in repetition frequency and exposure duration. Although no method currently exists to measure UWB fields inside the animal holder or the animal, we are certain that a broad range of frequencies was represented. Computed frequency spectra of measured UWB pulse electric field showed that more than an estimated 95% of pulse energy was carried by frequencies between 0 and 0.2 GHz (200 MHz). Because of the unipolar nature of the UWB pulses a substantial amount of this energy was at or near 0 Hz, which includes frequencies used in previous studies on effects of magnetic fields on nociception and activity. The estimated SARs of 3.7 mW/kg for pulses at 60/s and 37 mW/kg for pulses at 600/s were too small to cause detectable temperature rise. The SAR values were much smaller than 0.4 W/kg, the maximum allowable whole-body SAR used in radiofrequency/microwave exposure standards (12).

The animals in this study experienced two types of magnetic fields, those of the UWB pulses and those in the laboratory environment. Using a nominal UWB pulse amplitude of 100 kV/m and a wave impedance of 377 ohms in the GTEM cell, we estimated the propagating peak magnetic field of an individual pulse to be 3.3 G (0.33 mT). Due to the small fraction of time the pulses occupied, the time-averaged field was many times smaller, approximately $6 \cdot 10^{-8}$ and $6 \cdot 10^{-7}$ of the peak field for UWB pulses at 60/s and 600/s, respectively. The measured low-frequency magnetic fields in the laboratory of 0.04–2.80 mG ($4 \cdot 10^{-6}$–$2.8 \cdot 10^{-4}$ mT) were similar for all animals. In previous studies showing effects, static and low-frequency magnetic fields of 0.5–90 G (0.05–9.0 mT) for mice and snails (6,16,17,18,19,31) were larger than the measured laboratory fields. Microwave pulsed peak magnetic fields (25,26,27) estimated as 3.55 G (0.355 mT) for rats and pulsed magnetic fields with peaks of 0.01–0.05 G (0.001–0.005 mT) for rats (8,41) and 100 μT (0.1 mT) for snails (39,40) were also larger. Thus, the magnitude of effective magnetic fields in previous studies was similar to the magnitude of the peak magnetic field of individual UWB pulses, but they were larger than the time-averaged field of the pulses and the background laboratory low-frequency fields experienced by the animals in this study. The UWB pulse energy was also different from that of the static and low-frequency fields because it was distributed across a wideband of frequencies and was delivered in 1 ns or so, a small fraction of the pulse repetition period. The lack of significant UWB effect can be ascribed to the time-averaged energy at effective frequencies being much lower than that used in previous studies finding effects of magnetic fields. Because of their relatively small contribution to UWB pulse energy and their relative ineffectiveness in altering function (33), radio-frequency, and microwave components would be expected not to contribute directly to an effect of UWB pulses.

The trend of morphine back-paw latency of CF-1 mice to increase after UWB exposure, indicating enhanced antinociception, may be related to the antinociception in rats and snails (8,39,40) and the altered learning in rats (41) caused by pulsed magnetic fields. This may indicate an importance of the pulsatile nature of the energy delivered during exposure to electromagnetic fields. The time sequence of magnetic-field pulses can also be a factor (40).

In summary, the UWB pulses used here did not have a significant effect on the nociception and activity endpoints tested. The tests of thermal nociception and spontaneous locomotor activity

had been selected because of their use in previous work with low-frequency magnetic fields. Because opioid receptors are involved in the effects seen previously, the UWB pulses seemed not able to affect the receptors, or other neural components, as in previous work. The lack of significant effect could have been due to insufficient energy at known effective frequencies. Trends in the results with morphine seen with higher UWB pulse repetition frequency may indicate an effect that increases with increased energy at effective frequencies.

ACKNOWLEDGEMENTS

This work is supported by the U.S. Army Medical Research and Materiel Command under contract DAMD17–94-C-4069 awarded to McKesson BioServices. We are grateful to M. Kavaliers for advice in the early stages of the project and to Y. Akyel, B. Stuck, A. Thomas, and F. Prato for comments on draft manuscripts. We are also grateful to M. Belt, D. Cox, and J. Lee for continuous, reliable operation of the UWB exposure system, P. Henry for technical assistance in early experiments, and T.-S. Lu for discussions on estimating SAR. We also thank D. Cox for design and construction of the heated surface device and the animal holders.

The views, opinions, and/or findings contained in this report are those of the author(s) and should not be construed as an official Department of the Army position, policy, or decision unless so designated by other documentation. In conducting research using animals, the investigator(s) adhered to the "Guide for the Care and Use of Laboratory Animals," prepared by the Committee on Care and Use of Laboratory Animals of the Institute of Laboratory Animal Resources, National Research Council (National Institutes of Health Publication No. 86–23, Revised 1985). The U.S. Air Force Armstrong Laboratory at Brooks Air Force Base is fully accredited by the Association for Assessment and Accreditation of Laboratory Animal Care, International (AAALAC).

REFERENCES

1. Agee, F. J.; Scholfield, D. W.; Prather W.; Burger, J. W. Powerful ultra-wide band RF emitters: Status and challenges. SPIE Proc. Series 2557:98–109; 1995.
2. Alkana, R. L.; Davies, D. L.; Morland, J.; Parker, E. S.; Bejanian, M. Low-level hyperbaric exposure antagonizes locomotor effects of ethanol and *n*-propanol but not morphine in C57BL mice. Alcohol. Clin. Exp. Res. 19:693–700; 1995.
3. Bao, J. Z. Picosecond domain electromagnetic pulse measurements in an exposure facility: An error compensation routine using deconvolution techniques. Rev. Sci. Instrum. 68:2221–2227; 1997.
4. Baum, C. E.; Carin, L.; Stone, A. P., eds. Ultra-wideband, short-pulse electromagnetics 3. New York: Plenum; 1997.
5. Belknap, J. K.; Noordewier, B.; Lame, M. Genetic dissociation of multiple morphine effects among C57BL/6J, DBA/2J and C3H/HeJ inbred mouse strains. Physiol. Behav. 46:69–74; 1989.
6. Betancur, C.; Dell'Omo, G.; Alleva, E. Magnetic field effects on stress-induced analgesia in mice: Modulation by light. Neurosci. Lett. 182:147–150; 1994.
7. Cowan, A. Effects of opioids on the spontaneous behavior of animals. In: Herz, A.; Akil, H.; Simon, E. J., eds. Handbook of experimental pharmacology, 104/II: Opioids II. Berlin: Springer–Verlag; 1993:393–428.
8. Fleming, J. L.; Persinger, M. A.; Koren, S. A. Magnetic pulses elevate nociceptive thresholds: Comparisons with opiate receptor compounds in normal and seizure-induced brain-damaged rats. Electro- Magnetobiol. 13:67–75; 1994.
9. Frey, A. H. An integration of the data on mechanisms with particular reference to cancer. In: Frey, A. H., ed. On the nature of electromagnetic field interactions with biologic systems. Austin: Landes; 1994: 9–28.
10. Gebhart, G. F.; Mitchell, C. L. Strain differences in the analgesic response to morphine as measured on the hot plate. Arch. Int. Pharmacodyn. 201:128–140; 1973.
11. Harrison, L. M.; Kastin, A. J.; Weber, J. T.; Banks, W. A.; Hurley, D. L.; Zadina, J. E. The opiate system in invertebrates. Peptides 15:1309–1329; 1994.
12. IEEE IEEE C95. 1–1991: IEEE standard for safety levels with respect to human exposure to radio frequency electromagnetic fields, 3 kHz to 300 GHz. New York: Institute of Electrical and Electronics Engineers; 1992.
13. Jauchem, J. R.; Frei, M. R.; Ryan, K. L.; Merritt, J. H.; Murphy, M. R. Lack of effects on heart rate and blood pressure in ketamine-anesthetized rats briefly exposed to ultra-wideband electromagnetic pulses. IEEE Trans. Biomed. Eng. (in press, 1998).
14. Jauchem, J. R.; Seaman, R. L.; Lehnert, H. M.; Mathur, S. P.; Ryan, K. L.; Frei, M. R. Ultra-wideband electromagnetic pulses: Lack of effects on heart rate and blood pressure during two-minute exposures of rats. Bioelectromagnetics 19:330–333, 1998.
15. Kavaliers, M.; Eckel, L. A.; Ossenkopp, K. P. Brief exposure to 60 Hz magnetic fields improves sexually dimorphic spatial learning performance in the meadow vole, *Microtus pennsylvanicus*. J. Comp. Physiol. A 173:241–248; 1993.
16. Kavaliers, M.; Ossenkopp, K. P. Exposure to rotating magnetic fields alters morphine-induced behavioral responses in two strains of mice. Neuropharmacology 24:337–340; 1985.
17. Kavaliers, M.; Ossenkopp, K. P. Magnetic fields differentially inhibit mu, delta, kappa and sigma opiate-induced analgesia in mice. Peptides 7:449–453; 1986.
18. Kavaliers, M.; Ossenkopp, K. P. Stress-induced opioid analgesia and activity in mice: Inhibitory influences of exposure to magnetic fields. Psychopharmacology 89:440–443; 1986.
19. Kavaliers, M.; Ossenkopp, K. P. Magnetic fields inhibit opioid-mediated "analgesic" behaviours of the terrestrial snail, *Cepaea nemoralis*. J. Comp. Physiol. A 162:551–558; 1988.
20. Kavaliers, M.; Ossenkopp, K. P. Repeated naloxone treatments and exposures to weak 60-Hz magnetic fields have "analgesic" effects in snails. Brain Res. 620:159–162; 1993.
21. Kavaliers, M.; Ossenkopp, K. P.; Prato, F. S.; Carson, J. J. L. Opioid systems and the biological effects of magnetic fields. In: Frey, A. H., ed. On the nature of electromagnetic field interactions with biological systems. Austin: Landes; 1994:181–194.
22. Kavaliers, M.; Ossenkopp, K. P.; Prato, F. S.; Innes, D. G. L.; Galea, L. A. M.; Kinsella, D. M.; Perrot-Sinal, T. S. Spatial learning in deer mice: Sex differences and the effects of endogenous opioids and 60 Hz magnetic fields. J. Comp. Physiol. A 179:715–724; 1996.
23. Lai, H. Neurological effects of radiofrequency electromagnetic radiation. In: Lin, J. C., ed. Advances in electromagnetic fields in living systems, vol. 1. New York: Plenum; 1994:27–80.
24. Lai, H. Spatial learning deficit in the rat after exposure to a 60 Hz magnetic field. Bioelectromagnetics 17:494–496; 1996.
25. Lai, H.; Carino, M. A.; Horita, A.; Guy, A. W. Opioid receptor subtypes that mediate a microwave-induced decrease in central cholinergic activity in the rat. Bioelectromagnetics 13:237–246; 1992.
26. Lai, H.; Horita, A.; Chou, C. K.; Guy, A. W. Psychoactive-drug response is affected by acute low-level microwave irradiation. Bioelectromagnetics 4:205–214; 1983.
27. Lai, H.; Horita, A.; Guy, A. W. Microwave irradiation affects radial-arm maze performance in the rat. Bioelectromagnetics 15:95–104; 1994.
28. Maillefer, R. H.; Quock, R. M. Naltrexone-sensitive analgesia following exposure of mice to 2450-MHz radiofrequency radiation. Physiol. Behav. 52:511–514; 1992.
29. Marrazzi, M. A.; Mullings-Britton, J.; Stack, L.; Powers, R. J.; Lawhorn, J.; Graham, V.; Eccles, T.; Gunter, S. Atypical endogenous opioid systems in mice in relation to an auto-addiction opioid model of anorexia nervosa. Life Sci. 47:1427–1435; 1990.
30. Morland, J.; Jones, B. L.; Palomares, M. L.; Alkana, R. L. Morphine-6-glucuronide: A potent stimulator of locomotor activity in mice. Life Sci. 55:PL163–168; 1994.
31. Ossenkopp, K. P.; Kavaliers, M. Morphine-induced analgesia and exposure to low-intensity 60-Hz magnetic fields: Inhibition of noctur-

nal analgesia in mice is a function of magnetic field intensity. Brain Res. 418:356–360; 1987.
32. Prato, F. S.; Kavaliers, M.; Ossenkopp, K. P.; Carson, J. J. L.; Drost, D. J.; Frappier, J. R. H. Extremely low frequency magnetic field exposure from MRI/MRS procedures. Ann. NY Acad. Sci. 649:44–58; 1992.
33. Prato, F. S.; Ossenkopp, K. P.; Kavaliers, M.; Sestini, E.; Teskey, G. C. Attenuation of morphine-induced analgesia in mice by exposure to magnetic resonance imaging: Separate effects of the static, radiofrequency and time-varying magnetic fields. Magn. Reson. Imaging 5:9–14; 1987.
34. Saito, H. Inhibitory and stimulatory effects of morphine on locomotor activity in mice: Biochemical and behavioral studies. Pharmacol. Biochem. Behav. 35:231–235; 1990.
35. Sherry, C. J.; Blick, D. W.; Walters, T. J.; Brown, G. C.; Murphy, M. R. Lack of behavioral effects in non-human primates after exposure to ultrawideband electromagnetic radiation in the microwave frequency range. Radiat. Res. 143:93–97; 1995.
36. Stevens, C. W.; Rothe, K. S. Supraspinal administration of opioids with selectivity for μ-, δ-, and κ-opioid receptors produces analgesia in amphibians. Eur. J. Pharmacol. 331:15–21; 1997.
37. Szekely, J. I.; Miglecz, E.; Ronai, A. Z. Biphasic effects of a potent enkephalin analogue (D-Met^2,Pro^5)-enkephalinamide and morphine on locomotor activity in mice. Psychopharmacology 71:299–301; 1980.
38. Teskey, G. C.; Prato, F. S.; Ossenkopp, K. P.; Kavaliers, M. Exposure to time varying magnetic fields associated with magnetic resonance imaging reduces fentanyl-induced analgesia in mice. Bioelectromagnetics 9:167–174; 1988.
39. Thomas, A. W.; Kavaliers, M.; Prato, F. S.; Ossenkopp, K. P. Pulsed magnetic field induced "analgesia" in the land snail, *Cepaea nemoralis*, and the effects of μ, δ, and κ opioid receptor agonists/antagonists. Peptides 18:703–709; 1997.
40. Thomas, A. W.; Kavaliers, M.; Prato, F. S.; Ossenkopp, K. P. Antinociceptive effects of a pulsed magnetic field in the land snail, *Cepaea nemoralis*. Neurosci. Lett. 222:107–110; 1997.
41. Thomas, A. W.; Persinger, M. A. Daily posttraining exposure to pulsed magnetic fields that evoke morphine-like analgesia affects consequent motivation but not proficiency in maze learning in rats. Electro-Magnetobiol. 16:33–41; 1997.
42. Tysdale, D. M.; Lipa, S. M.; Ossenkopp, K. P.; Kavaliers, M. Inhibitory effects of 60-Hz magnetic fields on opiate-induced "analgesia" in the land snail, *Cepaea nemoralis*, under natural conditions. Physiol. Behav. 49:53–56; 1991.
43. Walters, T. J.; Mason, P. A.; Sherry, C. J.; Steffen, C.; Merritt, J. H. No detectable bioeffects following acute exposure to high peak power ultra-wide band electromagnetic radiation in rats. Aviat. Space Environ. Med. 66:562–567; 1995.
44. Wenger, G. R. The role of control activity levels in the reported strain differences to the behavioral effects of drugs in mice. Pharmacol. Biochem. Behav. 32:241–247; 1989.

Bioelectromagnetics 18:324–334 (1997)

Search for Frequency-Specific Effects of Millimeter-Wave Radiation on Isolated Nerve Function

A.G. Pakhomov,[1] H.K. Prol,[2] S.P. Mathur,[2] Y. Akyel,[2] and C.B.G. Campbell[1]

[1]Microwave Bioeffects Branch, U. S. Army Medical Research Detachment of the Walter Reed Army Institute of Research, Brooks Air Force Base, San Antonio, Texas
[2]McKesson BioServices, Brooks Air Force Base, San Antonio, Texas

Effects of a short-term exposure to millimeter waves (CW, 40–52 GHz, 0.24–3.0 mW/cm^2) on the compound action potential (CAP) conduction were studied in an isolated frog sciatic nerve preparation. CAPs were evoked by either a low-rate or a high-rate electrical stimulation of the nerve (4 and 20 paired pulses/s, respectively). The low-rate stimulation did not alter the functional state of the nerve, and the amplitude, latency, and peak latency of CAPs could stay virtually stable for hours. Microwave irradiation for 10–60 min at 0.24–1.5 mW/cm^2, either at various constant frequencies or with a stepwise frequency change (0.1 or 0.01 GHz/min), did not cause any detectable changes in CAP conduction or nerve refractoriness. The effect observed under irradiation at a higher field intensity of 2–3 mW/cm^2 was a subtle and transient reduction of CAP latency and peak latency along with a rise of the test CAP amplitude. These changes could be evoked by any tested frequency of the radiation; they reversed shortly after cessation of exposure and were both qualitatively and quantitatively similar to the effect of conventional heating of 0.3–0.4 °C. The high-rate electrical stimulation caused gradual and reversible decrease of the amplitude of conditioning and test CAPs and increased their latencies and peak latencies. These changes were essentially the same with and without irradiation (2.0–2.7 or 0.24–0.28 mW/cm^2), except for attenuation of the decrease of the test CAP amplitude. This effect was observed at both field intensities, but was statistically significant only for certain frequencies of the radiation. Within the studied limits, this effect appeared to be dependent on the frequency rather than on the intensity of the radiation, but this observation requires additional experimental confirmation. *Bioelectromagnetics 18:324–334, 1997.* © 1997 Wiley-Liss, Inc.

Key words: nerve conduction; compound action potential; frequency-specific bioeffects

INTRODUCTION

One of the most intriguing problems in modern electromagnetobiology is the existence and physiological significance of frequency-specific, resonance-type biological effects of millimeter waves [MMW, see for example Grundler et al., 1977; Keilmann, 1985; Grundler and Kaiser, 1992; Kataev et al., 1993; Belyaev et al., 1992, 1994]. Many investigators are rather skeptical about such effects and regard them as experimental artifacts [Gandhi et al., 1980; Bush et al., 1981; Furia et al., 1986]. At the same time, in the former Soviet Union the effects of low-level MMW have not only been demonstrated in a multitude of studies, but have been used for years in clinical practice. Diseases reported to be successfully treated by MMW range from peptic ulcers to cardiomyopathy, stenocardia, hypertension, wound infections, etc. Experience claimed with more than 100 000 clinical cases [Sit'ko et al., 1992; Betzky, 1992] should be considered and may provide evidence for the reality of specific or nonthermal biological effects of MMW electromagnetic radiation.

Of particular interest are recent experimental data for MMW effects on excitable tissue and cell membrane function. Burachas and Mascoliunas [1989] have demonstrated a pronounced MMW-induced suppression of compound action potentials (CAPs) in isolated frog sciatic nerves. After 10–20 min of irradiation at 77.7 GHz, 10 mW/cm^2, CAP amplitude decreased ex-

Contract Grant sponsor: U.S. Army Medical Research and Materiel Command; Contract Grant number: DAMD17-94-C-4069.
*Correspondence to: Dr. A. Pakhomov, USA-MCMR, U. S. Army Medical Research Detachment, 8308 Hawks Road, Building 1168, Brooks Air Force Base, San Antonio, TX 78235-5324. E-mail: akyel@rfr.brooks.af.mil

Received for review 13 February 1996; revision received 18 November 1996

© 1997 Wiley-Liss, Inc.

ponentially and fell 10-fold within the next 40–90 min. The CAP decrease due to the second and the subsequent exposures became increasingly steeper, taking only 10–15 min. In addition to this "slow" response, switching the field on increased CAP amplitude instantaneously by 5–7%, and switching the field off caused the opposite short-term reaction.

Chernyakov et al. [1989] carried out a complex study of effects induced by MMW in various excitable structures. Exposure of an isolated frog tailor's muscle (*m. sartorius*) at 0.1–0.15 mW/cm^2 in the range of 53–78 GHz decelerated the natural loss of transmembrane potential in myocytes and reduced the overshoot voltage, diminishing CAP amplitude by 7–25% and conduction velocity by 10–20%. Exposure of isolated frog sciatic nerves for 20–40 min altered the late CAP components or caused an abrupt "rearrangement" of CAPs: position, magnitude, and even polarity of CAP peaks (the initial CAP was polyphasic) suddenly changed in an unforeseeable manner. Sinoatrial area pacemakers changed their firing rate after just a few seconds of irradiation at 1 mW/cm^2, when microwave heating of the preparation did not exceed 0.005 °C.

Sazonov and Rizshkova [1995] reported that exposure at 42.19 ± 0.15 GHz facilitates isolated frog nerve recovery after a 1-kHz electrical stimulation train. The time needed for CAP restoration in exposed preparations decreased to 60–80% of the control group values.

Kataev et al. [1993] used voltage-clamp techniques to study MMW effects on membrane currents in the alga *Nitellopsis obtusa* (*Characea*). Irradiation for 30–60 min at 41, 50, and 71 GHz (5 mW/cm^2) suppressed the chloride current to zero with no recovery for 10–14 hr. The greater part of other tested frequencies in the range 38–78 GHz enhanced the chloride current, in some cases up to 200–400% (49, 70, 76 GHz). This activation was reversible, and recovery to the initial value took 30–40 min after the treatment. Neither activating nor inhibitory effects could be reproduced or explained by MMW heating.

In contrast to the above findings, Kazarinov et al. [1984] observed only thermal changes in the isolated frog skin potential under exposure to 35- to 41.6 GHz radiation. Khramov et al. [1991] demonstrated that all types of alterations in electrical activity of slow-adapting neurons of crayfish stretch receptor caused by 34–78 GHz MMW resulted from microwave heating. Motzkin and Feinstein [1989] did not find any effects of 5 mW/cm^2, 51.72 or 51.81 GHz radiation on miniature end plate potentials in rat neuromuscular junctions.

The purpose of the present study was to verify the existence of specific effects of MMW on excitable tissues under precisely controlled experimental conditions. High MMW sensitivity of CAP conduction in isolated frog sciatic nerve, as reported by other authors, motivated us to choose this preparation for our investigation. We used an approach which is standard for analysis of functional changes in excitable preparations, which is an electrical stimulation by paired pulses at either a low or a high pulse repetition rate. These techniques allow one to reveal changes in CAP conduction, nerve refractory properties, and to evaluate its ability to sustain a high-rate stimulation.

MATERIALS AND METHODS

Nerve Preparation and Data Acquisition

All experiments were performed on isolated nerve preparation (*n. ischiadicus* + *n. peroneus*) of the frog *Rana berlandieri.* Active adult frogs (males) were kept in vivarium conditions (22–25 °C, 30–70% relative humidity, 12-hr light/12-hr dark diurnal light cycle) for at least 1 week before experiments. After animal immobilization by pithing the brain and the spinal cord, sciatic nerves from both legs were isolated in a conventional manner, ligated and submerged into chilled Ringer's solution containing: $NaCl$ – 102.6; KCl – 1.0; $NaHCO_3$ – 0.7; $CaCl_2$ – 0.9 (mmol/l); pH 7.4–7.6. Then the two nerves were transferred into individual exposure and control chambers made of polyvinylchloride. These chambers had identical design and dimensions (145 mm length, 40 mm width, 58 mm height) with a 13 mm wide, 10 mm deep slot at the top. The nerve preparation was laid in this slot, open to MMW irradiation from the top.

The research described in this report was conducted in compliance with the Animal Welfare Act and other federal statutes and regulations relating to animals and experiments involving animals and adheres to the principles stated in the Guide for the Care and Use of Laboratory Animals, NIH publication 85–23.

The depth of MMW penetration into water ranges from 0.1 to 0.5 mm [Ryakovskaya and Shtemler, 1983], and it is even less in saline. Therefore, we exposed nerves under a thin layer of mineral oil (0.3–0.5 mm), which is almost transparent to MMW and effectively prevents nerve drying. Artifact-free nerve stimulation and CAP recording were accomplished via two pairs of saline bridge electrodes that contacted the opposite ends of the nerve and also limited the MMW-reachable area. These electrodes were made of 12 mm long pieces of silicone tubing (2.5 mm inner diameter, 1.5 mm wall thickness). They were permanently mounted on the bottom of the slot and filled with Ringer's solution. Thus, CAPs propagated from stimulating to recording

electrodes through a 30-mm middle portion of the nerve covered with oil and exposed to MMW. The saline electrodes were designed so as to provide exactly the same positioning of every nerve preparation, about 7 mm above the bottom of the slot. To eliminate biphasic CAP signals, the nerve was crushed between two recording electrodes connected to the amplifier.

CAPs were evoked by paired square pulses from a Grass Instruments Stimulator S8800 and recorded on a Tektronics 2430 digital oscilloscope. Usually, we used a supramaximal nerve stimulation (0.2-ms pulse width, 2–3 V amplitude). The relative refractory period lasted for 9.5–12 ms, and the interpulse interval was chosen to be 9 ms. Stimulating pulses were continually delivered at a rate of either 4 pairs/s (low-rate stimulation, LRS) or 20 pairs/s (high-rate stimulation, HRS). Automatic averaging of 16 consecutive CAP records was used in most of the experiments, to improve the signal-to-noise ratio and to deemphasize the incidental CAP variability. The amplitude, latency, and peak latency of conditioning and test CAPs (A, L, PL, and A_t, PL_t, see Fig. 1) were measured every 2 or 5 minutes throughout the experiment.

Both the chambers were cooled to 11–12 °C by constant flow of chilled water from a thermostabilized water bath. This attenuated but did not prevent nerve heating by the radiation because of slow heat conduction through mineral oil. Actual temperature in the chambers was monitored by a Luxtron Instruments model 850 multichannel fluoroptic thermometer; the fluoroptic probe was situated in the oil 1.5–2 mm from the middle of the nerve. This probe was primarily intended to measure conventional heating of the nerve. To quantify MMW heating of the preparation, we used an original "biological" technique, which will be described in detail in the "Results" section.

Most experimental reports about microwave bioeffects are based on a comparison of the data with either a control, or a sham-exposed population. A parallel control can be performed synchronously with the exposure, but has to be in a different physical location; sham exposures can be performed in exactly the same physical location as microwave exposures, but only at a different time. Though neither of the two approaches can entirely exclude the possible impact of uncontrolled factors other than irradiation, use of both sham and parallel controls in the same series of experiments can make a strong case that a difference (if observed) was in fact a result of irradiation. To make the experimental conditions as strict as possible, this "duplicative control" protocol was used in all experiments with HRS.

Control and exposed nerve chambers were situated in the same Faraday cage, but the control chamber

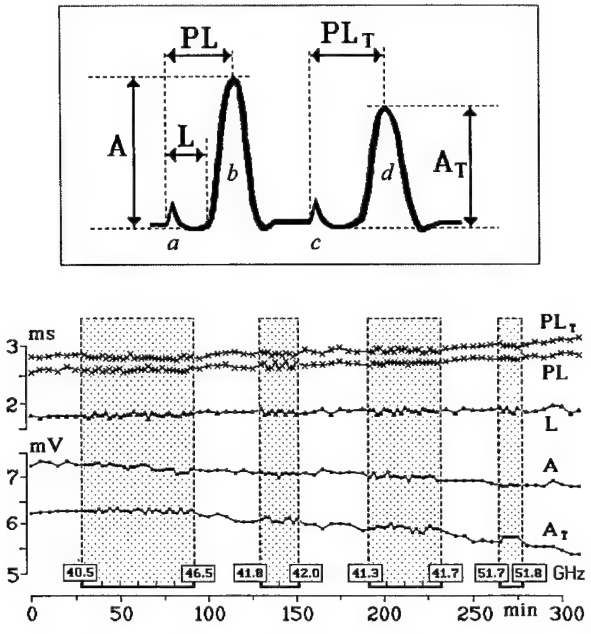

Fig. 1. Isolated nerve performance with a low-rate stimulation (4 paired pulses/s) and repetitive millimeter wave exposure. Periods of irradiation are shown by dotted areas. The indicated radiation frequencies are those at the beginning and at the end of each exposure; during irradiation, the frequency is increased stepwise at either 0.01 or 0.1 GHz/min; the incident power density for all the exposures is 2.2–2.8 mW/cm^2 (see Table 1 for details). The inset at the top shows the compound action potentials (CAPs) as evoked by paired pulses (*a*, *c*) with a 9-ms interval and defines the CAP parameters: A, PL and L are the amplitude, peak latency, and latency of the conditioning CAP (*b*), A_t and PL_t are the amplitude and peak latency of the test CAP (*d*).

was shielded from the radiation. Nerves in the exposed chamber could be either MMW-irradiated or sham-irradiated. To provide the sham exposure conditions, we tuned the waveguide attenuators to maximum, leaving all other devices and the microwave generator turned on. The incident power density still reaching the preparation during sham exposures was calculated to be about 10^{-8} mW/cm^2. The parallel control nerves were never exposed, but underwent all the same stimulation routines simultaneously with exposed and sham-exposed preparations. Statistical comparisons were done between exposed and sham-exposed data sets and then between their respective parallel controls. Any significant difference in performance of exposed and sham-exposed preparations should only be taken into account if it was not accompanied by a similar difference between their parallel controls.

Irradiation and Dosimetry

The microwave power generator (model G4-141, made in Russia) operated in a CW regime in the fre-

quency range 37–53 GHz. This generator uses a backward-wave oscillator and has the half-power bandwidth of less than 5 MHz. The waveguide line included two attenuators, a 10-dB bidirectional coupler, a slotted section with a broadband probe for standing wave measurements, and a horn antenna at its end. The horn was situated 52 mm above the isolated nerve in the exposed chamber so that the nerve was aligned with the E-field. Exact radiation frequency and net input power to the horn were monitored via the coupler by an M3-21 wattmeter and Ch3-34/Ch5-16 frequency meter (Russia) or by an EIP model 548A frequency counter (EIP Microwave Inc., USA). These devices were used to tune the MMW generator to the desired output power and frequency before each irradiation. If needed, these parameters could be adjusted during irradiation, but usually their drift was not considerable.

As a result of the intense absorption of MMW at the surface of biological tissues, the incident power density (IPD), rather than the specific absorption rate, should be used for characterization of exposure conditions. However, no IPD meters calibrated for the 37–53 GHz range could be found on the market. The most appropriate device proved to be a broadband electric field probe (Narda Microwave Corp., model 8623), which is calibrated from 300 kHz to 38 GHz and also at 94 GHz, but not between 38 and 94 GHz. It was the opinion of the probe manufacturer, that the design of the probe is suitable for the entire range, and no substantial variations of its sensitivity should be expected. To verify this, we calibrated the probe against IPD values calculated by a free-space standard field method (see Appendix for details). Theoretical IPD per unit of the net input power to the horn irradiator was calculated for frequencies from 37 to 78 GHz and for various far field distances from the horn. Theoretical and measured IPD differed by no more than ±1.5 dB throughout the entire frequency range. Most of this difference could be attributed to the combined error of the theoretical model and the net input power measurements, so the probe was concluded to be sufficiently accurate. Close IPD values were obtained later by another probe rated up to 45.5 GHz (Narda model 8721).

Both of these probes, although accurate, were much too big (53 mm diameter) for near-field dosimetry or field mapping. For these purposes we used a miniature flat crystal detector (Narda part 4824). A custom-made holder for the detector minimized field distortion and enabled precise movements in any direction over the irradiated area. The detector was calibrated in the far field against the other probe (8623) individually at every frequency of interest. The detector's sensitivity markedly varied within the frequency range, but always remained perfectly linear, at least in the studied interval from 0.1 to 8 mW/cm^2. More details on the performance of this crystal detector and field mapping are to be presented in a separate paper.

IPD values measured by the broadband probe and the crystal detector were normalized per unit of the net input power to the horn, and plotted against the distance from the horn. These plots proved to be rather similar for different frequencies, even in the near field. For the 52-mm distance from the horn, the normalized IPD measured from 45 to 65 (μW/cm^2)/mW, which did not exceed the presumed inaccuracy of the meters. Therefore, these variations were ignored; the mean coefficient of 55 (μW/cm^2)/mW was used to calculate IPD from the measured net input power values. For individual frequencies from the 38 to 53 GHz range, the field non-uniformity along the exposed site of the nerve was found to be no more than ±2 dB.

RESULTS

Low-Rate Stimulation (LRS) Experiments

The effectiveness of various regimens of irradiation, which are summarized in Table 1, was tested in a total of 49 experiments. Six regimens of exposure were focused on possible immediate frequency-specific effects of MMW; the radiation frequency during an exposure was constantly increased by steps of either 0.01 or 0.1 GHz/min. Most of the preparations were exposed several times with 20- to 60-min intervals between exposures. LRS continued throughout the experiment without interruption, and CAPs were measured every 2 min during irradiation and every 5 min between exposures. Other regimens used various constant frequencies chosen from three supposedly effective frequency bands. As measured by the fluoroptic probe, the maximum temperature rise under irradiation at 2.2–2.8 mW/cm^2 was 0.3–0.5 °C, and at lower IPD it was negligible.

LRS by itself did not affect the functional state of the nerve, even if continued for hours. The nerve performance and parameters of conditioning and test CAPs remained essentially stable regardless of repeated MMW exposures (Fig. 1). The only noticeable and repeatable reaction to the irradiation was a subtle and transient decrease of the test CAP peak latency (PL_t) and increase of its amplitude (A_t). Although these changes did not exceed a few percent, they could be statistically significant ($P < .05$) in comparison with both the control preparations and with the preexposure values (Figure 2A and B).

This effect occurred only at the highest tested IPD, apparently without any dependence on the radiation frequency, thus suggesting that it could be caused

TABLE 1. Millimeter-Wave Irradiation Experiments with the Low-Rate Stimulation Protocol

Frequency band (GHz)	Stepping rate (GHz/min)	Exposure time (min)	Intensity (mW/cm^2)	No. of exper./ No. of nerves	Summary of findings[d]
40.50–46.50[a]	0.1	60	2.2–2.6	4/4	(+)
41.30–41.70[a]	0.01	40	2.2–2.5	6/6	(+)
41.80–42.00[a]	0.01	20	2.3–2.5	5/5	(+)
41.80–42.00[a]	0.01	20	0.23–0.25	3/3	(−)
49.50–53.50[a]	0.1	40	2.4–3.0	4/4	(+−)
51.70–51.80[a]	0.01	10	2.7–2.8	6/6	(+)
41.15–41.30[b]	—	30	0.26; 1.0; 2.6	14/10	(−); (−); (+)
41.70–42.10[b]	—	30	2.3; 2.6	3/3	(−); (+−)
51.60–51.70[b]	—	30	0.28; 2.8	4/3	(−); (+−)
			Total:	49/24[c]	

[a]Radiation frequency was increased stepwise to cover the entire band during the exposure period.
[b]Irradiation was performed at various constant frequencies chosen from the specified band. Only one frequency was used per experiment.
[c]One nerve could be exposed several times in different regimens, so that the total (24) is less than the arithmetic sum of the upper rows.
[d](+) refers to a consistent thermal effect (gradual simultaneous decrease in the test CAP peak latency and increase in its amplitude, such as shown in Fig. 2); (+−) indicates changes analogous to this thermal effect, but lacking statistical significance; (−) shows absence of any considerable MMW effects.

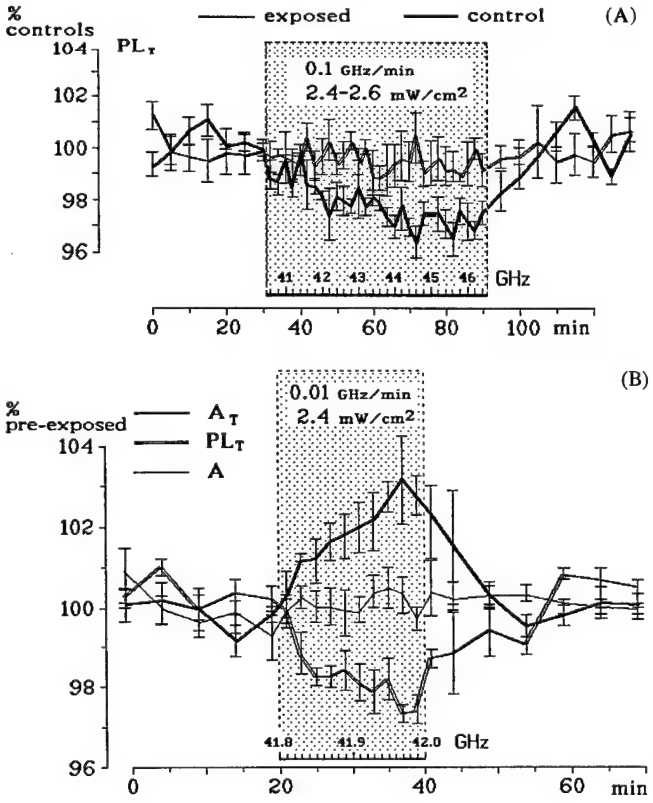

Fig. 2. Millimeter wave-induced alterations of compound action potential (CAP) conduction compared with (**A**) control experiments or with (**B**) the pre-exposure values. In both parts, CAP parameters are shown as percentage of the average preexposure value. Each datapoint is the mean ± SE from four to six independent experiments. Other designations are the same as in Fig. 1.

merely by general heating of the preparation by microwaves. To verify it, we studied the effects of conventional heating on nerve performance (Fig. 3). As can be seen from this graph, the pattern of the conventional heating-induced CAP changes (concurrent decrease of L, PL, Pl_t, and increase of A_t, while A stays almost stable) is the same as observed with the MMW exposures (Fig. 2).

Alterations of CAP indices due to small temperature changes (1–2 °C) could be approximated well by linear functions (Figure 4). This chart makes it possible to establish quantitatively whether the MMW-induced CAP changes could be regarded as produced by MMW

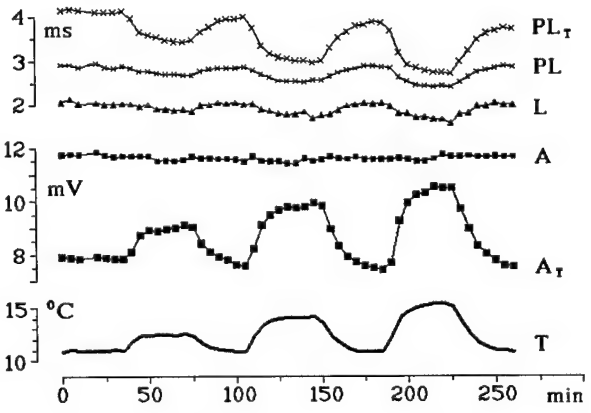

Fig. 3. Alterations of an isolated nerve performance by conventional heating. The lower trace, T, is the preparation temperature; other designations are the same as in Figure 1.

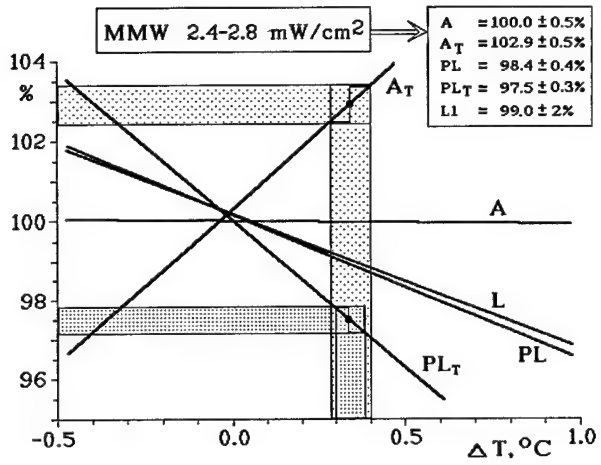

Fig. 4. Comparison of nerve performance alterations caused by millimeter-wave irradiation and conventional heating. The abscissa is the temperature change (°C) and the ordinate is the CAP parameters, in percent, to their values at the initial temperature. The lines A_t, A, L, etc., are obtained by differentiation and linear approximation of the data shown in Figure 3. A window at the top summarizes CAP changes observed under irradiations at 2.4–2.8 mW/cm^2. Dotted horizontal sectors on the chart show the range of values for A_t and PL_t observed under MMW irradiation; vertical dotted columns show the range of the corresponding values of temperature elevation. Other designations are the same as in Figure 1. See text for more explanation.

heating. At the initial temperature (zero temperature change), all CAP parameters were taken as 100% (they are not exactly 100% on the graph, because approximations were based on real experimental data and this introduced a small error). Experiments with MMW established that exposure at 2.4–2.8 mW/cm^2 increases A_t to 102.9 ± 0.5% and decreases PL_t to 97.5 ± 0.3% (these values are marked by two horizontal dotted bars on the graph). These changes can be explained by heating only if their magnitudes correspond to one and the same temperature rise. One can see from the graph that the corresponding temperature rise is indeed the same and equals 0.3–0.4 °C (it is marked by vertical dotted bars).

The same analysis was performed for other CAP parameters, and the correspondence of changes observed under MMW exposure and under conventional heating was essentially perfect. Thus, all MMW effects found in the LRS series could be attributed to microwave heating of the preparation. In turn, the level of MMW heating of the nerve could be measured indirectly from the MMW-induced alterations of CAP. We infer heating of the nerve preparation by 0.3–0.4 °C at an IPD of 2.4–2.8 mW/cm^2.

It is important to note that this use of the nerve itself as a thermometer did not reveal any substantial variations of temperature rise at different frequencies of irradiation. Within the accuracy of such measurements, heating depended on the IPD only. This fact not only confirms the correctness of our IPD measurements, but also shows the absence of any "geometrical resonances" which, hypothetically, could lead to a markedly increased MMW absorption and heating at certain "resonance" frequencies.

Our failure to find any frequency-specific effects in the LRS series did not necessarily mean the absence of such effects. Possibly, the LRS procedures used were not sensitive enough to reveal the effects. In earlier studies with 915 MHz microwaves [Pakhomov et al., 1992], use of a functional test with a high-rate stimulation detected nerve state changes that were otherwise undetectable. Therefore, this sensitive test was used next to study the effects of several selected MMW frequencies.

High-Rate Stimulation (HRS) Experiments

The principal difference between LRS and HRS is that LRS by itself does not alter the nerve functional state, while HRS does. Under HRS, the interval between pairs of stimuli is not long enough for complete recovery after conduction of the preceding CAPs, thus leading to nerve fatigue with gradual decrease of CAPs' amplitude and conduction velocity (Fig. 5).

After positioning the exposed and control nerves in the chambers, they were continually stimulated at 4 pairs/s until a reasonable stabilization of CAPs was

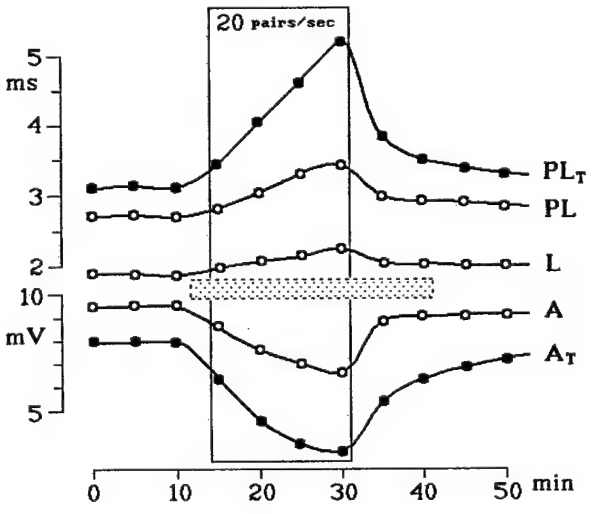

Fig. 5. Pattern of changes in compound action potential parameters and recovery in experiments with high-rate stimulation (20 paired pulses/s from the 14th until the 31st min of experiment; otherwise the rate is 4 paired pulses/s). Exposure or sham exposure (dotted bar) starts at 12 min and continues for 30 min. See Figure 1 for other designations.

obtained (60 min at least). Nerves with unstable or multi-peak potentials were usually discarded. Successful nerve preparations underwent from three to seven experiments lasting for 50 min each, with intervals sufficient for nerve recovery. MMW or sham exposure began on the 12th min of an experiment and continued for 30 min; HRS was turned on after 2 min of exposure and continued for 17 min. CAPs were recorded every 5 min, that is 3 datapoints before, 6 datapoints during, and 2 datapoints after exposure (Fig. 5). LRS was applied throughout a series of experiments with no interruptions other than HRS; LRS also continued between the experiments, when no data were collected.

MMW exposures were performed at a power density of either 2.0–2.7 mW/cm^2 (41.42, 42.04, 45.90 GHz, and 51.41 GHz), or 0.24–0.28 mW/cm^2 (41.22 and 50.91 GHz), as summarized in Table 2. The acceptable inaccuracy of adjustment of the radiation frequency was within 20 MHz from the indicated nominal values. As demonstrated in the LRS series, and confirmed by the Luxtron thermometer measurements, nerve heating at 2.0–2.7 mW/cm^2 was about 0.3–0.4 °C, and at 0.2–0.3 mW/cm^2 it was negligible. Different exposure regimens and sham exposures were randomized, except for the first experiment in a series, which was always performed without irradiation. The data from this first experiment were used only for evaluation of the individual nerve's ability to tolerate HRS and were not included in the statistical analysis. The same procedures, excluding irradiation, were simultaneously applied to the parallel control preparations.

Data processing was organized so as to maximally deemphasize individual differences between the nerve preparations and unforced functional changes during a series of experiments. This was accomplished by introduction of relative indices (*RI*) of the HRS tolerance, which were calculated as following:

$$RI = ({}^{e}V_n/{}^{e}V_i)/({}^{c}V_n/{}^{c}V_i) \cdot 100\%,$$

where ${}^{c}V_i$ is the value of a CAP parameter (amplitude, latency, etc.) before the HRS start in the first experiment in a series; ${}^{c}V_n$ is the value on the n min of the first experiment (during or after the HRS); ${}^{e}V_i$ and ${}^{e}V_n$, are the respective values in a succeeding experiment when HRS was accompanied by either MMW or sham irradiation. Calculation of relative indices from original data is also illustrated in Figure 6. If the nerve performance during an experiment with MMW irradiation is the same as in the first experiment in a series (which was always performed without irradiation), the relative indices will stay at 100%. If a relative index differs from 100%, this difference may indicate an aftereffect

TABLE 2. Millimeter-Wave Irradiation Experiments with the High-Rate Stimulation Protocol

Intensity (mW/cm^2)	Frequencies tested (GHz)	No. of experiments (exposed + parallel control)	Relative index values in exposed nerves (mean ± SE, %, at 30 min)[a]					
			Conditioning action potential			Test action potential		
			Amplitude	Peak latency	Latency	Amplitude	Peak latency
Sham	—	6 + 6	102.1 ± 2.9	90.4 ± 2.9	95.5 ± 1.2	92.9 ± 4.1	81.2 ± 4.5
0.24–0.28	41.22, 50.91	11 + 11	105.8 ± 1.2	90.3 ± 1.6	95.8 ± 1.0	109.3 ± 4.4*	92.1 ± 2.9
2.0–2.7	41.42, 42.04, 45.90, 51.41	22 + 22	107.5 ± 1.7	93.0 ± 2.7	94.4 ± 0.8	109.8 ± 3.8*	92.0 ± 4.6

[a]The 30-min time point corresponds to 16 min of the high-rate stimulation and 18 min of irradiation. The data within the intensity ranges were pooled together irrespective of the frequency of the radiation.
*$P < 0.02$ compared with the sham exposure. Differences in data values between the respective parallel control groups (not included in the table) were not statistically significant.

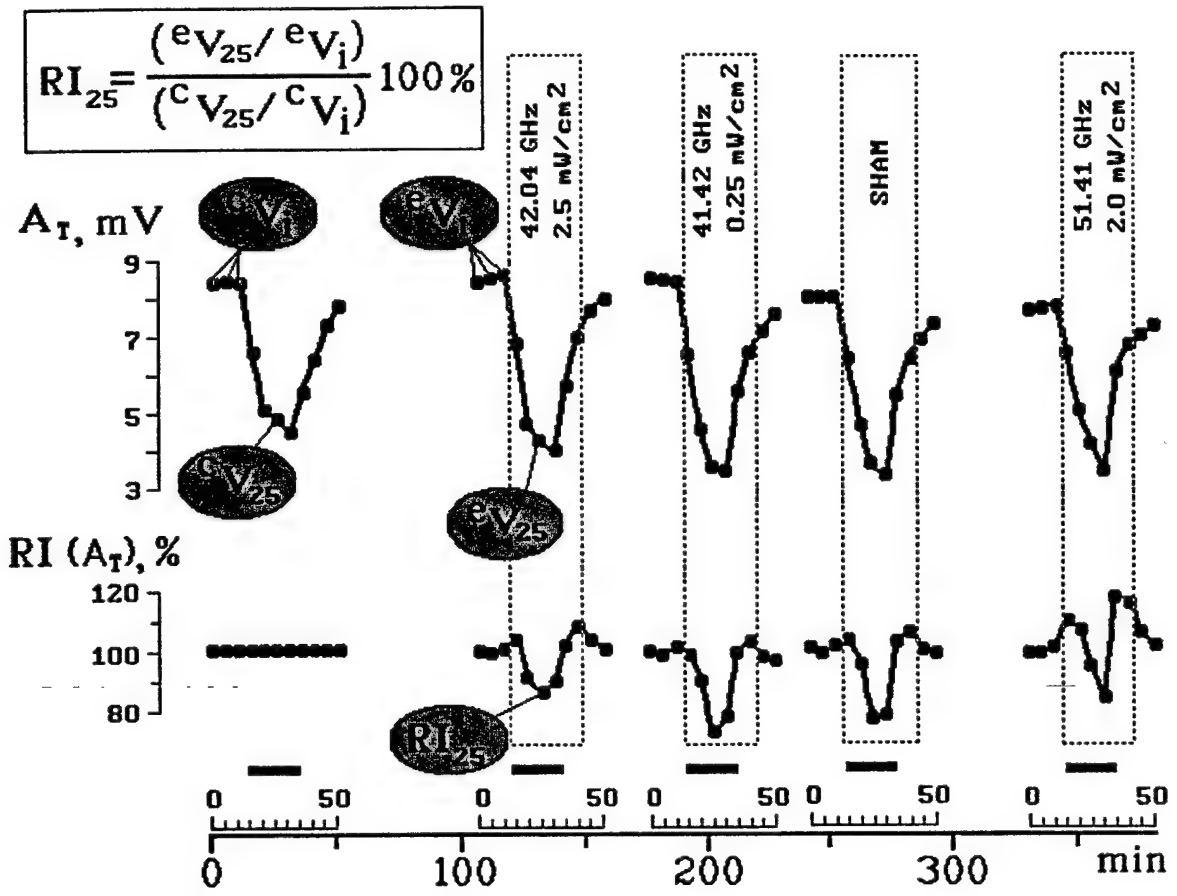

Fig. 6. Isolated nerve performance in a series of high-rate stimulation (HRS) experiments with one nerve preparation and the analysis of data. Horizontal axes: elapsed time (below) and time scales for each HRS experiment. Periods of the HRS (20 paired pulses/s) are shown by horizontal bars; otherwise, the rate was 4 paired pulses/s. Dotted line boxes indicate periods of microwave and sham exposure. Vertical axes: amplitude of the test compound action potential (A_t, mV), and its relative index $RI(A_t)$, in percent. The *RI* is used to assess quantitatively the individual nerve's HRS tolerance in each of the HRS experiments. For example, for a 25-min datapoint of the second experiment in the series, the relative index RI_{25} is calculated by the equation at the top of the graph. $^{c}V_i$ is the initial A_t value in the first experiment in a series (average of 3 datapoints before the HRS); $^{c}V_{25}$ is the A_t value on the 25th min of the experiment. $^{e}V_i$ and $^{e}V_{25}$ are the same values in the next experiment with exposure. Similarly, *RI* is calculated for every datapoint in all subsequent experiments with this nerve preparation. Note that *RI* deviation from 100% in these experiments does not necessarily indicate an effect of irradiation, it could come up as an aftereffect of the previous HRS trains, spontaneous changes in the nerve state, etc.

of the previous HRS, an effect of MMW, chance variations, or an impact of other uncontrolled factors. To identify the effect of MMW, if any, we randomized the sequence of exposures and sham exposures and averaged the data from the experiments with different nerve preparations. The statistical significance of the MMW-induced changes was estimated in comparison with the sham-treatment data by a two-tailed Student's *t* test. All the same data processing applied to the parallel control experiments.

A total of 78 experiments on 26 nerve preparations were carried out. For the initial analysis, the data for experiments with the high (2–2.7 mW/cm^2) and low (0.24–0.28 mW/cm^2) incident power densities were pooled together, regardless of the frequency of the radiation. This analysis established that the changes in CAP conduction reached maximum at 30 min into the experiment; that was the last datapoint during the HRS train. The average relative index values for this datapoint are provided in the Table 2. Irradiation at either field intensity induced no statistically significant changes in CAP parameters ($P > .05$), except for the

increase in the relative index of the test CAP amplitude (A_t, $P < .02$). The difference in this parameter between the sham-exposed group and both the exposed groups was the same (about 17%), despite the 10-fold difference in the field intensity. It is important to note that no statistically significant differences were found between the respective parallel control groups.

On the whole, the results indicated that MMW irradiation could attenuate the A_t decrease during the HRS train. The equivalence of magnitudes of this effect in the two MMW-exposed groups inferred that an irradiation parameter other than intensity could be essential for producing this effect. Hence, we analyzed the data separately for each frequency of the radiation.

The mean increase of the A_t relative index by the end of the HRS train ranged from about 6 to 22% for different radiation frequencies (as compared with the sham exposure data). Only minimal changes of 6 to 9% (nonsignificant) were observed under exposure with 42.04 and 41.42 GHz MMW at 2.4–2.7 mW/cm^2, even though the microwave heating was 0.3–0.4 °C. Irradiation at the same incident power, but at a different frequency of 45.9 GHz, caused a 21% increase of this index ($P < .05$). The other tested frequencies produced a statistically significant effect of the similar magnitude (13–22%, $P < .05$), despite reduction of the incident power density to 2 mW/cm^2 (51.41 GHz) and even to 0.24–0.28 mW/cm^2 (41.22 and 50.91 GHz, see Fig. 7).

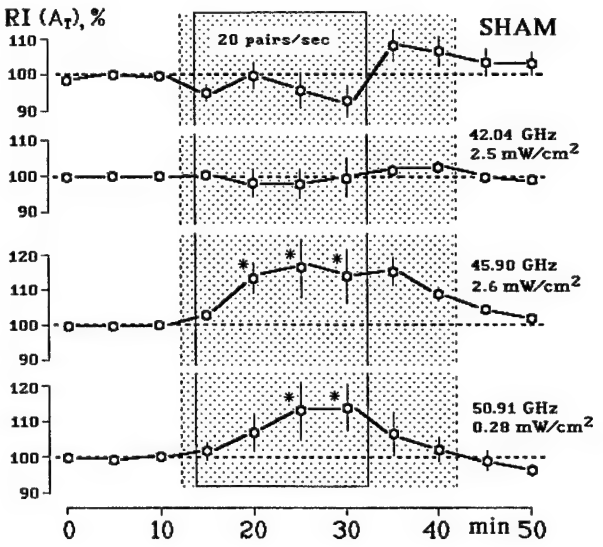

Fig. 7. Effect of millimeter waves on the nerve tolerance to high-rate stimulation. The vertical axes show the relative index of the test CAP amplitude (mean ± SE, five to seven independent experiments in each group). See text and Fig. 6 for the method of the relative index calculation. Periods of high-rate stimulation (20 paired pulses/s) and irradiation are shown by a box and dotted areas, respectively. Radiation frequency and incident power density are given to the right of the graphs. Asterisks indicate significant difference from the sham exposure data ($P < .05$).

DISCUSSION

Our experiments failed to confirm observations of severe MMW-induced alterations of CAP conduction, such as reported by other authors [Burachas and Mascoliunas, 1989; Chernyakov et al., 1989]. For the low-rate electrical stimulation of the nerve, MMW irradiation either did not cause any effect or, at high enough power levels, produced effects that were exactly the same as those produced by the equivalent conventional heating. One should note, however, that irradiation and other experimental conditions used in these two studies were substantially different from those in our work.

Another observed MMW effect, namely the increase of the A_t relative index by the end of the HRS train, deserves a more detailed analysis. This effect testifies to an attenuation of the HRS-induced A_t suppression or, in other words, to an ability of MMW to facilitate nerve recovery after conduction of a spike. This result fits well with the recent findings of Sazonov and Rizshkova [1995] that MMW exposure of the isolated frog sciatic nerve significantly decreases the time needed for CAP restoration after a high-rate (1 kHz) electrical stimulation train. According to our present data, this effect depends on the frequency of the radiation, but has almost the same magnitude at 10-fold different field intensities. These results suggest that the mechanism of the MMW action was different from general heating of the preparation, unless one assumes that at the same IPD level MMW absorption and heating at some frequencies could be more than tenfold greater than at others. This assumption does not seem feasible and also contradicts the results of the LRS experiments: Reverse calculation of the preparation heating from the nerve function changes ("use of the nerve as a thermometer") revealed no indications of extremely increased or decreased MMW absorption at any particular frequencies.

Instead of general MMW heating, the formation of so-called "hot spots" could be a more reasonable explanation for the effect. The spatial distribution and intensity of the local field maxima are very much dependent on the frequency of the radiation [Khizhnyak and Ziskin, 1994], so frequency-specific bioeffects could be produced by different patterns of "hot spots." One should also take into account the possibility of frequency-specific nonthermal interactions, which are often claimed to be characteristic for the MMW band [Chernyakov et al., 1989; Kataev et al., 1993; Rebrova, 1992; and others].

At this point, we consider it more important to

make sure that the observed frequency-specific effect of MMW on nerve function is real, rather than to speculate about underlying physical or physiological mechanisms. Our experimental procedures were organized so as to collect more physiological data and test more exposure regimens while using fewer animals and trying to rule out the possible impact of any factors other than microwaves. However, this made the statistical interpretation of the data very complicated. The experimental procedures had several features that influence the statistical confidence that can be placed in the findings: (1) Several treatment groups were compared with one sham-exposed group. (2) Both MMW and sham exposure experiments were supplemented with respective parallel controls, and there were no considerable differences between the parallel control groups. (3) A_t was not the only parameter measured, and we did not know *a priori* which parameter will reveal an effect. (4) The same effect occurred not just in an isolated timepoint, but in several adjacent and functionally related timepoints of the experiment. Conditions 1 and 3 decrease the statistical confidence that the effect was real, whereas conditions 2 and 4 increase it.

There are established techniques that can address some of these conditions separately (such as the Dunnet's test [1955] to compare several treatments with one control; see Winer [1971] for review), but no known method can quantitatively assess the cooperative impact of all these factors together. At the present time, the reality of this MMW effect cannot be addressed by statistical analysis, no matter whether we use the *t* test or more sophisticated procedures. The confidence levels reported in this paper should be regarded as an estimation only and are not necessarily correct. Instead of statistical manipulations, a solid proof of the effect can only be made by its reproduction in independent experiments.

ACKNOWLEDGMENTS

The work was performed while A.G. Pakhomov held a National Research Council-AMRMC Research Associateship and was supported by the U.S. Army Medical Research and Materiel Command under contract DAMD17-94-C-4069 awarded to McKesson BioServices. The views, opinions and findings contained in this report are those of the authors and should not be construed as an official Department of the Army position, policy or decision.

REFERENCES

Belyaev IYa, Alipov YD, Shcheglov VS (1992): Chromosome DNA as a target of resonance interaction between Escherichia coli cells and low-intensity millimeter waves. Electro Magnetobiol 11:97-108.

Belyaev IYa, Alipov YD, Shcheglov VS, Polunin VA, Aizenberg OA (1994): Cooperative response of Escherichia coli to the resonance effect of millimeter waves at super low intensity. Electro Magnetobiol 13:53-66.

Betzky OV (1992): Use of low-intensity electromagnetic millimeter waves in medicine. Millimetrovie Volni v Biologii i Meditcine 1:5-12 (in Russian).

Burachas G, Mascoliunas R (1989): Suppression of nerve action potential under the effect of millimeter waves. In Devyatkov ND (ed): "Millimeter Waves in Medicine and Biology." Moscow: Radioelectronica, pp 168-175 (in Russian).

Bush LG, Hill DW, Riazi A, Stensaas LJ, Partlow LM, Gandhi OP (1981): Effects of millimeter-wave radiation on monolayer cell cultures. III. A search for frequency-specific athermal biological effects on protein synthesis. Bioelectromagnetics 2:151-159.

Chernyakov GM, Korochkin VL, Babenko AP, Bigdai EV (1989): Reactions of biological systems of various complexity to the action of low-level EHF radiation. In Devyatkov ND (ed): "Millimeter Waves in Medicine and Biology." Moscow: Radioelectronica, pp 141-167 (in Russian).

Dunnet CW (1955): A multiple comparison procedure for comparing several treatments with a control. J. Am Stat Assoc 50:1096-1121.

Furia L, Hill DW, Gandhi OP (1986): Effect of millimeter wave irradiation on growth of Saccharomyces cerevisiae. IEEE Trans Biomed Eng 33:993-999.

Gandhi OP, Hagmann MJ, Hill DW, Partlow LM, Bush L (1980): Millimeter wave absorption spectra of biological samples. Bioelectromagnetics 1:285-298.

Grundler W, Keilman F, Froehlich H (1977): Resonant growth rate response of yeast cells irradiated by weak microwaves. Phys Lett 62A:463-466.

Grundler W, Kaiser F (1992): Experimental evidence for coherent excitations correlated with growth. Nanobiology 1:163-176.

Kataev AA, Alexandrov AA, Tikhonova LL, Berestovsky GN (1993): Frequency-dependent effects of the electromagnetic millimeter waves on the ion currents in the cell membrane of Nitellopsis: Nonthermal action. Biofizika 38:446-462.

Kazarinov KD, Sharov VS, Putvinskii AV, Betskii OV (1984): The effect of continuous millimeter low-intensity radiation on the Na^+ ion transport in the frog skin. Biofizika 29:480-482.

Keilmann F (1985): Resonant biological effects of microwaves. Physik in unserer Zeit 16:33-39.

Khizhnyak EP, Ziskin MC (1994): Heating patterns in biological tissue phantoms caused by millimeter wave electromagnetic radiation. IEEE Trans Biomed Eng 41:865-873.

Khramov RN, Sosunov EA, Koltun SV, Ilyasova EN, Lednev VV (1991): Millimeter-wave effects on electric activity of crayfish stretch receptors. Bioelectromagnetics 12:203-214.

Larsen, EG (1978): Techniques for producing standard EM fields from 10 kHz to 10 GHz for evaluating radiation monitors. In "Electromagnetic Fields in Biological Systems," Proceedings of a symposium, International Microwave Power Institute, Ottawa, Canada, pp 96-112.

Motzkin S, Feinstein, J (1989): Simultaneous intracellular and fluorescence monitoring of miniature end plate potentials in rat neuromuscular preparations during millimeter wave exposure. Tucson, AZ: 11th Annual Meeting of the Bioelectromagnetics Society, June, 1989, pp 6-7.

Pakhomov AG, Dubovick BV, Kolupayev VE, Pronkevich AN (1992): Microwave-induced changes in nerve conduction: effect of modulation. In: "Proceedings of the 14th Annual International Con-

ference, Part 1." Paris: IEEE Engineering in Medicine and Biology Society, pp 293–294.

Rebrova TB (1992): Effect of millimeter-range electromagnetic radiation on the vital activity of microorganisms. Millimetrovie volni v Biologii i Meditcine 1:37–47 (in Russian).

Ryakovskaya ML, and Shtemler, VM (1983): Absorption of electromagnetic waves of millimeter range in biological preparations with a plane-layer structure. In: Devyatkov ND (ed): "Effect of Nonthermal Action of Millimeter Radiation on Biological Subjects." Moscow: USSR Academy of Sciences, pp 172–181 (in Russian).

Sazonov AYu, Rizshkova LV (1995): Effects of electromagnetic radiation of millimeter range on biological subjects of various complicacy. Moscow, Russia: 10th Russian Symposium "Millimeter Waves in Medicine and Biology," April, 1995 (Digest of papers). Moscow: IRE RAN, pp 112–114 (in Russian).

Sit'ko SP, Zhukovsky VD, Montgomery GA (1992): Microwave resonance therapy (MRT) - a new non-invasive therapy for treatment of neuro-musculosceletal disorders. Lake Buena Vista, FL: First World Congress for Electricity and Magnetism in Biology and Medicine, June, 1992, pp 88–89.

Winer BJ (1971): "Statistical Principles in Experimental Design." New York: McGraw-Hill Book Company.

Appendix: Calculation of On–Axis Power Density for Horn Antennas

Methods for calibration of field strength-measuring probes/devices include free–space standard field methods, guided wave methods, and transfer probe methods. For calibrating field strength measuring probes/devices in the millimeter wave range, guided wave and transfer probe methods are inappropriate. The dimensions of transmission lines become very small, and dipoles in the transfer probe method become increasingly difficult to fabricate due to the small wavelengths involved. In free–space standard field methods, standard gain horns are commonly used to establish highly accurate electromagnetic field intensities in the frequency range above 1 GHz. We have used horn antennas in the frequency range 37 to 53 GHz and 53 to 78 GHz to generate standard field intensity at various distances from the horn antenna.

The on–axis incident power density (IPD) at an on–axis field point in free–space is computed using the equation

$$S = P_T G/4\pi r^2 \quad (1)$$

where S is the power density (W/m^2), P_T is the net input power into the horn (W), G is the absolute numerical power gain of the horn antenna, and r is the distance from the horn antenna aperture to the on–axis field point (m).

On–axis gain of the horn antenna is calculated from equations given by Larsen [1978] as

$$G(dB) = 10\log(AB) + 10.08 - R_H(dB) - R_E(dB) \quad (2)$$

where A is the wavelength normalized width of the horn aperture, B is the wavelength normalized height of the horn aperture, R_H is the gain reduction factor due to the H–plane flare of the horn, and R_E is the gain reduction factor due to the E–plane flare of the horn. The gain reduction factors are given by

$$R_H(dB) = (0.01\alpha)(1 + 10.19\alpha + 0.51\alpha^2 - 0.097\alpha^3) \quad (3)$$

$$R_E(dB) = (0.1\beta^2)(2.31 + 0.053\beta) \quad (4)$$

$$\alpha = A^2(1/L_H + 1/r) \quad (5)$$

$$\beta = B^2(1/L_E + 1/r) \quad (6)$$

where L_E and L_H are wavelength normalized values of the slant lengths and r is the wavelength normalized distance from the aperture of the horn to the on–axis field point.

For given horn dimensions, on–axis gain was calculated at each frequency of interest at distances from 40 to 500 mm. The net input power to the horn is determined from forward and reflected power measurements at the feed to the horn using a bidirectional coupler, and the incident power density S is then calculated using the gain computed from equations (2)–(6). All calculations for S are expressed in mW/cm^2 per mW of net input power to the horn.

Bioelectromagnetics 19:128–130 (1998)

Brief Communication

Ultra-Wide Band Electromagnetic Radiation Does Not Affect UV-Induced Recombination and Mutagenesis in Yeast

Olga N. Pakhomova,* Michelle L. Belt, Satnam P. Mathur, Jonathan C. Lee, and Yahya Akyel

McKesson BioServices, Microwave Bioeffects Branch, U. S. Army Medical Research Detachment of the Walter Reed Army Institute of Research, Brooks Air Force Base, San Antonio, Texas

Cell samples of the yeast *Saccharomyces cerevisiae* were exposed to 100 J/m^2 of 254 nm ultraviolet (UV) radiation followed by a 30 min treatment with ultra-wide band (UWB) electromagnetic pulses. The UWB pulses (101–104 kV/m, 1.0 ns width, 165 ps rise time) were applied at the repetition rates of 0 Hz (sham), 16 Hz, or 600 Hz. The effect of exposures was evaluated from the colony-forming ability of the cells on complete and selective media and the number of aberrant colonies. The experiments established no effect of UWB exposure on the UV-induced reciprocal and non-reciprocal recombination, mutagenesis, or cell survival. *Bioelectromagnetics 19:128–130, 1998.* © 1998 Wiley-Liss, Inc.

Key words: UWB; recombination; mutagenesis; yeast; ultraviolet light

INTRODUCTION

Ultra-wide band (UWB) systems have recently been developed for use as radars and as a means to suppress electronically vulnerable targets. UWB radiation is produced as short high-voltage pulses with an extremely fast rise, providing for the spectral bandwidth from 0 Hz to 2 GHz. The unusual properties of UWB radiation have raised concerns about its bioeffects and possible health hazards to personnel.

At present time, only a few studies of UWB bioeffects have been carried out, and they were focused on behavioral and physiological effects in laboratory animals [Walters et al., 1995; Sherry et al., 1995]. There have been no studies of cellular or genetic UWB effects, though evaluation of genetic risks is necessary for any potentially hazardous environmental factors (radiations, chemicals, etc.). In addition, a number of studies have suggested that cell DNA may be a target for various types of electromagnetic radiations [Blank et al., 1997; Lai et al., 1997; Belyaev et al., 1996].

To address this issue, we used the yeast *Saccharomyces cerevisiae* strain D7 specifically designed for screening of mutagenic and recombinagenic effects [Zimmermann et al., 1975]. Our recent experiments with this cell model demonstrated no UWB effect on spontaneous mutagenesis, recombinagenesis, or colony-forming ability [Pakhomova et al., 1997]. The purpose of the present work was to establish whether UWB exposure alters the induction of heritable chromosome aberrations by ultraviolet light (UV), a standard mutagenic factor.

The employed yeast strain D7 carries specific gene markers *ade2-40/ade2-119, trp5-12/trp5-27,* and *ilv1-92/ilv1-92*, which make it possible to detect certain mutagenic and recombinagenic events. Mutation induction by true reverse or allele non-specific suppresser mutation in *ilv1-192* is followed by appearance of iso-

Contract grant sponsor: US Army Medical Research and Material Command; contract grant number: DAMD17-94-C-4069 to McKesson BioServices.

*Correspondence to: Dr. O. Pakhomova, USA-MCMR, US Army Medical Research Detachment, 8308 Hawks Road, Building 1168, Brooks Air Force Base, San Antonio, TX 78235-5324; E-mail: pakhomov@netxpress.com

Received for review 19 May 1997; final review received 21 August 1997

© 1998 Wiley-Liss, Inc.

TABLE 1. Yeast Cell Survival and the Rates of Genetic Aberrations after Sequential UV and UWB Exposures

	Survival %	Crossovers per 10^2 survivors	Segregants per 10^2 survivors	Convertants per 10^5 survivors	Revertants per 10^6 survivors
Exposed (UV + 0 Hz UWB, $n = 6$)[a]	66.8 ± 3.7 (10179)[b]	1.83 ± 0.27 (179)	7.87 ± 0.79 (783)	196 ± 12 (16213)	290 ± 24 (3493)
Control (UV only, $n = 6$)	66.6 ± 4.9 (10019)	1.78 ± 0.22 (176)	7.82 ± 0.45 (776)	200 ± 11 (16310)	294 ± 22 (3652)
Exposed (UV + 16 Hz UWB, $n = 5$)	64.6 ± 5.3 (8385)	1.75 ± 0.23 (150)	7.47 ± 0.74 (618)	201 ± 17 (14362)	285 ± 40 (2915)
Control (UV only, $n = 5$)	62.2 ± 6.5 (8166)	1.71 ± 0.23 (136)	7.61 ± 0.55 (602)	211 ± 25 (14193)	282 ± 38 (2947)
Exposed (UV + 600 Hz UWB, $n = 6$)	62.3 ± 5.9 (9291)	2.01 ± 0.32 (179)	8.06 ± 0.72 (735)	209 ± 14 (15406)	275 ± 26 (3189)
Control (UV only, $n = 6$)	62.0 ± 7.0 (9246)	1.92 ± 0.33 (169)	8.54 ± 0.67 (782)	209 ± 20 (14936)	299 ± 25 (3335)

[a]Shown are the repetition rate of UWB pulses, Hz (0 Hz corresponds to sham exposure), and the number of independent experiments in each series, *n*.

[b]All the data values are given as an average (mean ± SE) for *n* experiments. Numbers in brackets indicate the actual number of colonies scored in all experiments with a particular type of exposure.

leucine non-requiring colonies on isoleucine-free media. Mitotic gene conversion is monitored by appearance of tryptophan non-requiring colonies on selective media. The alleles involved are *trp5-12* and *trp5-27*. Mitotic crossing-over is detected visually as pink and red twin sectored colonies due to formation of homozygous cells *ade2-40/ade2-40* (deep red) and *ade2-119/ade2-119* (pink) from the originally heteroallelic condition (white). Occurrences such as aneuploidy, point mutations, etc., give rise to more types of colored aberrant colonies, which are regarded below as segregants.

Preliminary experiments established that the threshold UV dose for a noticeable decrease of cell survival is about 50 J/m^2. Production of mutations and recombinations increased with increasing the UV dose up to about 150 J/m^2 and then reached a plateau or decreased. Hence, an intermediate dose of 100 J/m^2 was chosen for the main set of the experiments.

UWB pulses were produced by an exposure system designed at Sandia National Laboratories. UWB irradiation lasted for 30 min at a pulse repetition rate of 0 (sham), 16, or 600 Hz. Within 30 min, the suspension remained virtually uniform, showing no visible signs of sedimentation of cells. Based on measurements of the electric field using an EG&G D-dot sensor (model ACD-1A), the parameters of UWB pulses at the repetition rate of 16 Hz were as following (mean ± SE): 103.7 ± 0.57 kV/m peak amplitude, 1.019 ± 0.004 ns pulse width, and 164.8 ± 0.6 ps rise time. The respective values for the pulse repetition rate of 600 Hz were 101.5 ± 0.3 kV/m, 1.014 ± 0.005 ns, and 165.2 ± 0.9 ps. The exposure system's performance and dosimetry have been described in more detail by Bao et al. [1995]. Possible heating effect of the UWB exposure was evaluated with a Vitek Electrothermia Monitor (model 101) using a non-perturbing probe (#2427). Temperature changes in samples exposed for 30 min at 600 Hz did not exceed ambient temperature fluctuations.

Prior to exposures, yeast cells were grown for three days on YPD agar (1% yeast extract, 2% peptone, 2% dextrose, 2% agar), and suspended in distilled water at a titer of 5×10^6 cells/ml. Samples of 2.5 ml of this suspension in a Petri dish (36 mm diameter) were exposed to 254 nm UV radiation (Cole Parmer lamp model VL-6.LC) at 2.25 J/m^2/s up to the total dose of 100 J/m^2. To prevent possible recovery of genetic lesions by photoreactivation, these and subsequent manipulations were performed in dim red light. Two 1-ml samples of the UV-exposed suspension were transferred into identical polystyrene tubes. One tube was subjected to UWB or sham exposure, and the other one was used as a parallel control. The time interval between the completion of the UV exposure and the onset of the UWB exposure did not exceed 2 min. The sham exposure conditions were equivalent to the actual UWB exposure with zero pulse repetition frequency: All devices were turned on, but no trigger pulses were delivered to cause the high-voltage discharge across the spark gap. To enable a more vigorous experimental data analysis, sham exposures were accompanied with parallel control as well. All the three types of exposure (16 Hz, 600 Hz, and sham) were performed during the same day and using the same original cell suspension. The sequence of these exposures varied randomly from day to day and was not disclosed until the completion of the study to achieve double-blind conditions.

Immediately after the UWB or sham exposure, the samples were appropriately diluted according to

the expected yield of viable clones and plated onto minimal and selective media. The minimal medium was composed of 0.67% Difco yeast nitrogen base without amino acids, solidified with Difco agar (2%) and supplemented with the following growth factors: adenine sulfate (5 mg/l), L-isoleucine (60 mg/l), and L-tryptophan (10 mg/l). The selective media excluded L-isoleucine or L-tryptophan. The plates were incubated at 30 °C in the dark for 6 days. Survivals, mitotic crossovers, and segregants were scored as white or colored colonies formed on the minimal medium (10 plates per sample). Mutants to isoleucine independence and gene convertants to tryptophan independence were scored on the respective selective media (5 plates per sample). The parallel controls were always processed in the same way and simultaneously with respective UWB- and sham-exposed samples.

The experimental results are provided in the Table 1. The UV exposure decreased cell survival to 60–70%, and this level was not altered by the UWB exposure. The frequencies of segregations, mutations to the isoleucine independence, and recombinagenic events (mitotic crossing-over and conversion to tryptophan independence) were remarkably close in the UWB-exposed and parallel control samples, as well as in the UWB-exposed and sham-treated cells. The data showed no statistically significant effects (Student's *t*-test and χ^2 test) or even trends in any of the studied groups.

Our previous study has shown that UWB pulses per se do not provoke any mutagenic or recombinagenic events [Pakhomova et al., 1997]. Current research has supplemented this result, proving that acute exposure to UWB pulses does not affect UV-induced mutagenesis and recombinagenesis.

ACKNOWLEDGMENTS

The work was supported by the US Army Medical Research and Material Command under contract DAMD17-94-C-4069 awarded to McKesson BioServices. The views, opinions and findings contained in this report are those of the authors and should not be construed as an official Department of the Army position, policy or decision.

REFERENCES

Bao J-Z, Lee JC, Lu S-T, Seaman RL, Akyel Y (1995): Analysis of ultra-wide-band pulses in GTEM cell. In Brandt HE (ed): "Intense Microwave Pulses III". Proceedings of SPIE 2557, pp 237–248.

Belyaev IY, Shcheglov VS, Alipov YD, Polunin VA (1996): Resonance effect of millimeter waves in the power range from 10^{-19} to 3×10^{-3} W/cm^2 on *Escherichia coli* cells at different concentrations. Bioelectromagnetics 17:312–321.

Blank M, Goodman R (1997): Do electromagnetic fields interact directly with DNA? Bioelectromagnetics 18:111–115.

Lai H, Singh NP (1997): Acute exposure to a 60 Hz magnetic field increases DNA strand breaks in rat brain cells. Bioelectromagnetics 18:156–165.

Pakhomova ON, Belt ML, Mathur SP, Lee JC, Akyel Y (1997): Lack of genetic effects of ultrawide-band electromagnetic radiation in yeast. Electro Magnetobiology 16:195–201.

Sherry CJ, Blick DW, Walters TJ, Brown GC, Murphy MR (1995): Lack of behavioral effects in non-human primates after exposure to ultrawideband electromagnetic radiation in the microwave frequency range. Radiat Res 143:93–97.

Walters TJ, Mason PA, Sherry CJ, Steffen C, Merrit JH (1995): No detectable bioeffects following acute exposure to high peak power ultra-wide band electromagnetic radiation in rats. Aviat Space Environ Med 66:562–567.

Zimmermann FK, Kern R, Rasenberger H (1975): A yeast strain for simultaneous detection of induced mitotic crossing over, mitotic gene conversion and reverse mutation. Mutation Res 28:381–388.

Picosecond domain electromagnetic pulse measurements in an exposure facility: An error compensation routine using deconvolution techniques

Jian-Zhong Bao
McKesson BioServices and U.S. Army Medical Research Detachment, Brooks Air Force Base, Texas 78235

(Received 8 August 1996; accepted for publication 22 January 1997)

This article presents a two-step deconvolution routine to compensate for the measurement distortions of transient electrical fields in the picosecond domain in an electromagnetic pulse exposure facility. Because of the low-pass nature of connection cables and the limited bandwidth of a transient digitizer (Tektronix SCD 5000), the measured signal is a distorted output of D-dot (dD/dt, where D is the electric displacement) sensors. An empirical transfer function of the cable-digitizer system was evaluated using a reference impulse generated by a picosecond pulse generator. The reference impulse was injected into the connection cable at the D-dot sensor end and measured with the SCD 5000 while the cable was kept in the same position as for making D-dot measurements to ensure an in-position compensation. Two types of asymptotic conical dipole (ACD) D-dot sensors were utilized as the electrical field sensing devices: an axial model ACD-1(A) and a radial model ACD-1(R). Due to its right-angle structures, the ACD-1(R) gives a different output from that of ACD-1(A) to the same pulse, especially to the fast leading edge. The right-angle bends in ACD-1(R) cause reflections of a sensed signal in the sensor. To correct the errors due to the reflections, the impulse response of the ACD-1(R) D-dot sensor was proposed as a summation of the δ function and the parameters were determined with a pulse measurement using the ACD-1(A) D-dot sensor and an optimization procedure with the Levenberg–Marguardt algorithm. With this routine the measurement accuracy for the electrical pulse in picosecond domain has been improved significantly. [S0034-6748(97)01105-2]

I. INTRODUCTION

It is still a challenge to make an accurate transient measurement on electromagnetic pulses in the picosecond domain because of the limitations of measurement components.[1–5] This article presents a two-step deconvolution routine to compensate for the measurement distortions in a short electromagnetic pulse (EMP) exposure facility for studying biological effects. As depicted in Fig. 1, this facility, which was designed and built at the Sandia National Laboratories,[6] mainly consists of a pulse generator and an exposure cell. The generator includes a charging network and a RG220 coaxial cable. The exposure cell is a tapered transverse electromagnetic (TEM) cell with a centered septum. The RG220 cable connects a plasma switch to the TEM cell. When the charging circuit is triggered, a pulse with a magnitude of about 60 kV is generated and sent down to the spark gap. When the voltage across the gap reaches the breakdown voltage of the gas in it, a pulse with a much faster leading edge is formed in the RG220 and delivered to the cell. The exposure facility was installed in a shielded room, and the control and measurement devices were located outside. The pulse repetition frequency was controlled by an external trigger. The measurement system includes a Tektronix SCD 5000 transient digitizer (4.5 GHz bandwidth), an UT141 semirigid coaxial cable, and two asymptotic conical dipole (ACD) D-dot (dD/dt, where D is the electric displacement) sensors:[7,8] ACD-1(A), which is an axial model and mounted on the top ground wall of the cell for real time monitoring during exposures, and ACD-1(R), which is a radial model and used to map the field on the bottom ground wall of the cell where the biological specimens are placed. The SCD 5000 is connected to a D-dot sensor through a connection cable and triggered with a signal obtained from the RG220.

Because of the low-pass nature of the connection cables, which is attributed to the skin depth effect and dielectric dispersions,[9] and the limited bandwidth of the SCD 5000, the measured signal is a distorted output of the D-dot sensors. An empirical transfer function of the cable-digitizer system was evaluated using a reference impulse that was generated by a Pico Second Pulse Lab (PSPL) 4050B step generator with a 5210 impulse forming network (IFN) and characterized with a Tektronix CSA 803 communication signal analyzer with a SD 30 sampling head (40 GHz bandwidth). The reference impulse was injected into the connection cable at the D-dot sensor end and measured with the SCD 5000 while the cable was kept in the same position as for making a field measurement to ensure an in-position compensation.

Due to its right-angle structures, the ACD-1(R) D-dot sensor gives a different output from that of the ACD-1(A) to the same pulse, especially to the fast leading edge although the sensing elements for both sensors are the same. The right-angle bends in the ACD-1(R) cause reflections of a sensed signal in the sensor. For the first time, the impulse response of the ACD-1(R) was formulated as a summation of a δ function in order to correct the error resulted from the reflections. The parameters of the impulse response were determined with a symmetric reference measurement using the ACD-1(A) D-dot sensor and a nonlinear optimization procedure with the Levenberg–Marguardt algorithm.[10]

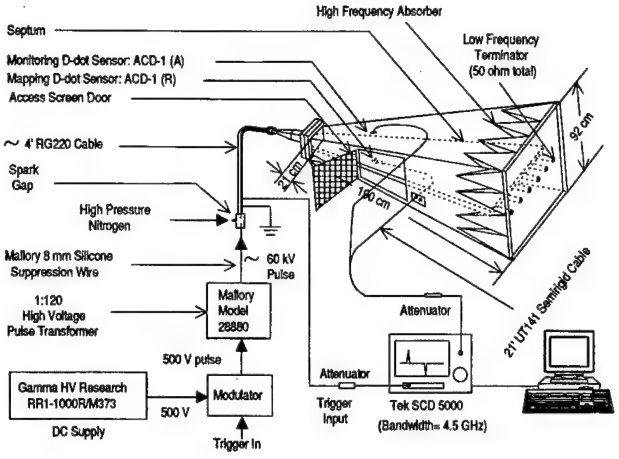

FIG. 1. Schematic diagram of the short electromagnetic pulse (EMP) exposure facility and the picosecond domain pulse acquisition system.

II. ERROR COMPENSATION: DECONVOLUTION

Deconvolution techniques are effective tools for data reconstruction in many areas[11–14] and were applied here to compensate the distortions in electrical pulse measurements. By assuming that the measurement system is linear and time invariant (LTI), we can have

$$u(t)=v(t)*h(t)+n(t)=\int_{-\infty}^{+\infty} v(\tau)h(t-\tau)d\tau+n(t), \qquad (1)$$

where $u(t)$ is the measured signal, $v(t)$ is the true signal before any degradations, $h(t)$ is the system impulse response, $n(t)$ is the additive noise, and $*$ denotes convolution, which smears fast changing features in $v(t)$. Here we have an inverse problem: finding $v(t)$ from $u(t)$, $h(t)$, and $n(t)$, i.e., deconvolution, which is an ill-posed problem mathematically.[15] Small changes in $u(t)$ can be mapped into large changes in $v(t)$. This is such a serious problem that an effective noise-control procedure has to be implemented because none of the measurements are noise free. Performing a Fourier transform on Eq. (1), we get

$$U(f)=V(f)H(f)+N(f), \qquad (2)$$

where upper case letters are Fourier transforms of the corresponding lower case letters, respectively, $H(f)$ is the system transfer function, and f is the frequency. Now $v(t)$ can be solved by performing inverse Fourier transform:

$$v(t)=F^{-1}\left(\frac{U(f)-N(f)}{H(f)}\right), \qquad (3)$$

where F^{-1} stands for inverse Fourier transform. If we had an exact knowledge about $U(f)$, $N(f)$, and $H(f)$ in the entire frequency range, and if the measurement system, as assumed, were LTI, $v(t)$ could be recovered exactly. Unfortunately, LTI condition may not be rigorously true and none of the above information can be obtained perfectly in practice because of the ever presence of noise and error. In general, the noise spectra $N(f)$ cannot be separated from the measured signal spectra $U(f)$ unless there are other information or assumptions available. So, Eq. (3) can only be applied

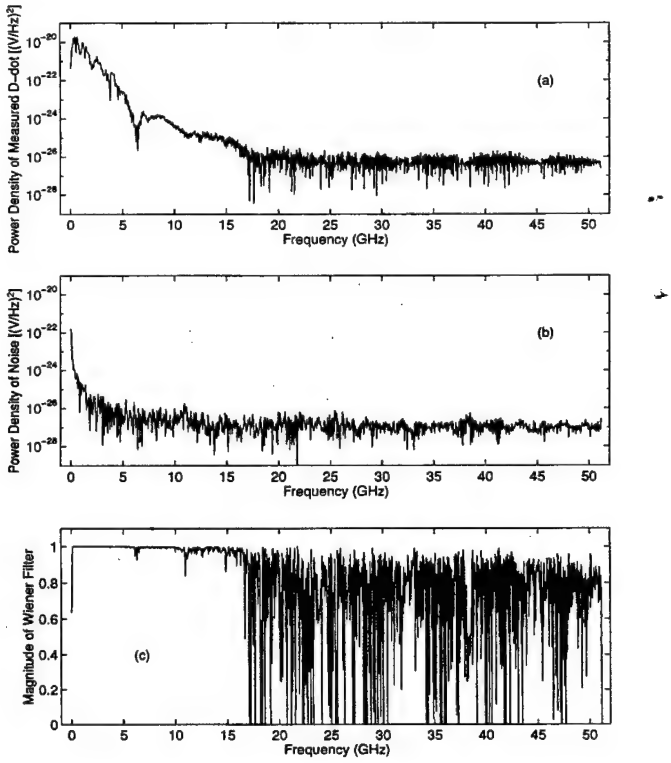

FIG. 2. (a) A typical power spectrum of output voltage of the ACD-1(A) D-dot sensor, (b) a typical power spectrum of the noise obtained remote after a pulse excitation, and (c) their corresponding Wiener filter.

approximately with $U(f)-N(f)\approx U(f)$. However, a Wiener filter minimizes the error caused by $N(f)$ in the least-squares sense, and is defined as[10]

$$\Phi(f)=1-\frac{|N(f)|^2}{|U(f)|^2}. \qquad (4)$$

If we presume that the power spectra of noise $|N(f)|^2$ with a pulse excitation is the same as that after the excitation, we can obtain it from a measurement in a time window of the same size that is remote after the excitation. Figure 2 shows the power spectra of a typical output voltage of the ACD-1(A) D-dot sensor under a pulse excitation and a typical noise signal obtained remote after the pulse excitation, and their corresponding Wiener filter. The noise spectrum exhibits a typical $1/f$ characteristics, which might be attributed to the fluctuations in the SCD 5000.[16,17]

In this study, the wave forms obtained with the SCD 5000 were digitized with 1024 points in a 10 ns window, which implies a maximum frequency of 51.15 GHz. The reference impulse was sampled with 1000 points in a 10 ns window using the CSA 803 and interpolated into 1024 points in the same window. All the wave forms were the average of 200 to remove random noises and increase the signal-to-noise ratio. All the raw data was pretreated before applying the fast Fourier transform (FFT). The pretreatment includes taking off base-line offset, converting attenuator factor, zero padding to avoid aliases and to make u periodically causal,[18] and data windowing to avoid sharp changes at the edges.

Since the signal was over sampled, a low-pass filter was mandatory. With a Wiener and a low-pass filter, Eq. (3) can be rewritten as

$$v(t)=F^{-1}\left(\frac{U(f)\Phi(f)L(f)}{H(f)}\right), \tag{5}$$

where $L(f)$ is a low-pass filter. Its cutoff edge was a half Hann window[10] and cutoff frequency was chosen as 12.5 GHz to retain all the frequency contents which might be obtained by the D-dot sensors.[19] The imperfection (e.g., nonlinearities) of the wave-form recorders (SCD 5000 and CSA 803) was not considered in this work. The most critical task in deconvolution is the evaluation of the transfer function, and it can be classified as the empirical or semiempirical method. The following two sections show how we obtain the transfer function empirically (Sec. III) and semiempirically (Sec. IV).

III. COMPENSATION FOR CONNECTION CABLE AND TRANSIENT DIGITIZER

A PSPL 4050B step generator with a 5210 IFN was utilized to generate an impulse with a magnitude of 2.8 V and a pulse width of 58 ps as the reference. Since the output impulses from the IFN are basically identical and repetitive, they can be characterized by a CSA 803 with a SD 30 sampling head. A different position configuration of connection cables gives a different impulse response, especially to the high-frequency contents. To take this effect into account, a characterized picosecond impulse was injected into the connecting cable between the D-dot sensor and the SCD 5000 at the D-dot sensor end while keeping the cable's position the same as for a real field measurement. Figure 3 shows the reference impulse characterized by the CSA 803, the impulse measured by the SCD 5000 through the connection cable, and the respective Fourier transform. There is a significant difference between the reference and the measured impulses in both time and frequency domain. The magnitudes of the Fourier spectra indicate that the reference impulse is much stronger than measured impulse in a wide frequency range (dc, 20 GHz), which gives us the physical basis that we can numerically expand the bandwidth of the measurement hardware to a wider frequency range[20] and compensate the distortions due to the connection cable and the SCD 5000. The extent of the bandwidth expansion is largely determined by the reference impulse.

Rearranging Eq. (1) to a form for the evaluation of a system transfer function, we have

$$x_{\text{out}}(t)+n_{\text{out}}(t)=[x_{\text{in}}(t)+n_{\text{in}}(t)]*h_{\text{cd}}(t), \tag{6}$$

where $x_{\text{out}}(t)+n_{\text{out}}(t)$ is the output impulse measured by the SCD 5000, in which $x_{\text{out}}(t)$ is the desired signal we want to obtain and $n_{\text{out}}(t)$ is the additive noise, $x_{\text{in}}(t)+n_{\text{in}}(t)$ is the input impulse characterized by the CSA 803, in which $x_{\text{in}}(t)$ is the real signal and $n_{\text{in}}(t)$ is the noise, and $h_{\text{cd}}(t)$ is the impulse response of the cable–digitizer system to be obtained from the measurements. By taking Fourier transform on Eq. (6), we can get the frequency domain form:

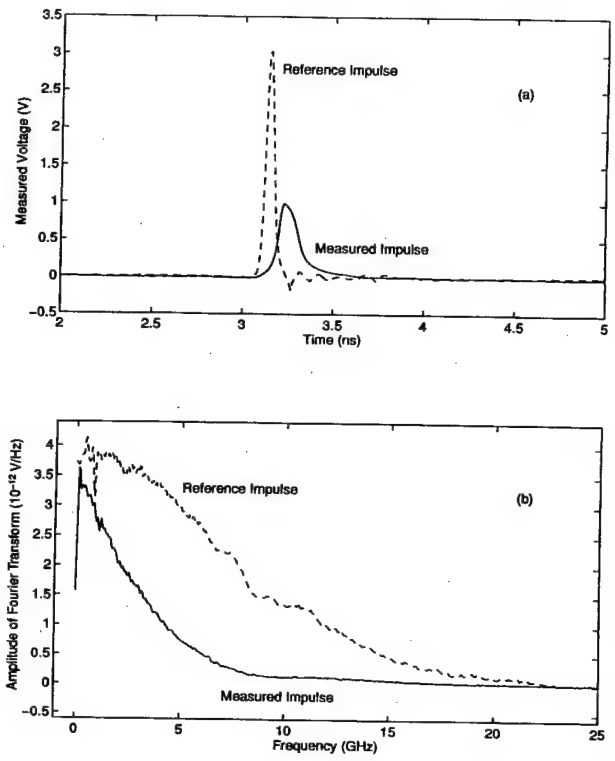

FIG. 3. Comparison between the reference impulse characterized using a CSA 803 with a SD 30 sampling head and the measured impulse with a SCD 5000 through an UT141 connection cable (a) in time domain and (b) in frequency domain.

$$H_{\text{cd}}(f)=\frac{X_{\text{out}}(f)+N_{\text{out}}(f)}{X_{\text{in}}(f)+N_{\text{in}}(f)}$$

$$=H(f)\,\frac{1+N_{\text{out}}(f)/X_{\text{out}}(f)}{1+N_{\text{in}}(f)/X_{\text{in}}(f)}, \tag{7}$$

where the upper case letters stand for the Fourier transform of the corresponding lower case letters, respectively, and

$$H(f)=\frac{X_{\text{out}}(f)}{X_{\text{in}}(f)} \tag{8}$$

is the true transfer function. The fraction term behind $H(f)$ in Eq. (7) is the noise contribution, which is close to one at the frequencies at which the signal-to-noise ratios of both input and output impulses are very large. At the frequencies where $X_{\text{in}}(f)$ is close to zero, $X_{\text{out}}(f)$ should be close to zero, too. When the frequencies are far away from the measurement band of the recording instrument, no matter how large $X_{\text{in}}(f)$ is, $X_{\text{out}}(f)$ is just noise. Consequently, at these frequencies, $H_{\text{cd}}(f)$ contains only noise. Since $H(f)$ can only be obtained approximately in practice, an exact deconvolution is inherently impossible.[21,22]

$H_{\text{cd}}(f)$ given by Eq. (7) was utilized in Eq. (5) as the transfer function, $H(f)$, to compensate the effect of the connection cable and the SCD 5000. Since the spectra of reference and measured impulses were the average of 200, the contributions from the random noise were substantially canceled. It can be observed from Fig. 3(b) that both spectra

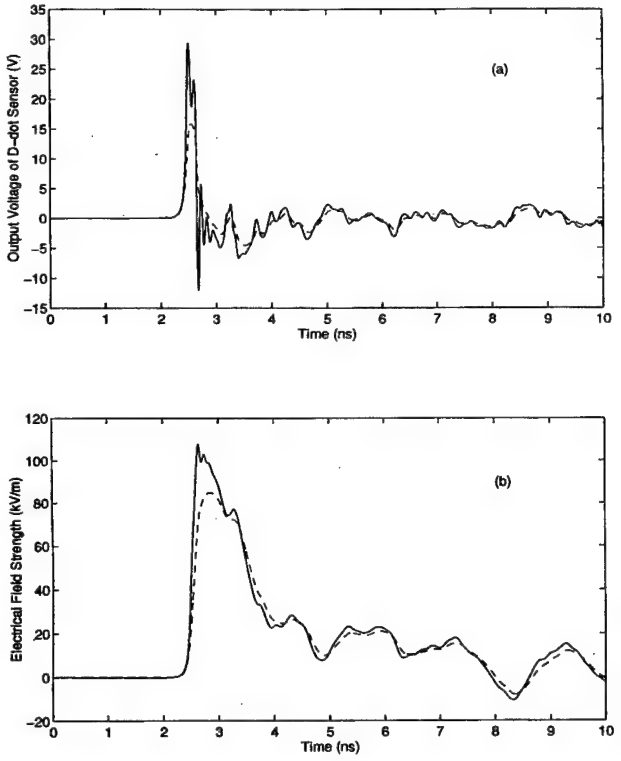

FIG. 4. (a) Comparison between output voltage of ACD-1(A) D-dot sensor without any compensation (dashed lines) and that after the cable-digitizer compensation (solid lines). (b) Comparison between the corresponding electrical fields. The measurement was done at a pulse repetition frequency of 60 Hz. The comparison of pulse parameters are listed in Table I.

have a sensible magnitude up to 15 GHz so that Eq. (7) is a good approximation to Eq. (8) in the frequency range that concerns us.

All the electrical fields in this article were calculated with a simple summation,

$$E(t_n)=c\sum_{k=0}^{n}\dot{D}(t_k), \tag{9}$$

where $E(t_n)$ is the transient electrical field, $\dot{D}(t_k)$ is the measured or compensated transient output voltage of D-dot sensors, and c is a converting coefficient given by $c=\Delta t/(\epsilon_0\epsilon_r A_{eq}R)$, in which Δt is the sampling time interval of SCD 5000, ϵ_0 is the permittivity of vacuum, ϵ_r is the relative permittivity of the medium in which the sensor is, A_{eq} is the equivalent area of the sensor, and R is the load impedance.

Figure 4(a) shows the comparison between the measured and the cable-digitizer compensated output voltage of the ACD-1(A) D-dot sensor at a pulse repetition frequency of 60 Hz. The sensor was mounted on the top ground wall of the TEM cell. Figure 4(b) presents the comparison between their corresponding electrical fields. Clearly, the compensated electrical field gives a faster rise time and a higher magnitude than that directly measured. The comparison between their pulse parameters is listed in Table I.

TABLE I. Comparison of pulse parameters between the uncompensated and the cable-digitizer compensated electrical fields presented in Fig. 4(b). The measurement was done using an ACD-1(A) D-dot sensor at a pulse repetition frequency of 60 Hz.

Electrical field	Rise time (10–90%) (ps)	Magnitude (kV/m)	Pulse width (ns)
Uncompensated	234	84.8	1.11
Compensated	166	107.6	0.98

IV. COMPENSATION FOR REFLECTIONS IN *D*-DOT SENSOR ACD-1(R)

The sensing elements in both ACD-1(R) and ACD-1(A) D-dot sensors are the same while they are connected to the respective SMA connectors differently. In the ACD-1(A), the sensing element and the SMA connector are joined in the axial direction directly, while in the ACD-1(R) they are connected by a coaxial line through three right-angle bends in the radial direction, as schematically drawn in Fig. 5. The right-angle bends of the ACD-1(R) D-dot sensor cause reflections of a sensed signal in the sensor. The reflections result in a magnitude reduction and a "shoulder" on the falling edge of the first spike in the output voltage of the ACD-1(R) D-dot sensor, as shown in Fig. 6(a). Although there are only minor influences on its slow variation part, there is a clear consequence on the fast leading edge of the pulse, which is illustrated in Fig. 6(b). The leading edge is important for estimating the rise time.

If we do not consider any dispersions which may be associated with the sensors, the output of an ACD-1(R) D-dot sensor is the transmission of the original signal plus down-scaled and delayed replicas of the original signal, therefore its impulse response can be approximated as

$$h(t)=a_0\delta(t)+a_1\delta(t-\tau_1)+a_2\delta(t-\tau_2), \tag{10}$$

where a_k ($k=0,1,2$) are the scaled coefficients and τ_k ($k=1,2$) are the delay times. The physical constrains for the parameters are $0<a_k<1$ and $\tau_k>0$. The effects of the sensing element were not taken into account because the sensor has a bandwidth $\geqslant$10 GHz,[19] and the low-pass nature of the coaxial line and the SMA connector was ignored. The first δ function in Eq. (10) is for the transmitted D-dot signal through the right-angle bends, and the rest of them are for

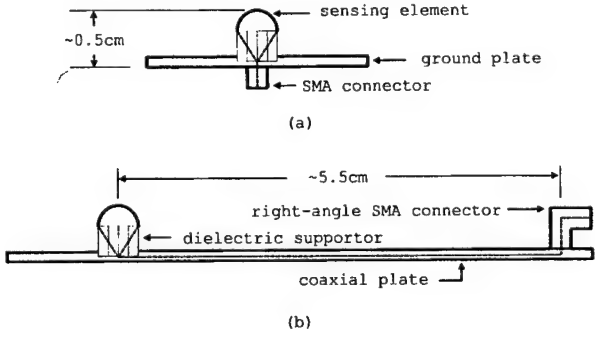

FIG. 5. Geometric configurations and dimensions of the asymptotic conical dipole D-dot sensors: (a) the axial model ACD-1(R) and (b) the radial model ACD-1(A).

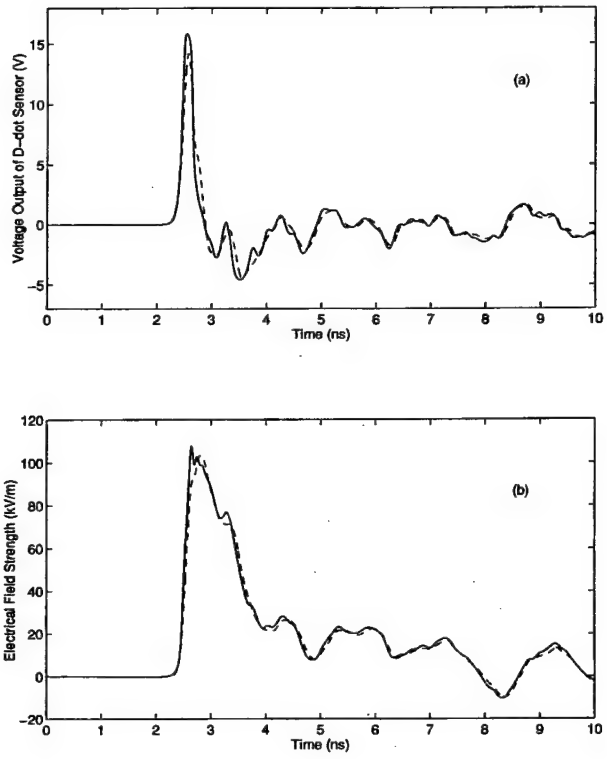

FIG. 6. (a) Comparison between measured output voltage of the ACD-1(A) D-dot sensor (solid lines) and that of the ACD-1(R) D-dot sensor (dashed lines). The two sensors were located at a symmetric pair of locations on the top and the bottom ground wall of the TEM cell, respectively. (b) Comparison between their corresponding electrical fields with the respective cable-digitizer compensation.

the reflections. If the sensed signal were a δ function and there were no dispersion associated with the sensor, and if the digitizer were infinitely fast, all the reflections would be separated. From Fig. 6(a), it seems that only the first reflection had an obvious effect on the electrical field, so only two reflections were considered. The number of the δ function included in Eq. (10) is mainly decided by the high frequency contents in the pulse. The sharper the pulse is, the more δ functions might be needed. For a given set of parameters, $\mathbf{P}=\{a_0,a_1,\tau_1,\ldots\}$, the distortion due to the reflections in the ACD-1(R) D-dot sensor and the limitations of the cable-digitizer system can be compensated together with

$$w_{\mathrm{rec}}(t,\mathbf{P})=F^{-1}\left(\frac{U(f)\Phi(f)L(f)}{H_{\mathrm{cd}}(f)H_{\mathrm{dd}}(f,\mathbf{P})}\right), \tag{11}$$

where $H_{\mathrm{dd}}(f,\mathbf{P})$ is the transfer function given by

$$H_{\mathrm{dd}}(f,\mathbf{P})=a_0+a_1e^{-j\omega\tau_1}+a_2e^{-j\omega\tau_2}, \tag{12}$$

where ω is the angular frequency. For a different $\mathbf{P}$ we get a different w_{rec}. To determine the optimal $\mathbf{P}$, the Levenberg–Marguardt algorithm[10] was utilized to minimize an objective function defined as

$$S(\mathbf{P})=\sum_{n=0}^{N/2-1}W(t_n)[E_{\mathrm{ref}}(t_n)-E_{\mathrm{rec}}(t_n,\mathbf{P})]^2, \tag{13}$$

where N is the total number of data points including zero padding, W is the weighting factor, $E_{\mathrm{ref}}(t_n)$, used as a reference, is the electrical field obtained with the cable-digitizer compensated output voltage of ACD-1(A) D-dot sensor. $E_{\mathrm{rec}}(t_n,\mathbf{P})$ is the electrical pulse to be optimized through adjusting $\mathbf{P}$. It was calculated with the output voltage of ACD-1(R) D-dot sensor after cable-digitizer *and* D-dot sensor compensation. The measurement using the ACD-1(R) D-dot sensor was done at a specific location on the bottom ground wall that was symmetric to the ACD-1(A) about the center septum, as indicated in Fig. 1. By the symmetry of the cell, E_{rec} and E_{ref} should be very close to each other, and the observed difference is mainly due to the reflections in the ACD-1(R). Adjusting W in Eq. (13) allows us to emphasize a specific portion of the wave form, e.g., the leading edge. An additional phase term may be needed in Eq. (12) to synchronize $E_{\mathrm{ref}}(t_n)$ and $E_{\mathrm{rec}}(t_n,\mathbf{P})$ for the nonlinear least-squares optimization. The reason for utilizing the electrical field rather than the output voltage of D-dot sensors is that the former gives a better recovery to its leading edge.

In this iterative minimization procedure the parameters were adjusted in time domain while the derivatives were calculated in frequency domain and then transformed back to time domain. The derivatives, which are needed in the Levenberg–Marguardt algorithm, were calculated as[10]

$$\frac{\partial S(\mathbf{P})}{\partial p_k}=\sum_{n=0}^{N/2-1}2W(t_n)[E_{\mathrm{rec}}(t_n,\mathbf{P})-E_{\mathrm{ref}}(t_n)]\frac{\partial E_{\mathrm{rec}}(t_n,\mathbf{P})}{\partial p_k} \tag{14}$$

and

$$\frac{\partial^2 S(\mathbf{P})}{\partial p_k\partial p_l}=\sum_{n=0}^{N/2-1}2W(t_n)\frac{\partial E_{\mathrm{rec}}(t_n,\mathbf{P})}{\partial p_k}\frac{\partial E_{\mathrm{rec}}(t_n,\mathbf{P})}{\partial p_l}, \tag{15}$$

where p_k and p_l are the kth and lth parameters in $\mathbf{P}$, respectively, and

$$\begin{aligned}\frac{\partial E_{\mathrm{rec}}(t_n,\mathbf{P})}{\partial p_k}&=c\sum_{l=0}^{n}\frac{\partial w_{\mathrm{rec}}(t_l,\mathbf{P})}{\partial p_k}\\&=c\sum_{l=0}^{n}F^{-1}\left(-\frac{U(f)\Phi(f)L(f)}{H_{\mathrm{cd}}(f)H_{\mathrm{dd}}^2(f,\mathbf{P})}\frac{\partial H_{\mathrm{dd}}(f,\mathbf{P})}{\partial p_k}\right),\end{aligned} \tag{16}$$

where $\partial H_{\mathrm{dd}}(f,\mathbf{P})/\partial p_k$ is given by one of the following:

$$\begin{aligned}\frac{\partial H_{\mathrm{dd}}(f,\mathbf{P})}{\partial a_0}&=1,\\\frac{\partial H_{\mathrm{dd}}(f,\mathbf{P})}{\partial a_i}&=e^{-j\omega\tau_i},\\\frac{\partial H_{\mathrm{dd}}(f,\mathbf{P})}{\partial \tau_i}&=-ja_i\omega e^{-j\omega\tau_i},\end{aligned} \tag{17}$$

where $i=1,2$. When $f=0$, the terms in the bracket for F^{-1} in Eq. (16) is real. Since there always is a low-pass filter to eliminate high-frequency noises because of oversampling, we can force $\partial H_{\mathrm{dd}}(f,\mathbf{P})/\partial p_k|_{f=f\max}=0$. The above conditions ensure that the inverse Fourier transform in Eq. (16) gives a real result. The details of the formulation and the iterative procedure can be found in Ref. 23. The best fitted parameters are listed in Table II. The delay time and the

TABLE II. Optimal parameters for Eqs. (10) and (12) for the compensation of reflections in ACD-1(R) D-dot sensor. The parameters were determined with a nonlinear least-squares procedure.

a_0	a_1	τ_1 (ps)	a_2	τ_2 (ps)
0.72	0.28	81.2	0.01	510

magnitude of the second δ function suggest that the first reflection occurs at the joint between the sensing element and the coaxial plate, considering the dimensions of the sensor. It is the first reflection that exhibits the strongest effect. The second reflection that occurs at a bend of the SMA connector is very minor, at least to this specific type of pulses. Since **P** was estimated from a least-squares routine with the measured wave forms, $H_{dd}(f,\mathbf{P})$ would not be zero in this frequency range.

Figure 7 was plotted in a smaller time window to illustrate the details. Beyond this window, the effects of Eq. (12) to the electrical pulse form are very small. Figure 7(a) shows the comparison between the output voltage of the ACD-1(A) D-dot sensor with cable-digitizer compensation, that of the ACD-1(R) D-dot sensor with cable-digitizer compensation, and that of the ACD-1(R) D-dot sensor with cable digitizer *and* D-dot sensor compensation. Figure 7(b) presents the comparison between their corresponding electrical fields. There is a step (dashed line) at the leading edge of the electrical field obtained with ACD-1(R) D-dot sensor with only

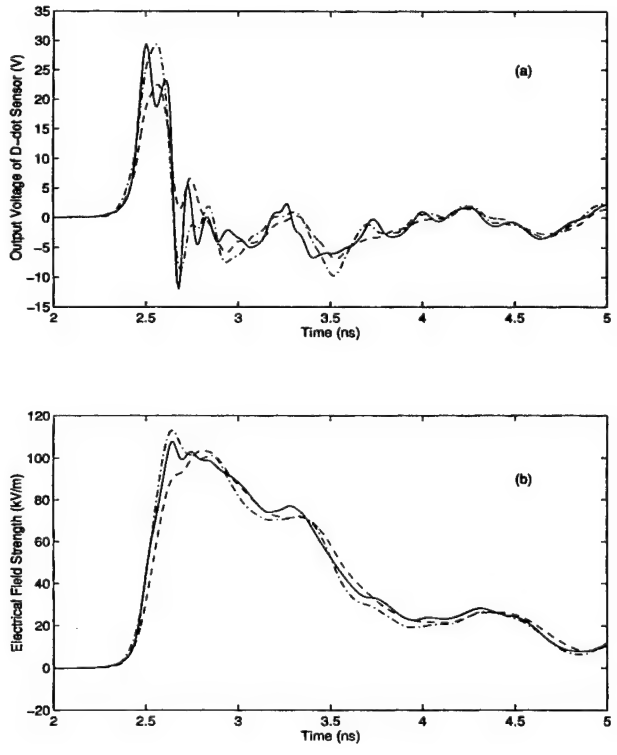

FIG. 7. (a) Comparison between output voltage of the ACD-1(R) D-dot sensor with cable-digitizer compensation (dashed line), that of the ACD-1(R) D-dot sensor with both cable-digitizer and D-dot sensor compensation (dash-dot line), and that of the ACD-1(A) D-dot sensor with cable-digitizer compensation (solid line). (b) Comparison between their corresponding electrical fields.

cable-digitizer compensation although it only affects the fast change part of the peak field. Because the fully compensated electrical pulse is much closer to the reference pulse, it gives a more accurate estimation of the rise time than that of partially compensated one. Despite the fact that the semi-empirical method requires more computation, it has following advantages over the empirical method:

(i) more clear physics;
(ii) only a few parameters are needed for the transfer function of a specific type sensor; and
(iii) wider valid frequency range to some extent as long as the analytical model is sound.

The degree of the overall improvement to the measurement accuracy is determined by the reference pulses, the nature of the measurement hardware, and the validity of the analytical model of impulse response for the D-dot sensor.

V. DISCUSSION

The problems associated with transient electrical field measurements in the picosecond domain in an electromagnetic exposure facility have been discussed. An approach with a two-step deconvolution routine has been presented. The transfer function for the connection cable and the SCD 5000 transient digitizer was empirically evaluated with a reference impulse from a picosecond pulse generator. The right-angle bands in the ACD-1(R) D-dot sensor causes reflections. For the first time, the impulse response for the reflections was formulated as a summation of δ function. The parameters in the δ functions were determined with a symmetric pulse measurement using an ACD-1(A) D-dot sensor and an iterative procedure for time domain optimization using frequency domain derivatives. With this routine, the measurement accuracy has largely been improved. This method can be easily extended to other fast pulse measurement systems.

ACKNOWLEDGMENTS

This work is supported by the U.S. Army Medical Research and Materiel Command under Contract No. DAMD 17-94-C-4069 awarded to McKesson BioServices. The views, opinions, and/or findings contained in this report are those of the author and should not be construed as an official Department of Army position, policy, or decision unless so designated by other documentation. The author wishes to thank J. C. Lee for some assistance with measurement instruments, M. E. Belt, and D. D. Cox for improving the pulse generator, and S.-T. Lu for drawing Fig. 1.

[1] N. S. Nahman, IEEE Trans Instrum. Meas. **32**, 117 (1983).
[2] N. S. Nahman, Proc. IEEE **66**, 441 (1978).
[3] W. L. Gans, Proc. IEEE **74**, 86 (1986).
[4] R. A. Lawton, S. M. Riad, and J. R. Andrews, Proc. IEEE **74**, 77 (1986).
[5] G. Casalegno, Electromagnetics **9**, 17 (1989).
[6] G. J. Rohwein, J. F. Aurand, C. A. Forst, L. D. Roose, and S. R. Babcock, in 21st International Power Modulator Symposium, Costa Mesa, CA (1994).
[7] C. E. Baum, in *Fast Electrical and Optical Measurements*, edited by J. E. Thompson and L. H. Luessen (Martinus Nijhoff, Boston, 1986).
[8] M. Kanda, in *Time-Domain Measurements in Electromagnetics*, edited by

E. K. Miller (Van Nostrand Reinhold, New York, 1986).
[9] J. D. Jackson, *Classical Electrodynamics*, 2nd ed. (Wiley, New York, 1975).
[10] W. H. Press, B. P. Flannery, S. A. Teukolsky, and W. T. Vetterling, *Numerical Recipes in C*, 2nd ed. (Cambridge University Press, Cambridge, 1992).
[11] J. V. Candy, R. W. Ziolkowski, and D. KentLewis, J. Acoust. Soc. Am. **88**, 2235 (1990).
[12] N. H. Younan, A. B. Kopp, D. B. Miller, and C. D. Taylor, IEEE Trans. Power Deliv. **6**, 501 (1991).
[13] J. D. Perez, C. Liu, L. Lawson, T. E. Moore, and C. R. Chappell, Ann. Geophys. (France) **11**, 889 (1993).
[14] W. D. Blair, J. E. Conte, and T. R. Rice, IEEE Trans. Educ. **38**, 211 (1995).
[15] T. K. Sarkar, D. D. Weiner, and V. K. Jain, IEEE Trans. Antennas Propag. **29**, 373 (1981).
[16] H. J. Siweris and B. Schiek, IEEE Trans. Microwave Theory Tech. **30**, 233 (1985).
[17] S. Sinha, Phys. Rev. E **53**, 4509 (1996).
[18] A. V. Oppenheim and R. W. Schafer, *Discrete-Time Signal Processing* (Prentice–Hall, Englewood Cliffs, 1989).
[19] EG&G Washington Analytical Services Center, Inc., Albuquerque, NM. Specification of ACD *D*-dot Sensor (Data Sheet 1119), 1987.
[20] J. F. Aurand, P. E. Patterson, and C. A. Forst, in Conference on Precision Electromagnetic Measurements, Boulder, Colorado, 1994.
[21] N. S. Nahman, in *Fast Electrical and Optical Measurements, Volume I*, edited by J. E. Thompson and L. H. Luessen (Martinus Nijhoff, Boston, 1986).
[22] S. M. Riad, Proc. IEEE **74**, 82 (1986).
[23] J.-Z. Bao, C. C. Davis, and R. E. Schmukler, IEEE Trans. Biomed. Eng. **40**, 364 (1993).

Complex Dielectric Measurements and Analysis of Brain Tissues in the Radio and Microwave Frequencies

Jian-Zhong Bao, *Senior Member, IEEE*, Shin-Tsu Lu, and William D. Hurt, *Senior Member, IEEE*

***Abstract*—We present *in-vitro* complex dielectric measurements of gray and white matter of rat brains in the frequency range between 45 MHz and 26.5 GHz at body and room temperatures using the open-ended coaxial probe technique with an HP8510B network analyzer. The measurement data exhibited two separated dispersions, and were analyzed by means of a complex nonlinear least-squares technique. We suggest two empirical models to describe the experimental data: one containing two Cole–Cole functions was applied to the data from this paper, and another including one Havriliak–Negami and one Cole–Cole function was utilized to a combination of past and present literature data in a wider frequency range from 100 kHz to 26.5 GHz. The adoption of previously published data at the frequencies below 45 MHz increases the valid frequency range of the model.**

***Index Terms*—Brain tissues, complex dielectric constant, complex nonlinear modeling, open-ended coaxial probe technique, radio and microwave frequencies.**

I. Introduction

THE lack of sufficient data at super-high frequencies and accurate models in a wide frequency range for complex dielectric properties of tissues has presented an obstacle for both theoretical and experimental studies of electromagnetic energy deposition in human or animal bodies. Most of the early studies were at a few discrete frequency bands or scattered frequency points, and in frequencies below 5 GHz. There are also very few published data above 10 GHz, and virtually no model covers a wide frequency range [1]–[3]. It is important to establish a reliable database and empirical models for each organ in a wide frequency range for studies of the interaction between electromagnetic wave and biological bodies [4], especially for pulse situations. The dielectric information is also of importance for clinical applications [5].

In this paper, we report *in-vitro* complex dielectric measurements of gray and white matter from rat brains in the frequency range between 45 MHz and 26.5 GHz using the open-ended coaxial probe technique with a computer-controlled HP8510B network analyzer and the complex nonlinear modeling of experimental data. The measurements were performed at 37 °C

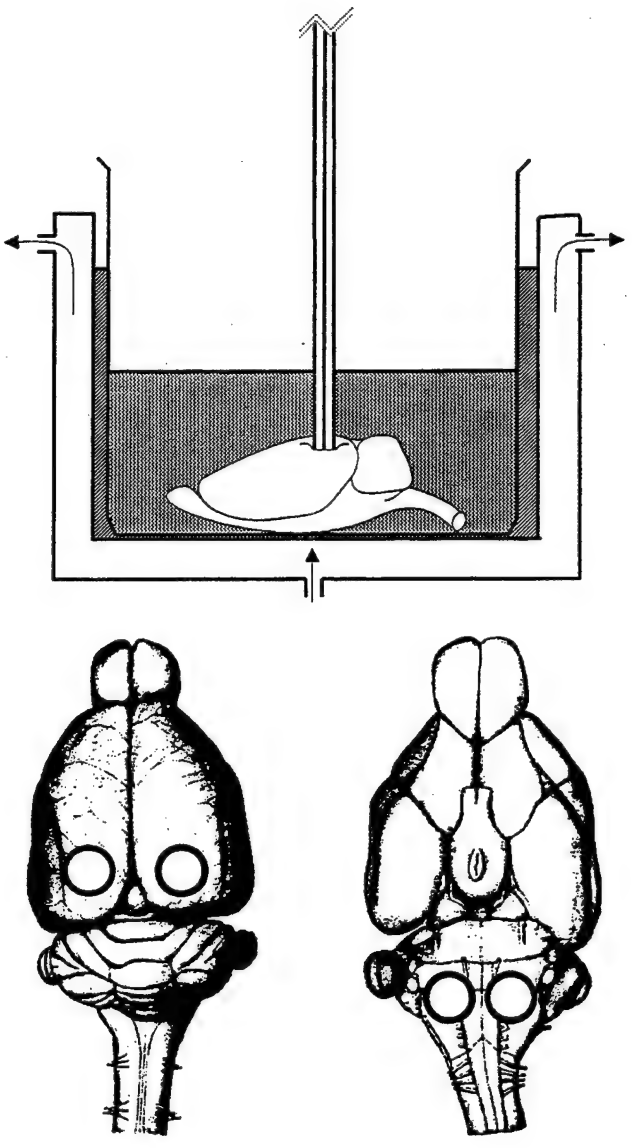

Fig. 1. Tissue and probe configuration and measurement locations on the surface of a rat brain. The circles indicate the locations on the (a) cerebral cortex for gray matter and on the (b) medulla oblongata for white matter measurements.

Manuscript received February 27, 1997; revised June 20, 1997. This work was supported by the U.S. Army Medical Research and Materiel Command under Contract DAMD17-94-C-4069 awarded to McKesson BioServices.

J.-Z. Bao is with McKesson BioServices and the U.S. Army Medical Research Detachment, Brooks Air Force Base, San Antonio, TX 78235 USA (e-mail: jian@abba.brooks.af.mil).

S.-T. Lu is with McKesson BioServices and the U.S. Army Medical Research Detachment, Brooks Air Force Base, San Antonio, TX 78235 USA.

W. D. Hurt is with Armstrong Laboratory, Brooks Air Force Base, San Antonio, TX 78235 USA.

Publisher Item Identifier S 0018-9480(97)07109-3.

0018–9480/97$10.00 © 1997 IEEE

TABLE I
BEST-FITTED PARAMETERS IN (3) FOR THE GRAY AND WHITE MATTER OF RAT BRAINS AT ROOM AND BODY TEMPERATURES. THE CORRESPONDING COMPARISONS BETWEEN THE EXPERIMENTAL DATA AND THEIR FITTING ARE IN FIGS. 5 AND 6

	gray matter		white matter	
	24 °C	37 °C	25 °C	37 °C
$\Delta\epsilon_1$	269.7 ± 2.6	309.8 ± 7.8	110.4 ± 6.6	130.3 ± 9.1
τ_1 (ns)	5.59 ± 0.04	5.12 ± 0.11	6.24 ± 0.35	5.31 ± 0.40
α_1	0.910 ± 0.003	0.892 ± 0.026	0.840 ± 0.005	0.806 ± 0.007
$\Delta\epsilon_2$	50.26 ± 0.04	46.68 ± 0.11	31.19 ± 0.14	28.12 ± 0.16
τ_2 (ps)	6.74 ± 0.06	4.87 ± 0.12	5.20 ± 0.22	3.04 ± 0.17
α_2	0.907 ± 0.002	0.939 ± 0.004	0.732 ± 0.059	0.760 ± 0.007
ϵ_h	5.11 ± 0.02	4.54 ± 0.04	4.79 ± 0.02	4.40 ± 0.03
σ_0 (S/m)	0.366 ± 0.002	0.368 ± 0.005	0.234 ± 0.003	0.241 ± 0.005

and 24 °C for gray and at 37 °C and 25 °C for white matter. The measured data were analyzed with two empirical models. One of these included two Cole–Cole functions [6] and was utilized with the data from this paper to obtain a model for the frequencies between 45 MHz and 26.5 GHz. The other model contained a Havriliak–Negami [6] and a Cole–Cole function, and was applied to the combined data from this paper and results of [7], [8] at the frequencies below 45 MHz to construct a model which covers a wider frequency range between 100 kHz and 26.5 GHz. Although the first model gives a better fit to the measured spectra in general, the second one simulates the complex dielectric spectra in a much wider frequency range.

II. MEASUREMENTS

A. Open-Ended Coaxial Probe Technique

The open-ended coaxial probe technique has been extensively employed for the dielectric measurements of materials, especially biological samples [9]–[13]. With this technique, the complex dielectric spectra can be easily acquired in a wide frequency range and in an almost continuous form. The technique is especially suitable for liquids. The measurements for solids are much more tedious, and the main problem is to assure a good and tight contact between the open end of the coaxial probe and the sample surface [14], [15]. A very tiny air gap could introduce a very large error, especially to the high dielectric constant materials [16]. For soft solids such as tissues, a good contact can be realized by applying moderate pressure.

The measured complex reflection coefficient (ρ_m) contains the desired information from the interface between the open end of a probe and the material under measurement as well as the undesired effects of the network analyzer (which was not calibrated), connectors, and coaxial line. With a linear model for the interface, ρ_m can be converted to the complex relative dielectric constant ($\epsilon = \epsilon' - j\epsilon''$, where $j = \sqrt{-1}$) with [17], [18]

$$\epsilon = \frac{A_1\rho_m - A_2}{A_3 - \rho_m} \tag{1}$$

where the complex coefficients A_1, A_2, and A_3 were determined with a calibration procedure using three reference measurements: an open, a short, and standard saline. This simple rational expression maps *one* point in the complex ρ_m plane to *one* point in the complex ϵ plane. Although this relation is based on assumptions and simplifications, using standards in the calibration procedure will compensate for the measurement errors to a large extent, especially when the dielectric properties under investigation are close to one of the standards used for the calibration [18]. The advantage of (1)

TABLE II
BEST-FITTED PARAMETERS IN (4) FOR THE GRAY AND WHITE MATTER OF RAT BRAINS WITH THE ADOPTION OF EARLY PUBLISHED LOW-FREQUENCY DATA OF A DOG BRAIN. THE CORRESPONDING COMPARISONS BETWEEN THE EXPERIMENTAL DATA AND THEIR FITTING ARE IN FIGS. 7 AND 8

	gray matter		white matter	
	24 °C	37 °C	25 °C	37 °C
$\Delta\epsilon_1$	7703	9217	7961	8502
τ_1 (ns)	59.1	182.1	24.9	605.5
α_1	0.300	0.364	0.214	0.348
β_1	3.190	2.297	5.010	2.300
$\Delta\epsilon_2$	45.27	40.76	29.01	26.38
τ_2 (ps)	6.12	4.27	4.35	2.96
α_2	0.999	0.997	0.787	0.817
ϵ_h	4.92	5.18	4.55	4.81
σ_0 (S/m)	0.155	0.163	0.102	0.128

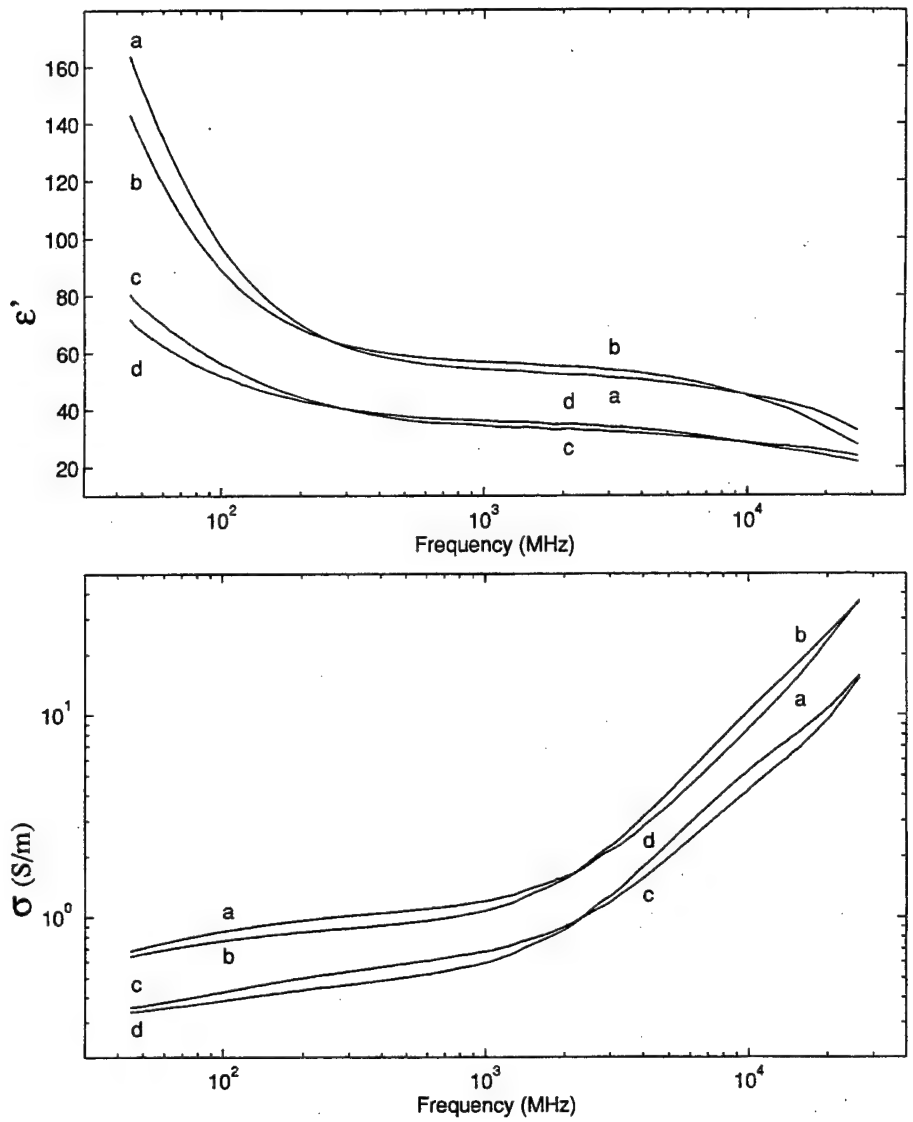

Fig. 2. Permittivity and conductivity spectra of gray matter at *a*: 37 ± 0.5 °C, *b*: 24 ± 0.5 °C; white matter at *c*: 37 ± 0.5 °C, and *d*: 25 ± 0.5 °C.

TABLE III
COMPARISON OF VALUES FROM (3) AND (4) USING THE PARAMETERS LISTED IN TABLES I AND II, RESPECTIVELY, WITH THE EXPERIMENTAL DATA FOR GRAY MATTER AT 37 °C AT SOME SELECTED FREQUENCY POINTS. THESE POINTS ARE IN CURVES *a* OF FIGS. 6 AND 8. THE EXPERIMENTAL DATA AT 0.1, 1, AND 10 MHz ARE FROM [1] AND [7]. N/A STANDS FOR NOT APPLICABLE

	ϵ'			σ (S/m)		
frequencies (MHz)	value of Eq. (3)	value of Eq. (4)	experimental data	value of Eq. (3)	value of Eq. (4)	experimental data
0.1	N/A	3934	3800	N/A	0.173	0.170
1.0	N/A	1570	1250	N/A	0.231	0.210
10.0	N/A	395	366 ± 14	N/A	0.427	0.365 ± 0.015
99.9	97.1	101	96.9 ± 7.0	0.851	0.798	0.850 ± 0.040
901.8	54.3	54.2	54.4 ± 3.0	1.19	1.34	1.18 ± 0.10
10179.8	45.8	44.1	45.0 ± 2.0	8.83	7.93	8.67 ± 0.85
26500.0	32.2	32.6	32.6 ± 2.3	32.1	30.7	36.7 ± 2.7

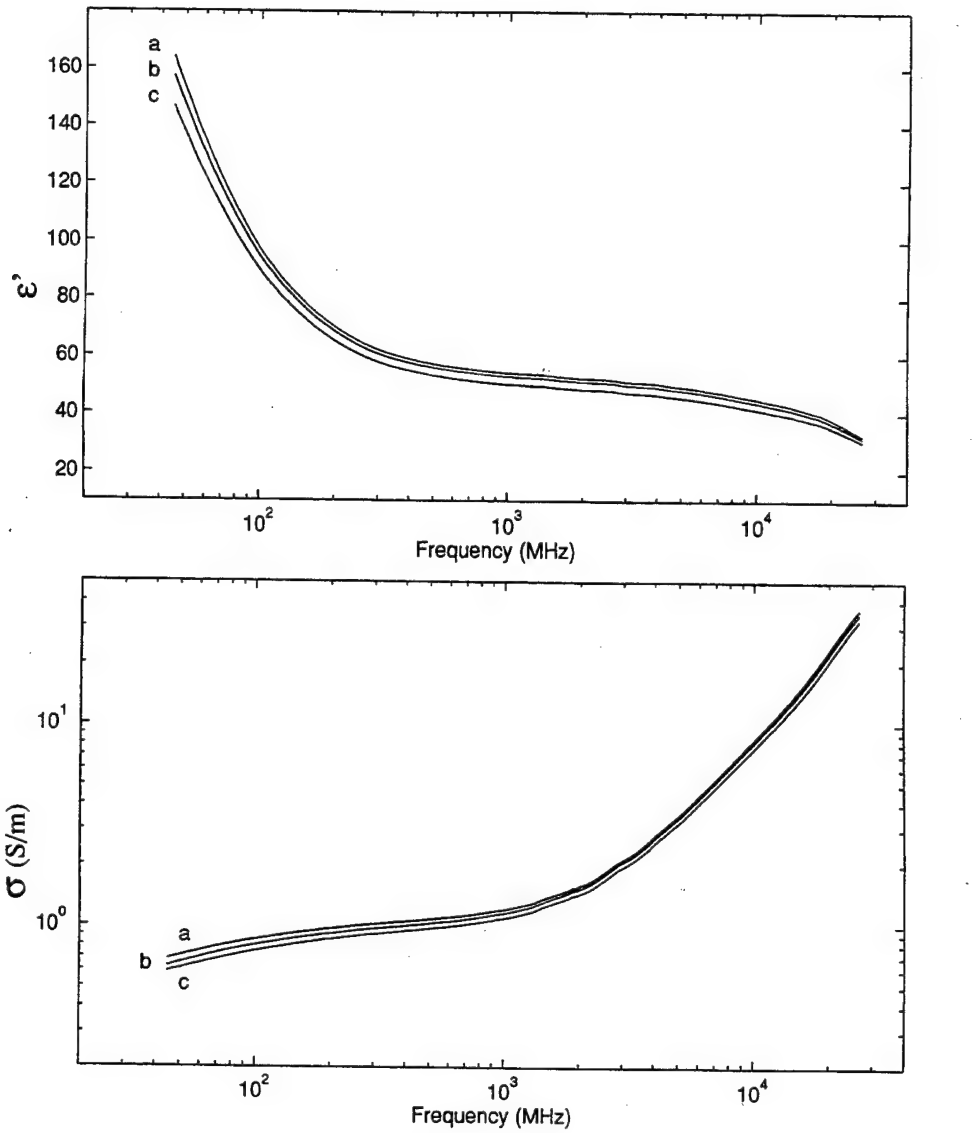

Fig. 3. The systematic time variation of the permittivity and conductivity spectra of gray matter of one typical measurement setup at *a*: 1 min, *b*: 11 min, and *c*: 21 min after the probe contacted the sample surface at 37 ± 0.5 °C.

TABLE IV

COMPARISON OF VALUES FROM (3) AND (4) USING THE PARAMETERS LISTED IN TABLES I AND II, RESPECTIVELY, WITH THE EXPERIMENTAL DATA FOR WHITE MATTER AT 37 °C AT SOME SELECTED FREQUENCY POINTS. THESE POINTS ARE IN CURVES *b* OF FIGS. 6 AND 8. THE EXPERIMENTAL DATA AT 0.1, 1, AND 10 MHz ARE FROM [1] AND [7]. N/A STANDS FOR NOT APPLICABLE

	ϵ'			σ (S/m)		
frequencies (MHz)	value of Eq. (3)	value of Eq. (4)	experimental data	value of Eq. (3)	value of Eq. (4)	experimental data
0.1	N/A	2354	2680 ± 720	N/A	0.135	0.135 ± 0.015
1.0	N/A	767.8	685 ± 142	N/A	0.168	0.165 ± 0.025
10.0	N/A	183.4	186 ± 23	N/A	0.256	0.255 ± 0.045
99.9	56.9	56.1	56.1 ± 5.0	0.433	0.416	0.425 ± 0.042
901.8	34.9	35.0	34.9 ± 2.0	0.682	0.692	0.662 ± 0.075
10179.8	28.8	28.7	28.3 ± 1.5	4.17	4.07	4.32 ± 0.57
26500.0	23.7	23.8	23.7 ± 1.5	13.8	14.0	15.2 ± 1.5

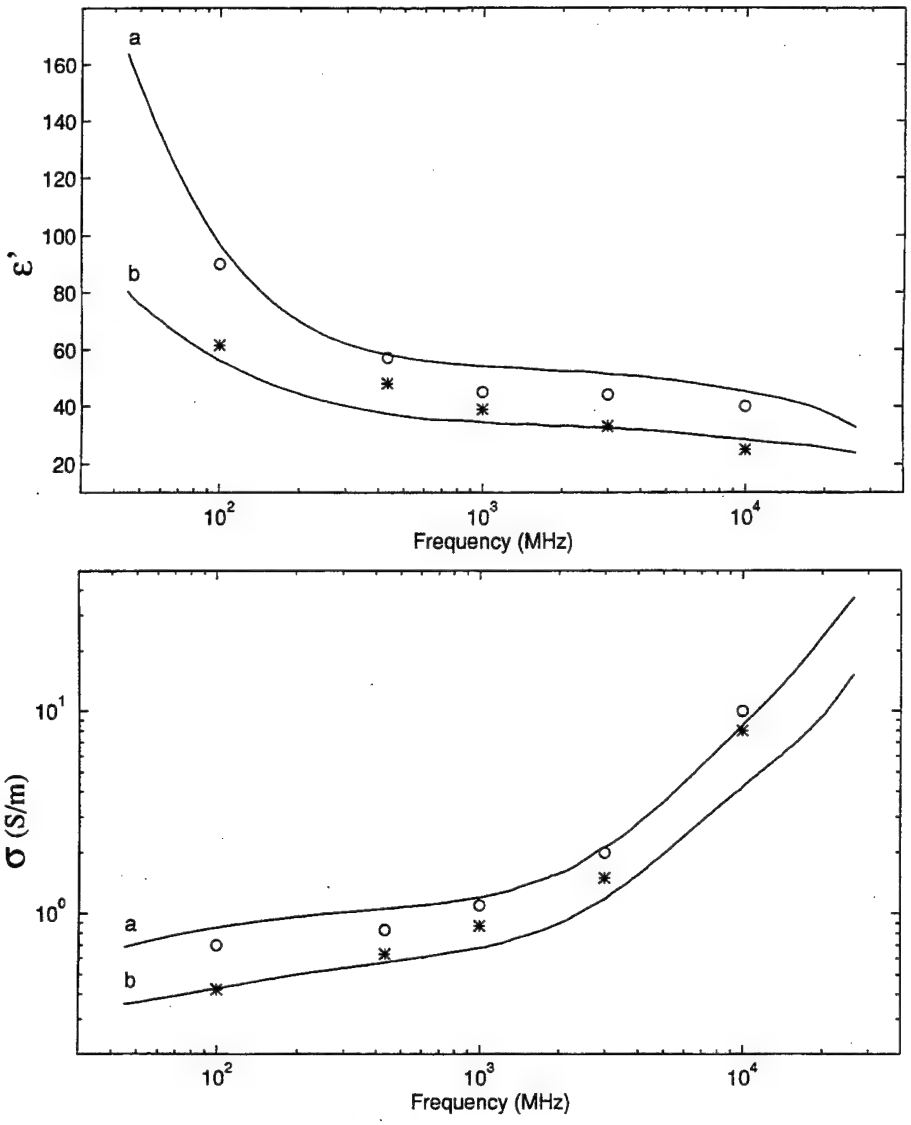

Fig. 4. Comparison of permittivity and conductivity spectra of rat brain tissues between this paper (solid lines) and previously published data of dog brain tissues by Foster *et al.* [20] (o and *) at body temperature. Lines *a* and open circles (o) are for gray matter and lines *b* and stars (*) are for white matter.

TABLE V

COMPARISON OF VALUES FROM (3) AND (4) USING THE PARAMETERS LISTED IN TABLES I AND II, RESPECTIVELY, WITH THE EXPERIMENTAL DATA FOR GRAY MATTER AT 24 °C AT SOME SELECTED FREQUENCY POINTS. THESE POINTS ARE IN CURVES *a* OF FIGS. 5 AND 7. THE EXPERIMENTAL DATA AT 0.1, 1, AND 10 MHz ARE FROM [8] AT 24.5 °C. N/A STANDS FOR NOT APPLICABLE

	ϵ'			σ (S/m)		
frequencies (MHz)	value of Eq. (3)	value of Eq. (4)	experimental data	value of Eq. (3)	value of Eq. (4)	experimental data
0.1	N/A	2816	2806 ± 6	N/A	0.161	0.150 ± 0.020
1.0	N/A	1197	923 ± 3	N/A	0.202	0.177 ± 0.008
10.0	N/A	338	265 ± 5	N/A	0.356	0.295 ± 0.005
99.9	88.6	94.4	88.8 ± 8.6	0.765	0.671	0.764 ± 0.034
901.8	57.0	55.4	57.0 ± 3.0	1.06	1.13	1.04 ± 0.15
10179.8	45.0	44.6	44.6 ± 2.1	10.8	10.1	10.6 ± 0.8
26500.0	28.0	27.3	27.7 ± 2.2	33.0	34.9	36.1 ± 4.1

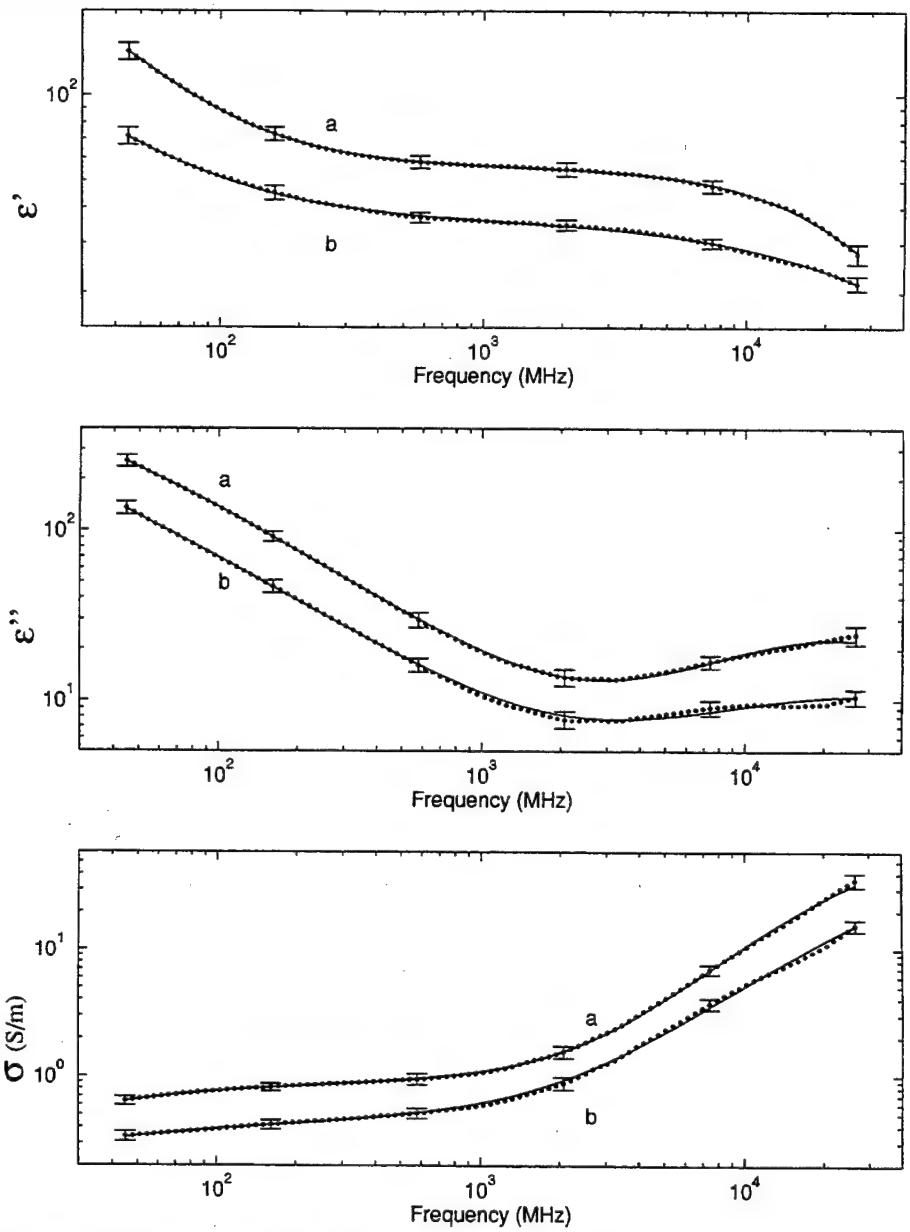

Fig. 5. Comparison between the measured data (•) and their CNLS fitting (solid lines) with (3). Curves *a* are for gray matter at 24 ± 0.5 °C while curves *b* are for white matter at 25 ± 0.5 °C. The best-fitted parameters are listed in Table I. The error bars stand for the standard deviations.

is that its inversion is unique so that no efforts were needed to distinguish the solutions and is much easier than that with a more complicated model.

B. Sample Preparation and Experimental Setup

Male Wistar–Kyoto rats were used as tissue donors. They were euthanized by CO_2 inhalation until the time of death. The brain and approximately 5 mm of the spinal cord were dissected free of skull and dura matter of the meninges in less than 10 min after death. The cerebral cortex consists of approximately a 2-mm-thick surface layer of gray matter and about a 6-mm-thick layer underneath a mixing region of gray and white matter. Since the gray matter was in direct contact with the open end of the probe and the measurement thickness into the specimen is about 2 mm [19], gray matter contributed the most to the measurements. Therefore, gray matter was used to represent the cerebral cortex. Medulla oblongata was constituted nearly solely by white matter and used to signify the white matter. Its thickness is about 7 mm. The specimens were washed with and immersed in 0.9% saline during the temperature adjusting process and measurements. Keeping the specimens in saline has the following advantages:

1) maintaining the tissues in a more physiologically friendly environment than in air;
2) making the temperature control easier;
3) avoiding any air bubbles which would possibly exist between the flat open end of the probe and the specimen surface if the specimen were kept in air.

Measurements at room temperature were done within 40 min, and at body temperature within 60 min after the euthanasia of

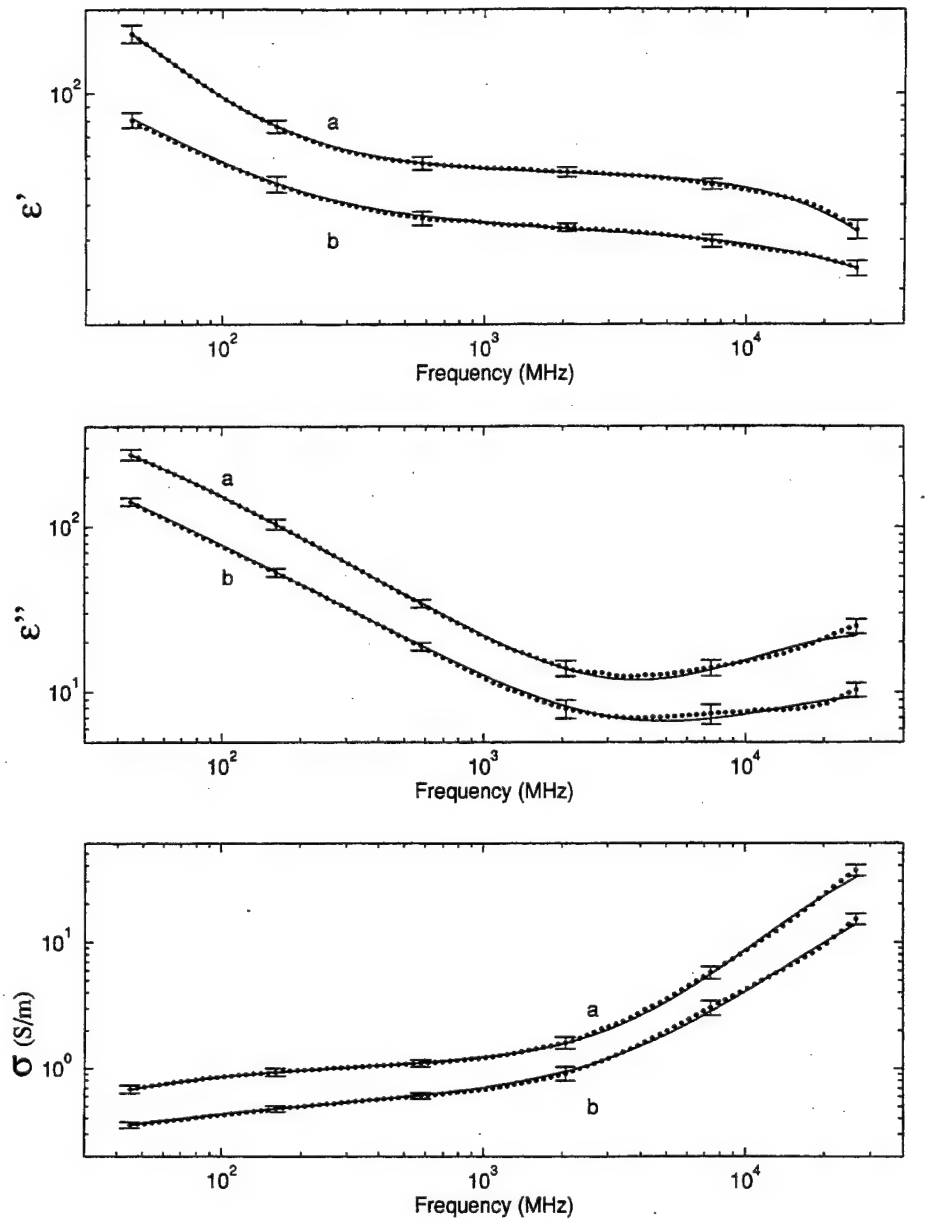

Fig. 6. Comparison between the measured data (•) and their CNLS fitting (solid lines) with (3) at 37 ± 0.5 °C. Curves *a* are for gray matter and curves *b* are for white matter. The best-fitted parameters are listed in Table I. The error bars stand for the standard deviations.

the rats. The whole brain tissue was kept intact, and one brain specimen was used only once at one temperature to ensure that the measurements were on fresh tissues. A total of 12 rat brains were utilized in this study. The probe position and the geometry of the sample container were kept the same during the saline reference and the tissue measurements to minimize environmental influences. The surface of specimens was in good and tight contact with the flat open-end of the probe. The measurement system is very similar to the one which has been described in [17], [18]. Measurements were done on the surface of specimens using an HP8510B network analyzer with a semirigid right-angle coaxial probe of 2.2-mm diameter and 15-cm length. Frequency range from 45 MHz to 26.5 GHz was swept on a logarithmic scale over 201 points in less than 1 min. The temperature was controlled by a water circulator, and measured on the surface of tissue specimens. Fig. 1 shows the tissue-probe configuration and measurement locations of a probe on the surface of a rat brain. The complex dielectric spectra were measured at different locations on the surface of specimen for gray and white matter, respectively.

III. Measurement Results

The dielectric properties of tissues in radio and microwave frequencies depend on their cellular and subcellular structures and constituents. Fig. 2 exhibits the measured permittivity (ϵ') and conductivity (σ) spectra of gray matter at 37 °C and 24 °C, and of white matter at 37 °C and 25 °C in the frequency range between 45 MHz and 26.5 GHz. σ is defined as $\sigma = \omega\epsilon_0\epsilon''$, where ϵ_0 is the permittivity in a vacuum, and ω is the angular frequency. Each of the spectra presents two well-separated major dispersions, which are commonly

TABLE VI
COMPARISON OF VALUES FROM (3) AND (4) USING THE PARAMETERS LISTED IN TABLES I AND II, RESPECTIVELY, WITH THE EXPERIMENTAL DATA FOR WHITE MATTER AT 25 °C AT SOME SELECTED FREQUENCY POINTS. THESE POINTS ARE IN CURVES *b* OF FIGS. 5 AND 7. THE EXPERIMENTAL DATA AT 0.1, 1, AND 10 MHz ARE FROM [8] AT 24.5 °C. N/A STANDS FOR NOT APPLICABLE

	ϵ'			σ (S/m)		
frequencies (MHz)	value of Eq. (3)	value of Eq. (4)	experimental data	value of Eq. (3)	value of Eq. (4)	experimental data
0.1	N/A	1365	1425 ± 25	N/A	0.106	0.150 ± 0.050
1.0	N/A	540	401 ± 1	N/A	0.125	0.120
10.0	N/A	165	120 ± 5	N/A	0.191	0.165 ± 0.005
99.9	51.5	56.2	51.8 ± 5.2	0.387	0.343	0.385 ± 0.060
901.8	36.5	35.9	36.4 ± 1.5	0.597	0.622	0.572 ± 0.075
10179.8	28.5	28.4	28.1 ± 1.2	5.23	4.89	5.37 ± 0.50
26500.0	21.6	21.9	21.7 ± 1.3	15.5	15.6	15.6 ± 1.6

referred to as β- and γ-dispersion [1], although only the high frequency tail of the β-dispersion is covered in this frequency range. The β-dispersion, centered in the megahertz frequency range, is largely due to the occurrence of Maxwell–Wagner effects at the interface between the cell membrane and the surrounding aqueous phase. The γ-dispersion, centered in the gigahertz frequency range, is attributed to the relaxation of water molecules in the aqueous phase or bound to macromolecules. Besides the long tails of β-dispersion, our spectra do not show a distinct so-called β'-dispersion. If it existed, it would be covered in our frequency range. Gray and white matter display a distinct dielectric property in this frequency range, where ϵ' and σ of gray matter constantly yield a higher value than those of white matter at both body and room temperatures, respectively. The temperature dependence of the spectra shows a crossing feature: ϵ' increases with temperature at low and high frequency ranges of this spectra and decreases in the middle, while σ increases with temperature in the low frequency range and decreases in the high frequency range. This feature is consistent with an earlier observation in a different cell system [18].

Fig. 3 illustrates a typical time-course of the measured ϵ' and σ spectra of grey matter at body temperature. Since the tissue samples were pressed against the probe, minor damage took place on their surface. The surface damage in turn caused a change of the interfacial properties with time. The systematic variation with time may be resulted from the leakage of the extracellular and intercellular fluid and/or elastic deformation of the tissues around the open-end of the probe, but not due to temperature variation, which shows a different feature (Fig. 2). To minimize the influence caused by the damage, a measurement should be performed as quickly as possible after a tissue specimen is placed in good contact with the probe.

Fig. 4 represents the comparison between the measured spectra of this paper and previously published data of a canine brain by Foster *et al.* [20] at 37 °C. Although our data constantly show a larger difference for both ϵ' and σ between gray and white matter, they are in reasonable agreement with the early data considering the factors such as using different measurement techniques and tissues from different species. One possible reason for the larger difference in our data is that we were using much fresher specimens. In addition, our spectra cover a wider frequency range.

IV. COMPLEX NONLINEAR ANALYSIS

To analyze these two well-separated dispersions, we need at least two dispersion functions. The measured spectra were analyzed using two models with and without considering previously published data at frequencies below 45 MHz, respectively. The adoption of early literature data in this modeling extends the valid frequency range of the model. The parameters of models are determined by means of a complex nonlinear least-squares (CNLS) fit, which simultaneously fits the real and imaginary parts to ensure a complete fit:

$$S(\vec{P}) = \sum_{k=1}^{N} \{W_k^r[\epsilon_m^r(\omega_k, \vec{P}) - \epsilon_e^r(\omega_k)]^2 + W_k^i[\epsilon_m^i(\omega_k, \vec{P}) - \epsilon_e^i(\omega_k)]^2\} \quad (2)$$

where N is the number of frequency points, ϵ_e is the experimental data, ϵ_m is given by an empirical model [see (3) or (4)], superscript r and i denote the real and imaginary parts, respectively, W is a weighting factor, and $\vec{P}$ represents the set of real parameters in the model. The best-fit values of these parameters are evaluated by minimizing S using the Levenberg–Margaret algorithm [21]. The procedure of our fitting routine can be found in [22].

The model utilized for the data solely from this paper contains two Cole–Cole functions:

$$\epsilon_m(\omega) = \epsilon_h + \frac{\Delta\epsilon_1}{1 + (j\omega\tau_1)^{\alpha_1}} + \frac{\Delta\epsilon_2}{1 + (j\omega\tau_2)^{\alpha_2}} + \frac{\sigma_0}{j\omega\epsilon_0} \quad (3)$$

where ϵ_h is the high-frequency limit of the dielectric constant, $\Delta\epsilon$ is the dielectric decrements of the dispersion, τ is the relaxation times, α are exponents, and σ_0 is the dc conductivity. The two Cole–Cole functions are for the two dispersions, and

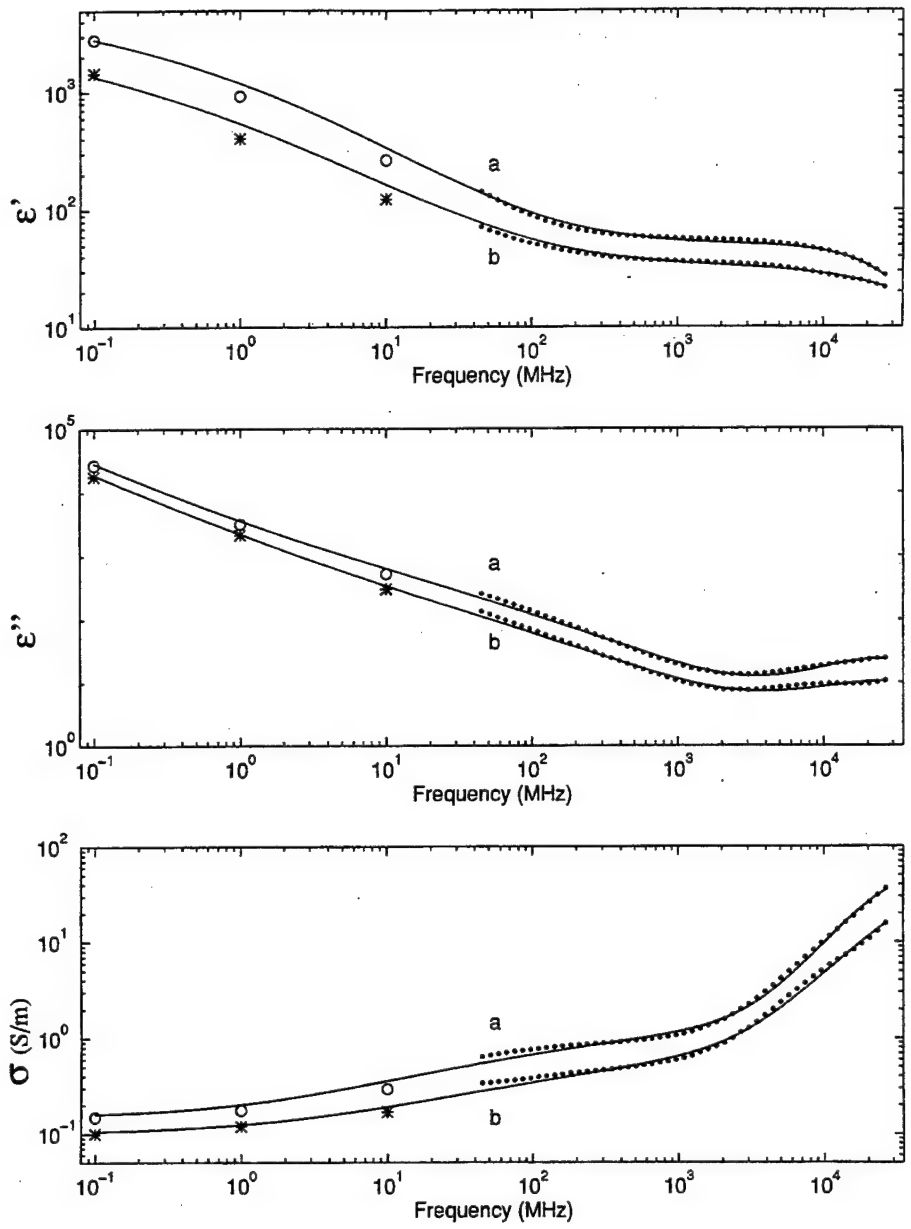

Fig. 7. Comparison between the measured data from this paper (•) plus previously published data of canine and bovine brain tissues at 24.5 °C by Surowiec *et al.* [8] (o and ∗) and the CNLS fitting (solid lines) with (4). Curves *a* and open circles (o) are for gray matter and curves *b* and stars (∗) are for white matter. The best-fitted parameters are listed in Table II.

subscripts 1 and 2 represent the dispersions at low- and high-frequency ends, respectively. Since the data from this paper covers a very small portion of the β-dispersion, it is impossible to retrieve the entire β-dispersion from these data alone, and the parameters ($\Delta\epsilon_1$ and τ_1) obtained with the fitting do not reflect the β-dispersion. A large part of the γ-dispersion was in our measurement range so that the recovery of γ-dispersion is relatively more reliable. Nevertheless, we suggest that the extracted parameters in the model should only be used in the frequency range where the experimental data reside. Fig. 5 shows that the comparison between the measurement data and their CNLS fitting for gray and white matter at 24 °C and at 25 °C, respectively, and Fig. 6 shows a similar comparison at 37 °C. Only half of the measured data were plotted to make the fitting lines more visible in these two figures. Despite some small discrepancy in the imaginary part at high frequencies, (3) generally gives a good fit. The corresponding best-fitted parameters for (3) are listed in Table I.

Because the difference between the dielectric properties of the same organ but in different species is small [19], [23], and to the best of our knowledge there is no published low-frequency data (<45 MHz) for rat brains at the temperatures we were working with, we adopted the data of canine's gray and white matter at lower frequencies (10 MHz, 1 MHz, and 100 kHz) by Stoy *et al.* [7] at body temperature and Surowiec et al. [8] at room temperature. Utilizing the published data as references (even from different species) at frequencies below our measurement range in the fitting can increase the frequency range of validity of the model. There are only a few available published data for white and gray matter, regardless

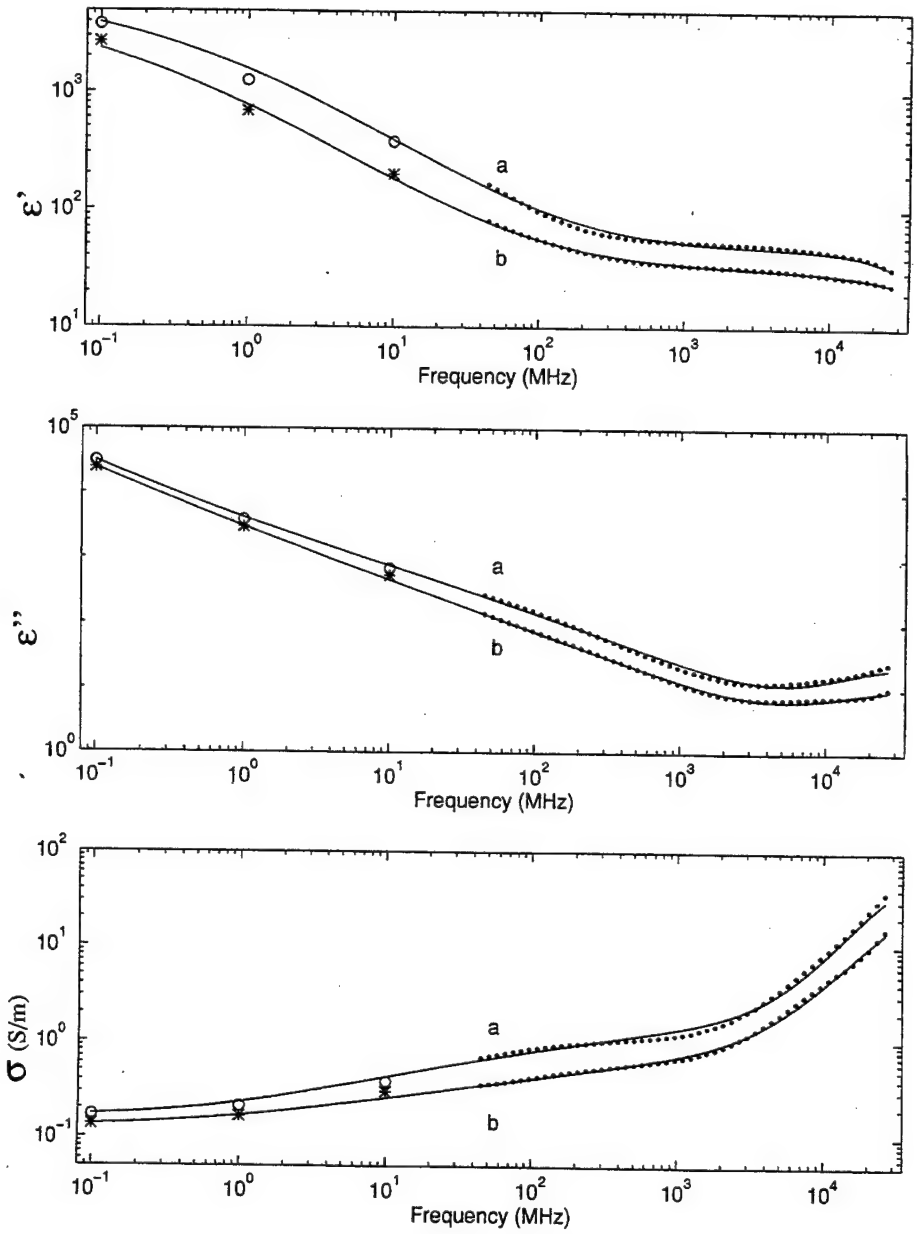

Fig. 8. Comparison between the measured data from this paper (•) plus previously published data of dog brain tissues by Stoy *et al.* [7] (o and ∗) and the CNLS fitting (solid lines) with (4) at 37 °C. Curves *a* and open circles (o) are for gray matters and curves *b* and stars (∗) are for white matters. The best-fitted parameters are listed in Table II.

of the frequencies, temperatures, techniques, and species [2], [23], [24]. The extended dispersion at the low-frequency end was modeled with a Havriliak–Negami rather than Cole–Cole function to increase the flexibility of the model, and so (3) becomes

$$\epsilon_m(\omega) = \epsilon_h + \frac{\Delta\epsilon_1}{[1+(j\omega\tau_1)^{\alpha_1}]^{\beta_1}} + \frac{\Delta\epsilon_2}{1+(j\omega\tau_2)^{\alpha_2}} + \frac{\sigma_0}{j\omega\epsilon_0} \quad (4)$$

where β_1 is another exponent. Fig. 7 shows that the comparison between the combined data and their CNLS fitting for gray and white matter at room temperatures, while Fig. 8 shows a similar comparison at body temperature. Only one quarter of the measured data from this paper were plotted to make the fitting lines more visible. Although the quality of fit with (4) to the combined data is not as good as that with (3) to the present data, (4) covers a wider frequency range. The closest available room temperature data is at 24.5 °C [8], which is a half degree higher than our gray-matter temperature and a half degree lower than our white-matter temperature. The transition from our measured spectra to the early published data are fairly smooth for body temperature but less smooth for room temperature, which might be a partial result of the 0.5 °C difference between the temperatures at which the data were collected. The best-fitted parameters for the gray and white matter in the extended frequency range are listed in Table II. Since the combined data was applied to extract its best-fit parameters, (4) can be regarded for the *general* gray and white matter in the frequency range between 100 kHz and 26.5 GHz. Tables III and VI shows the comparison of calculated values from (3) and (4) using the parameters listed in Tables I and II, respectively, with the experimental data for gray and

white matter at body and room temperatures at several selected frequency points. These points are around curves *a* or *b* of Figs. 5–8, respectively. Although, in general, (3) presents a better values in a smaller frequency range, both (3) and (4) can yield reasonably close values to the measurement data if the experimental uncertainty are taken into account.

V. Conclusions

The complex dielectric spectra of gray and white matter of rat brains have been measured with the open-ended coaxial-probe technique in the frequency range between 45 MHz and 26.5 GHz at body and room temperatures. This paper's data have been analyzed with two Cole–Cole functions and a combination of early and current literature data has been analyzed with one Havriliak–Negami and one Cole–Cole function using CNLS technique in a frequency range from 100 kHz to 26.5 GHz. Furthermore, we explicitly show the time variation of the spectra due to the damage of the sample surface. Our data and models complement a few existing data, especially for the high frequencies above 10 GHz.

VI. Acknowledgments

The authors thank M. E. Belt and D. D. Cox for building the temperature control system, and P. J. Henry for help with the animals. Author J.-Z. Bao wishes to thank Prof. C. C. Davis for the data acquisition software. The views, opinions, and/or findings contained in this paper are those of the authors and should not be construed as an official Department of Army position, policy, or decision unless so designated by other documentation.

References

[1] K. R. Foster and H. P. Schwan, "Dielectric properties of tissues," in *Handbook of Biological Effects of Electromagnetic Fields*, C. Polk and E. Postow, Eds. New York: CRC, 1996, pp. 25–102.

[2] M. A. Stuchly, T. W. Athey, S. S. Stuchly, G. M. Samaras, and G. Taylor, "Dielectric properties of animal tissues in vivo at frequencies 10 MHz–1 GHz," *Bioelectromagnetics*, vol. 2, pp. 93–103, 1981.

[3] M. A. Stuchly and S. S. Stuchly, "Dielectric properties of biological substances—Tabulated," *J. Microwave Power*, vol. 15, pp. 19–26, 1980.

[4] C.-K. Chou, H. Bassen, J. Osepchuk, R. Petersen, M. Meltz, R. Cleveland, J. C. Lin, and L. Heynick, "Radio frequency electromagnetic exposure: Tutorial review on experimental dosimetry," *Bioelectromagnetics*, vol. 17, pp. 195–208, 1996.

[5] C.-K. Chou, "Evaluation of microwave hyperthermia applicators," *Bioelectromagnetics*, vol. 13, p. 581, 1992.

[6] C. J. F. Bottcher and P. Bordewijk, *Theory of Electric Polarization—Volume II*, 2nd ed. New York: Elsevier, 1978.

[7] R. D. Stoy, K. R. Foster, and H. P. Schwan, "Dielectric properties of mammalian tissues from 0.1 to 100 MHz: A summary of recent data," *Phys. Med. Bio.*, vol. 27, pp. 501–513, 1982.

[8] A. Surowiec, S. S. Stuchly, and A. Swarup, "Postmortem changes of the dielectric properties of bovine brain tissues at low radio-frequencies," *Bioelectromagnetics*, vol. 7, pp. 31–43, 1986.

[9] E. C. Burdette, F. L. Cain, and J. Seals, "In vivo probe measurement technique for determining dielectric properties at VHF through microwave frequencies," *IEEE Trans. Microwave Theory Tech.*, vol. MTT-28, pp. 414–427, Apr. 1980.

[10] T. W. Athey, M. A. Stuchly, and S. S. Stuchly, "Measurement of radio frequency permittivity of biological tissues with an open-ended coaxial line: Part I." *IEEE Trans. Microwave Theory Tech.*, vol. MTT-30, pp. 82–86, Jan. 1982.

[11] M. A. Stuchly, A. W. Athey, G. M. Samaras, and G. E. Taylor, "Measurement of radio frequency permittivity of biological tissues with an open-ened coaxial line: Part II—Experimental results," *IEEE Trans. Microwave Theory Tech.*, vol. MTT-30, pp. 87–92, Jan. 1982.

[12] L. L. Li, B. Ismail, L. S. Taylor, and C. C. Davis, "Flanged coaxial microwave probes for measuring thin moisture layers," *IEEE Trans. Bio-Med. Eng.*, vol. 39, pp. 49–57, Jan. 1992.

[13] C. Gabriel, T. Y. A. Chan, and E. H. Grant, "Admittance models for open ended coaxial probes and place in dielectric spectroscopy," *Phys. Med. Biol.*, vol. 39, pp. 2183–2200, 1994.

[14] S. Bringhurst and M. F. Iskander, "Open-ended metallized ceramic coaxial probe for high-temperature dielectric properties measurements," *IEEE Trans. Microwave Theory Tech.*, vol. 44, pp. 926–935, June 1996.

[15] G. Q. Jiang, W. H. Wong, E. Y. Raskovich, W. G. Clark, W. A. Hines, and J. Sanny, "Open-ended coaxial-line technique for the measurement of the microwave dielectric constant for low-loss solids and liquids," *Rev. Sci. Instrum.*, vol. 64, pp. 1614–1621, June 1993.

[16] J. Baker-Jarvis, M. D. Janezic, P. D. Domich, and R. G. Geyer, "Analysis of an open-ended coaxial probe with lift-off for nondestructive testing," *IEEE Trans. Instrum. Meas.*, vol. 43, pp. 711–718, Oct. 1994.

[17] J.-Z. Bao, C. C. Davis, and M. L. Swicord, "Microwave dielectric measurements of erythrocyte suspensions," *Biophys. J.*, vol. 66, pp. 2173–2180, 1994.

[18] J.-Z. Bao, M. L. Swicord, and C. C. Davis, "Microwave dielectric characterization of binary mixtures of water, methanol, and ethanol," *J. Chem. Phys.*, vol. 104, pp. 4441–4450, 1996.

[19] M. A. Stuchly, K. A. Stuchly, and A. M. Smith, "Dielectric properties of animal tissues in vivo at radio and microwave frequencies: comparison between species," *Phyiscs in Medicine and Biology*, vol. 27, pp. 927–1159, 1982.

[20] K. R. Foster, J. L. Schepps, R. D. Stoy, and H. P. Schwan, "Dielectric properties of brain tissue between 0.01 and 10 GHz," *Phys. Med. Biol.*, vol. 24, pp. 1177–1187, 1979.

[21] W. H. Press, B. P. Flannery, S. A. Teukolsky, and W. T. Vetterling, *Numerical Recipes in C*, 2 ed. Cambridge, U.K.: Cambridge Univ. Press, 1992.

[22] J.-Z. Bao, C. C. Davis, and R. E. Schmukler, "Impedance spectroscopy of human erythrocytes: System calibration and nonlinear modeling," *IEEE Trans. Bio-Med. Eng.*, vol. 40, pp. 364–378, Apr. 1993.

[23] J. C. Lin, "Microwave properties of fresh mammalian brain tissues at body temperature," *IEEE Trans. Bio-Med. Eng.*, vol. BME-22, pp. 74–76, Jan. 1975.

[24] N. R. V. Nightingale, A. W. J. Dawkins, R. J. Sheppard, E. H. Grant, V. D. Goodridge, and J. L. Christie, "The use of time domain spectroscopy to measure the dielectric properties of mouse brain at radiowave and microwave frequencies," *Phys. Med. Biol.*, vol. 25, pp. 1161–1165, 1980.

Jian-Zhong Bao (M'92–SM'96) was born in Beijing, China, in 1958. He received the B.S. degree in physics from Northwestern University, Xian, China, in 1982, and the Ph.D. degree in chemical physics from the University of Maryland at College Park (UMCP), in 1991.

From 1982 to 1985, he was a Faculty Member at Xidian University, Xian, China. From 1986 to 1991, he was a Graduate Research Assistant in the Department of Electrical Engineering, UMCP, working on electrical impedance measurements and modeling of red-blood cells in the frequencies from 1 Hz to 10 MHz, membrane phase transition, and electrical-field simulation, and from 1992 to 1994, he was a Research Associate, working on dielectrometry of macromolecules, binary solutions of simple molecules, and simple cellular systems in gigahertz range. Since 1994, he has been with McKesson BioServices, as a Senior Research Engineer with the U.S. Army Medical Research Detachment, Brooks Air Force Base, San Antonio, TX. He has been working on various projects that include signal processing of picosecond electromagnetic pulses and electromagnetic simulation with the finite-difference time-domain method. His current research interest is the application of object-oriented methodologies to electromagnetic modeling. He has authored over 20 publications in the areas of impedance and microwave dielectric measurements and characterization of materials, measurements and signal processing of electromagnetic pulses, and computer simulation of electromagnetics.

Dr. Bao is a member of the American Physical Society, Bioelectromagnetics Society, Biophysical Society, and Computer Society, and his name is listed in *American Men and Women of Science* and *Who's Who in Science and Engineering*.

Shin-Tsu Lu was born in Taipei, Taiwan, R.O.C., in 1943. He received the B.V.M. degree in veterinary medicine in 1968 from National Taiwan University, Taipei, and the M.S. and Ph. D. degrees in radiation biology from the University of Rochester, Rochester, NY, in 1973 and 1977, respectively.

From 1972 to 1990, he served as a Staff and Faculty Member at the University of Rochester, School of Medicine, Department of Medicine, Cardiology Unit, Department of Radiation Biology and Biophysics, Aerosol Research Laboratory, and Department of Biophysics. He also served as a Scientific Consultant to various private and governmental research laboratories and a Scientific Reviewer on publication and grant applications. Since 1990, he has been the Senior Research Physiologist of the McKesson BioServices at the U.S. Army Medical Research Detachment, Microwave Bioeffects Branch at Brooks AFB, San Antonio, TX. His research has concentrated on biological effects of radio-frequency radiation and ELF fields.

Dr. Lu is a member of the Bioelctromagnetics Society, Engineering in Medicine and Biology Society, and ANSI C95.4.

William D. Hurt (SM'78) was born in Georgetown, TX, on March 16, 1942. He received the B.S. degree and the M.S. degree in physics from St. Mary's University, San Antonio, TX, in 1964 and 1971, respectively, and the M.S. degree in engineering from the University of Texas at Austin, in 1976.

He is a Research Physicist at the Armstrong Laboratory, Brooks Air Force Base, San Antonio.

Mr. Hurt is a member of the IEEE Standards Coordinating Committee 28, Subcommittee I, Techniques, Procedures, and Instrumentation.

Bioelectromagnetics 20:216–223 (1999)

Pulsed Microwave Induced Light, Sound, and Electrical Discharge Enhanced by a Biopolymer

Johnathan L. Kiel,[1]* Ronald L. Seaman,[2] Satnam P. Mathur,[2] Jill E. Parker,[1] John R. Wright,[3] John L. Alls,[1] and Pedro J. Morales[1]

[1]*Directed Energy Bioeffects Division, Air Force Research Laboratory, Brooks AFB, Texas*
[2]*McKesson BioServices and U.S. Army Medical Research Detachment, Brooks AFB, Texas*
[3]*Department of Physical Sciences, Southeastern Oklahoma State University, Durant, Oklahoma*

Intense flashes of light were observed in sodium bicarbonate and hydrogen peroxide solutions when they were exposed to pulsed microwave radiation, and the response was greatly enhanced by a microwave-absorbing, biosynthesized polymer, diazoluminomelanin. A FPS-7B radar transmitter, operating at 1.25 GHz provided pulses of 5.73 ± 0.09 μs in duration at 10.00 ± 0.03 pulses/s with 2.07 ± 0.08 MW forward power (mean ± standard deviation), induced the effect but only when the appropriate chemical interaction was present. This phenomenon involves acoustic wave generation, bubble formation, pulsed luminescence, ionized gas ejection, and electrical discharge. The use of pulsed microwave radiation to generate highly focused energy deposition opens up the possibility of a variety of biomedical applications, including targeting killing of microbes or eukaryotic cells. The full range of microwave intensities and frequencies that induce these effects has yet to be explored and, therefore, the health and safety implications of generating the phenomena in living tissues remain an open question. Bioelectromagnetics 20:216–223, 1999. Published 1999 Wiley-Liss, Inc.†

Key words: radio frequency radiation; diazoluminomelanin; free radicals

INTRODUCTION

A peroxidizing mixture of diazoluminomelanin (DALM), a microwave absorbing polymer, can generate thermochemiluminescence (TCL), steady-state luminescence based on the temperature, when exposed to microwave radiation [Kiel et al., 1990; Kiel and O'Brien, 1991]. TCL will not proceed without the presence of hydrogen peroxide and a source of carbon dioxide (sodium carbonate or bicarbonate can be used in place of the gas). The polymer, formed in bacteria, makes them sensitive to a profound microwave biological effect as well. A moderate rate of energy absorption (100 mW/g) of 2450-MHz radiation has previously shown a large magnitude of kill (5 logs) of *Bacillus anthracis* (Anthrax bacteria), when the bacteria were held at 37 °C during exposure under peroxidizing conditions, after cultivation on medium inducing DALM biosynthesis [Bruno and Kiel, 1993]. In 1989, we [Kiel and Seaman, unpublished data] observed flashes of light in peroxidizing solutions of the water-soluble TCL polymer DALM with applied microwave pulses. In those preliminary experiments, microwave energy at 2450 MHz was delivered as 40-μs pulses at 1–3 pulses/s. Application was made with 3.6-mm OD open-ended semirigid coaxial cable connected to an EPSCO PG5KB/5238H source, in contact either with sample fluid or with the outside of its cuvette; both approaches were successful in generating flashes of light. Here, we provide evidence for a pulsed-microwave

Published 1999 Wiley-Liss, Inc. †This article was prepared by a group consisting of both United States government employees and non-United States government employees, and as such is subject to 17 U.S.C. Sec. 105.

Grant sponsor: United States Air Force Office of Scientific Research and the U.S. Army Medical Research and Materiel; Grant number: DAMD17-94-C-4069.

The views, opinions, and/or findings contained in this report are those of the authors and should not be construed as an official Department of the Army or Department of the Air Force position, policy, or decision unless so designated by other documentation.

*Correspondence to: J.L. Kiel, AFRL/HEDB, 2503 Gillingham Drive, Bldg. 175E, Brooks AFB, TX, 78235-5102. E-mail: johnathan.kiel@aloer.brooks.af.mil

Received for review 14 August 1997; Final revision received 7 August 1998

mechanism for light production and focusing of energy deposition that is enhanced by DALM.

MATERIALS AND METHODS

Chemicals and Biosynthesis

Luminol (5-amino-2,3-dihydro-1,4-phthalazinedione), 3-amino-L-tyrosine dihydrochloride (3AT), sodium nitrite, and potassium nitrate were obtained from Sigma (St. Louis, MO). Diazoluminol was prepared by mixing 0.17 g of luminol and 0.65 g of $NaNO_2$ in 120 ml of distilled water and stirring for 35 min. The solution was filtered twice. In the case of luminol and bicarbonate solutions used, clear supernatants were collected off saturated aqueous solutions of luminol and $NaHCO_3$.

Biosynthetic DALM solutions were prepared from *Escherichia coli* JM109, pIC2ORNR$_{1.1}$ bacteria (American Type Culture Collection # 69905) grown on medium containing 3-amino-L-tyrosine, luminol, and potassium nitrate in a tryptocase soy broth base (U.S. Patent 5,156,971) for 5 days. The unfrozen pigmented supernatant was removed from above the ice of frozen cultures and was diluted as noted below. The 1:10 dilutions of DALM were made in sodium bicarbonate/luminol saturated solutions, except that when determining their optical absorptions at 350 nm, deionized water was used instead. Optical absorption of 1:10 DALM solution at 350 nm wavelength was 0.15. Poly-diazotyrosine (pDAT) was synthesized like DALM, as previously reported [Kiel and O'Brien, 1991], but with the exclusion of luminol, and was dissolved in water until its optical absorption at 350 nm matched that of the respective DALM solutions. These proportions were preserved when solutions prepared with sodium bicarbonate/luminol saturated solutions were substituted for water.

Reaction Mixtures

Premixed reaction mixtures for 1:10 DALM or pDAT contained 1.8 ml of saturated sodium bicarbonate/luminol and 0.2 ml of DALM or pDAT neat solution, respectively, to which was added 1.2 ml of diazoluminol solution and additional 0.33 ml of saturated sodium bicarbonate/luminol solution, with or without 0.495 ml of 3% hydrogen peroxide (added last). Solutions of 1:100 DALM or pDAT differed from the 1:10 solutions in containing 1.2 ml 1:10 dilution of diazoluminol solution and 0.2 ml 1:10 DALM or pDAT in sodium bicarbonate/luminol saturated solutions, with additional 0.66 ml saturated sodium bicarbonate/luminol solution, with or without 0.66 ml of 3% hydrogen peroxide. Except for the 3% hydrogen peroxide, which was added to samples previously exposed to microwave radiation, when components of the reaction mixtures were deleted, saturated sodium bicarbonate/luminol solution was substituted for the excluded components. This substitution was not made when sodium bicarbonate solution, deionized water, or hydrogen peroxide or any of these used in combination (Table 1) were exposed. All reactions were begun at room temperature (23 °C) but were bulk heated with forced hot air from 23.3 °C to 54.5 °C for DALM and pDAT samples without hydrogen peroxide and from 28.2 °C to 54.4 °C for those same samples with hydrogen peroxide. This scanning of temperature was required because we did not know what the optimal temperature or level of thermochemiluminescence was required to observe the pulse effects.

Microwave Exposure

Samples were placed in 15-ml polystyrene tubes without tops. As shown in Figure 1, a single tube was held by a polyvinyl support beam attached to a section of WR-650 microwave waveguide with a flangeless opening of 16.5 × 8.3 cm. The long dimension of the waveguide opening was horizontal, providing a vertical electrical field. When placed in a hole in the beam, a tube was vertical with its center 7.6 cm from the waveguide opening and was centered horizontally with respect to the opening. Microwave pulses were generated by a FPS-7B radar transmitter operating at 1.25 GHz. The transmitter provided pulses of 5.73 ± 0.09 μs in duration at 10.00 ± 0.03 pulses/s with 2.07 ± 0.08 MW forward power (mean ± standard deviation). During exposures, temperature was monitored by means of nonperturbing Vitek 101 Electrothermia Monitor and Luxtron probes in and near the bottom of the sample. Specific absorption rates (SAR) determined in separate exposures of duplicate samples are listed in Table 1. These values were calculated from the rate of rise of temperature (°C/s) in respective samples measured by nonperturbing fiberoptic Luxtron MPM probes: SAR = c(dT/dt). Specific heat c was taken to be that of water, 4180 J/kg/°C, for all samples. Equivalent peak SAR of the pulses was approximately 2×10^4 times the time-averaged SARs reported in Table 1.

Sound and Light Recordings

Sound was recorded on the audio track of videotape by using an RCA BK-6B M-11017A microphone outside of the anechoic chamber. Sound was directed to the microphone through a plastic tube (1.9-cm ID) connected to a plastic funnel positioned 15 cm above the sample tube. The acoustic path between the top of the sample tube and the microphone was 4.63 m long, with a calculated propagation delay of approximately 13.4 ms. The video images for analysis were recorded with an ITT model #F4577 low-light sensitive black/white camera at a normal video frame recording rate. Images to spatially re-

TABLE 1. Summary of Flash Responses Observable on Video Recordings*

Sample	SAR (W/kg)	Onset delay (s)	Flash burst type	Number of bursts	Maximum burst duration (s)	Duration observed (s)
Deionized water	50 ± 0.0[a]	N/A	None	—	—	472
H_2O_2	40 ± 20	N/A	None	—	—	464
$NaHCO_3$	340 ± 40	N/A	None	—	—	429
w/H_2O_2	370 ± 20	94	Sporadic	14	115	454
Luminol						
$NaHCO_3$	300 ± 50	301	Sporadic	3	<1	471
w/H_2O_2	400 ± 20	12	Continuous	1	242	254
Luminol diazoluminol						
$NaHCO_3$	360 ± 20	N/A	None	—	—	482
w/H_2O_2	370 ± 60	N/A	None	—	—	438
DALM						
(1:10)	570 ± 230	68	Sporadic	4	9	424
w/H_2O_2	480 ± 60	10	Sporadic	8	38	390
DALM						
(1:100)	360 ± 50	10	Sporadic	6	47	315
w/H_2O_2	610 ± 150	63	Sporadic	20	20	444
pDAT						
(1:10)	370 ± 60	N/A	None	—	—	461
w/H_2O_2	440 ± 70	290	Sporadic	6	<1	571
pDAT						
(1:100)	320 ± 100	85	Sporadic	12	93	432
w/H_2O_2	400 ± 60	134	Sporadic	10	<1	677

* SAR is the average (spatial and temporal) specific absorption rate of microwave energy. DALM (diazoluminomelanin) and pDAT (polydiazotyrosine) solutions all contained luminol, diazoluminol, and sodium bicarbonate.
[a] ± one standard deviation; n = 2 to 6.

solve the light source were recorded with an Optronics DEI-470 integrating color camera at various frame integration times. The arrangement of this apparatus is shown in Figure 2. The exposure was performed in an anechoic chamber sealed off from external light sources. The cameras were placed in screen-wire Faraday cages with holes cut in the cages so as not to block the light path to the lenses.

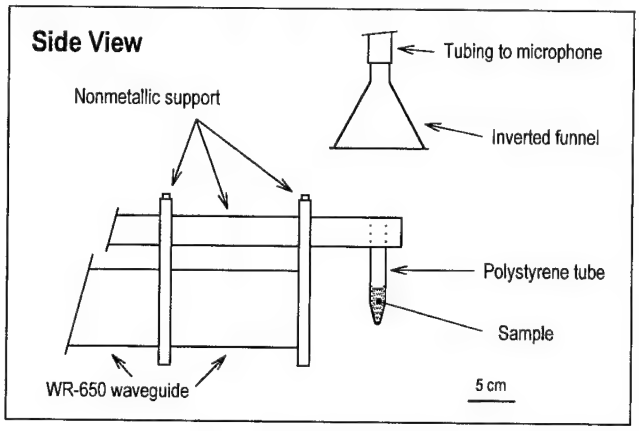

Fig. 1. Side view of sample positioned for exposure. The 15-ml polystyrene tube containing the sample was held by a nonmetallic support beam made of polyvinylchloride. The beam was securely fastened to the WR-650 waveguide by brackets made of the same material. The inverted plastic funnel directed sound produced in the sample through tubing connected to a microphone outside the anechoic chamber. Not shown in the sketch are secondary support braces and nonperturbing temperature probe.

For analysis, videotape was played on a Panasonic TV/Recorder AG-560 (27-cm diagonal screen) with contrast set at maximum and brightness at minimum. The video image of an activated, luminescing solution was approximately 3.5 cm from the bottom of the sample tube to the fluid meniscus and 1.7 cm wide.

For sensing the light emissions, a sensing element of an EXTECH Light Adapter 4010201 was securely fastened to a vertical plate having a variable aperture. The plate was held in place in front of the monitor screen by stereotaxic manipulators, which allowed precise placement of the aperture-sensor combination. The signal from the light adapter was amplified by a Krohn-Hite 3322 Dual Filter (20 dB, low pass max flat, 51 kHz), and then by a Gould Model 20-4615-58 Universal Amplifier (ext. mV, 1 V F.S., DC-30 Hz) and displayed on a Tektronix 2430A Digital Oscilloscope and/or recorded on a Gould TA2000 Chart Recorder.

The audio output of the monitor was amplified by a Krohn-Hite filter (0 dB, high-pass RC, 900 Hz) and by a Rockland Model 1022F Dual Hi/Lo filter (20 dB, high-

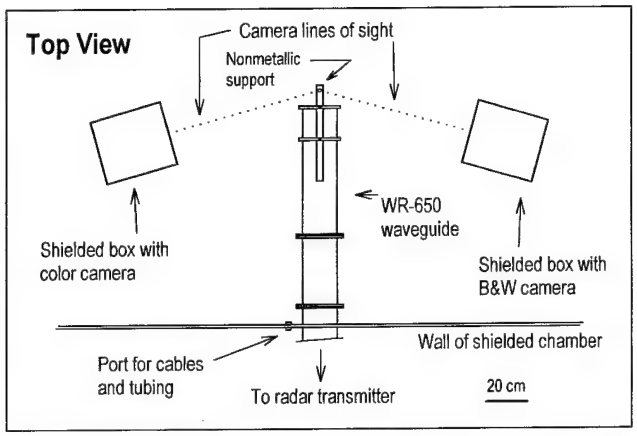

Fig. 2. Top view of the experimental apparatus inside the anechoic chamber. The shielded boxes containing cameras were supported from the floor and were approximately 76 cm from the sample tube. Lines of sight to the sample are shown as dotted lines. Not shown are cables from the cameras, tubing for sound transmission, and the nonperturbing temperature probe, which all passed through the cable port to instrumentation outside the chamber. Microwave absorbing material lining the interior wall of the chamber, secondary support braces, and funnel for sound pick up are also not shown.

pass RC, 11 Hz). The output of the latter was connected to the second Rockland amplifier (0 dB, low pass, 60 Hz) through a 1N914B signal diode to provide a rectified signal. The amplified signal or the amplified and rectified signal was displayed and/or recorded along with the light signal.

RESULTS

We first attempted to reproduce the original 1989 observation by formulating DALM solutions with maximal TCL. One such solution contained sources of carbon dioxide and hydrogen peroxide, which are required for DALM, itself a complex mixture of a polymer of tyrosine and covalently and noncovalently linked luminol and diazoluminol, to luminesce. Another solution was made by adding a polymer formed from diazotyrosine (pDAT), that shows similar TCL to DALM. When exposed to pulsed (10/s) 1.25-GHz microwave radiation, these solutions generated flashes that were clearly distinguishable on video recordings by low-light intensity video cameras.

Figure 3 shows sequential video frames that demonstrate baseline TCL and flashes induced by microwave pulses. As in the original observations in 1989, the flashes appeared in bursts, i.e., not with every microwave pulse, and were accompanied by audible pops. The intensity of the pops correlated with the intensity of the flashes, as clearly shown by the examples of processed sound and light signals in Figure 4. In Figure 4D, the first of each pair of peaks in the sound signal from a DALM solution was due to a signal induced on the audio channel by operation of the microwave transmitter. The earlier peak provided a convenient reference for timing. Note the low baseline luminescence (dashed lines in Fig. 4) and rapid increases in luminescence indicating flashes. Ripples on the light signal were due to the video frame rate. In Figure 4B, the luminescence was higher than in A (see inserted scale) because of the activation by hydrogen peroxide. The 10 pulse/s variations in luminescence occurred in synchrony with the microwave pulses. In Figure 4C, by using only luminol, bicarbonate, and hydrogen peroxide, the luminescence was high and the flashing was persistent. However, not all the flashes were accompanied by a loud pop. In Figure 4D, where the tracing time scale for activated 1:100 DALM solution was expanded, the microwave artifact (brief, coincident with the flashes later in the record) and pops (longer, damped fall off recordings), due to the sound propagation, there was a 13.5 to 14 ms delay. The small waves seen in the light signal were attributable to the video frame rate. Within the time resolutions of the recorded signals and analysis procedures, recorded flashes and pops seem to be occurring at the same time, coincident or nearly coincident with each microwave pulse. Figure 4 also illustrates that lower intensity pops occurred without flashes before and sometimes after bursts of flashes, that were, in turn, accompanied by higher intensity pops.

Integrated imaging (Fig. 3) clearly demonstrates that flashes originated from discrete areas in the meniscus of the sample. Flashes were apparently independent of TCL in liquid below the meniscus. The images strongly suggest discharges in gas above the liquid. In all cases in which flashes were frequent and intense, bubbles were observed in liquid samples during and after microwave exposure. The high-intensity flash among the series of less intense flashes of ITT camera images in Figure 3 was attributable to inherent differences in flash intensity or the missing of the peak of the short-duration flash between video frames.

To further investigate the source of the flashes, we examined the components of DALM solutions separately and in combination using equal sample volumes and the same incident microwave pulses (Table 1). Deionized water, sodium bicarbonate, and hydrogen peroxide solutions all failed to demonstrate TCL and flashes, despite extended exposure to microwave pulses. Biosynthetic DALM solutions without hydrogen peroxide activation displayed bursts of flashes with greater regularity, but lower intensity, than the same solutions with hydrogen peroxide added. When DALM was excluded, solutions containing diazoluminol and luminol, as well as sodium bicarbonate with and without hydrogen peroxide, showed no flashes, although the peroxide-activated solutions

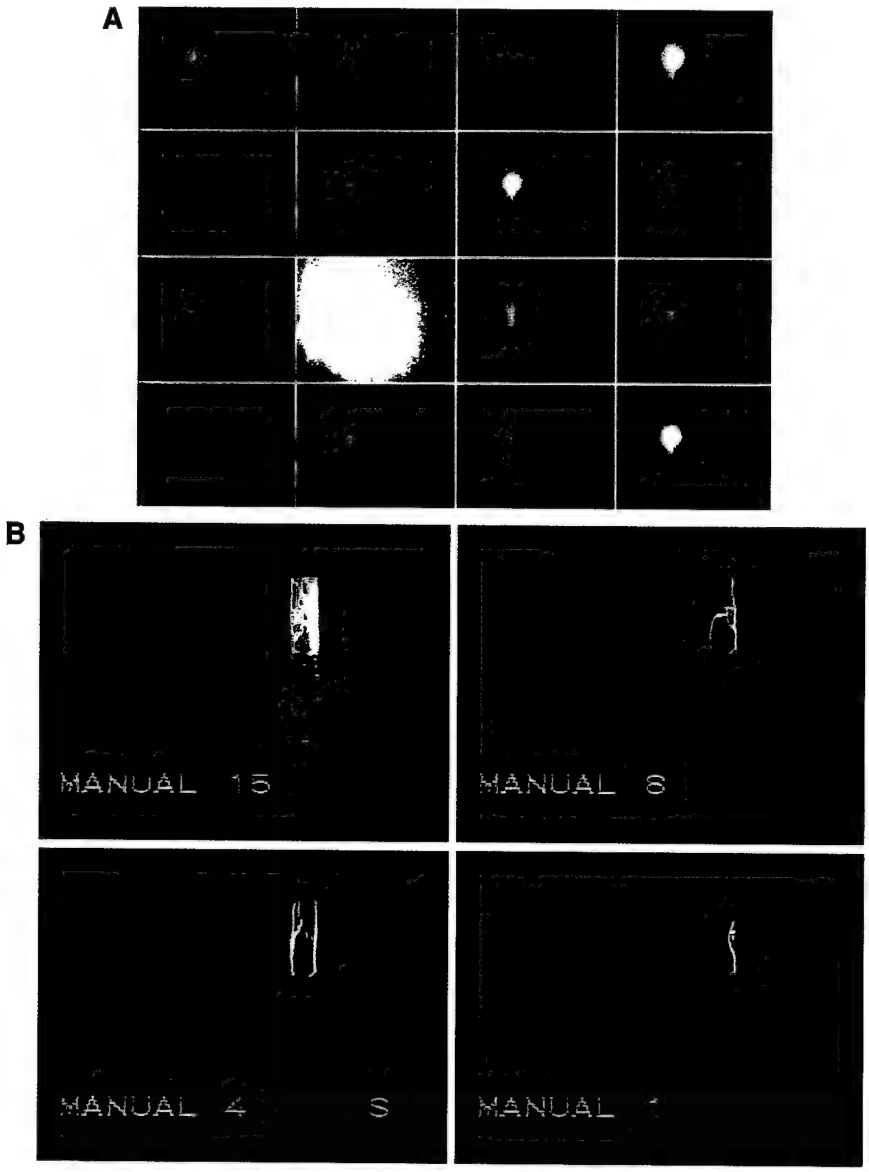

Fig. 3. Two series of video frames showing repetitive flashes with microwave exposures in samples of sodium bicarbonate and H_2O_2 solution with and without luminol added. **A:** (luminol added) Images from an ITT model #F4577 low-light sensitive black/white camera, normal video frame rate recording; each frame is a sequential frame representing 33 ms of integration time. **B:** (no luminol) Images from an Optronics DEI-470 integrating camera, recording at various frame integration times (15, 8, 4, or 1 s).

showed strong background luminescence. When the diazoluminol was excluded from the luminol and bicarbonate solutions, flashes occurred sporadically without hydrogen peroxide, but more intensely in the peroxide-activated solutions. These flashes arose from discrete locations on the menisci, discharging into the air space above the tube but not outside the tube. Finally, when exposed to microwave pulses, sodium bicarbonate and hydrogen peroxide solution produced bright flashes that were sustained for several seconds.

In all cases in which flashes were observed, a delay was observed after initiation of microwave pulses until the firing of the first flash. The delay ranged from 10 and 12 s for hydrogen-peroxide-activated DALM and luminol solutions, respectively, to 5 min for nonactivated luminol solutions. This observation and the presence of gas bubbles in all cases in which flashes were noted suggest that formation of gas bubbles that collected in the menisci was necessary for the flash. DALM seemed to catalyze the formation of bubbles in nonactivated solu-

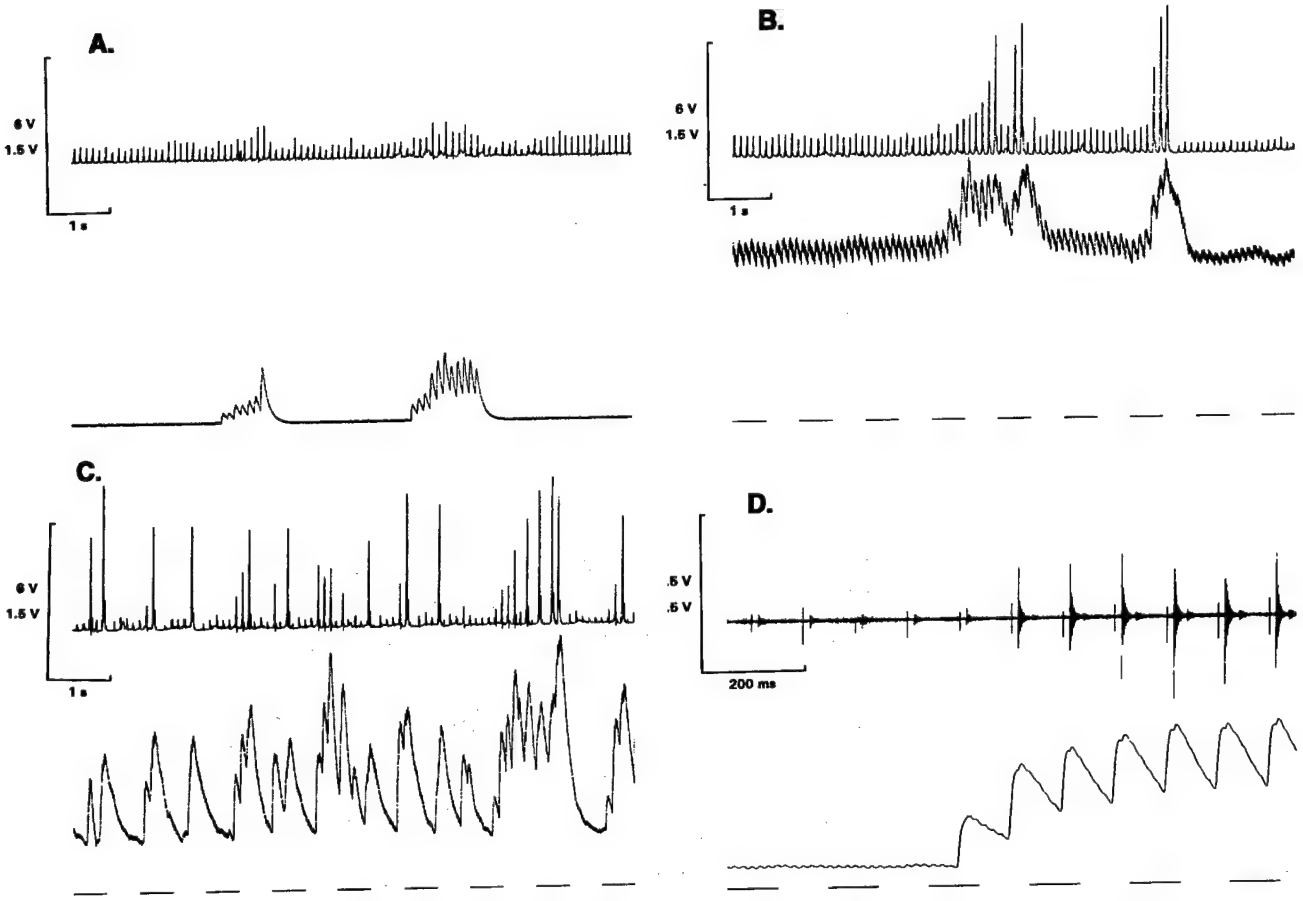

Fig. 4. Processed sound (top in each set) and light (bottom in each set) signals from videotape records from an ITT low-light sensitive camera. The scale insets are the chart recorder deflections in volts (6 and 1.5 V for sound and light intensities, respectively, for A, B, and C and 0.5 V for D) and the time scale in seconds for A, B, and C and milliseconds for D. **A:** Sample rectified-sound and light signals from diazoluminomelanin (DALM) (1:10) solution. Aperture open full. **B:** Sample rectified-sound and light signals from DALM (1:10) solution with H_2O_2. Aperture approximately 1-cm diameter to reduce baseline luminescence signal. **C:** Sample rectified-sound and light signals from an aqueous solution containing luminol, $NaHCO_3$, and H_2O_2. Aperture approximately 1 cm. **D:** Sample sound and light signals from DALM solution (1:100) with H_2O_2 on an expanded time scale at the onset of a flash burst. Aperture full open. The amplified or rectified-amplified audio signal was recorded at 1 V/cm for A–C and 0.25 V/cm for D. In D, output of a Rockland filter (0 dB) was connected directly to the chart recorder. The light signal was recorded at 0.25 V/cm for A–D.

tions because the flashes were more sustained than in luminol solutions alone.

DISCUSSION

An intermediate acoustic mechanism may play a role in the phenomenon observed here through thermoelastic expansion caused by rapid temperature rise due to the microwave pulse [Foster and Finch, 1974; Borth and Cain, 1977; Lin, 1980; Chou et al., 1982]. It should be noted that the specific absorption per microwave pulse in our experiments, 20–50 J/kg, was at least three orders of magnitude larger than for microwave pulses known to elicit auditory sensations [Seaman and Lebovitz, 1989]. However, we have recently generated the acoustic part of the effects enhanced by DALM with 6 kW peak power pulses (10 PPS; 1.5-ms pulse width) of 2.06 GHz radiation. This level is 3×10^{-3} times the level described in this paper (unpublished results).

The effects reported here could be explained by the following sequence: (1) the products of the chemical reactions produce enhanced absorption of the microwave energy; (2) the pulse form of the radiation and the specific molecular absorption stimulates vibrations that become sound; (3) the container resonates at certain frequencies of the sound; (4) the resonance amplifies the sound; (5) the sound leads to cavitation, bubble formation, and bubble collapse yielding luminescence; (6) fi-

nally, the gas is ejected as a plasma (gas ionized by heat from high pressures generated in the bubble collapse) because of the anisotropic (ellipsoidal) bubble collapse near the surface of the liquid sample [Glanz, 1996; Barber et al., 1997]. This latter result produces a supersonic jet of hot, ionized gas that then electrically discharges because of the microwave radiation's electric field. The spectacular "lightning in a bottle" effect imaged in Figure 3 is the consequence. The lack of discharge above the tube opening and the absence of an electrical arc to the microwave waveguide also support this conclusion and rule out other sources of electrical discharge. Also, the building of sound intensity with the burst of flashes suggests a build up of hot ionized gas before the discharge. The sporadic nature of the flashes, especially when major discharges were observed, suggests a possible depletion of the ionized gas that must again build up for subsequent flashes. The popping observed has also been heard in classic ultrasonic-induced sonluminescence (SL) and is believed to result from the rebounding of the shock wave [Walton and Reynolds, 1984; Glanz, 1996; Barber et al., 1997]. The popping reported here is not from boiling, because the sound that leads to the pops is not chaotic. It follows the pulse rate of the microwave radiation, and the pops show evidence of a build up of the sound pulses corresponding to the microwave radiation pulse rate (see Fig. 4).

The lack of flashes and the lack of pulsed sound generation in sodium bicarbonate and hydrogen peroxide solutions alone suggest that specific gases may be necessary for the effect that occurs when these reactants are in solution together. Also, the high nonphysiologic level of carbonate used here was not sufficient to generate the effect. Therefore, it was not merely dependent on high ion concentration. The carbonate radical has been previously reported as the major product of mixtures of sodium bicarbonate or sodium carbonate and hydrogen peroxide [Michelson and Maral, 1983]. Other possibilities are superoxide, hydroxyl, and formate radicals. We also suspect that peroxycarbonate may be formed. These substances may be released in hot vapors or as gases. The absence of flashes when diazoluminol was present in luminol, bicarbonate, and hydrogen peroxide solutions suggests that this compound is quenching the reactive radical or ion that mediates the phenomenon. The quenching is not because diazoluminol is not responsive to SL. It has been recently reported to be a SL-enhancing compound, when ultrasound is the inducing source [Maddox et al., 1998]. When DALM or pDAT was present, the quenching was reversed. This reversal suggests that DALM or pDAT can assist in the generation of light and sound by pulsed-microwave radiation and that free radicals are likely to be involved. The interaction of diazoluminol with the radicals was probably responsible for the increased chemiluminescence observed.

In both the pulse effects reported here and the killing of anthrax bacteria, the average temperature was not sufficient to explain the results. Both studies required the same kind of chemical reactions and conditions to produce the effects observed. Although the killing of anthrax was done with continuous wave microwave radiation, the specific absorption rate was high and the temperature was actively maintained by air cooling. This approach led to a large flux of energy through the bacteria. By itself, this thermal flux was not sufficient to kill the bacteria unless they contained DALM that was being peroxidized in the presence of carbon dioxide or carbonate at the same time. These similarities suggest a mechanism, other than frank heating, that focuses energy on vulnerable structures and is accentuated by pulsing of the microwave radiation.

CONCLUSIONS

Pulsed microwave radiation interacting with certain reduction/oxidation-type biochemical reactions can enhance localized absorption of microwave radiation leading to sound and light generation and electrical discharge. The evidence for this conclusion includes (1) the necessity for certain chemical reactions to generate the phenomena; (2) the necessity for sound generation by the microwave radiation to produce light that follows the microwave pulse rate, (3) the surface ejection of plasma from the reaction liquid, and (4) electrical discharge as a result of the interaction of the microwave radiation electric field with the ejected plasma. The phenomenon we describe here opens up the possibility of a microwave bioeffect mechanism unique to pulsed microwave radiation and the potential for applying pulsed microwave radiation to surface sterilization and focal tissue destruction.

ACKNOWLEDGMENTS

We thank B.E. Stuck and P.K. Kennedy for comments on earlier drafts and D.D. Cox for design and fabrication of the sample support beam. We also thank the Navy Medical Research Institute Detachment of the Triservice Radiofrequency Radiation Facility for providing access to the FPS transmitter.

REFERENCES

Barber BP, Hiller RA, Löfstedt R, Putterman SJ, Weninger KR.1997. Defining the unknowns of sonoluminescence. Phys Rep 281:65–143.

Borth DE, Cain CA. 1977. Theoretical analysis of acoustic signal generation in materials irradiated with microwave energy. IEEE Trans Microwave Theory Tech 25:944–954.

Bruno JG, Kiel JL. 1993. Effect of radio-frequency radiation (RFR) and diazoluminomelanin (DALM) on the growth potential of bacilli. In: Blank M, editor. Electricity and magnetism in biology and medicine. San Francisco: San Francisco Press. p 231–233.

Chou CK, Guy AW, Galambos R. 1982. Auditory perception of radio-frequency electromagnetic fields. J Acoust Soc Am 71:1321–1334.

Foster KR, Finch ED. 1974. Microwave hearing: evidence for thermoacoustic auditory stimulation by pulsed microwaves. Science 185:258–258.

Glanz J. 1996. The spell of sonoluminescence. Science 274:718–719.

Kiel JL, O'Brien GJ. 1991. Diazoluminomelanin and a method for preparing same. U.S. Patent 5,003,050.

Kiel JL, Gabriel C, Simmons DM, Erwin DN, Grant EH. 1990. Diazoluminomelanin: a conductive luminescent polymer with microwave and radiowave absorptive properties. In: Pedersen PC, Onaral B, editors. Proceedings of the twelfth annual international conference of the IEEE Engineering in Medicine and Biology Society, Vol.12, No. 4, Philadelphia: IEEE. p 1689–1690.

Lin JC. 1980. The microwave auditory phenomenon. Proc IEEE 68:67–73.

Maddox L, Reeves M, Wood K, Roberts K, Studer J, Wetzel J, Smith T, Holwitt E, Alls J, Kiel J, Wright JR. 1998. Acoustic wave dosimetry based on diazotized luminol solutions. Microchem J 58:209–217.

Michelson AM, Maral J. 1983. Carbonate anions: effects on the oxidation of luminol, oxidative hemolysis, γ-irradiation and the reaction of activated oxygen species with enzymes containing various active centres. Biochimie 65:95–104.

Seaman RL, Lebovitz RL. 1989. Thresholds of cat cochlear nucleus neurons to microwave pulses. Bioelectromagnetics 10:147–160.

Walton AJ, Reynolds GT. 1984. Sonoluminescence. Adv Phys 33:595–660.

INT. J. RADIAT. BIOL 1999, VOL. 75, NO. 1, 115–120

Frequency of micronuclei in the blood and bone marrow cells of mice exposed to ultra-wideband electromagnetic radiation

VIJAYALAXMI†*, R. L. SEAMAN‡, M. L. BELT‡, J. M. DOYLE‡, S. P. MATHUR‡ and T. J. PRIHODA§

(Received 15 May 1998; accepted 18 August 1998)

Abstract.
Purpose: To investigate the extent of genetic damage in the peripheral blood and bone marrow cells of mice exposed to ultra-wideband electromagnetic radiation (UWBR).
Materials and methods: CF-1 male mice were exposed to UWBR for 15 min at an estimated whole-body average specific absorption rate of 37 $mW\,kg^{-1}$. Groups of untreated control and positive control mice injected with mitomycin C were also included in the study. After various treatments, half of the mice were killed at 18 h, and the other half at 24 h. Peripheral blood and bone marrow smears were examined to determine the extent of genotoxicity, as assessed by the presence of micronuclei (MN) in polychromatic erythrocytes (PCE).
Results: The percentages of PCE and the incidence of MN per 2000 PCE in both tissues in mice killed at 18 h were similar to the frequencies observed in mice terminated at 24 h. There were no significant differences in the percentage of PCE between control and the mice with or without UWBR exposure; the group mean values ($\pm$ standard deviation) were in the range of 3.1 ± 0.14 to 3.2 ± 0.23 in peripheral blood, and 49.0 ± 3.56 to 52.3 ± 4.02 in bone marrow. The mean incidence of MN per 2000 PCE in control and in mice with or without UWBR exposure ranged from 7.7 ± 2.00 to 9.7 ± 2.54 in peripheral blood and 7.4 ± 2.32 to 10.0 ± 3.27 in bone marrow. Pairwise comparison of the data did not reveal statistically significant differences between the control and mice with or without UWBR exposure groups (excluding positive controls).
Conclusion: Under the experimental conditions tested, there was no evidence for excess genotoxicity in peripheral blood or bone marrow cells of mice exposed to UWBR.

1. Introduction

Electromagnetic devices capable of producing signals with pulse widths of a few nanoseconds and electric field amplitudes exceeding 100 000 $V\,m^{-1}$ are being considered in the USA and elsewhere for use in warfare settings, for example electronic countermeasures to identify and track incoming armour-piercing rounds that threaten ground vehicles (Fuerer 1991, Taylor 1991, Toevs *et al.* 1992). Ultra-wideband electromagnetic radiation (UWBR) in the radiofrequency range is in this category of signal, and can be characterized as having a large band spread of up to 2 GHz, a rapid rise time of less than 0.2 ns, and a pulse duration of a few ns. It is conceivable that personnel could be exposed to such signals while operating and/or working in the vicinity of radar or communications-jamming equipment, and/or by similar friendly or enemy equipment (Sherry *et al.* 1995). Such potential exposure to UWBR raises issues related to possible bioeffects and/or possible human health hazards.

Recently, Albanese *et al.* (1994) described possible useful applications of ultra-short electromagnetic pulses in medical settings. These included electroporation, which would allow chemotherapeutic drugs to enter more readily and kill cancer cells, and the development of new techniques for imaging tissue structures. The authors also associated their theoretical considerations with undesirable health effects resulting from potential tissue damage mechanisms, including macromolecular conformation changes, alterations in chemical reaction rates, membrane effects and temperature-mediated adverse responses. Merritt *et al.* (1995) subsequently challenged most of these associations, and indicated the limited availability of experimental (biological) data. The small number of published scientific reports has not indicated any discernible physiological or behavioural change in rats and monkeys exposed to UWBR (Sherry *et al.* 1995, Walters *et al.* 1995).

The potential of UWBR exposure to induce genetic damage, if any, is important for risk assessment related to mutation and cancer induction. Recently, Pakhomova *et al.* (1997, 1998) reported an absence of mutagenic effects of UWBR exposure on the D7 strain of the yeast *Saccharomyces cerevisiae*. As far as is known, an examination of the genetic effects of

*Author for correspondence.
†Department of Radiology, Division of Radiation Oncology, and Center for Environmental Radiation Toxicology, The University of Texas Health Science Center at San Antonio, 7703 Floyd Curl Drive, San Antonio, TX 78284, USA. e-mail: vijay@uthscsa.edu
‡McKesson BioServices and Microwave Bioeffects Branch, US Army Medical Research Detachment, Brooks Air Force Base, San Antonio, TX 78235, USA.
§Department of Pathology, The University of Texas Health Science Center at San Antonio, 7703 Floyd Curl Drive, San Antonio, TX 78284, USA.

International Journal of Radiation Biology ISSN 0955-3002 print/ISSN 1362-3095 online © 1999 Taylor & Francis Ltd
http://www.tandf.co.uk/JNLS/rab.htm
http://www.taylorandfrancis.com/JNLS/rab.htm

UWBR exposure of mammalian cells, either *in vitro* or *in vivo*, has not been reported in the literature. The rodent micronucleus (MN) test has been widely accepted as an *in vivo* test system for detecting genotoxic agents, and has become a standard assay used in regulatory testing in several countries (Auletta *et al.* 1993, Health Protection Branch Genotoxicity Committee (Canada) 1993, Kirkland 1993, Sofuni 1993). The objective of the present investigation was to assess the extent of genetic damage, as determined from the incidence of MN, in peripheral blood and bone marrow cells of mice exposed to UWBR for 15 min.

2. Materials and methods

A protocol approved by the Institutional Animal Care and Use Committee of the United States Air Force Armstrong Laboratory, Brooks Air Force Base was followed. The Standard Operating Procedures were compatible with the requirements of the United States National Toxicology Program.

2.1. *UWBR exposure*

The UWBR exposure facility is located at Brooks Air Force Base in San Antonio. Mice were exposed to UWBR pulses in a giga-transverse-electromagnetic (GTEM) cell comprised of a tapered rectangular coaxial transmission line with a square cross section (originally constructed by Sandia National Laboratory, Albuquerque, NM, USA). The outer ground conductor had a square cross section measuring 11–71 cm inside the cell (the range results from the tapered structure of the cell). The centre conductor was 7.8–56.3 cm wide in the same region, and was 2.6 cm thick throughout the cell. An approximate volume of $20 \times 20 \times 40$ cm was available on each broad side of the centre conductor for placing a single mouse in a circular plastic holder. A modified RG-220 coaxial cable connected the GTEM cell to a high voltage source. Ionization of pressurized nitrogen gas in a spark gap in the cable resulted in high voltage pulses that led to UWBR pulses in the GTEM cell. In this system, the electric field was directed from the centre conductor to the ground conductor.

The propagating UWBR pulses in the GTEM cell were monitored during exposures of mice using signals from a time-derivative (D-dot) probe mounted in the wall of the cell. Stored wave forms were later processed using a correction algorithm to give the electric field strength versus time (Bao 1997). Pulses were triggered at 600 pulses per second by an external pulse generator. The peak amplitude of the UWBR pulse was 91.1–102.9 $kV\,m^{-1}$ at the location of the centre of the animal holder. The pulse rise time was 146.6–166.1 ps and the pulse duration was 0.92–0.97 ns. The whole-body specific absorption rate (SAR) was estimated to be 37 $mW\,kg^{-1}$. This was done by integrating the product of the power spectrum, computed from the corrected UWBR pulse field strength, and the normalized SAR ($W\,kg^{-1}$ per $mW\,cm^{-2}$) for a prolate spheroidal model of a medium-sized mouse (Durney *et al.* 1986) in the frequency domain. The average for k- and H-polarizations of the animal was used to account for the movement of the animal in the UWBR field.

2.2. *Mice and maintenance*

CF-1 male mice aged 10–12 weeks old, weighing 33–48 g, were obtained from Charles River Laboratories (Portage, MI, USA). Upon arrival they were housed two to four per cage in an animal facility at Brooks Air Force Base. The room was maintained at a temperature of 22 ± 1°C and a relative humidity of 50 ± 5%, with an air-flow rate of 10–15 exchanges per hour. A time-controlled system provided a daily 05.00–17.00 light and 17.00–05.00 dark cycle. All mice were given *ad libitum* access to Purina rodent chow and to tap water.

After a 10 day quarantine period, a total of 61 mice were distributed into separate groups using a randomized block design. There were nine mice in the untreated control group, 12 mice in the positive control group and 10 mice in each of UWBR exposure groups. Each mouse was placed in a circular plastic holder that did not restrict the movement of the animal. The mouse in its holder was placed in the GTEM cell for UWBR exposure for 15 min at 600 pulses per second (+UWBR), or to no pulses (−UWBR); the exposure was carried out at room temperature, one mouse at a time. The selection of the 15 min duration of the UWBR exposure was based on an earlier observation (unpublished), which indicated a potential UWBR exposure time-related effect on morphine-induced analgesia in these mice. After each UWBR exposure, the holder was removed from the GTEM cell and the mouse was taken out. All mice were returned to their cages and kept in the animal facility until sacrifice at 18 or 24 h when the peripheral blood and bone marrow cells were collected for the genetox study reported here.

2.3. *Positive controls*

Mice in this group were given an i.p. injection of mitomycin C (MMC; 1 $mg\,kg^{-1}$ body weight) (Sigma; St Louis, MO, USA) at 18 or 24 h before sacrifice.

MMC is a known clastogen that has been shown to induce MN (Heddle *et al.* 1984).

2.4. *Peripheral blood and bone marrow smears*

From each group, half of the mice were killed at 18 h, and the remaining half at 24 h. From each mouse, before sacrifice, a small drop of peripheral blood was collected on a clean microscope slide by snipping the end of the tail. A thin smear was made over an area of 2–3 cm by pulling the blood behind a coverglass held at a 45° angle. Following sacrifice, bone marrow from both femurs was flushed with 0.5 ml of foetal calf serum into a microfuge tube using a 1 ml syringe fitted with a 22 G needle. The cells were concentrated by gentle centrifugation at 600*g* for 1–3 min and a small drop of resuspended cells was placed on a clean microscope slide to make a smear as described above. All smears were air-dried, fixed in absolute methanol and stained using acridine orange.

Coded slides were examined under ×1000 magnification using a fluorescence microscope equipped with appropriate filters. Immature erythrocytes (PCE) were identified by their orange-red colour, mature erythrocytes by their green colour and the MN by their yellowish colour. For each mouse, 1000 erythrocytes in peripheral blood and 200 erythrocytes in bone marrow were examined to obtain the percentage of PCE. In addition, for each mouse, 2000 consecutive PCE were examined in peripheral blood and in bone marrow to determine the incidence of MN. Decoding of the slides was done after completing the microscopic analysis.

2.5. *Statistical analysis*

The statistical methods used were descriptive statistics of mean, standard deviation and analysis of variance of the groups used in the experiment. Pairwise multiple comparisons of individual means of different groups were done to compare the controls, +UWBR and −UWBR exposures, and MMC group for sacrifice times at 18 and 24 h. Residuals were analysed to determine whether the best skewness and kurtosis were with the raw data or the usual transformations for small percentages and for small frequency counts (Zar 1974). In addition, deleted residuals versus raw residuals were plotted to verify that no one observation had undue influence on the results. A final plot of residuals versus predicted values was used to verify normality of distribution, homogeneity of variance and lack of outliers, yielding a valid analysis.

3. Results

The mean percentages of PCE and the average incidence of MN per 2000 PCE for the mice in the control, +UWBR/−UWBR-exposed and positive control groups (killed at 18 and 24 h) are shown in table 1.

3.1. *Peripheral blood*

The percentages of PCE in the control, +UWBR and −UWBR mice killed at 18 and 24 h were all within the range of 3.1 ± 0.14 to 3.2 ± 0.23 ($p = 0.1326$ for the overall effect of UWBR). The positive control mice injected with MMC exhibited decreased percentages of PCE when killed at 18 h (2.9 ± 0.14) and at 24 h (2.6 ± 0.17).

The frequencies of MN per 2000 PCE in control mice killed at 18 and 24 h were 8.3 ± 3.30 and 9.2 ± 2.68, respectively. The indices for MN per 2000 PCE in +UWBR and −UWBR-exposed mice killed at 18 and 24 h were similar, ranging from 7.7 ± 2.00

Table 1. The percentages of polychromatic erythrocytes (PCE) and the incidence of micronuclei (MN) in the peripheral blood and bone marrow cells of mice exposed to ultra-wideband electromagnetic radiation (UWBR) for 15 min.

Group	Group mean* % PCE (±SD)	Group mean MN per 2000 PCE (±SD)
Peripheral blood		
Mice sacrificed at 18 h after UWBR exposure		
Controls	3.1 (0.17)	8.3 (3.30)
UWBR−	3.2 (0.23)	7.7 (2.00)
UWBR+	3.1 (0.17)	9.7 (2.54)
Mitomycin C	2.9 (0.14)	99.2 (3.31)
Mice sacrificed at 24 h after UWBR exposure		
Controls	3.1 (0.14)	9.2 (2.68)
UWBR−	3.2 (0.23)	8.8 (2.20)
UWBR+	3.1 (0.20)	9.4 (2.88)
Mitomycin C	2.6 (0.17)	107.3 (8.07)
Bone marrow		
Mice sacrificed at 18 h after UWBR exposure		
Controls	49.0 (3.56)	8.8 (2.06)
UWBR−	51.4 (3.04)	7.4 (2.32)
UWBR+	51.2 (2.61)	8.7 (2.00)
Mitomycin C	44.6 (3.07)	102.7 (9.09)
Mice sacrificed at 24 h after UWBR exposure		
Controls	52.3 (4.02)	9.8 (2.86)
UWBR−	50.5 (3.55)	8.1 (2.28)
UWBR+	50.0 (1.42)	10.0 (3.27)
Mitomycin C	42.3 (2.14)	114.8 (14.88)

* For each mouse, 1000 consecutive erythrocytes in the peripheral blood and 200 consecutive erythrocytes in the bone marrow were examined.

to 9.7±2.54 (p=0.0975 for the overall effect of UWBR). The positive control mice treated with MMC exhibited a significantly increased incidence of MN per 2000 PCE when killed at both 18 h (99.2±3.31) and 24 h (107.3±8.07) (p=0.0001).

3.2. *Bone marrow*

The percentages of PCE in control mice killed at 18 and 24 h were 49.0±3.56 and 52.3±4.02, respectively. In +UWBR and −UWBR-exposed mice, the percentage of PCE (at both times of sacrifice) ranged between 50.0±1.42 and 51.4±3.04 (p=0.705 for the overall effect of UWBR). The positive control mice exhibited a decrease in the percentage of PCE when killed at 18 h (44.6±3.07) and at 24 h (42.3±2.14).

The frequencies of MN per 2000 PCE in control mice killed at 18 and 24 h were 8.8±2.06 and 9.8±2.86, respectively. The indices for MN per 2000 PCE in +UWBR and −UWBR-exposed mice terminated at 18 and 24 h ranged between 7.4±2.32 and 10.0±3.27 (p=0.072 for the overall effect of UWBR). The positive control mice treated with MMC exhibited significantly increased frequencies of MN per 2000 PCE when killed at both 18 h (102.7±9.09) and at 24 h (114.8±14.88) (p= 0.0001).

4. Discussion

In mammals, during erythroblastosis, for a still unknown reason, the main nucleus is expelled and lagging chromosomal fragments and/or whole chromosomes that are not incorporated into daughter nuclei during cell division persist as easily recognizable micronuclei in immature erythrocytes (PCE). The first appearance of MN in PCE occurs 10–12 h after a clastogenic exposure. This lag period results from the time required for the erythroblast to divide, to expel its main nucleus to become the polychromatic erythrocyte, and any mitotic delay induced by the genotoxic agent (Heddle *et al.* 1984). Once induced, the MN persists in the PCE for about 30 h (Jenssen and Ramel 1978). Hence, the clastogenic and/or aneugenic effect of a given treatment can be detected at any point during this time interval (Heddle *et al.* 1984). The main requirement of the treatment and/or sampling schedule is to obtain at least one sample at or near to the time of the maximum incidence of micronucleated PCE (MacGregor *et al.* 1987). In the present study, peripheral blood and bone marrow cells were examined at 18 and 24 h following UWBR exposure.

There were no significant differences in the percentage of PCE between the controls and the +UWBR and −UWBR-exposed mice, and this indicates that the time required for nucleated erythropoietic cells to become PCE is not altered by *in vivo* exposure of mice to +UWBR and −UWBR used in this study; a marked reduction in the frequency of PCE would have indicated that the division and maturation of the nucleated erythropoietic cells had been inhibited (MacGregor *et al.* 1987).

The incidence of MN observed in the bone marrow cells of control mice was comparable with values reported earlier for adult CF-1 mice (average of 4 MN per 1000 PCE) (Okine *et al.* 1983). The influence of UWBR exposure on the incidence of MN per 2000 PCE in both the peripheral blood and bone marrow cells determined by pairwise analysis did not indicate significant differences between control and +UWBR and −UWBR-exposed mice. In recently published genetoxicity investigations, Pakhomova *et al.* (1997) observed no significant difference in the occurrence of chromosome recombinations, mutations and abnormal colonies (i.e. mitotic crossovers, segregations, revertants and convertants) between the UWBR-exposed and sham-exposed D7 strain of yeast *Saccharomyces cerevisiae*; in that study, the UWBR exposure was for 30 min, with a pulse repetition rate of 16–600 Hz, a pulse duration of 1.01–1.02 ns and a pulse rise time of 164–166 ps. This gives a bandwidth of 190% (Foster *et al.* 1995) and a peak electric field strength of 101–104 kV m^{-1}. In a subsequent paper, the same authors reported no significant effect of similar UWBR exposure on the incidence of ultraviolet light- (UV; 2.25 J m^{-2} s^{-1} and a total exposure of 100 J m^{-2}) induced reciprocal and non-reciprocal recombination or mutagenesis, or on UV-induced cytotoxicity (Pakhomova *et al.* 1998).

Earlier investigations in rats, mice and monkeys exposed to UWBR did not demonstrate any altered physiological responses. Walters *et al.* (1995) reported no significant differences in a swimming performance test, in blood chemistry, or in the expression of c-fos protein in brain cells, between control rats and those exposed to UWBR for 2 min (pulse repetition rate 60 Hz, pulse duration 7–8 ns, bandwidth 0.25–2.5 GHz, peak E-field strength 250 kV m^{-1}, and far field equivalent peak power density of 1.7×10^9 W cm^{-2}). In a recent report, Jauchem *et al.* (1997) indicated no significant differences in heart rate and arterial blood pressure between UWBR-exposed (pulse repetition rate 1 kHz, pulse rise time 300 ps and E-field strength 21 kV m^{-1}) and control rats. Sherry *et al.* (1995) exposed six monkeys to UWBR for 2 min (pulse frequency 60 Hz, pulse duration 5–10 ns, a total of 7200 pulses, bandwidth

100 MHz to 1.5 GHz, peak E-field strength of 250 kV m^{-1}, and a whole-body SAR calculated to be 0.5 mW kg^{-1}). Each monkey was exposed to UWBR twice, with an interval of 6 days between exposures. The mean primate equilibrium platform performance for all monkeys after UWBR exposure was not different from that observed before each UWBR exposure. Seaman *et al.* (1998) reported that exposure of mice to UWBR for 30 min (60–600 pulses per second, pulse duration 1.0 ns, rise time 200 ps, pulse amplitude 100 kV m^{-1} and a calculated bandwidth of 184.3% (Foster *et al.* 1995)) did not result in significant changes in normal or morphine-induced nociception and locomotor activity. In contrast, an *in vitro* exposure of murine macrophages to UWBR (with similar exposure conditions), under certain conditions of macrophage stimulation, resulted in an increase in the production of nitric oxide (Seaman *et al.* 1996).

The results from this investigation did not indicate excess genotoxicity in both peripheral blood and bone marrow cells of mice exposed to UWBR for 15 min.

Acknowledgements

This work was supported by the United States Army Medical Research and Material Command under contract DAMD17-94-C-4069 awarded to McKesson BioServices, and by the United States Air Force Office of Scientific Research grant No. F49620-95-1-0337. The authors thank T.-S. Lu for discussions on the estimate of SAR and and W. D. Hurt for SAR calculation.

The views, opinions and/or findings contained in this report are those of the authors and should not be construed as an official Department of the Army position, policy or decision unless so designated by other documentation.

In conducting the research using animals, the investigator(s) have adhered to the 'Guide for the Care and Use of Laboratory Animals' prepared by the Committee on Care and Use of Laboratory Animals of the Institute of Laboratory Animal Resources, National Research Council (NIH Publication # 86-23, Rev. 1985).

References

Albanese, R., Blaschak, J., Medina, R. and Penn, J., 1994, Ultrashort elecromagnetic signals: biophysical questions, safety issues, and medical opportunities. *Aviation Space and Environmental Medicine*, **65,** A116–A120.

Auletta, A. E., Dearfield, K. L. and Cimino, M. C., 1993, Mutagenicity test schemes and guidelines: US EPA Office of Pollution Prevention and Office of Pesticide Programs. *Environmental and Molecular Mutagenesis*, **21,** 38–45.

Bao, J.-H., 1997, Picosecond domain electromagnetic pulse measurements in an exposure facility: an error compensation routine using deconvolution techniques. *Review of Scientific Instruments*, **68,** 2221–2227.

Durney, C. H., Massoudi, H. and Iskander, M. F., 1986, *Radiofrequency Radiation Handbook*, 4th edition, Report TR-85-73 (San Antonio, TX: USAF School of Aerospace Medicine, Brooks Air Force Base).

Foster, P. R., Halsey, J. D. and Hussain, G. M., 1995, Ultra-wideband antenna technology. In *Introduction to Ultra-Wideband Radar Systems*, edited by J. D. Taylor (Boca Raton, FL: CRC Press), pp. 145–286.

Fuerer, D., 1991, Electronic countermeasures in wideband spectrum systems. In *Propagation Limitations for Systems Using Band Spreading*, (Neuilly Sur Seine: AGARD) LS-172, pp. 1–11.

Health Protection Branch Genotoxicity Committee (Canada), 1993, The assessment of mutagenicity: Health Protection Branch Mutagenicity Guidelines. *Environmental and Molecular Mutagenesis*, **21,** 15–37.

Heddle, J. A., Stuart, E. and Salamone, M. F., 1984, The bone marrow micronucleus test. In *Handbook of Mutagenicity Test Procedures*, edited by B. J. Kilbey, M. Legator, W. Nichols and C. Ramel (Amsterdam: Elsevier), pp. 441–457.

Jauchem, J. R., Frei, M. R., Ryan, K. L., Merritt, J. H. and Murphy, M. R., 1997, Lack of effects on heart rate and blood pressure in ketamine-anesthetized rats briefly exposed to ultrawideband electromagentic pulses. *IEEE Transactions on Biomedical Engineering* (in press).

Jenssen, D. and Ramel, C., 1978, Factors affecting the induction of micronuclei at low doses of X-rays, MMS and dimethylnitrosamine in mouse erythroblasts. *Mutation Research*, **58,** 51–65.

Kirkland, D. J., 1993, Genetic toxicology testing requirements: official and unofficial views from Europe. *Environmental and Molecular Mutagenesis*, **21,** 8–14.

MacGregor, J. T., Heddle, J. A., Hite, M., Margolin, B. H., Ramel, C., Salamone, M. F., Tice, R. R. and Wild, D., 1987, Guidelines for the conduct of micronucleus assays in mammalian bone marrow erythrocytes. *Mutation Research*, **189,** 103–112.

Merritt, J. H., Kiel, J. L. and Hurt, W. D., 1995, Considerations for human exposure standards for fast-rise-time high-peak-power electromagnetic pulses. *Aviation Space and Environmental Medicine*, **66,** 586–589.

Okine, L. K. N., Ioannides, C. and Parke, D. V., 1983, Studies on the possible mutagenicity of b-adrenergic blocker drugs. *Toxicology Letters*, **16,** 167–174.

Pakhomova, O. N., Belt, M. L., Mathur, S. P., Lee, J. C. and Akyel, Y., 1997, Lack of genetic effects of ultrawide-band electromagnetic radiation in yeast. *Electro- and Magnetobiology*, **16,** 195–201.

Pakhomova, O. N., Belt, M. L., Mathur, S. P., Lee, J. C. and Akyel, Y., 1998, Ultra-wide band electromagnetic radiation does not affect UV-induced recombination and mutagenesis in yeast. *Bioelectromagnetics*, **19,** 128–131.

Seaman, R. L., Belt, M. L., Doyle, J. M. and Mathur, S. P., 1998, Ultra-wideband electromagnetic pulses and morphine-induced changes in nociception and activity in mice. *Physiology and Behavior* (in press).

Seaman, R. L., Kiel, J. L., Parker, J. E., Grubbs, T. R. and Prol, H. K., 1996, Effects of ultra-wide-band pulses on nitric oxide production in murine macrophages. *Eighteenth*

Annual Meeting of The Bioelectromagnetics Society (Frederick, MD, The Bioelectromagnetic Society), p. 213.

SHERRY, C. J., BLICK, D. W., WALTERS, T. J., BROWN, G. C. and MURPHY, M. R., 1995, Lack of behavioral effects in non-human primates after exposure to ultrawideband electromagnetic radiation in the microwave frequency range. *Radiation Research*, **143,** 93–97.

SOFUNI, T., 1993, Japanese guidelines for mutagenicity testing. *Environmental and Molecular Mutagenesis*, **21,** 2–7.

TAYLOR, J. D., 1991, Ultrawideband radar. *IEEE International Microwaves Symposium Digest*, **MTT-S-1,** 367–370.

TOEVS, J. W., SMITH, D. R., BYRNE, D. P. and ROSS, G. F., 1992, UWB radar for ground vehicle self protection. *IEEE International Microwaves Symposium Digest*, **MTT-S-3,** 1492–1494.

WALTERS, T. J., MASON, P. A., SHERRY, C. J., STEFFEN, C. and MERRITT, J. H., 1995, No detectable bioeffects following acute exposure to high peak power ultra-wide band electromagnetic radiation in rats. *Aviation Space and Environmental Medicine*, **66,** 562–567.

ZAR, J. H., 1974, *Biostatistical Analysis* (Englewood Cliffs, NJ: Prentice Hall).

ELECTRO- AND MAGNETOBIOLOGY, 17(2), 115–125 (1998)

A PILOT STUDY OF THE MILLIMETER-WAVELENGTH RADIATION EFFECT ON SYNAPTIC TRANSMISSION

Andrei G. Pakhomov, H. Kenneth Prol, and Yahya Akyel
McKesson BioServices
Microwave Bioeffects Branch
U.S. Army Medical Research Detachment of the
Walter Reed Army Institute of Research
Brooks Air Force Base
San Antonio, Texas 78235-5324

ABSTRACT

Effects of 41.34 GHz millimeter waves (MMWs) were studied in the isolated hemisected frog spinal cord preparation. The purpose of the work was to establish whether MMW irradiation alters conduction in a polysynaptic pathway from dorsal root (DR) afferent fibers to efferents of the respective ventral root (VR). After isolating and placement of the cord in the exposure bath, the DR_{IX} or DR_X was stimulated with single supramaximal pulses every 30 s. Experiments began after 30–160 min of stabilization and lasted for 65 min, without any changes or interruptions of the stimulation routine. Each experiment included two identical 5-min MMW exposures (2.8 mW/cm^2, at 25 and 50 min into the experiment). During the rest of the time the preparation was sham exposed. VR responses to the DR stimulation (DR-VRRs) represented a variable polyphasic wave with a latency of 8–15 ms, 0.5–3 mV peak amplitude, and 30–70 ms duration. All DR-VRRs recorded during the experiment were stored for automated

The use of animals in this study was in compliance with the Animal Welfare Act and other federal statutes and regulations relating to animals and experiments involving animals, and adhered to the principles stated in the Guide for the Care and Use of Laboratory Animals, NIH publication 85-23. The animal use protocol, No. AD4002, has been approved by the Armstrong Laboratory Animal Care and Use Committee.

Address correspondence to: Dr. A. Pakhomov, USA-MCMR, U.S. Army Medical Research Detachment, 8308 Hawks Road, Building 1168, Brooks Air Force Base, San Antonio, TX 78235-5324. Fax: (210) 536-5382. E-mail: pakhomov@netxpress.com

Copyright © 1998 by Marcel Dekker, Inc. **www.dekker.com**

analysis of spontaneous (unforced) waveform changes and MMW-induced changes. For the entire studied group of 13 preparations, the first MMW irradiation increased the waveform changes by 14% ($p < .02$ compared with the preceding sham exposure). Of this group, 9 preparations with the most pronounced reaction to the first MMW exposure had no reaction to the second exposure. In contrast, the other 4 preparations with subtle or no effect of the first exposure reacted strongly to the second exposure. The difference in the effect of two consequent and identical MMW exposures infers that this effect was not caused by MMW heating and involved regulatory physiological mechanisms, such as adaptation and sensitization.

INTRODUCTION

Until now, effects of low-intensity millimeter waves (MMWs, 30–300 GHz frequency range) have been studied in a limited number of excitable tissue preparations, i.e., isolated peripheral nerves (1–5), striated muscle and heart pacemaker (5), crayfish stretch receptor (6), and snail neurons (7). The present work is the first attempt to study MMW effects on key processes of interneuronal interaction, namely on the conduction of excitation in a polysynaptic pathway from primary afferents to motoneurons in the amphibian spinal cord.

This preparation offers a unique combination of features essential for this type of research. The highly organized neuronal circuitry of the spinal cord allows one to study virtually any known neuron function, including mono- and polysynaptic conduction via chemical and electrical synapses, pre- and postsynaptic inhibition, spatial and temporal summation, synaptic plasticity phenomena, and pacemaker activity. During exposure of the spinal cord to MMWs the roots and recording electrodes can be shielded from the radiation, which is very important for providing artifact-free conditions. The isolated frog spinal cord has good performance and viability *in vitro*, along with an appropriate size and shape for experiments with MMW, which do not penetrate deep into biological tissues. Most morphological and biochemical correlates of spinal cord electrical activity are known in great detail [see Kudo (8) for review], thus providing opportunities for understanding physiological mechanisms of MMW effects, if any are observed.

However, experimentation with the isolated spinal cord is quite laborious. Therefore, the present study was intended only to reveal possible MMW effects and to define adequate exposure techniques and biopotential analysis procedures for future studies.

Previously, we established that MMW irradiation of an isolated nerve preparation can significantly alter its ability to sustain a high-rate electrical stimulation (3,4). Among tested frequencies of the radiation, the frequency of 41.34 GHz (7.25-mm wavelength) was the most effective, and was therefore chosen for the spinal cord experiments.

MATERIALS AND METHODS

Spinal Cord Preparation and Data Acquisition

Experiments were performed on an isolated and hemisected spinal cord of the bullfrog *Rana catesbeiana* (1). Active adult frogs were kept in vivarium conditions

(22–25°C, 30–70% relative humidity, 12 h light/12 h dark diurnal light cycle) for at least 1 week prior to experiments. Animals were chilled for 15–20 min on ice and immobilized by mechanical destruction of the brain. The spinal cord was approached by a dorsal laminectomy and cut at the level of the upper thoracic segments. Dorsal and ventral roots (DR and VR) of segments IX and/or X needed for electrophysiological recording were cut as far from the cord as possible; all other roots were cut close to the cord. The cord was carefully removed from the vertebral column and placed in chilled Ringer's solution (NaCl 114; KCl 2.0; $NaHCO_3$ 2.0; $CaCl_2$ 1.8; glucose 5.5 (mM); pH 7.4–7.6). The solution was supplemented with hydrogen peroxide (0.004%) to improve tissue oxygenation and viability of the preparation *in vitro* (9). After a sagittal hemisection, one part of the cord was transferred to the exposure bath and laid lateral side downward. The roots were extended upward along the walls of the bath and put in contact with bipolar stimulating and recording electrodes. The electrodes were made of thin gold wire and permanently mounted on the walls of the bath.

The exposure bath was designed to keep the preparation viable for a long period (hours), and to enable artifact-free root stimulation and biopotential recording during MMW irradiation, which was performed from underneath, through the 0.5-mm-thick Plexiglas bottom of the bath. The spinal cord was continuously superfused, at a rate of 2.7 ml/min, with Ringer's solution chilled to 9–10°C. The solution layer above the cord was 1.5–2 mm thick, and the distal parts of the roots extending upward from the solution to the electrodes were covered with a mixture of petroleum jelly and mineral oil to prevent them from drying.

Special care was taken to avoid formation of any saline gap between the cord and the bottom of the chamber, which could strongly attenuate the MMW radiation. For this purpose, the area of segments IX and X of the cord was gently pressed down to the bottom of the bath with the help of a micromanipulator-driven plastic holder. In contrast, the roots in the area of their contact with electrodes were shielded from the radiation by the cord itself and the saline layer above it.

The electrodes were connected to a Grass Instruments Stimulator S8800 (USA) and BIOPAC Systems MP100 electrophysiological data acquisition system (USA). After positioning of the cord in the exposure bath, supramaximal electrical stimuli were applied to one of the DR (20–30 V, 0.6 ms width, 1 pulse per 30 s). If, for any reason (such as damage during isolation), this stimulation did not evoke VR responses (DR-VRRs), or if they were too weak, the stimulation was switched to the other DR. With the DR stimulation continuing, the preparation was left to stabilize for 30–160 min before the onset of the experiment. The stimulation routine was not altered or interrupted before completion of the entire experiment.

It should be emphasized that the only difference between the stabilization period and the experiment itself was that during stabilization we recorded DR-VRRs on the monitor, and during the experiment we also stored the records for subsequent analysis. In other words, there was no "signal" to the preparation by which it could recognize when the experiment actually began. We intentionally varied the duration of the stabilization period in order to avoid any specific timing between spinal cord isolation, onset of stimulation, and MMW exposures performed during the experiment.

Each successful spinal cord preparation was used in only a single experiment, which lasted for 65 min; for the convenience of data processing, this period was conditionally divided into 13 intervals of 5 min each. Two identical 5-min MMW exposures (2.8 mW/cm^2, 41.34 GHz) were performed during the 6th and the 10th intervals (25 and

50 min into the experiment); for the remainder of the time the preparation was sham-exposed. For the sham exposure, the waveguide attenuators were tuned to maximum (about 80 dB field attenuation), while the MMW generator and all other devices remained turned on. Switching from sham to MMW irradiation conditions was performed by rotation of attenuator control knobs, and was not accompanied by any vibrations, noise, or changes in the power frequency (60 Hz) fields.

During each 5-min interval, 10 DR-VRRs were recorded, stored, and measured. The measurements included latency, peak-to-peak and maximum amplitude, standard deviation of the amplitude (SDA), and subtended area of the DR-VRR signal. (The SDA is a measure of the instant amplitude variation during the course of the DR-VRR. In this respect, it is a characteristic of the signal shape, and has no relation to and should not be confused with statistical analysis of data.) All these parameters, excluding latency, were measured automatically by the MP100 software for the period between 10 and 60 ms after DR stimulation. In addition, a special method of analysis was applied to quantify changes in the DR-VRR waveform during the experiment (see the Results and Discussion section).

The measurement data were plotted against the time from the onset of the experiment and analyzed both directly (without any normalization or averaging), then with averaging for the 5-min intervals in each experiment, and with normalization and averaging for the entire group of preparations. Statistical analysis of differences in DR-VRRs recorded during MMW and sham-exposure intervals was done with a 2-tailed Student's t test and χ^2 test. Although the experimental conditions were not double-blind, the complete automatization of the stimulation, recording, storage of the records, and measurement procedures excluded any subjective impact of the experimenter on the results.

Irradiation and Dosimetry

The MMW exposure equipment, methods of dosimetry, and field mapping were described in detail in our previous publications (3,4). The microwave power generator (model G4-141, Russia) operated in a continuous-wave regimen at a frequency of 41.34 GHz. The output waveguide line terminated in a tapered dielectric rod antenna positioned vertically under the exposure bath; the bottom of the bath was 25 mm above the tip of the rod. At this distance, the field was virtually uniform, with the maximum (2.8 mW/cm^2) on the axis of the antenna. The field intensity decrease within a 5-mm radius from the axis of the antenna did not exceed 2 dB, while the exposed segment of the spinal cord was less than 2 mm wide and 4–6 mm long. The E-field was aligned with the long axis of the cord. Exact radiation frequency and net input power to the irradiating antenna were monitored through a bidirectional coupler, using an EIP model 548A frequency counter and M3-21 wattmeter (Russia). Fluctuations of the radiation frequency and intensity from one experiment to another did not exceed 2 MHz and 10%, respectively.

The temperature of the Ringer's solution at the outflow port of the exposure bath was monitored with a Luxtron Instruments model 850 multichannel fluoroptic thermometer. Within the accuracy of about 0.2°C, these measurements demonstrated no temperature changes during MMW exposures.

RESULTS AND DISCUSSION

A total of 13 experiments were performed, and 1690 DR-VRR records were analyzed. In most of the preparations, DR-VRR represented a variable polyphasic wave with a latency of 8–15 ms, 0.5–3 mV peak amplitude, and 30–70 ms duration. Figure 1 shows original DR-VRRs recorded before, during, and after the first MMW exposure in two different preparations. In these two experiments, as well as in the other ones, the irradiation caused no readily visible effects: the amplitude and shape of the biopotentials fluctuated within the same limits as without exposure, and the latency stayed quite stable throughout the experiment.

Usually, measured values of DR-VRR amplitude, SDA, and subtended area varied substantially from one stimulus to another. Nevertheless, in some preparations the data averaged for 5-min intervals showed a significant change during MMW irradiation, such as illustrated in Figure 2A. In this preparation, the first irradiation significantly decreased DR-VRR amplitude, SDA, and area as compared with the previous interval of sham exposure ($p < .01$). However, consecutive intervals of sham

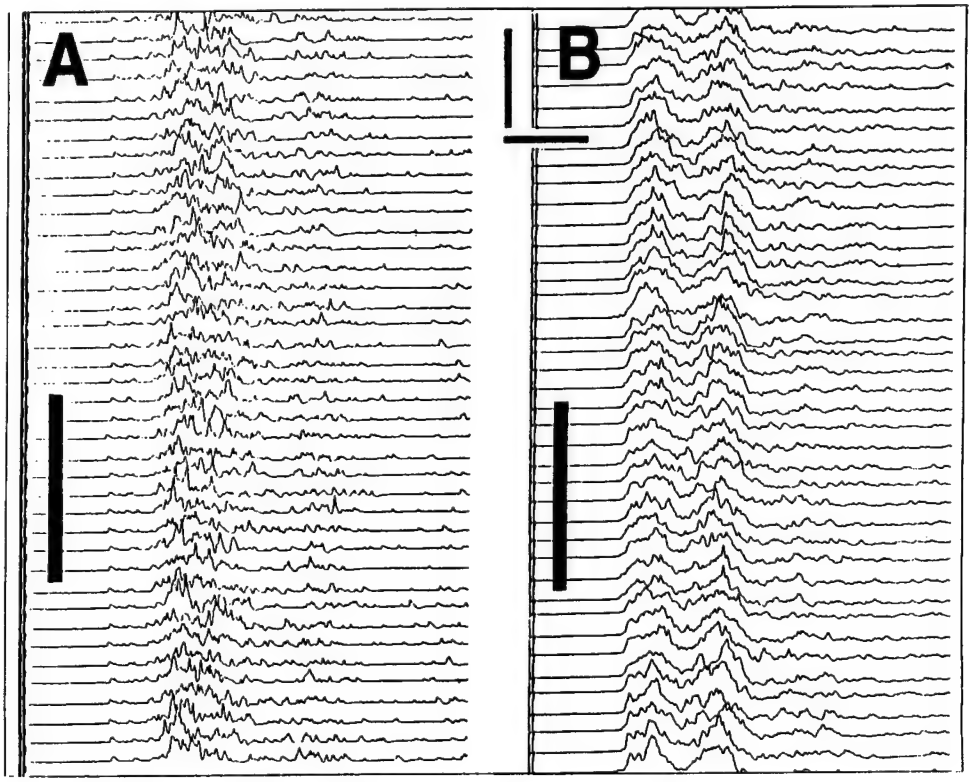

FIGURE 1. Sequential records (from top to bottom) of the ventral root (VR) discharges in two isolated spinal cord preparations (A and B). The discharges are evoked every 30 s by stimulation of the respective dorsal root (DR). Periods of millimeter wave (MMW) irradiation (41.34 GHz, 2.8 mW/cm^2 for 5 min) are shown by vertical black bars. Calibration: 10 ms, 3 mV (A); and 10 ms, 6 mV (B).

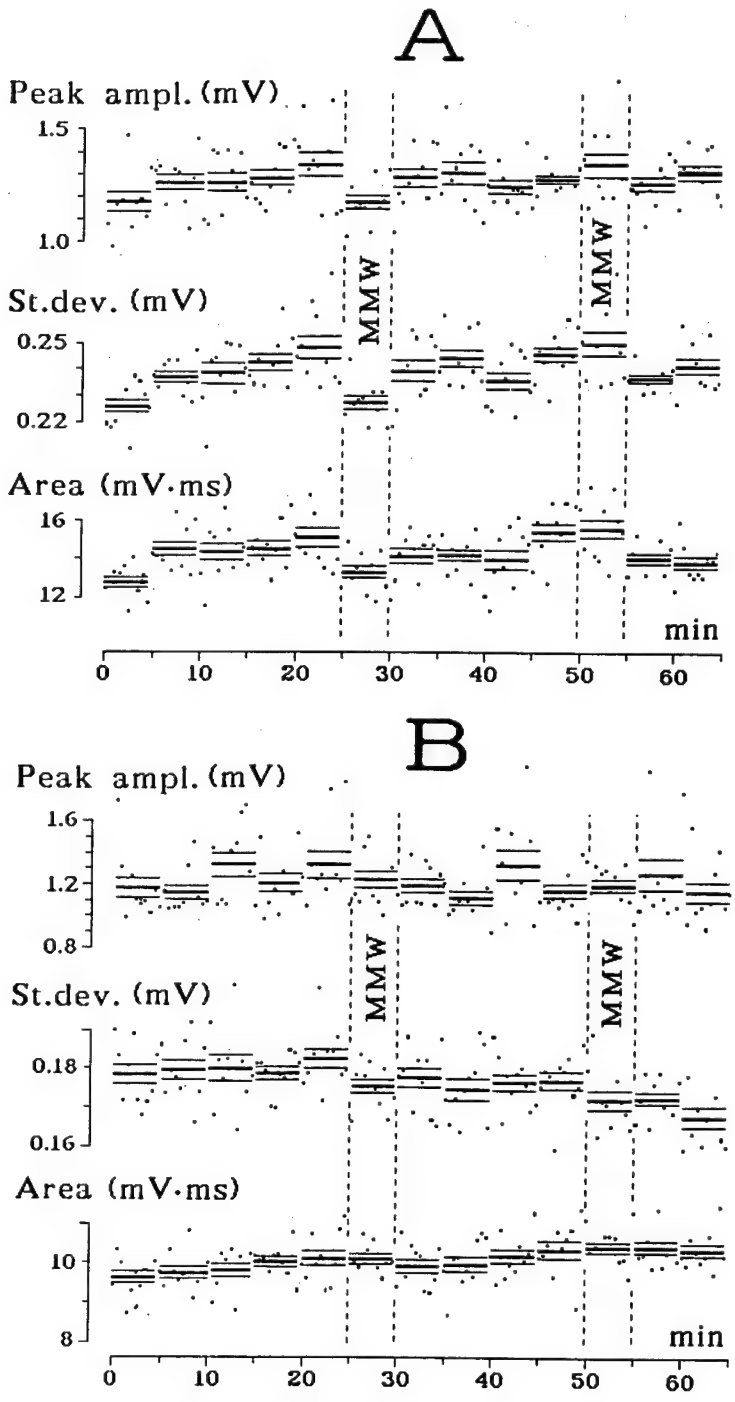

FIGURE 2. Effect of millimeter wave (MMW) irradiation on the area, peak amplitude, and standard deviation of the amplitude of ventral root responses to dorsal root stimulation (DR-VRRs). (A and B) Two different spinal-cord preparations. The dorsal root is stimulated every 30 s. Black dots indicate the original measured values of the parameters of each DR-VRR. Horizontal bars are the same values averaged for 5-min intervals (mean ± SE, n = 10). MMW exposures lasted from 25 to 30 min of the experiment, and from 50 to 55 min; the rest of the time the preparations were sham exposed.

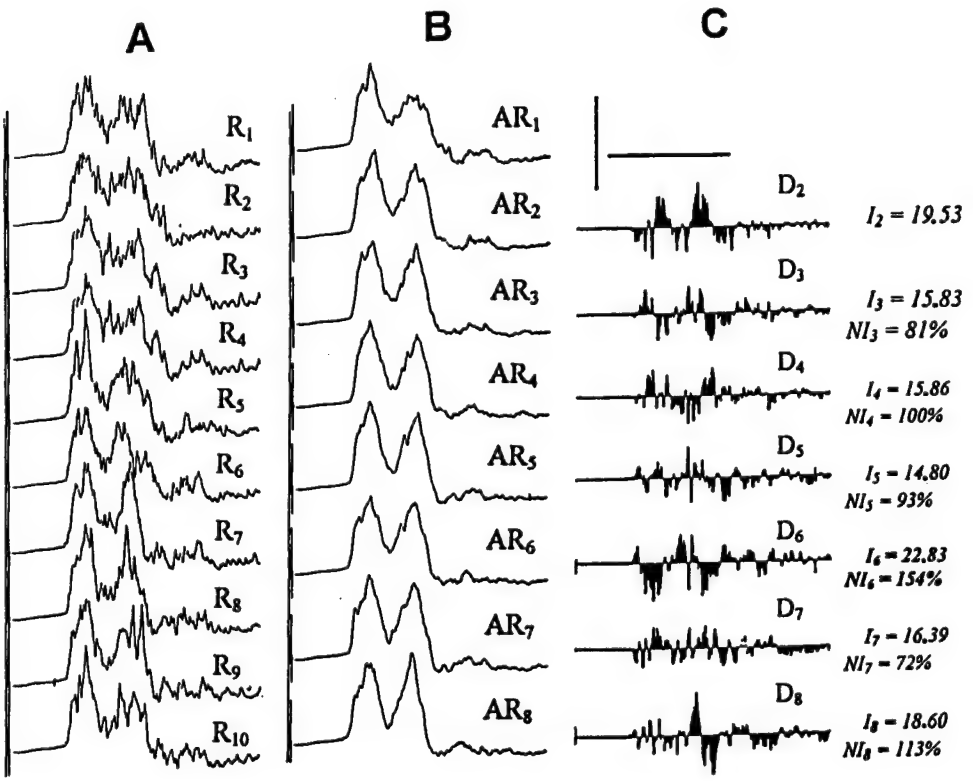

FIGURE 3. Illustration of the waveform data processing procedure. (A) Original records of ventral root responses to dorsal root stimulation (DR-VRR) taken every 30 s during the first 5-min interval (R_1, R_2, . . ., R_{10}). (B) DR-VRR records accumulated for sequential 5-min intervals (AR_n). AR_1 is a sum of waveforms R_1 through R_{10}, AR_2 is a sum of waveforms R_{11} through R_{20} (not shown), and so forth. (C) Difference (D_n) in sequential AR signals ($D_n = AR_n - AR_{n-1}$). I_n is the tracing integral of D_n (the area between the trace and the zero line, regardless of the sign, in mV • ms). NI_n is the normalized value of the total integral ($NI_n = 100\% I_n/I_{n-1}$). See text for further explanation. AR_6, D_6, I_6, and NI_6 correspond to the first millimeter-wave (MMW) exposure (records for the second exposure are not shown); all other records are for sham exposures. Calibration: 100 ms for all the fragments, 2 mV for A, 20 mV for B, and 10 mV for C.

exposure occasionally could also differ from each other (e.g., the first and second intervals in Fig. 2A), and some spinal cord preparations showed virtually no response to MMW (Fig. 2B).

Among the observed changes, the decrease in SDA due to the first exposure was the most consistent: It was statistically significant in the first 6 experiments performed, but, for unknown reasons, weakened or disappeared in the next experiments. Although these observations could not be taken as a proof of the MMW effect, they suggested that the measured DR-VRR parameters were not always adequate to reveal this effect. DR-VRR is a complex signal, produced by polysynaptic transmission from primary afferents to motoneurons and summation of excitation on the motoneurons; it is never

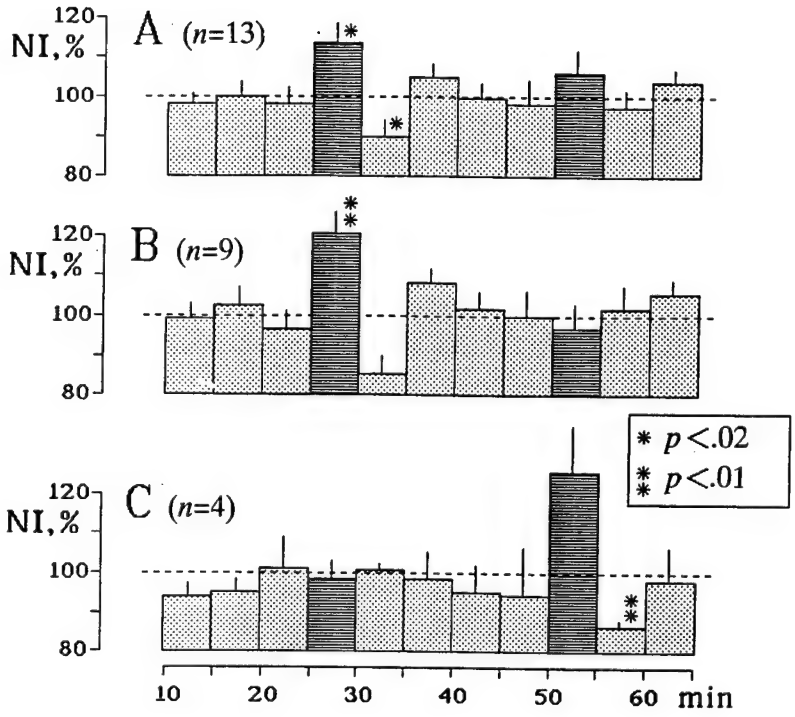

FIGURE 4. Millimeter wave (MMW) irradiation effect on changes in the waveform of the ventral root response to dorsal root stimulation (DR-VRR). The changes are expressed by the normalized integral (NI) of differences of waveforms accumulated for 5-min intervals (see text and Figure 3 for details of NI calculation). NI values are averaged (mean ± SE) for the entire studied group (A, n = 13), preparations with a pronounced response to the first exposure (B, n = 9), and for the remaining 4 preparations (C, n = 4). Periods corresponding to MMW exposures are outlined by a different shading (25–30 min and 50–55 min).

the same in shape, amplitude, or time course in any two spinal cord preparations. Depending on the DR-VRR particulars in each individual preparation, the MMW effect may or may not show up as changes in amplitude, area, or SDA. Then, demonstration of the MMW effect (if any) requires a different analysis procedure sensitive to any changes in the DR-VRR waveform, and also able to quantify them. This analysis was accomplished by using special waveform math and processing features included in the MP100 system software.

The waveform processing method employed is illustrated in Figure 3. First, all DR-VRR records within each 5-min interval were summed together, thus yielding one "accumulated" waveform for each interval (AR_1, AR_2, ..., AR_n, where n is the number of the 5-min interval, from 1 to 13). To evaluate the difference (D_n) between the sequential accumulated waveforms, they were subtracted from each other ($D_n = AR_n - AR_{n-1}$), yielding twelve D_n traces (from 2 to 13). One should note that this was a "geometrical" subtraction, i.e., one entire waveform was subtracted from another (this is principally different from subtraction of, say, peak amplitudes or subtended areas of the signal). The difference D_n was quantified by an automated measurement of the

tracing integral (I_n), which is the total area between the zero line and the D_n trace (regardless of the sign).

By this procedure, any alteration in the DR-VRR time course, shape, amplitude, etc., within a 5-min interval as compared with the previous 5-min interval is detected and quantified as I_n. Due to natural fluctuations of the DR-VRR, I_n is always a positive number. The MMW effect, if present, can be detected as an additional increase in I_n compared to the I_n in the preceding intervals of sham exposure.

For convenience of comparison of I_n in different preparations, we used the normalized integral (NI), which was calculated as: $NI_n = 100\% (I_n/I_{n-1})$. Obviously, if changes in the waveform during a given 5-min interval are equal to those during the previous interval, then NI = 100%. If for any reason the changes increase, the NI increases as well, and vice versa. One should note that for 13 analyzed intervals (1 to 13), this processing gives 12 I_n values (2 to 13) and 11 NI_n values (3 to 13).

The NI values, averaged for the entire group of 13 spinal cord preparations, are presented in Figure 4A. Before MMW exposure, NI showed only minor fluctuations and stayed virtually at 100%. The first MMW irradiation caused a pronounced and highly significant ($p < .02$) increase in NI, testifying that MMWs affected the function of the preparations. This effect was followed by a decrease in NI (perhaps only because the high I_n value from the previous interval with MMW exposure now was in the denominator for NI calculation), and stabilization at about 100%. The second MMW irradiation did not produce a statistically significant effect.

The next step was to find out whether this physiological effect could be attributed to MMW heating of the preparation or not. Although we observed no changes in the superfusing solution temperature, this does not mean that the temperature of the spinal cord itself also remained stable during exposure. For each particular preparation, the heating caused by the first and the second MMW exposures was exactly the same (preparations were never moved or altered in any other way from the onset of the stabilization period to the end of the entire experiment). In other words, the heating effect of the first and the second exposures was always the same, but their physiological effect was different.

Because the size of the spinal cord preparations and their position in the exposure bath could vary slightly, the MMW heating of the individual preparations could also be somewhat different. For the thermal mechanism of the MMW effect, the preparations with a greater response to the first exposure (because they were heated more than the others) should also have had a greater response to the second exposure (because the heating effect in both instances was the same). However, the actual situation proved to be the opposite.

As shown in Figure 4B, nine preparations selected for their greater response to the first MMW exposure showed no reaction to the second irradiation. And, quite unexpectedly, the remaining 4 preparations, which had a subtle or no response to the first exposure, reacted strongly to the second exposure (Fig. 4C).

This type of reaction to MMWs cannot be explained by a thermal mechanism. Earlier, we performed comprehensive studies of heating effects in the isolated frog spinal cord (10,11), as well as in other isolated preparations of excitable tissues of poikilothermic animals (4,12). In all of these preparations, a reaction to repetitive heating by 0.5–5°C depended solely on the increase in temperature, no matter how many times and how frequently the heating was done. In the present study, the pronounced difference in reactions to the first and the second MMW exposures makes a strong case

that the effect is not thermal and involves specific regulatory processes, such as adaptation and sensitization.

At this point, physiological interpretation of the established MMW effect appears exceedingly complicated. Conduction of a signal from dorsal to ventral roots in a frog spinal cord includes nerve conduction via terminals of the primary afferents, synaptic transmission (through both chemical and electrical synapses), summation of postsynaptic potentials on inter- and motoneurons, and the firing of these neurons. Any of these processes could be affected by MMWs, leading to an alteration of the motoneurons' discharge, which was detected as a change in the DR-VRR waveform. Without consistent changes in the amplitude, latency, or area of the potentials, this effect should be regarded as a mild modulation of the reflex conduction rather than its inhibition or facilitation.

An important conclusion from this study is that the effect of even a short MMW irradiation is not limited to changes taking place during this irradiation. The aftereffect of the first MMW exposure was not detectable by physiological indices, but manifested itself as a change in the sensitivity to the second exposure. Moreover, this aftereffect could be either a decrease or an increase in the sensitivity of the preparation, depending on whether the preparation responded to the first exposure or not. The possibility of this long-lasting alteration of MMW sensitivity must be taken into account in further experimentation, particularly when studying effects of prolonged or repetitive MMW exposures.

ACKNOWLEDGMENTS

The work described here was performed while A.G. Pakhomov held a National Research Council–AMRMC Research Associateship, and was supported by the U.S. Army Medical Research and Material Command under contract DAMD17-94-C-4069 awarded to McKesson BioServices. The views, opinions, and findings contained in this report are those of the authors, and should not be construed as an official Department of the Army position, policy, or decision.

REFERENCES

1. Burachas, G., and Mascoliunas, R.: Suppression of nerve action potential under the effect of millimeter waves, in *Millimeter Waves in Medicine and Biology*, N.D. Devyatkov, ed., Radioelectornica, Moscow, 168–175, 1989.
2. Sazonov A.Yu., and Rizshkova, L.V.: Effects of electromagnetic radiation of millimeter range on biological subjects of various complexity, in *Millimeter Waves in Medicine and Biology*, Digest of papers of the 10th Russian Symposium (April 1995, Moscow, Russia), IRE RAN, Moscow, 112–114, 1995.
3. Pakhomov, A.G., Prol, H.K., Mathur, S.P., Akyel, Y., and Campbell, C.B.G.: Frequency-specific effects of millimeter wavelength electromagnetic radiation in isolated nerve, Electro- Magnetobiol. *16*, 43–57, 1997.
4. Pakhomov, A.G., Prol, H.K., Mathur, S.P., Akyel, Y., and Campbell, C.B.G.: Search for frequency-specific effects of millimeter-wave radiation on isolated nerve function, Bioelectromagnetics *18*, 324–334, 1997.

5. Chernyakov, G.M., Korochkin, V.L., Babenko, A.P., and Bigdai, E.V.: Reactions of biological systems of various complexity to the action of low-level EHF radiation, in *Millimeter Waves in Medicine and Biology*, N.D. Devyatkov, ed., Radioelectronica, Moscow, 141–167, 1989.
6. Khramov, R.N., Sosunov, E.A., Koltun, S.V., Ilyasova, E.N., and Lednev, V.V.: Millimeter-wave effects on electric activity of crayfish stretch receptors, Bioelectromagnetics *12*, 203–214, 1991.
7. Alekseev, S.I., and Ziskin, M.C.: Millimeter waves thermally alter the firing rate of the *Lymnaea* pacemaker neuron, Bioelectromagnetics *18*, 89–98, 1997.
8. Kudo, Y.: The pharmacology of the amphibian spinal cord, Prog. Neurobiol. *11*, 1–78, 1978.
9. Walton, K., and Fulton, B.: Hydrogen peroxide as a source of molecular oxygen for *in vitro* mammalian CNS preparations, Brain Res. *278*, 387–393, 1983.
10. Pakhomov, A.G.: Effect of microwave irradiation and temperature on spontaneous ventral root discharges in frog spinal cord, Neurophysiology *20*, 723–728, 1988.
11. Pakhomov, A.G.: Effects of high-power microwaves on synaptic transmission in frog spinal cord, Sechenov Physiol. J. USSR *77*, 37–44, 1991.
12. Pakhomov, A.G., Dubovick, B.V., Kolupayev, V.E., and Pronkevich, A.N.: Absence of non-thermal microwave effects on the function of giant nerve fibers, J. Bioelectr. *10*, 185–203, 1991.

ERROR CORRECTION IN TRANSIENT ELECTROMAGNETIC FIELD MEASUREMENTS USING DECONVOLUTION TECHNIQUES

Jian-Zhong Bao, Jonathan C. Lee, Michael E. Belt, David D. Cox, Satnam P. Mathur, and Shin-Tsu Lu

McKesson BioServices and U.S. Army Medical Research Detachment
Brooks Air Force Base, Texas 78235

INTRODUCTION

It is difficult to make an accurate transient measurement on electromagnetic pulses in the pico-second domain because of the limitations of measurement components. In this paper, we present a two-step deconvolution routine to compensate for the measurement distortions in our short electromagnetic pulse (EMP) exposure facility for studying biological effects. As depicted in Figure 1, the facility mainly consists of a pulse generator and a GTEM cell. The measurement system includes a Tektronix SCD 5000 transient digitizer (4.5 GHz bandwidth), connection cables, and two Asymptotic Conical Dipole (ACD) D-dot (dD/dt) sensors: ACD-1(A), which is mounted on the top ground wall of the cell and utilized for real time monitoring during exposures, and ACD-1(R), which is used to map the field on the bottom ground wall of the cell where the specimens are placed.

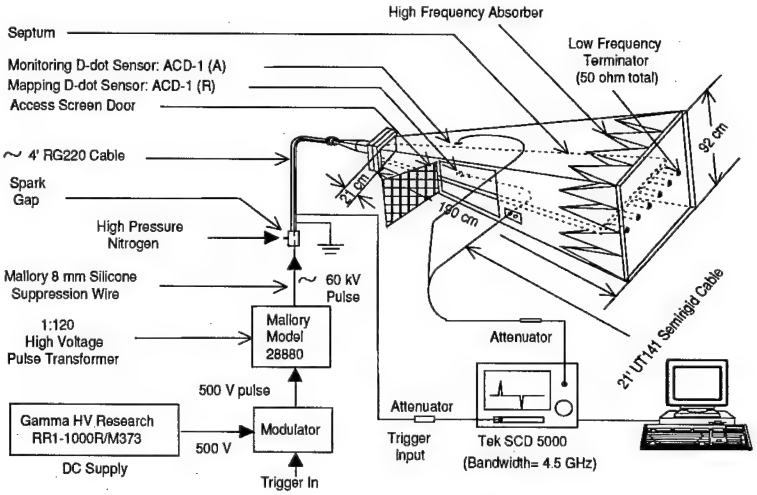

Figure 1: Short electromagnetic pulse (EMP) exposure facility and data acquisition system.

Ultra-Wideband, Short-Pulse Electromagnetics 3
Edited by Baum *et al.*, Plenum Press, New York, 1997

Because of the low-pass nature of the connection cables and the limited bandwidth of the SCD 5000, the measured signal is a distorted output of a D-dot sensor. An empirical transfer function of the cable-digitizer system is evaluated using a reference impulse generated by a Pico Second Pulse Lab (PSPL) 4050B step generator with a 5210 Impulse Forming Network (IFN) and characterized with a Tektronix CSA 803 communication signal analyzer with a SD 30 sampling head (40 GHz bandwidth). The reference impulse is injected into the connection cable at the D-dot sensor end and measured with the SCD 5000 while the cable is kept in the same position as for making D-dot measurements to ensure an in-place calibration.

Due to its right-angle structures, the ACD-1(R) gives a different output from that of ACD-1(A) to the same pulse, especially to the fast leading edge although the sensing elements for both sensors are the same. The right-angle bends in ACD-1(R) cause reflections of D-dot signals in the sensor. To correct the errors due to the reflections, we have developed a semi-empirical procedure: the impulse response of ACD-1(R) D-dot sensor is assumed as a summation of δ-function and its parameters are determined with a reference measurement using ACD-1(A) and an optimization procedure with Levenberg-Marguardt algorithm [1].

ITERATIVE CAUSAL DECONVOLUTION

By assuming that the measurement system is linear and time-invariant (LTI), we can have

$$u(t) = v(t) * h(t) + n(t) = \int_{-\infty}^{+\infty} v(\tau)h(t-\tau)d\tau + n(t), \tag{1}$$

where $u(t)$ is the measured signal, $v(t)$ is the true signal before any degradations, $h(t)$ is the system impulse response, $n(t)$ is the additive noise, and $*$ denotes convolution, which smears fast changing features in $v(t)$. Here we have an inverse problem: finding $v(t)$ from $u(t)$, $h(t)$, and $n(t)$, i.e., deconvolution, which is an ill-posed problem mathematically: small changes in $u(t)$ can be mapped into large changes in $v(t)$. This is such a serious problem that an effective noise-control procedure has to be implemented because none of the measurements are noise-free. Performing Fourier transform on Eq. (1), we get

$$U(f) = V(f)H(f) + N(f), \tag{2}$$

where upper case letters are Fourier transforms of the corresponding lower case letters, respectively, $H(f)$ is the system transfer function, and f is the frequency. Now $v(t)$ can be solved by performing inverse-Fourier transform:

$$v(t) = F^{-1}\{\frac{U(f) - N(f)}{H(f)}\}, \tag{3}$$

where F^{-1} stands for inverse Fourier transform. If we had an exact knowledge about $U(f)$, $N(f)$, and $H(f)$ in the entire frequency range, and if the measurement system, as assumed, were LTI, $v(t)$ can be recovered exactly. Unfortunately, none of the above information can be obtained exactly in practice because of the ever presence of noise and error. In general, the noise spectra $N(f)$ cannot be separated from the measured signal spectra $U(f)$ unless there are other information or assumptions available. So Eq. (3) can only be applied approximately with $U(f) - N(f) \approx U(f)$. To minimize the error due to $N(f)$ in the least square sense, we applied a Wiener filter[1]: $\Phi(f) = 1 - \mid N(f) \mid^2 / \mid U(f) \mid^2$. If we assume that the power spectra of noise $\mid N(f) \mid^2$ with a D-dot signal excitation is the same as that after the excitation, we can obtain it from a measurement in a time window of the same size that is remote after the excitation. In this study, all the waveforms were sampled with 1024 points in a 10 ns window, which gives a maximum frequency of 51.15 GHz, and are the average of 200 waveforms to remove random noises and increase the signal-to-noise ratio. All the raw data was pre-treated before applying the Fast Fourier Transform (FFT). The pre-treatment

includes subtracting baseline offset, converting attenuator factor, zero-padding to avoid aliases and to make u periodically causal, and data-windowing to avoid sharp changes at the edges. Since the signal is over sampled, a low pass filter, $L(f)$, is mandatory. With $\Phi(f)$ and $L(f)$, Eq. (3) can be rewritten as

$$v(t) \approx F^{-1}\{\tilde{V}(f)\} = F^{-1}\{\frac{U(f)\Phi(f)L(f)}{H(f)}\}, \tag{4}$$

where the cutoff edge of $L(f)$ is a half Hann window [1]. Another problem is that, in general, directly performing F^{-1} in Eq. (4) does not guarantee a causal $v(t)$ from band-limited frequency domain data, and the absence of causality may cause errors although an acausal inverse-transform generally gives satisfactory results. To enforce causality on $v(t)$, the real ($\tilde{V}_R$) and imaginary ($\tilde{V}_I$) part of $\tilde{V}(f)$ in Eq. (4) must follow the Hilbert transform[2]:

$$\tilde{V}(k) = \frac{1}{N}\sum_{m=0}^{N-1} \tilde{V}_R(m) Y_N(k-m), \quad \text{where} \quad Y_N(k) = \begin{cases} N, & k = 0, \\ -j2\cot(\pi k/2), & k = \text{odd}, \\ 0, & k = \text{even}, \end{cases} \tag{5}$$

where $j = \sqrt{-1}$ and N is the total number of data point including zero-padding,

$$j\tilde{V}_I(k) = \frac{1}{N}\sum_{m=0}^{N-1} \tilde{V}_R(m) Z_N(k-m), \qquad \text{and} \tag{6}$$

$$\tilde{V}_R(k) = \frac{1}{N}\sum_{m=0}^{N-1} j\tilde{V}_I(m) Z_N(k-m) + v(0) + (-1)^k v(N/2), \tag{7}$$

where $Z_N(k) = Y_N(k) - N\delta(k)$. In the time domain, above relations can be represented as:

$$v(n) = v_e(n) y_N(n), \qquad \text{and} \qquad v_o(n) = v_e(n) z_N(n), \tag{8}$$

where $y_N = \text{IFFT}\{Y_N\}/N$, $z_N = \text{IFFT}\{Z_N\}/N$, $v_e = \text{IFFT}\{\tilde{V}_R\}/N$, and $v_o = \text{IFFT}\{j\tilde{V}_I\}/N$, where IFFT stands for inverse FFT, v_e and v_o are even and odd parts of $v = v_e + v_o$, respectively. v is referred periodically causal if $v(n) = 0$ for $n \geq N/2$.

Eqs. (5) to (7) suggest that a causal v can be restored completely from the real part or almost from the imaginary part. In practice, since $\tilde{V}_R$ and $\tilde{V}_I$ may not follow the Hilbert transform, the causal v recovered from $\tilde{V}_R$ alone will not be consistent with that restored from $\tilde{V}_I$. To overcome this disagreement, we have improved an algorithm initially developed by Sarkar et al.[3] to extract the causal time domain sequence in an iterative manner. Our algorithm shows a faster and more stable convergence. In Eqs. (4) and (12), F^{-1} means the following iterative procedure:

1. Calculate an even and an odd time domain sequence with $v_e = \text{IFFT}\{\tilde{V}_R\}/N$ and $v_o = \text{IFFT}\{j\tilde{V}_I\}/N$, respectively, and calculate $S = \sum_{i=N/2}^{N-1}[v_e(i) + v_o(i)]^2$.

2. Create a new odd time domain sequence as
   $v_{o,new}(0 : N-1) = \{0, [v_o(1 : N/2-1) + v_e(1 : N/2-1)]/2,$
   $0, [v_o(N/2+1 : N-1) - v_e(N/2+1 : N-1)]/2\}$.

3. Calculate a new imaginary part of frequency domain data with $\tilde{V}_{I,new} = \text{FFT}\{v_{o,new}\}$.

4. Create an average imaginary part of frequency domain data as
   $\tilde{V}_{I,avg}(0 : N/2) = \{0, [\tilde{V}_I(1 : N/2-1) + \tilde{V}_{I,new}(1 : N/2-1)]/2, 0\}$, and
   $\tilde{V}_{I,avg}(N/2+1 : N-1) = -\tilde{V}_{I,avg}(N/2-1 : 1)$, where $\tilde{V}_{I,avg}(0 : N-1)$ has been forced to follow the symmetric property that ensures a real inverse transform.

5. Calculate another new odd time domain sequence with $v_{o,avg} = \text{IFFT}\{j\tilde{V}_{I,avg}\}/N$.

6. Create a new even sequence as
$v_{e,new} = \{v_e(0), [v_e(1:N/2-1) + v_{o,avg}(1:N/2-1)]/2,$
$v_e(N/2), [v_e(N/2+1:N-1) - v_{o,avg}(N/2+1:N-1)]/2\}$.

7. Calculate a new real part of frequency domain data with $\tilde{V}_{R,new} = \text{FFT}\{v_{e,new}\}$.

8. Create an average real part of frequency domain data as
$\tilde{V}_{R,avg}(0:N/2) = \{[\tilde{V}_R(0:N/2) + \tilde{V}_{R,new}(0:N/2)]/2\}$, and
$\tilde{V}_{R,avg}(N/2+1:N-1) = \tilde{V}_{R,avg}(N/2-1:1)$, where $\tilde{V}_{R,avg}(0:N-1)$ has been forced to follow the symmetric property that ensures a real inverse transform.

9. Calculate another even part of time domain sequence with $v_e = \text{IFFT}\{\tilde{V}_{R,avg}\}/N$.

10. Calculate a better causal sequence with $v = v_e + v_o$ and $S_{new} = \sum_{i=N/2}^{N-1}[v(i)]^2$. A smaller S_{new} implies a better periodically causal v.

11. Calculate $\mid S_{new} - S \mid /S_{new}$. If it is less than a sufficient resolution, say 10^{-5}, stop the iteration and output a causal time domain sequence v; otherwise, let $\tilde{V}_R = \tilde{V}_{R,new}$, $\tilde{V}_I = \tilde{V}_{I,new}$, $v_e = v_{e,new}$, $v_o = v_{o,new}$, and $S = S_{new}$, and go to step 2.

COMPENSATION FOR CONNECTION CABLE AND SCD 5000

A PSPL 4050B step generator with a 5210 IFN was utilized to generate an impulse with a magnitude of 2.8 V and a pulse-width of 58 ps as the reference. Since the output impulses from the IFN are identical, they can be characterized by a CSA 803 with a SD30 sampling head. The characterized pico-second impulse was injected into the connecting cable between the D-dot sensor and the SCD 5000 at the D-dot sensor end. Figure 2 shows the reference impulse characterized by the CSA 803, the impulse measured by the SCD 5000, and the respective Fourier spectra. There is a significant difference between the reference and the measured impulses in both time and frequency domain. The magnitudes of the FFT spectra suggest that the reference impulse is much stronger than measured impulse in a wide frequency range (DC-20 GHz), which gives us the physical basis that we can numerically expand the bandwidth of the measurement hardware to a wider frequency range.

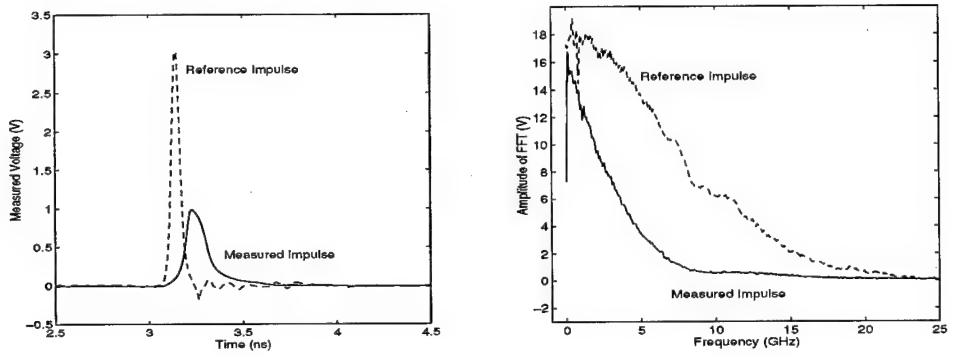

Figure 2: Comparison between the reference impulse characterized using a CSA 803 with a SD30 sampling head and the measured impulse with SCD 5000 in time and frequency domain.

Rearranging Eq. (1) to a form for the evaluation of system transfer function, we have:

$$x_{out}(t) + n_{out}(t) = [x_{in}(t) + n_{in}(t)] * h_{cd}(t), \tag{9}$$

where $x_{out}(t)+n_{out}(t)$ is the impulse measured by the SCD 5000, in which $x_{out}(t)$ is the desired signal we want to obtain and $n_{out}(t)$ is the additive noise, $x_{in}(t)+n_{in}(t)$ is the characterized impulse by the CSA 803, in which $x_{in}(t)$ is the real signal and $n_{in}(t)$ is the noise, and $h_{cd}(t)$ is the impulse response of the cable-digitizer system to be obtained from the measurements. By taking Fourier transform on Eq. (9), we can get the frequency domain form:

$$H_{cd}(f) = \frac{X_{out}(f) + N_{out}(f)}{X_{in}(f) + N_{in}(f)} = H(f) \cdot \frac{1 + N_{out}(f)/X_{out}(f)}{1 + N_{in}(f)/X_{in}(f)}, \tag{10}$$

where the upper case letters stand for the Fourier spectra of the corresponding lower case letters, respectively, and $H(f) = X_{out}(f)/X_{in}(f)$ is the true transfer function. The fraction term behind $H(f)$ is the noise contribution, which is close to one at the frequencies at which the signal-to-noise ratios of measured data are very large. At the frequencies where $X_{in}(f)$ is close to zero, $X_{out}(f)$ should be close to zero, too. Consequently, $H_{cd}(f)$ is just noise. Since $H(f)$ can only be obtained approximately in practice, an exact deconvolution is inherently impossible[4].

H_{cd} was utilized in Eq. (4) as the transfer function, H, to compensate the effect of the connection cable and the SCD 5000 for the measurements obtained with a mounted ACD-1(A) on the top ground wall. Figure 3 shows the measured and cable-digitizer compensated D-dot, E field, and energy density spectra of corresponding E field at a pulse repetition frequency of 60 Hz. Clearly, the compensated data give a faster rise time and a higher magnitude than those directly measured. The comparison of their pulse parameters is listed in Table 1.

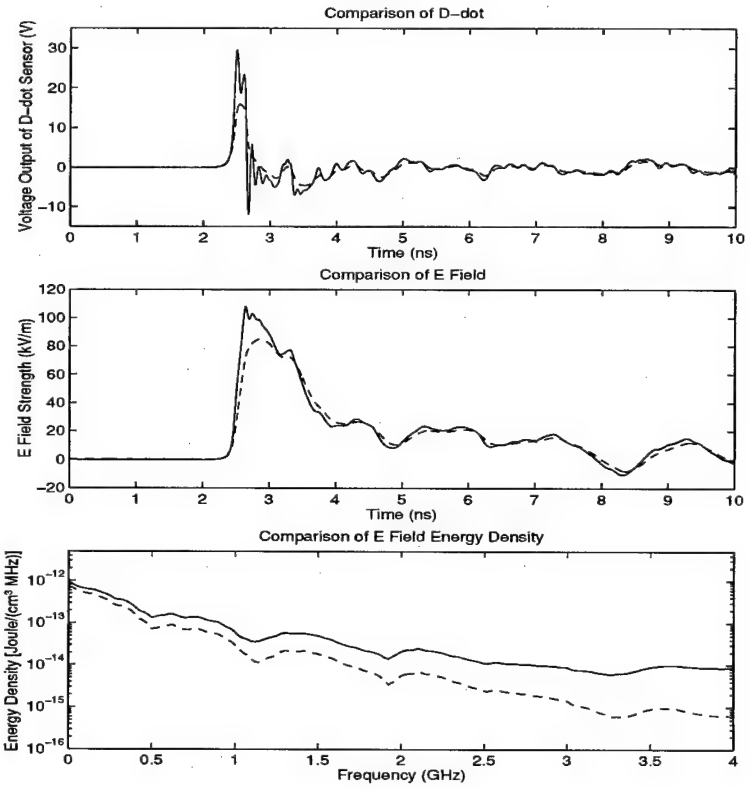

Figure 3: Comparison between cable-digitizer compensated (solid lines) and uncompensated (dashed lines) D-dot, E field, and energy density spectra of E field. The measurement was done with an ACD-1(A) D-dot sensor at a pulse repetition frequency of 60 Hz.

Table 1. Comparison of pulse parameters between the uncompensated and the cable-digitizer compensated E filed presented in Figure 3.

	rise time (ps)	magnitude (kV/m)	pulse width (ns)
uncompensated E field	234	84.8	1.11
compensated E field	166	107.6	0.98

COMPENSATION FOR REFLECTIONS IN D-DOT SENSOR ACD-1(R)

The sensing elements ("eggs") in both ACD-1(R) and ACD-1(A) are the same while they are connected to the respective SMA connectors differently. In ACD-1(A), the sensing element and the SMA connector are joined in the axial direction directly while, in ACD-1(R), they are connected by a coaxial line through three right-angle bends in the radial direction, as drawn in Figure 4.

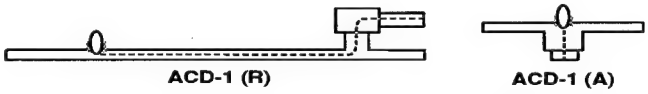

Figure 4: Schematic diagrams of ACD-1(R) and ACD-1(A) D-dot sensors.

The right-angle bends of ACD-1(R) cause reflections of D-dot signals in the sensor. The reflections result in a magnitude reduction and a "shoulder" on the falling edge of the first spike, as shown in Figure 5(a). Although there are only minor influences on its slow variation part, there is a clear effect on the fast leading edge of the pulse, as shown in Figure 5(b), which is important for estimating the rise time.

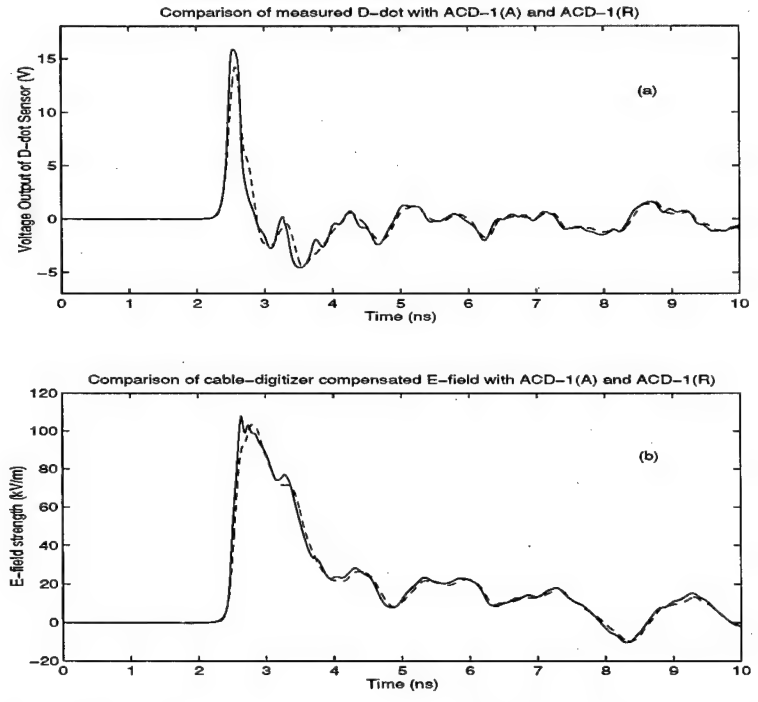

Figure 5: Comparison of (a) measured D-dot with ACD-1(A) (solid lines) and ACD-1(R) (dashed lines) at a symmetric pair of locations on the top and the bottom ground walls, respectively, and (b) their corresponding cable-digitizer compensated E field wave forms.

The output of ACD-1(R) is the transmission of the original signal plus scaled and delayed replicas of the original signal, therefore its impulse response can be modeled as

$$h(t) = a_0\delta(t) + a_1\delta(t-\tau_1) + a_2\delta(t-\tau_2), \tag{11}$$

where $a_k < 1, (k = 0, 1, 2)$ are the scaled coefficients, and $\tau_k > 0, (k = 1, 2)$ are the delay times. We did not take the effects of the sensing element into account because it has a bandwidth $\geq$ 10 GHz [5], and ignored the low pass nature of the coaxial line and the SMA connector. The first δ-function in Eq. (11) is for the transmitted D-dot signal through the right-angle bends, and rest of them are for the reflections. From Figure 5(a), it seems that only the first reflection has an obvious effect on the E field, so we only include two reflections: one for the right-angle band at the joint between the "egg" and the coaxial line, and another for a bend at SMA connector. For a given set of parameters, $\mathbf{P} = \{a_0, a_1, \tau_1, \cdots\}$, the distortion due to the reflections in ACD-1(R) and the cable-digitizer limitations can be compensated together with

$$w_{rec}(t, \mathbf{P}) = F^{-1}\{\frac{U(f)\Phi(f)L(f)}{H_{cd}(f)H_{dd}(f, \mathbf{P})}\}, \tag{12}$$

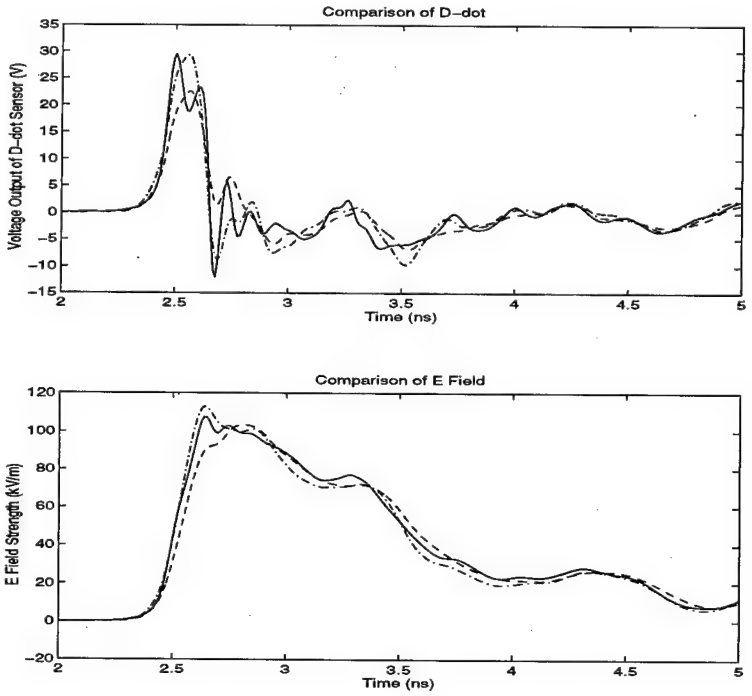

Figure 6: D-dot and E field measured using an ACD-1(R) compensated with Eq. (4) (dashed line) and Eq. (12) with the optimized parameters (dash-dot line), and those measured using an ACD-1(A) compensated with Eq. (4) (solid line).

where $H_{dd}(f, \mathbf{P})$ is the transfer function given by

$$H_{dd}(f, \mathbf{P}) = a_0 + a_1 e^{-j\omega\tau_1} + a_2 e^{-j\omega\tau_2}, \tag{13}$$

where ω is the angular frequency. For a different $\mathbf{P}$, we get a different w_{rec}. To determine $\mathbf{P}$, we have developed an optimization procedure which uses the Levenberg-Marguardt algorithm [1] to minimize an objective function (S): the parameters are adjusted in time domain while

the derivatives are calculated in frequency domain and then transformed back to time domain [6]. S is defined as

$$S(\mathbf{P}) = \sum_{n=0}^{N/2-1} W(t_n)[E_{ref}(t_n) - E_{rec}(t_n, \mathbf{P})]^2, \tag{14}$$

where W is the weighting factor, $E_{ref}(t_n) = c\sum_{k=0}^{n} v_{ref}(t_k)$, used as a reference, is the E field obtained from the cable-digitizer compensated D-dot measured using the mounted ACD-1(A), $E_{rec}(t_n, \mathbf{P}) = c\sum_{k=0}^{n} w_{rec}(t_k, \mathbf{P})$ is the E field after cable-digitizer *and* D-dot sensor compensation for a measurement using an ACD-1(R) at a specific location on the bottom ground wall that is symmetric to the ACD-1(A) about center septum, as indicated in Figure 1. c is a converting coefficient. By the symmetry of the cell, E_{rec} and E_{ref} should be very close to each other, and the observed difference is mainly due to the reflections in ACD-1(R). It has been found that utilizing the wave forms of E field in the optimization procedure gives a better recovery to its leading edge than that obtained with D-dot wave forms. Figure 6 shows the results for the best fitted parameters: $a_0 = .72$, $a_1 = .28$, $\tau_1 = 81.2$ ps, $a_2 = .01$, and $\tau_2 = 510$ ps, from which we can see the reflection at the SMA connector is very minor. Although the semi-empirical method requires more computation, it is of following advantages: (i) more clear physics, (ii) easier portability for transform function due to a small number of parameters, and (iii) wider valid frequency range because of using an analytical model.

In summary, we have presented an error compensation routine for the electromagnetic pulse measurements in the pico second domain, which includes an algorithm of an iterative causal deconvolution and evaluations of an empirical transfer function for a cable-digitizer system and a semi-empirical transfer function for an ACD-1(R) D-dot sensor.

ACKNOWLEDGMENTS

This work is supported by the U.S. Army Medical Research and Materiel Command under contract DAMD17-94-C-4069 awarded to McKesson BioServices. The views, opinions and/or findings contained in this report are those of the authors and should not be construed as an official Department of Army position, policy or decision unless so designated by other documentation.

REFERENCES

[1] W. H. Press, B. P. Flannery, S. A. Teukolsky, and W. T. Vetterling. *Numerical Recipes in C.* Cambridge University Press, Cambridge, UK, 2 edition, 1992.

[2] A. V. Oppenheim and R. W. Schafer. *Discrete-Time Signal Processing.* Prentice Hall, New Jersey, 1989.

[3] T. Sarkar, H. Wang, R. Adve, and M. Moturi. Evaluation of a causal time domain response from bandlimited frequency domain data. In H. L. Bertoni, L. Carin, and L. B. Felsen, editors, *Ultra-Wideband, Short-Pulse Electromagnetics*, pages 501–515, Plenum Press, New York, 1993.

[4] N. S. Nahman. Software correction of measured pulse data. In J. E. Thompson and L. H. Luessen, editors, *Fast Electrical and Optical Measurements. Volume I*, pages 351–417, Martinus Nijhoff Publishers, Boston, 1986.

[5] *Specification of ACD D-dot Sensor (Data Sheet 1119).* EG&G Washington Analytical Services Center, Inc., Albuquerque, New Mexico, 1987.

[6] J.-Z. Bao. Time domain optimization with frequency domain derivatives. To be published.

McKesson BioServices

Contract No.
DAMD17-94-C-4069

Technical Report on the Safety of Army Personnel from Exposure to Radiofrequency Radiation from Advanced Membrane Transducer Antenna

Submitted to:

Bruce E. Stuck, Director
U.S. Army Medical Research Detachment
Brooks Air Force Base, Texas

McKesson BioServices
14665 Rothgeb Drive
Rockville, MD 20850

Satnam Mathur, Ph. D.
Sr. Electrical Engineer

Shin-Tsu Lu, Ph. D.
Sr. Research Scientist

June 12, 1998

An Equal Opportunity Employer

Technical Report on the Safety of Army Personnel From Exposure to Radiofrequency Radiation from Advanced Membrane Transducer Antenna

The US Army Dismounted Battlespace Battle Lab (DBBL) ACT II Advanced Membrane Transducer (AMT) Antenna has been developed for the US Army to provide increased flexibility while operating in urban environment. It is intended to be attached directly to vehicles, radio systems or worn in a soldiers' BDU. A technical assesment of AMT antenna has been completed to determine if the radiofrequency radiation (RFR) from the antenna conforms to the permissible exposure limits (PEL) as defined in DoD Instruction Number 6055.11 (February 21, 1995). Even though AMT antenna was found to produce large electric fields close to the antenna surface, the specific absorption rate (SAR) was found to be lower than those prescribed in the safety guidelines. The induced currents in the ankle and wrist was also found to be within the safety limits. Specific recommendations regarding safe use of this device, when worn by a soldier, are included.

Introduction

The US Army DBBL ACT II AMT antenna is a planar, conformal antenna designed to be attached directly to vehicles, radio systems or worn in a soldiers' BDU. No additional hardware or ground plane is required. It is fed by a standard RG-58 cable and measures 19.6 cm by 14 cm in size. Typical operating parameters are: SINGCARS 30 - 88 MHz, 5 watts, though it has been effectively operated by US Forces from 1 W to 100 W.

Since, the AMT antenna is going to be mounted on a soldier's back, there is a need for quantifying maximum induced currents and local SAR distribution in the human body in the immediate vicinity of the antenna. Radio Frequency PELs (1) applicable to the intended use of the AMT antenna, in the frequency range of interest, are:

For controlled environments:

1. A spatial peak SAR, not exceeding 8 W/kg as averaged over any 1 g of tissue

2. The induced currents in the body conform with the maximum permissible exposure (MPE) in Table 1 of reference (a); viz, 100 mA through each foot of a free-standing individuals (not in contact with metallic objects).

For Uncontrolled Environments:

1. A spatial peak SAR, not exceeding 1.6 W/kg as averaged over any 1 g of tissue,
2. The induced currents in the body conform with the maximum permissible exposure (MPE) in Table 1 of reference (a); viz, 45 mA through each foot of a free-standing individuals (not in contact with metallic objects).

In addition, root mean square (RMS) electric field strengths would be restricted to 61.4 V/m for controlled environments and to 27.5 V/m for uncontrolled environments. However, for partial body exposures, which is the case with intended use AMT antenna, the peak value of mean squared electric field can be up to 20 times the values stated above, i.e., 754 kV^2/m^2 for controlled environments and 151.25 kV^2/m^2 for uncontrolled environments or peak electric field strengths of 274.6 V/m and 123 V/m for controlled and uncontrolled environments respectively.

The intended use of AMT antenna conforms to the definition of a controlled environment. For other personnel working in the vicinity, who will be exposed to the radiation from the antenna, limits for the uncontrolled environment will apply. If SAR and induced currents conform to limits placed on the controlled environment exposures, then it is likely to also conform to the uncontrolled environments as electromagnetic field will drop substantially away from the antenna.

It is to be noted that low power device exclusions mentioned in section 4.2 of the safety standards do not apply in this case since the device (AMT antenna) is designed to be used at a distance of less than 2.5 cm from the body.

Testing the AMT Antenna

The testing of the AMT antenna was divided into three distinct categories:

Free-space Tests: These tests were conducted to determine direction and amplitude of maximum fields, to determine if there are any RF hot spots, and to determine the rate at which electric field strength falls with distance. Following tests were conducted:

a. near-zone angular radiation pattern,
b. near-zone field distribution on a plane parallel to the antenna surface
c. variation of electric field with increasing axial distance from the antenna surface.

All free-space tests were conducted at a mid frequency of 50 MHZ. All the tests were conducted in an anechoic chamber appropriate for low frequency operation.

Tests to Determine Surface Heating: A muscle equivalent phantom of human torso was constructed according to the recipe given in RFR dosimetry handbook (2) for a frequency of 70 MHZ. This frequency was chosen because the recipe was available at frequencies of 40.68, 70 and 100 MHZ. Since the frequency of operation of AMT antenna is 30 - 88 MHZ, the recipe at 70 MHZ will model the electrical characteristics (conductivity and dielectric constant) of the muscle equivalent material fairly well from 30 to 88 MHZ. The conductivity of muscle equivalent material at 70 MHZ is 0.79 S/m. The conductivity is 12.7% higher at 100 MHZ (0.89 S/m) and 13.9 % lower at 40.68 MHZ (0.68 S/m). The dielectric constant of muscle equivalent material at 70 MHZ is 84.0 and it is 15.5% higher at 40.68 MHZ (97.0) and 14.6 % lower at 100 MHZ (71.7). Therefore, a muscle equivalent phantom of human torso at 70 MHZ yields a maximum error of ±15% at other frequencies of interest.

A thermographic camera system was also used to determine:

a. surface heating of the antenna and feed-cable system

b. possible thermal hot spots (temperature rise) on the surface of the phantom.

Three measurements were done at various frequencies of interest.

Induced Current and SAR Measurements

SAR Distribution: Spatial SAR distribution in the vicinity of expected RF hot spots in the phantom of human torso was measured using commercially available non-perturbing, fluroptic Luxtron probes embedded in the phantom. Temperature rise in the phantom, resulting from application of high input power to the antenna for 1 minute was measured. SAR was calculated from the measured temperature gradient. The measurement was done at various frequencies of interest.

Induced Currents: Induced currents in ankle and wrist were measured using commercially available induced current meters. The measurement was done for free standing individuals at various frequencies of interest.

Free-Space Test Setup

Figure 1a shows the setup for antenna radiation pattern measurement. Antenna is mounted on a plastic stand and base. The antenna can be mounted either vertically or horizontally (Figure 1b), and it can be rotated about the vertical axis from 0° (broadside to the probe) to ±90°. The probe is mounted on plastic stand that can be raised or lowered to facilitate alignment of the antenna and the probe. The probe used is an omnidirectional, E-field probe along with Holaday field strength meter. The probe measures the electric field radiated by the antenna in any polarization and the meter displays the power density in mW/cm^2. The power density displayed by the meter is based on the far field expression:

$$P_d \ (mW/cm^2) = \frac{E_{rms}^2 \ (V/m)}{3770 \ (Ohm)} \qquad (1)$$

In this test we are interested in measuring the near-zone field of the AMT antenna. Equation (1) was used to calculate the root mean square (RMS) value of near-zone electric field, E_{rms}, from the power density value, P_d, displayed by the meter.

Figures 1c and 1d show a simple setup to measure the near-zone electric field radiated by the antenna in a plane parallel to the plane of the antenna. A styrofoam template was used to position the probe along the plane at pre-determined locations. The horizontal and vertical resolution of the template is 1" (2.54 cm) and 1.5" (3.81 cm) respectively, which is at least $\lambda/158$ at 50 MHz, our test frequency. Figure 1d shows the distance of the probe tip (1.5 cm) from the antenna surface.

Measurement of the axial variation of the electric field was performed using the set up of Figure 1a, with the porbe aligned to the center of the antenna as shown. Figures 2a and 2b show the coordinate system and relative position of the probe and the antenna for free-space tests.

Free-space Test Results

Figure 3 shows the AMT antenna radiation patterns, a plot of relative power density versus angular deviation (θ), for the case when AMT antenna was mounted horizontally and the radiating side of the antenna was facing the probe. Radiation patterns were measured at 50 MHz and net input power to the antenna was 5W. As we can see from the polar plot, the maximum radiation occurs when the edges of the antenna face the probe (θ = 0 or 180 degrees). The distance of the probe from the surface of the antenna in the broadside position (θ = 90 degrees) was 10.5 cm. The angular radiation patterns are measured with the same radial distance from the center of the antenna surface. Thus, at θ = 0 or 180 degrees, the edges of the antenna were about 1.0 cm from the probe. A large power density (20 mW/cm^2 per watt input power) at the edges of the antenna is indicative of the complicated nature of the edge diffracted fields and that the edge diffracted fields add in phase at 1.0 cm from the edges to yield a high measured power density, and a corresponding high electric field.

The radiation pattern with the antenna mounted horizontally, but the back of the antenna (side which is supposed to be towards mounting surface) towards the probe, is shown in Figure 4. The radiation pattern has an assymetry in the radiation from the edges of the antenna but the maximum power density is still occurs at the edges.

The radiation pattern measurements for vertically mounted antenna (not shown) under the same test conditions, show a pronounced assymetry in power density measured from $\theta = 0$ and 180 degrees, but again the maximum power density is measured from one of the edges. Again, the front and back radiation patterns were identical.

Figure 5 shows the variation of the power density and the electric field with axial distance, z. The maximum electric field calculated from the measured power density is at z = 1 to 2 cm from the antenna surface. The maximum electric field is found to be about 300 V/m, which is slightly above the maximum peak field allowed for partial body exposres. The results for the vertical mounting were similar. Notice that field decays rapidly as z increases and is only approximately -15 dB at z = 12.5 cm from the antenna surface.

Figures 6 and 7 show relative electric field measured in a plane parrallel to the antenna surface and at a distance of z = 1.5 cm from the antenna surface. The field plots are similar with the front side or the back side towards the probe, though there are slight diffrences in the exact field distribution in the two cases. The contour plots show exact location of the maximum electric field. It is seen from Figure 7 that maximum field ocurrs at about 4.2 cm up and 2 cm in from the lower right corner of the antenna (x = 10 cm, and y = -7 cm). The actual electric field at the RF hot spot is measured to be 450 V/m. The contour plot also shows that the field pattern has a symmetry about x = 0 cm line.

Thermographic Measurements

The AMT antenna was mounted in front of a phantom model of the human torso, as

shown in Figure 8. The average distance of the antenna from the phantom model was about 2 cm. Infra red (IR) thermographic camera was used to record sequence of pre-exposure, exposure and post-exposure shots. Pre-exposure shots were taken just before the antenna was placed in front of the phantom and post exposure shots were taken just after antenna was removed from in front of the phantom, which was right after the RF power was turned off. The net temperature rise on the phantom surface is then calculated by subtracting the first post-exposure shot from the last pre-exposure shot.

The measurements were made at 50, 60, 70, and 80 MHZ. The net power into the antenna was 52 W at 50 MHZ to 16 W at 80 MHZ. This is due to the fact that the antenna is not well matched when mounted on or near a human body (phantom) and consequently there is a large reflected power which varies with frequency of operation. The exposure time was 90 s and 60 sequential recordings were made. Typical overall average temperature on the antenna surface was 23 °C (at 60 MHZ) and on the phantom surface was 20.8 °C (at 60 MHZ). As shown in Figure 8b and Figure 8c, there is a considerable amount of heat generated in the feed cable and on the feed structure, as well as on the antenna surface. For a net power input of 27 W at 60 MHZ, the maximum temperature on the cable was 26.8 °C. Figures 9 through 12 show the temperature rise on the surface of the phantom at various frequencies on the area of the phantom model which was directly behind the antenna. Note that the temperature difference plots in Figures 9 - 12 show a diffused pattern for 50 and 70 MHZ, but indicate a well defined thermal hot spots in the location of feed cable, feed structure, on the antenna surface and antenna mounts.

Thus, a surface heating of the antenna structure tends to obscure the heat actually generated on the surface of the phantom model at least at some frequencies. Maximum temperature difference observed on the surface of the phantom model at 50 MHZ and at 70 MHZ is about 0.4 to 0.6 °C, while at 60 and 80 MHZ the true temperature rise is masked by the excessive heating of the antenna surface.

SAR Measurements and Results

The thermographic measurements could not reveal any thermal hot spots due to heat

diffusion on the surface of the phantom and, at some frequencies, due to excessive surface heating of the antenna itself. The temperature rise was measured at 24 separate locations around the expected RF hot spot as shown in Figure 7, at 40, 50, 60, 70, and 80 MHZ. A Luxtron model 3000 fluro-optic thermometer with MAM-05 fluoro-optic probes were embeded approximately 0.3 cm into the phantom model as shown in Figure 13. Each of the MAM-05 Luxtron probe contains an array of four sensors, spaced 0.5 cm apart. The probes were so inserted into the phantom that the first sensor (sensor D, Figure 13) was placed at 1 cm from the near edge of the antenna. Two MAM-05 probes were used at the same time, and three pairs of runs were made at x=1 and 4 cm, at x=2 and 5 cm, and at x=3 and 6 cm from the lower edge of the antenna and at the same frequency to obtain 24 data points. Each measurement at each location and frequency was repeated three times. Each run was for 3 minutes, 1 minute pre-exposure, I minute exposure (RF ON) and 1 minute of post-exposure (RF OFF).

An average of the three runs at each point and each frequency was taken and plotted against time. Th data obtained was modeled by three separate equations (linear regression), representing the three line segments joined at their end points. The three distinct data segments corresponded to the pre-exposure, exposure and the post- exposure regimes. Then the slope of the exposure region was adjusted by a baseline obtained from the average slope of the pre- and post-exposure data (3). SAR was calculated from the measured temperature rise as given by the following equation:

$$SAR \ \ (W/kg) \ = \ C \ \ (J/kg \ ^\circ C) \ * \ \frac{\partial T}{\partial t} \ \ (^\circ C/s) \qquad (2)$$

where C is the specific heat capacity of the human muscle phantom and is equal to 3767.4 J/kg°C.

The results are shown in the tabulated form in Tables 1-5 and in graphical form in Figures 14 through 18.

SAR Table No. 1

(Normalized SAR in W/kg per watt input)

Luxtron Probes Used: MAM-05 - two probes were used at a time.

Total number of runs (n) = 9; three runs for every set of probe locations.

Probe depth (penetration) into the phantom = 0.3 cm

Total number of Data Points : N = 24

RF Parameters:

Frequency = 40 MHZ

Net Input Power (mean ±sd) = 22.45 ± 1.4 W (N = 24)

Phantom Characteristics (@ 70 MHZ):

Conductivity (σ) = 0.76 S/m

Relative Permittivity (ϵ_r) = 84.7

Coordinate	y1	y2	y3	y4	y5	y6
x1	unmeas.	0.043	0.16	0.521	0.13	0.14
x2	unmeas.	unmeas.	unmeas.	0.483	0.11	0.094
x3	0.0063	0.16	0.00065	**0.300**	0.096	0.12
x4	unmeas.	unmeas.	0.11	0.375	0.25	0.06

SAR Table No. 2

(Normalized SAR in W/kg per watt input)

Luxtron Probes Used: MAM-05 - two probes were used at a time.

Total number of runs (n) = 9; three runs for every set of probe locations.

Probe depth (penetration) into the phantom = 0.3 cm

Total number of data points: N = 24

RF Parameters:

Frequency = 50 MHZ

Net Input Power (mean ± sd) = 31.56 ± 2.74 W (N = 24)

Phantom Characteristics (@ 70 MHZ):

Conductivity (σ) = 0.76 S/m

Relative Permittivity (ϵ_r) = 84.7

Coordinate	y1	y2	y3	y4	y5	y6
x1	unmeas.	0.18	0.21	0.72	0.375	0.18
x2	0.049	0.27	0.26	0.54	0.23	0.26
x3	0.05	0.11	0.205	**0.52**	0.308	0.26
x4	0.081	0.099	0.19	0.41	0.31	0.32

SAR Table No. 3

(Normalized SAR in W/kg per watt input)

Luxtron Probes Used: MAM-05 - two probes were used at a time.

Total number of runs (n) = 9; three runs for every set of probe locations.

Probe depth (penetration) into the phantom = 0.3 cm

Total number of data points: N = 24

RF Parameters:

Frequency = 60 MHZ

Mean Net Input Power = 42.11 ± 9.24 W (N = 24)

Phantom Characteristics (@ 70 MHZ):

Conductivity (σ) = 0.76 S/m

Relative Permittivity (ϵ_r) = 84.7

Coordinate	y1	y2	y3	y4	y5	y6
x1	0.016	0.053	0.0075	0.433	0.019	0.027
x2	0.00	0.06	unmeas.	0.305	0.048	0.068
x3	0.095	0.05	0.012	**0.245**	unmeas.	0.06
x4	0.049	unmeas.	0.07	0.176	unmeas.	unmeas.

SAR Table No. 4

(Normalized SAR in W/kg per watt input)

Luxtron Probes Used: MAM-05 - two probes were used at a time.

Total number of runs (n) = 9; three runs for every set of probe locations.

Probe depth (penetration) into the phantom = 0.3 cm

Total number of data points: N = 24

RF Parameters:

Frequency = 70 MHZ

Mean Net Input Power = 28.89 ± 1.61 W (N = 24)

Phantom Characteristics (@ 70 MHZ):

Conductivity (σ) = 0.76 S/m

Relative Permittivity (ϵ_r) = 84.7

Coordinate	y1	y2	y3	y4	y5	y6
x1	unmeas.	0.051	0.0016	0.33	0.15	0.14
x2	0.075	0.122	0.084	0.31	0.23	0.287
x3	0.094	0.296	0.097	**0.32**	0.21	0.14
x4	0.040	0.135	0.097	0.29	0.20	0.103

SAR Table No. 5

(Normalized SAR in W/kg per watt input)

Luxtron Probes Used: MAM-05 - two probes were used at a time.

Total number of runs (n) = 9; three runs for every set of probe locations.

Probe depth (penetration) into the phantom = 0.3 cm

Total number of data points: N = 24

RF Parameters:

Frequency = 80 MHZ

Mean Net Input Power = 23.44 ± 0.58 W (N = 24)

Phantom Characteristics (@ 70 MHZ):

Conductivity (σ) = 0.76 S/m

Relative Permittivity (ϵ_r) = 84.7

Coordinate	y1	y2	y3	y4	y5	y6
x1	unmeas.	0.094	unmeas.	0.24	0.21	0.19
x2	0.005	0.076	unmeas.	0.16	0.09	0.205
x3	0.002	0.006	0.001	**0.21**	0.15	0.165
x4	unmeas.	unmeas.	0.005	0.22	0.21	unmeas.

Discussion of SAR Results

As the results presented in the SAR tables indicate, maximum normalized SAR is 0.72 W/kg per watt net power input to the antenna, at 50 MHZ. Net power input means the forward power minus the reverse power as measured by Bird wattmeter. A local SAR of 0.72 W/kg per watt means that one can operate up to 11.1 W net input power and be still with in the 8 W/kg

limit for the local SAR. Unmeas. Indicates that the temperature rise was unmeasurable. The bold face entry in Tables 1 -5 indicates the SAR at the location of the RF hot spot. Note that RF hot spot location is not the thermal hot spot location. The thermal hot spot appears 1 cm to the right of the RF hot spot. This is expected as thermal diffusion would change the location of thermal hot spot relative to the location of the maximum field point (RF hot spot).

Figures 14 - 18 show spatial distribution of the local SAR at frequencies from 40 to 80 MHz. Relevant statistics is also included in the figures. The XY plane shown in Figures 14 - 18 is the area covered under lower right quarter of the antenna. Figures 14 - 18 show that even though the location of the maximum SAR is the same for all frequencies, the distribution is quite different as a function of the frequency. This is not surprising given the results seen in the thermographic measurements.

Induced Current Measurements

Holaday ankle current coil and meter was used to measure induced currents in the ankle and wrist of four human volunteers, three male and one female, standing on a cement floor wearing rubber soled shoes (free-standing individuals). Induced ankle current was found to be a function of frequency. Maximum ankle current recorded was 33.6 mA at 30 MHz in the female volunteer, far below the 100 mA per foot limit. Table 6 summarizes the data concerning the volunteers. Figure 19 shows a plot of mean induced ankle current normalized to net input power, at each frequency. The scatter data points refer to each volunteer. Best result is obtained at 60 MHz where the mean is about 1 mA per watt and the worst case is at 30 MHz with a mean of 11 mA per watt and a worst case of 14 mA per watt. This means that a maximum power input of 7.14 W (100/14) can be allowed before the induced current limit of 100 mA per foot will be violated. The maximum wrist current measured was 0.82 mA per watt.

Table 6 : Induced Ankle Current Measurement Data

Volunteer #	Sex	Weight (kg)	Height (m)	Max. Ankel Current (mA)	Wrist current (mA)
1	M	83.9	1.73	33.0*	6.0 @ 30 Mhz
2	M	79.4	1.78	31.3	0.62 @ 80 MHz
3	F	68.5	1.58	33.6	1.14 @ 30 MHz
4	M	83.9	1.85	24.0	4.89 @ 80 MHz

* at 50 MHz. All other maximum ankel currents are at 30 MHz.

The results for induced currents do not reflect what the situation would be if the individual is standing on a metallic surface or is in contact with a metallic object. For conditions of possible contact with metallic bodies the IEEE/ANSI standards limit the contact current (as measured by contact current meter) to 45 mA through each foot from 0.1 to 100 MHz. We have not measured the contact current, since such a scenario is not envisioned in the intended use of the AMT antenna. Use of protective gloves and clothing will limit the contact current to maximum allowable limit and will prevent possible contact/shock burns.

As a byproduct of the induced current measurements, data on voltage standing wave ratio (VSWR) versus frequency was obtained. Figure 20 shows the result. VSWR is a measure of how well the antenna is matched to the load, in this case load is the antenna mounted on the backs of human volunteers. A VSWR of 17 was obtained at 30 MHz, while a VSWR of 4 was obtained at 80 MHz. An ideal VSWR of 1.0 means 100% power input to the antenna is transmitted (no reflection at the antenna input terminals). Correspondingly, a VSWR of 17.0 means that only 21% of the input power is transmitted, while a VSWR of 4.0 implies a 64% power transmission. It is clear that a better match needs to be obtained at all frequencies, but especially at 30 MHz. A VSWR of say less than 2.0, will ensure that there is no excessive heating of the feed cable as well as antenna surface itself. An almost 80% reflection of power is likely to impact adversly on the operation of the source connected to the antenna.

Conclusions and recommendations

The AMT device, as it is intended to be used, was found to produce local SAR of less than 8 W/kg. Induced currents for free-standing individuals were well within the maximum persible limits. No tests were conducted on individuals standing on a metallic ground or in contact with metallic surfaces. Use of protective clothing and/or gloves is recommended.

Based on SAR and induced current measurements, it is determined that AMT can not be operated safely at net input powers of more than 7.0 W. All these tests were performed assuming continuous operation in the transmitting mode. For a 9 to 1 duty cycle (9 minutes receive and 1 minute transmit), it is unlikely to cause any discomfort to the soldier at the intended power levels.

The AMT device is poorly matched when mounted on the human body. It is highly recommended that a braodband matching network be incorporated at the input end of the AMT antenna. As it is, a large VSWR especially at the lower end of the frequency band is likely to effect the operation of the transmitting source.

References

(1) Institute of Electrical and Electronic Engineers (IEEE) C95.1-1991, " IEEE Standard for Safety Levels with respect to Human Exposure to Radiofrequency Electromagnetic Fields, 3 kHz to 300 GHz", IEEE Press, April 27, 1992.

(2) Carl H. Durney, Massoudi, H, and Iskander M. " Radiofrequency Radiation Dosimetry Handbook (Fourth Edition)" prepared for USAF School of Aerospace Medicine, Aerospace Medical Division (AFSC), Brooks AFB, TX 78235, October 1966.

(3) Gambrill, C. S., DeAngelis, M. L., Lu, S. T. "Error Analysis of a Thermometric Microwave-dosimetry Procedure". In Blank, M., ed. Electricity and Magnetism in Biology and Medicine. San Francisco: San Francisco Press; 1993:593 - 595.

(4) Holaday Industries Application Note, " Units for RF Hazard Measurements", web site http:// www. holadayinc.com/page12.html. April 14 1998.

Acknowledgments

Authors gratefully acknowledge the all the technical help and cooperation extended to us by Dr. John A. D'Andrea and his staff, Naval Medical Research Institute Detachment at Brooks Air Force Base, Texas 78235. Authors would like to thank Mr. David D. Cox, McKesson BioServices, for design and fabrication of AMT antenna positioner and his technical support throughout this work. We would also like to thank Mr. Don Hatcher and Mr. Michael Belt for their help with thermographic measurements.

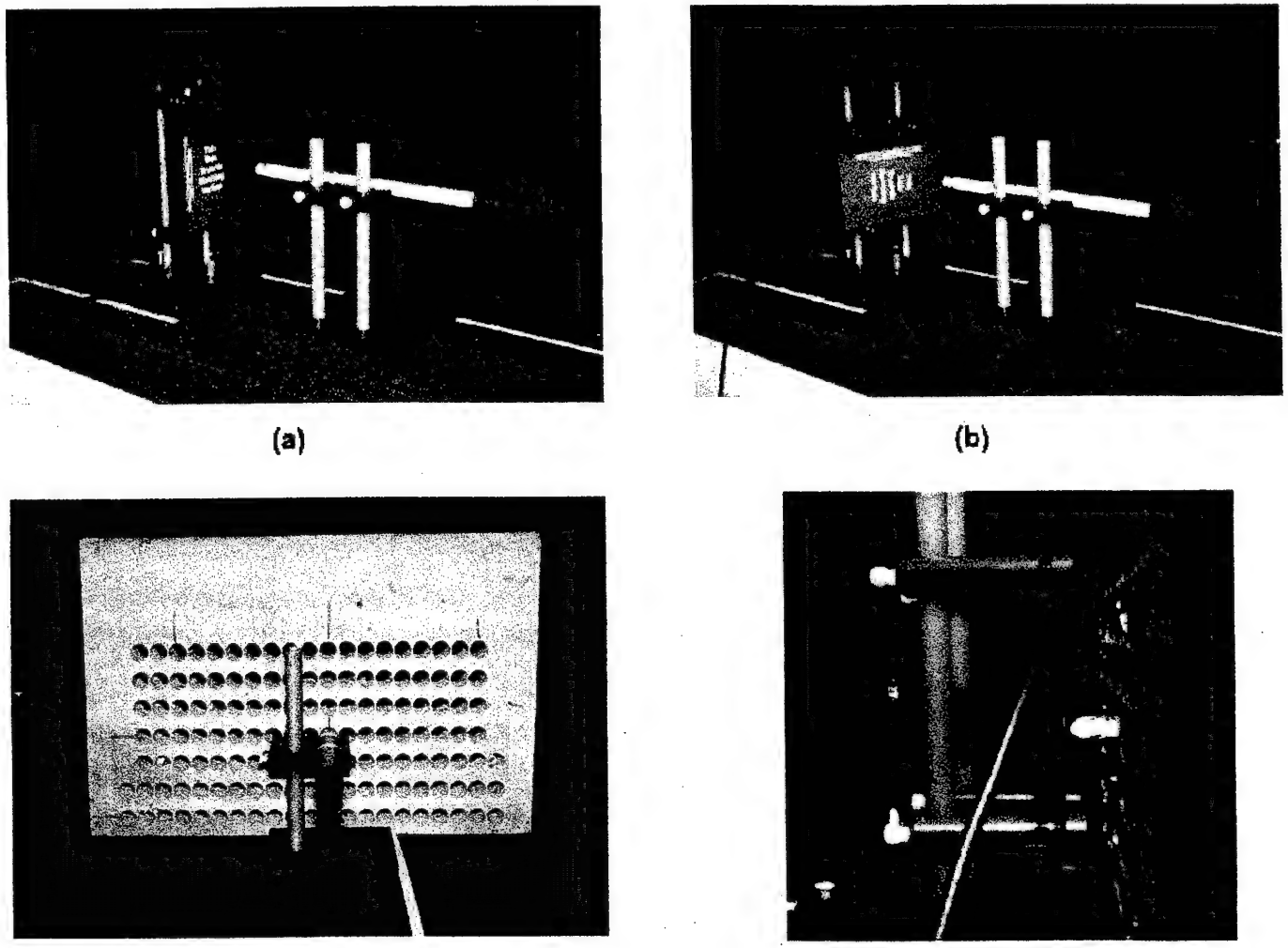

Figure 1. Antenna Pattern Measurement Setup : (a) Vertical mounting (antenna 90 deg. to probe) (b) Horizontal mounting (antenna 20 deg. to probe), (c) Planar scan setup showing probe and styrofoam template, (d) Planar scan setup showing probe tip and AMT antenna.

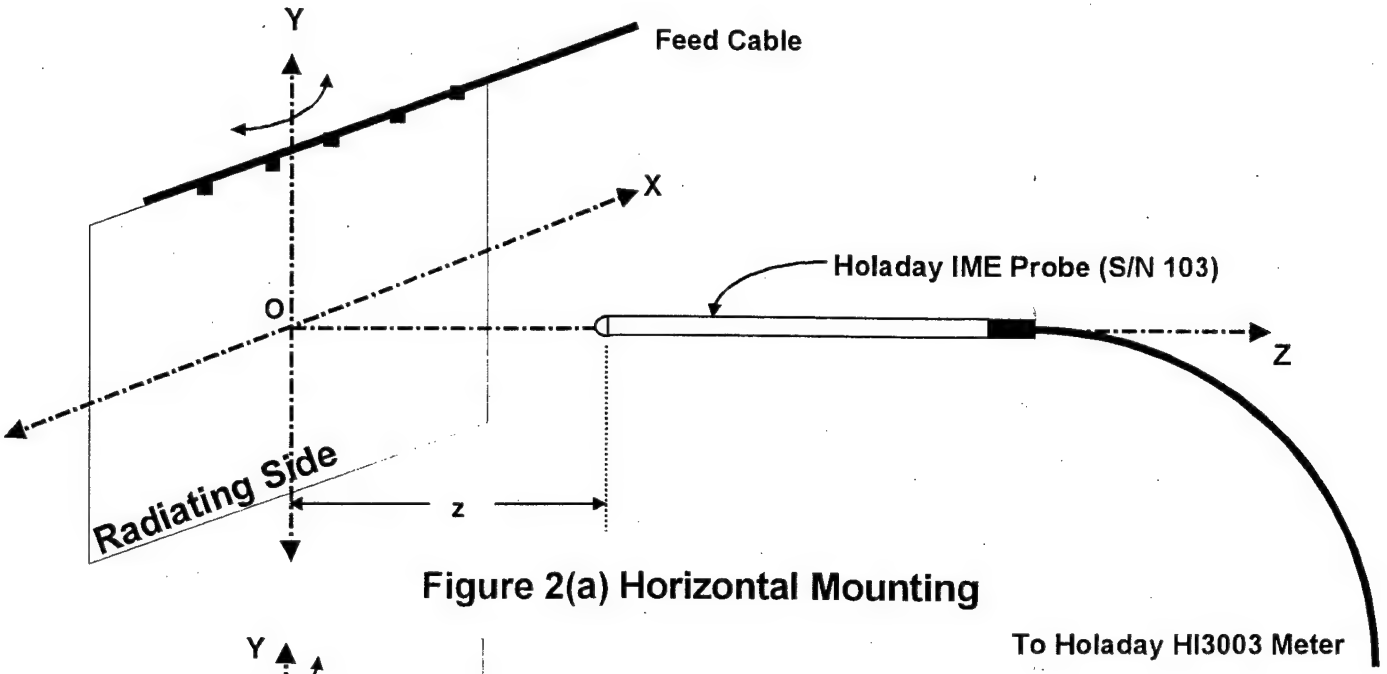

Figure 2(a) Horizontal Mounting

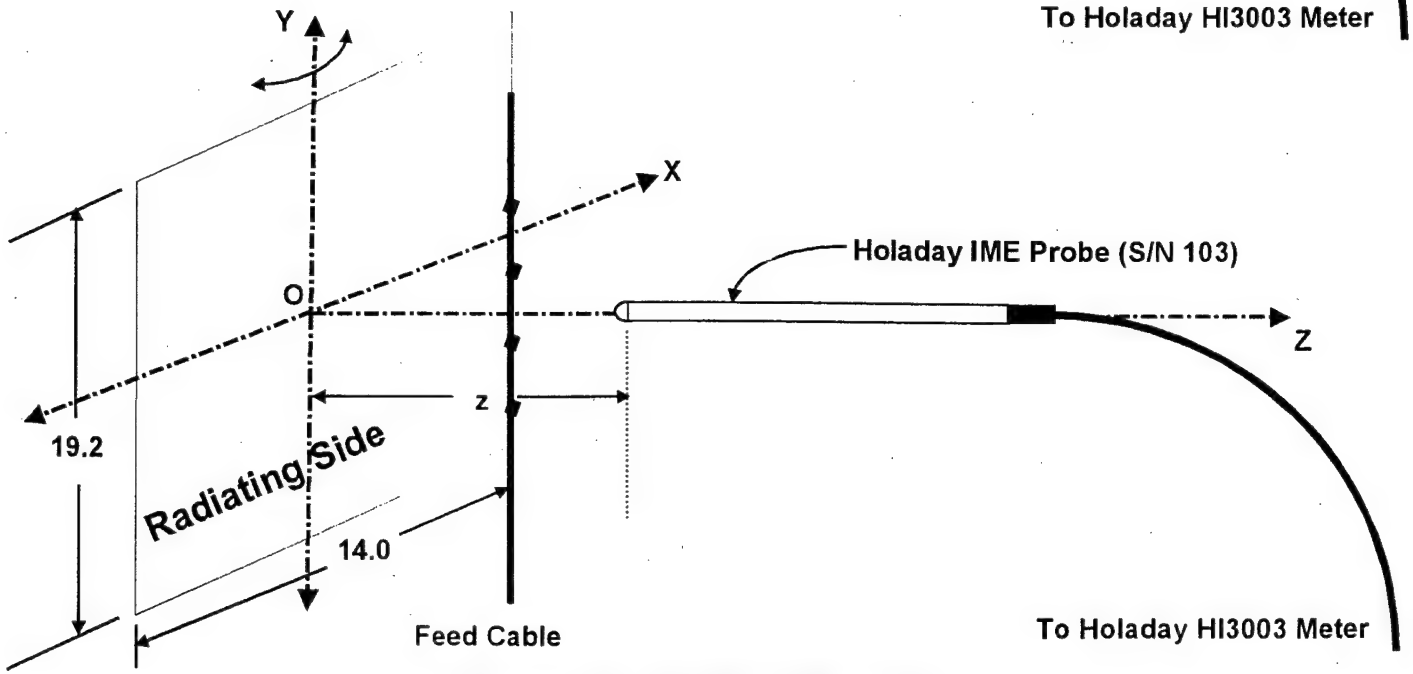

Figure 2(b) Vertical Mounting

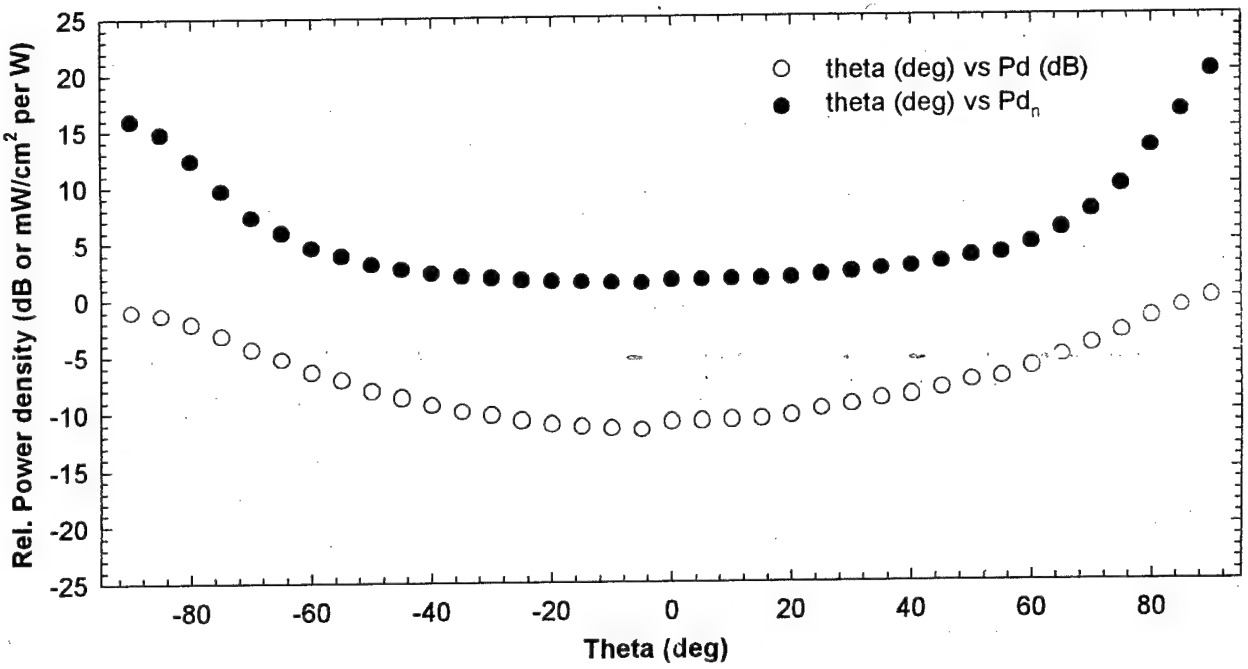

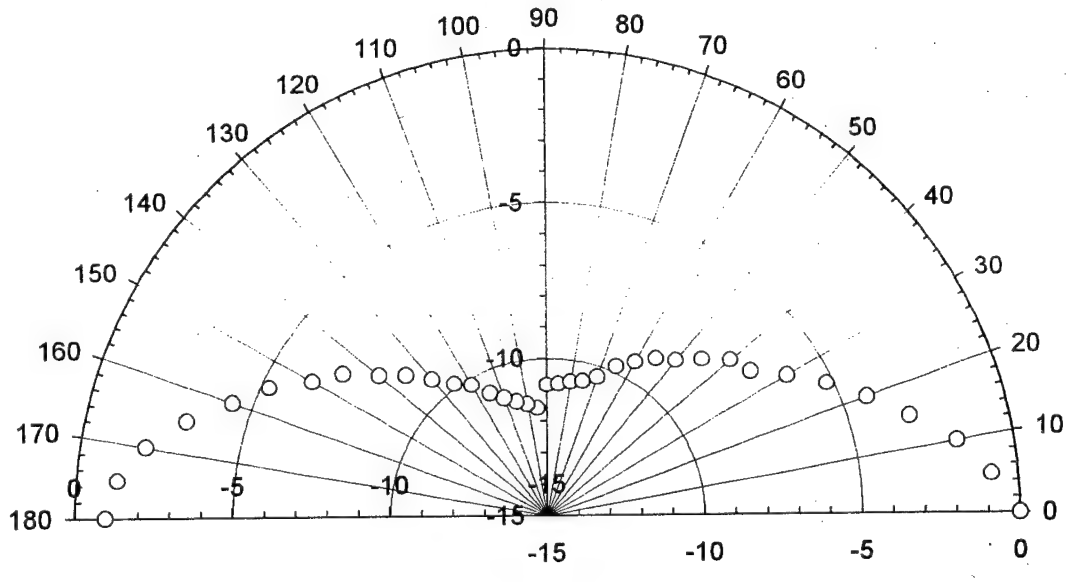

Figure 3. AMT Antenna Radiation Pattern (Front): 50 MHz, R = 10.5 cm (Antenna Mounted Horizontally)

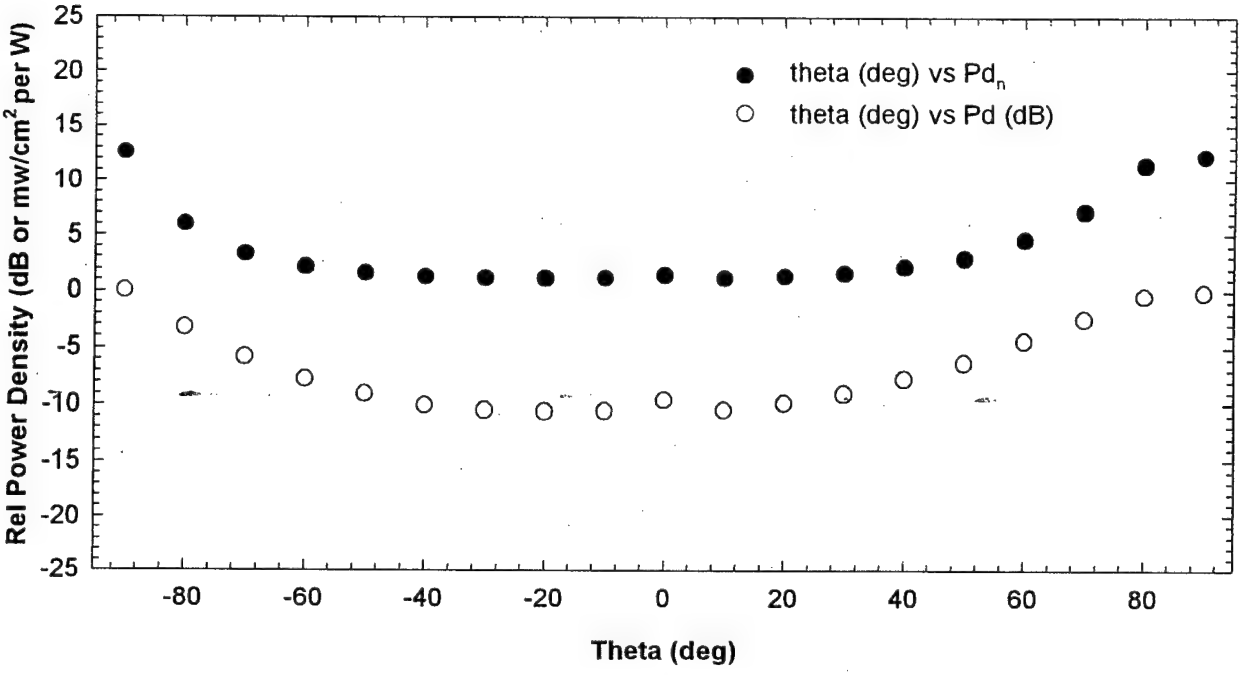

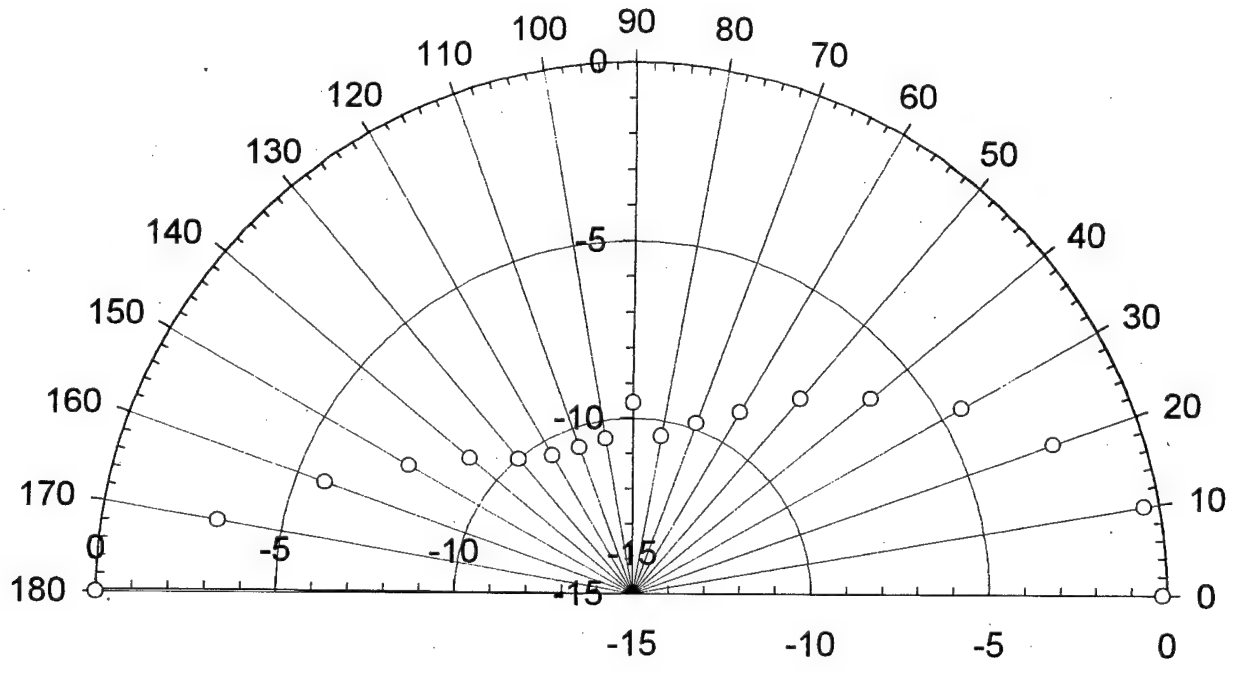

Figure 4: AMT Antenna Radiation Pattern (Back): 50 MHz, R = 10.5 cm (Antenna Mounted Horizontally)

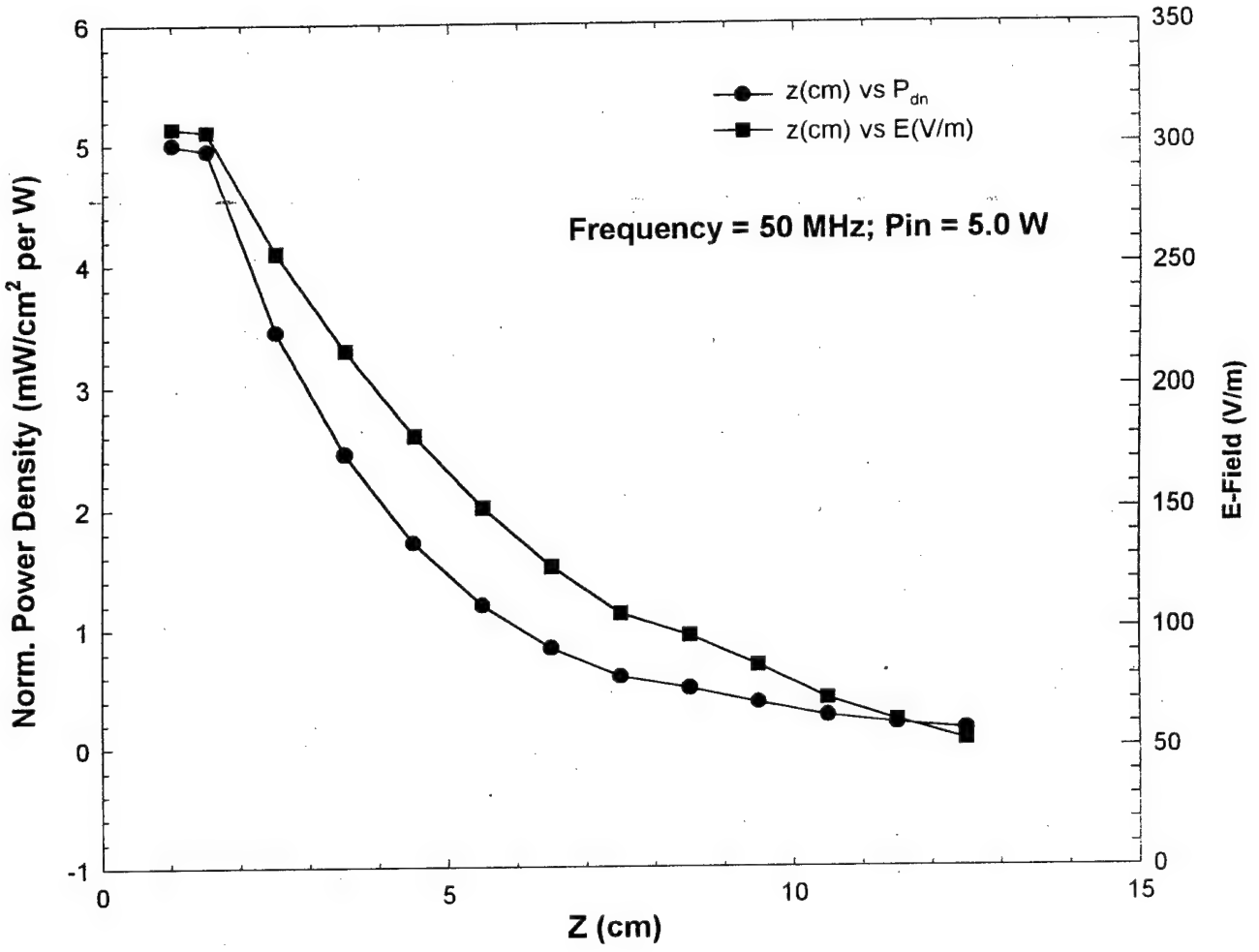

Figure 5: AMT Antenna: Broadside Z-axis Scan (Front); Horizontal mounting.

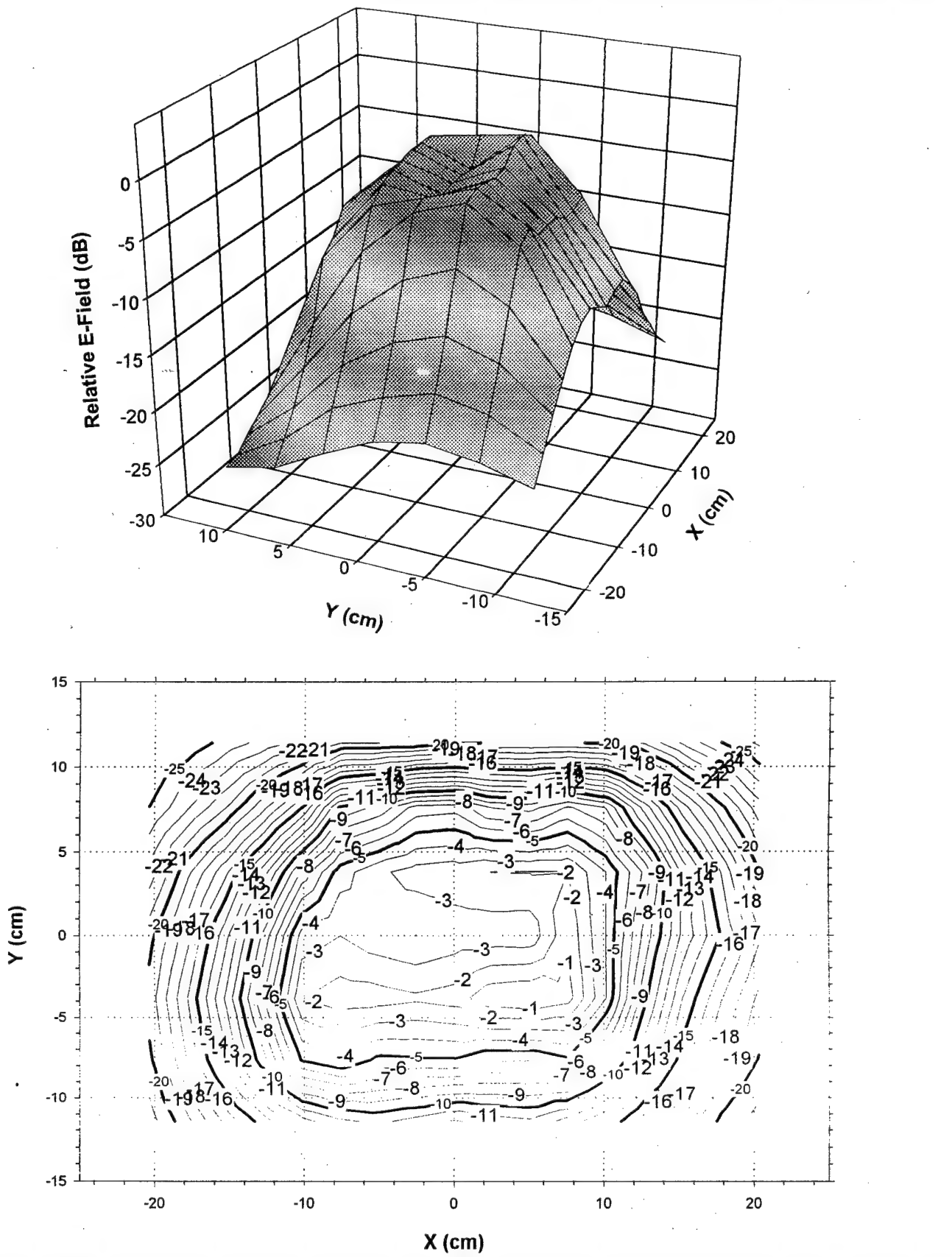

Figure 6: AMT Antenna: Planar Scan (Front); Relative E-Field Plots at z = 1.5 cm

Frequency = 50 MHz; Input Power = 5 W
Horizontal Mounting; Back Side towards Probe

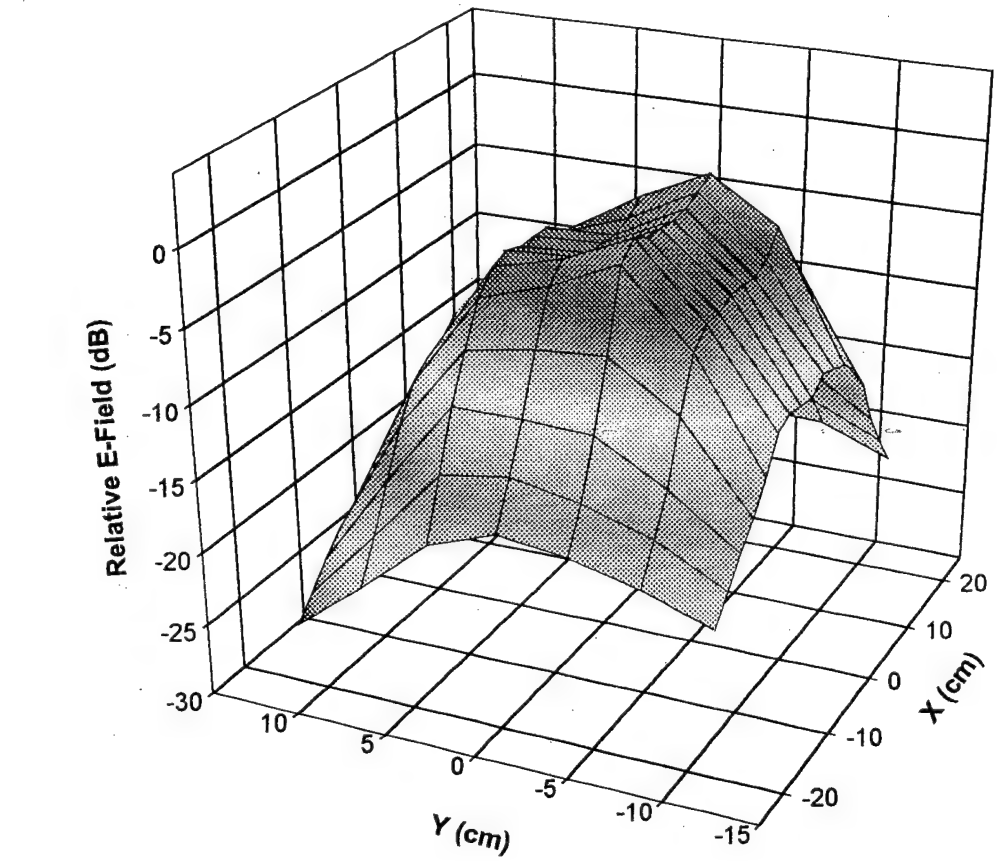

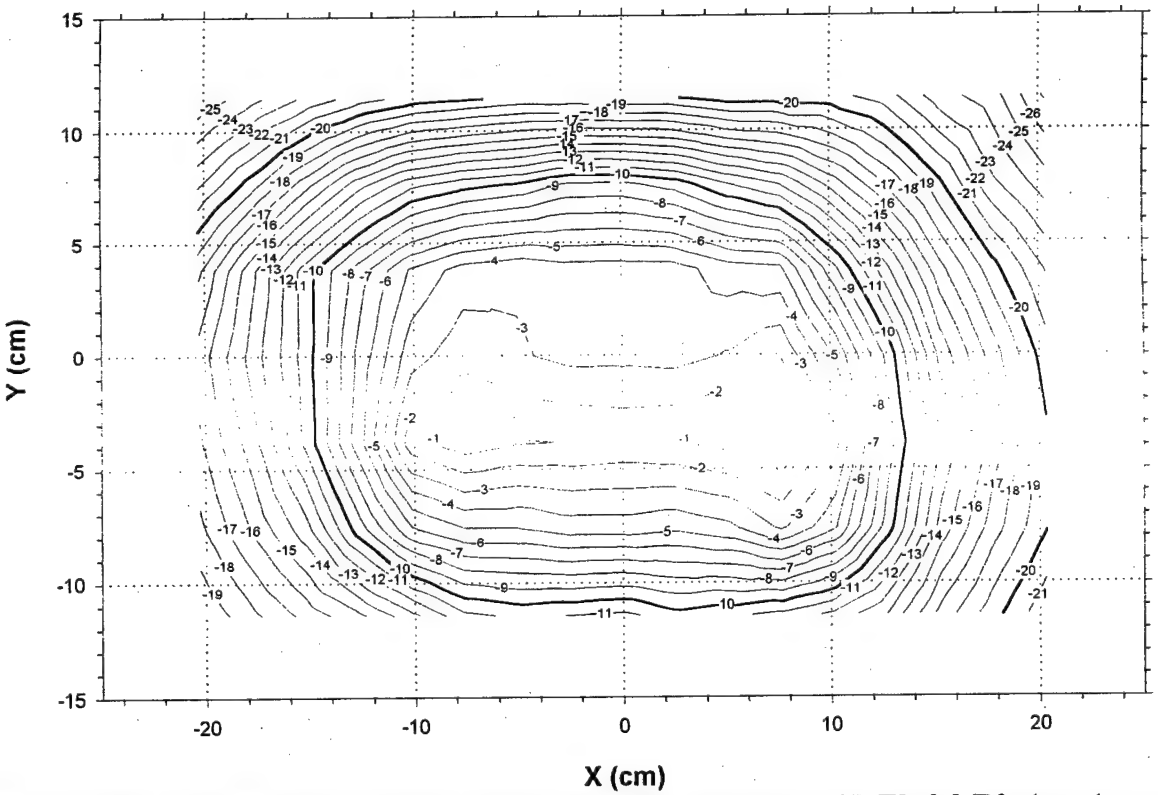

Figure 7: AMT Antenna: Planar Scan(Back); Relative E-Field Plots at z = 1.5 cm

(a) Human Torso Phantom - pre exposure shot

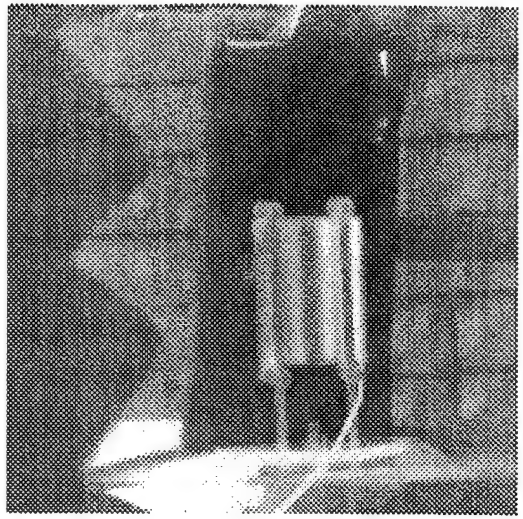

(b) AMT Antenna in front of Phantom : 1 s after RF ON

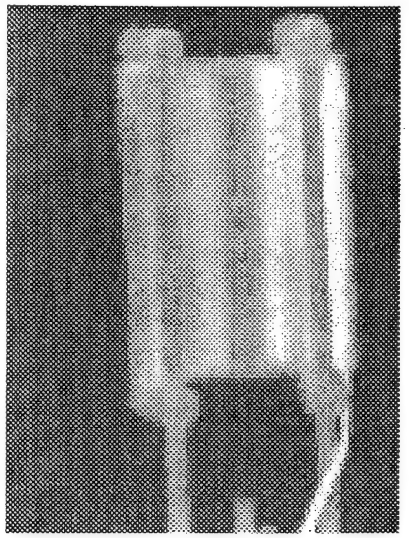

(c) Close up shot of AMT antenna showing surface heating : 2 s after RF ON

(d) Human Torso Phantom : Post Exposure Shot

Figure 8: Sequence of Thermographic Pictures (60 MHz)

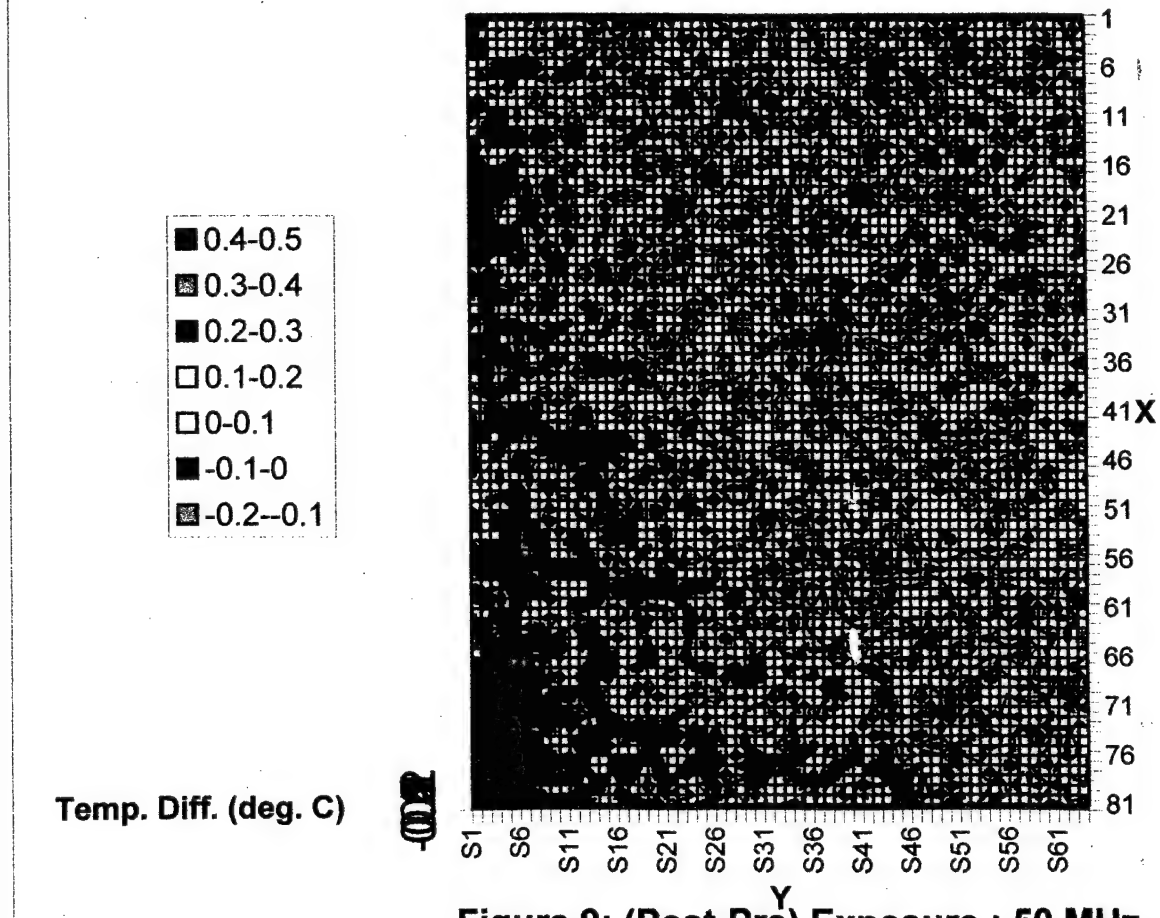

Figure 9: (Post-Pre) Exposure : 50 MHz

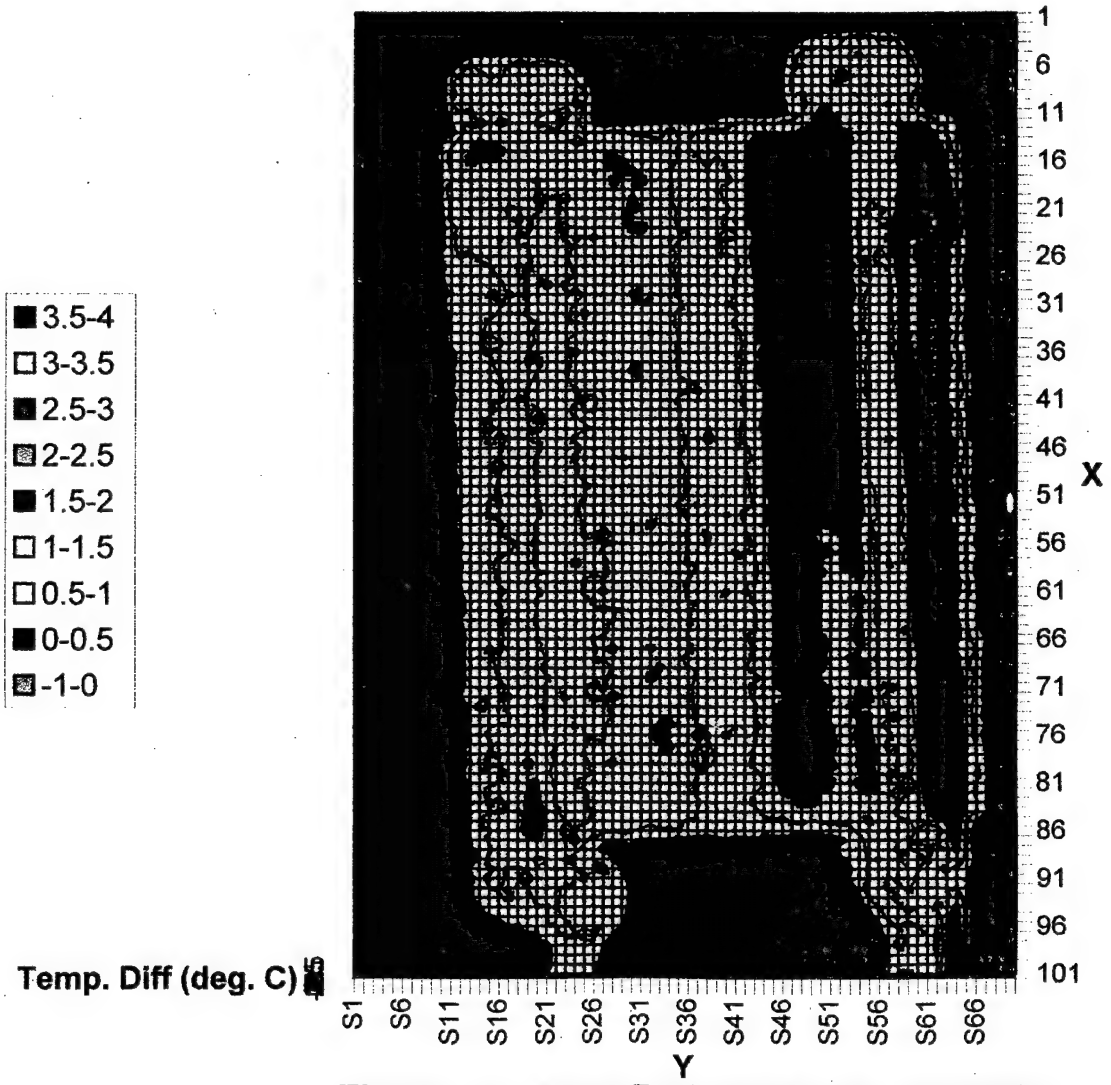

Figure 10: (Post-Pre) Exposure : 60 MHz

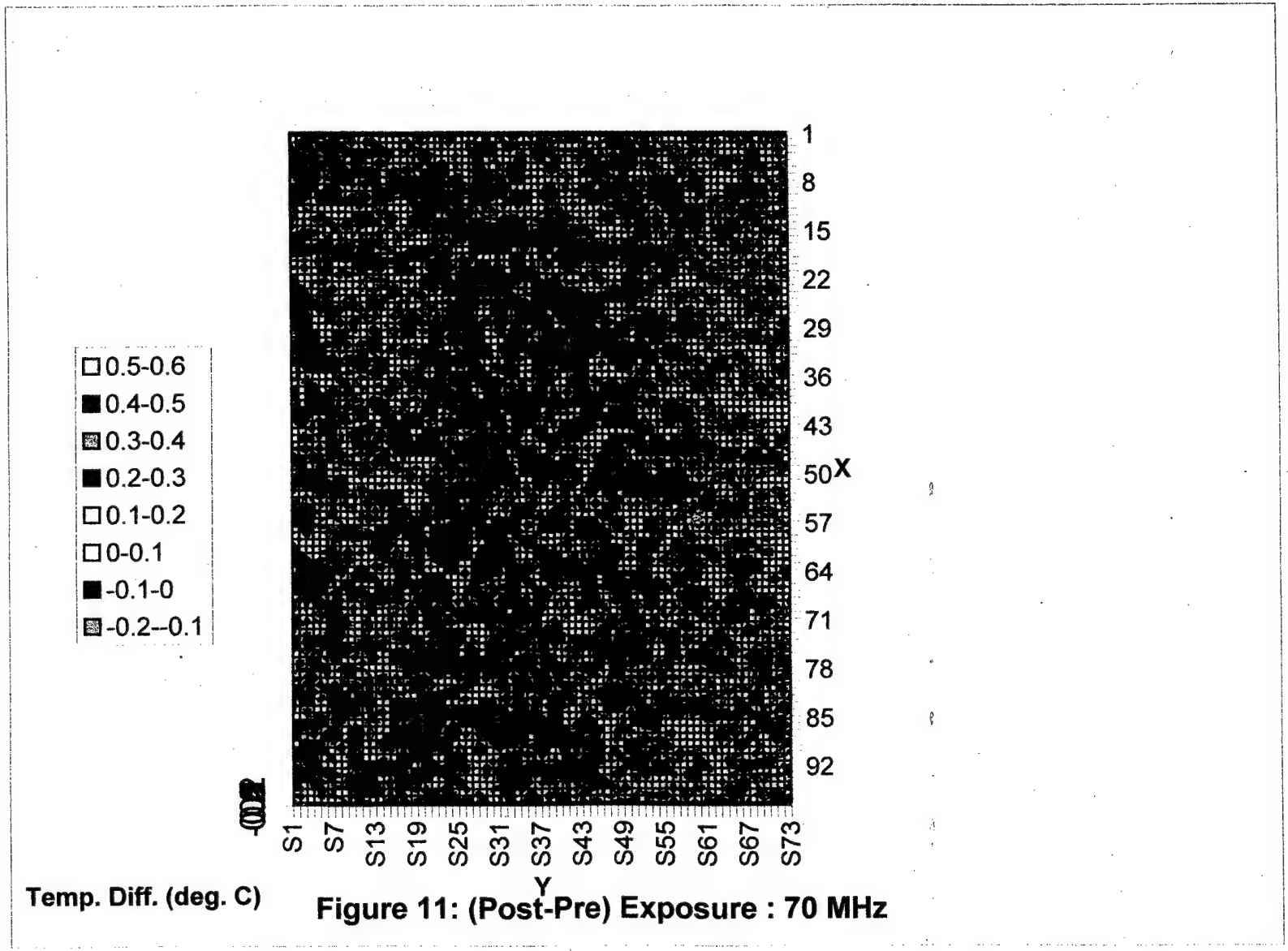

Figure 11: (Post-Pre) Exposure : 70 MHz

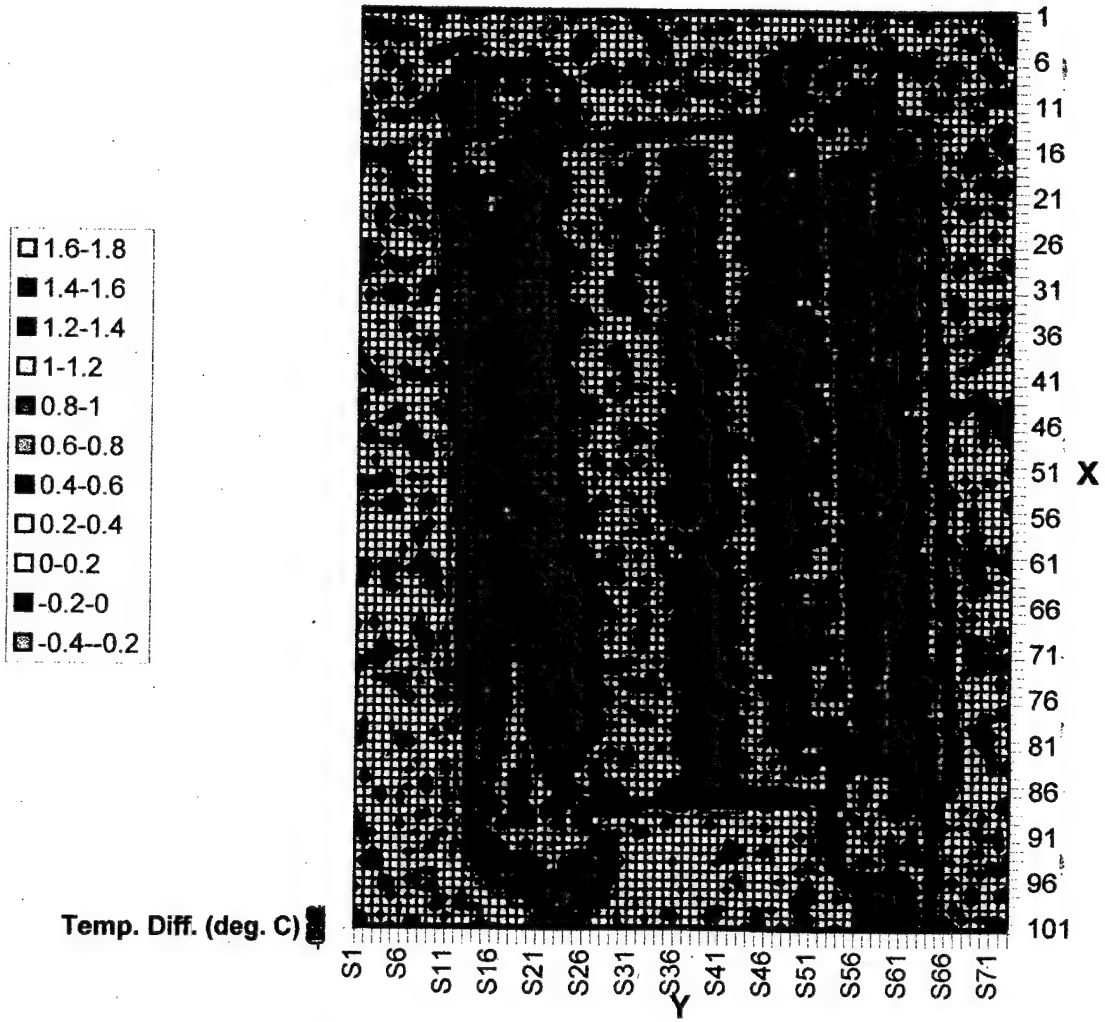

Figure 12: (Post-Pre) Exposure : 80 MHz

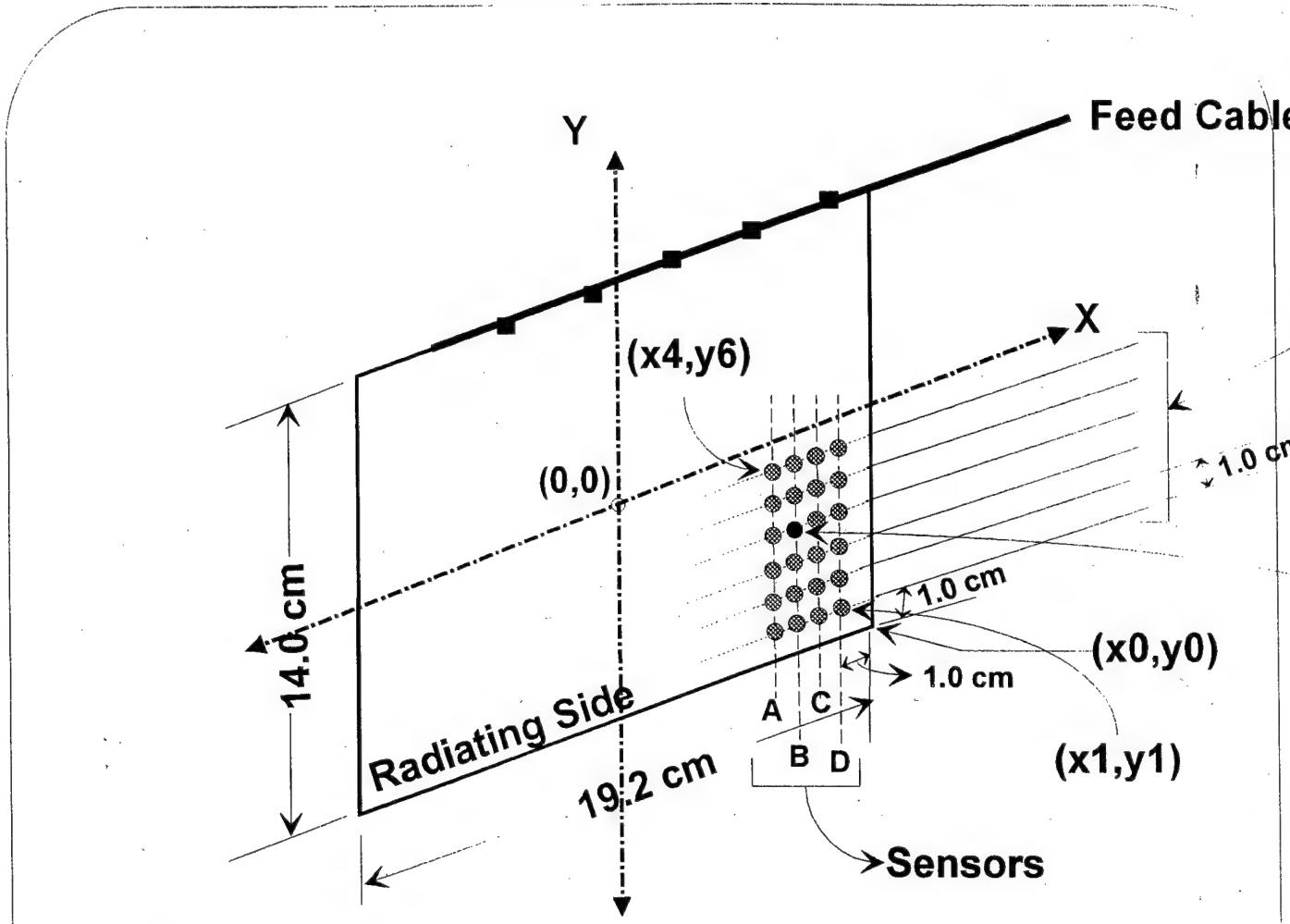

Sensor Coordinates (cm)

(Referred to point (x0,y0)

	y1	y2	y3	y4	y5	y6
x1	(1,1)	(1,2)	(1,3)	(1,4)	(1,5)	(1,6)
x2	(1.5,1)	(1.5,2)	(1.5,3)	(1.5,4)	(1.5,5)	(1.5,6)
x3	(2,1)	(2,2)	(2,3)	(2,4)	(2,5)	(2,6)
x4	(2.5,1)	(2.5,2)	(2.5,3)	(2.5,4)	(2.5,5)	(2.5,6)

NOTE: Spacing between sensors = 0.5 cm

Figure 13 : Geometry for SAR Measurements ; AMT Antenna mounted on a 70 MHz Human Muscle Phantom.

Number of data points (N) = 24
Net Input Power (W_t) = 22.45 +/- 1.4 W
Max. Norm. SAR = 0.521 W/kg per W_t @ (-1,4)
Norm. SAR (mean +/- sd) = 0.108 +/- 0.18 W/kg per W_t

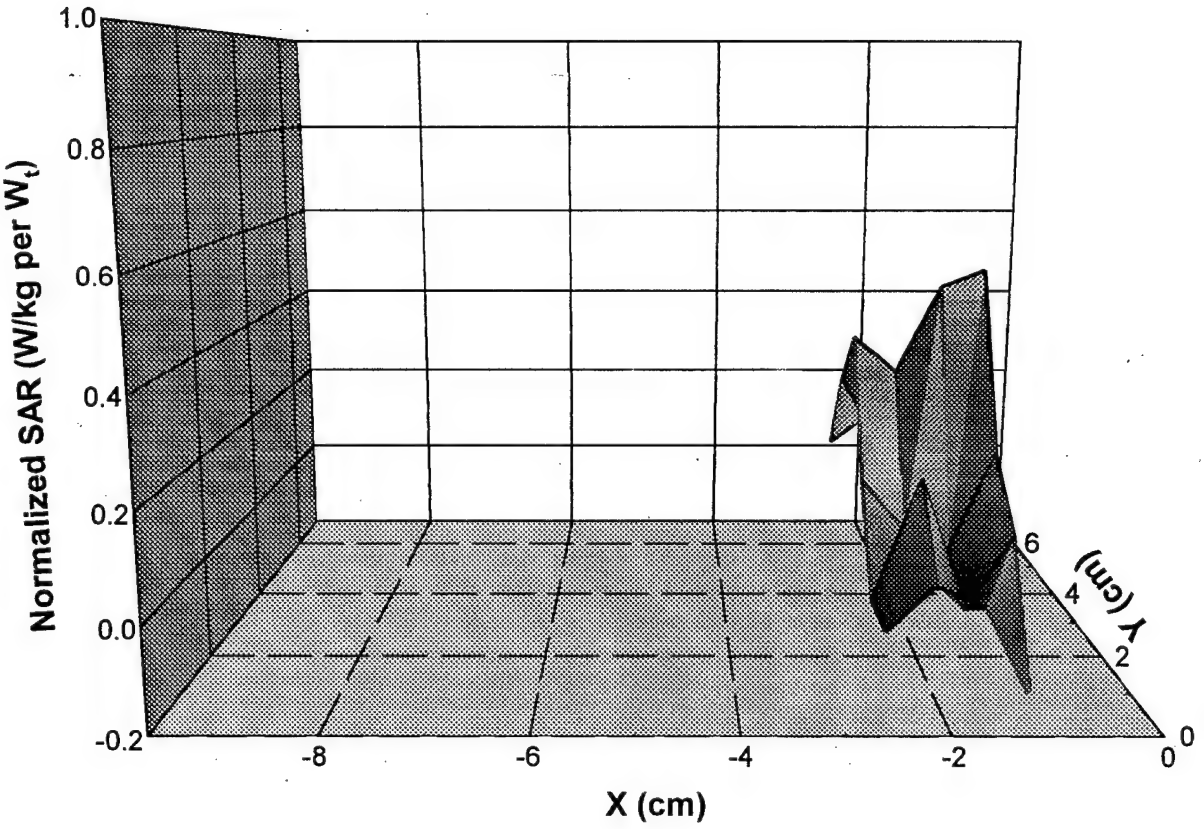

Figure 14: Normalized SAR Distribuiton : 40 MHz

Number of data points (N) = 24
Net Input Power (W_t)(mean +/- sd) = 31.56 +/- 2.74 W
Max. Norm. SAR = 0.72 W/kg per W_t @ (-1,4)
Norm. SAR (mean +/- sd) = 0.255 +/- 0.17 W/kg per W_t

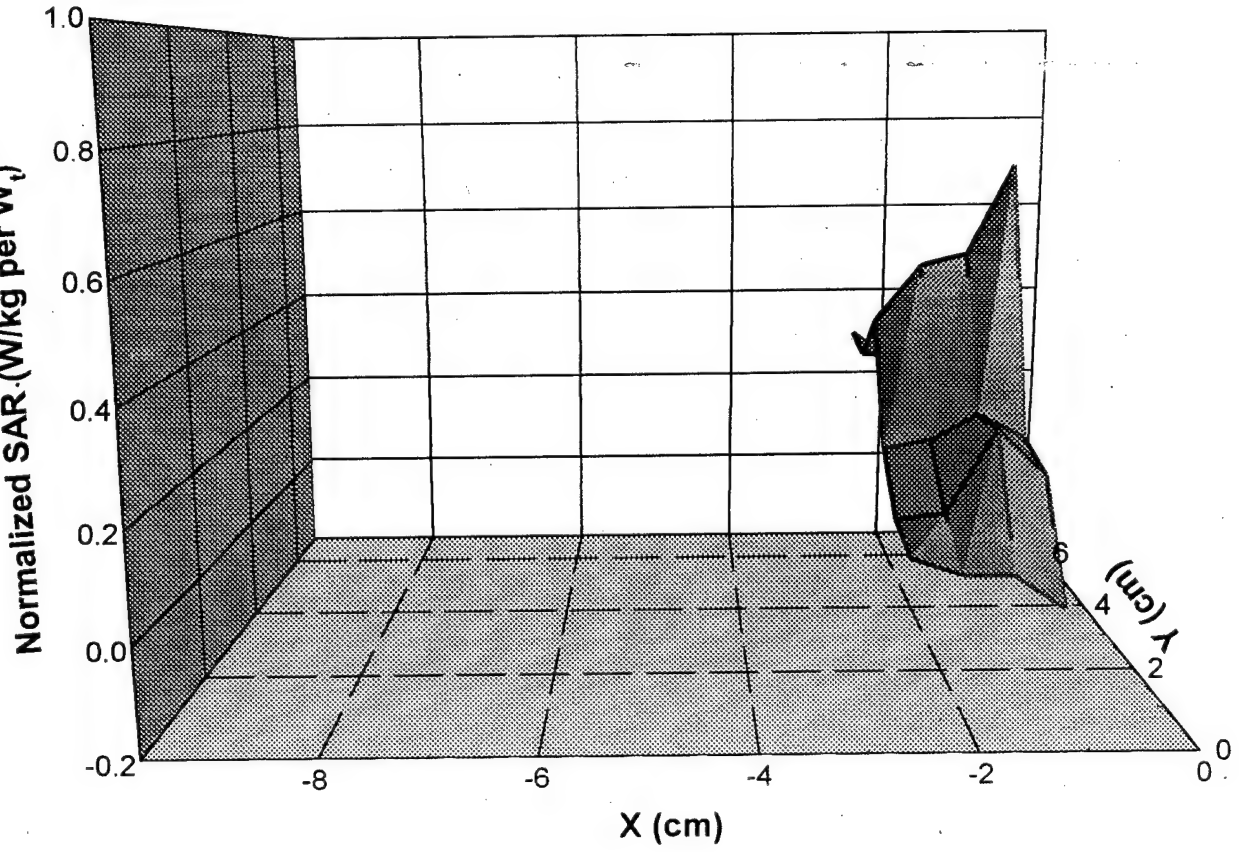

Figure 15: Normalized SAR Distribution : 50 MHz

Number of data points (N) = 24
Net Input Power (W_t)(mean +/- sd) = 42.11 +/- 2.74 W
Max. Norm. SAR = 0.433 W/kg per W_t @ (-1,4)
Norm. SAR (mean +/- sd) = 0.066 +/- 0.12 W/kg per W_t

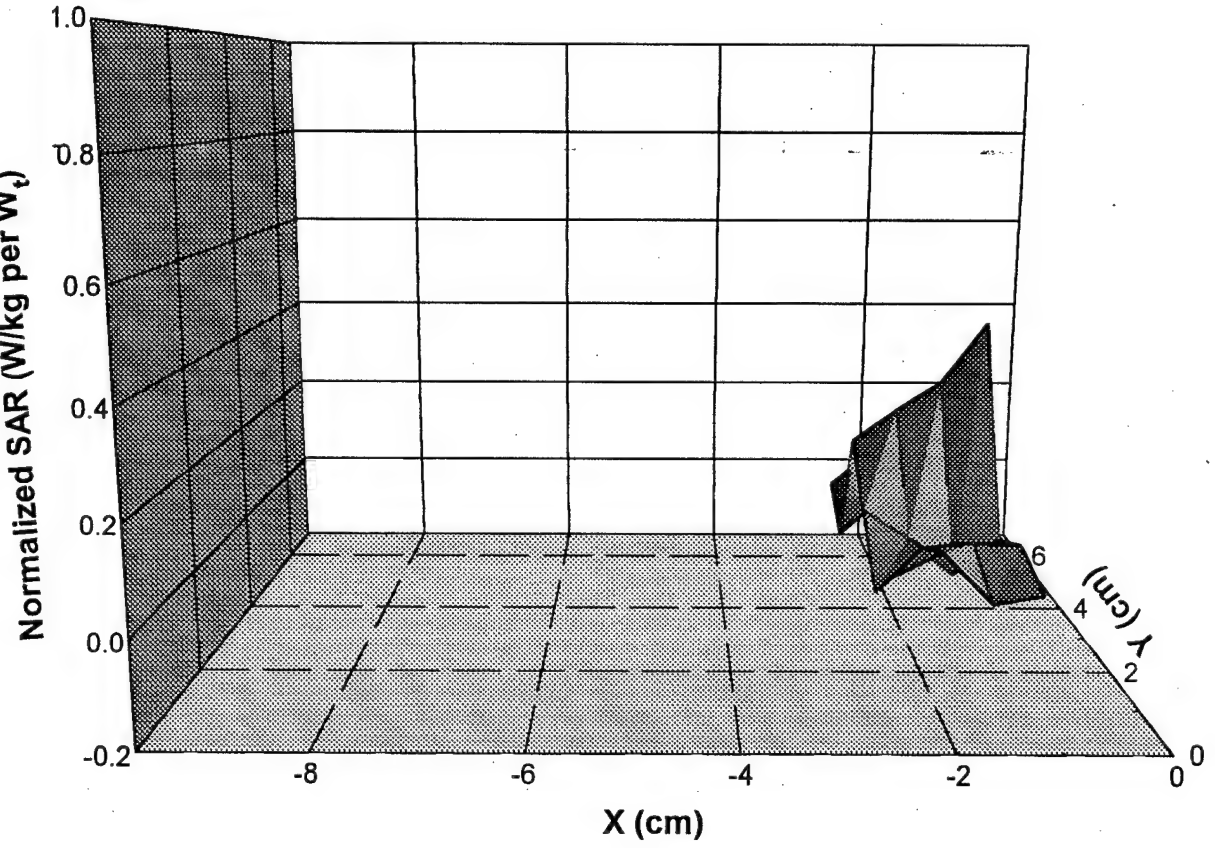

Figure 16: Normalized SAR Distribution : 60 MHz

Number of data points (N) = 24
Net Input Power (W_t)(mean +/- sd) = 28.89 +/- 1.605 W
Max. Norm. SAR = 0.33 W/kg per W_t @ (-1,4)
Norm. SAR (mean +/- sd) = 0.157 +/- 0.105 W/kg per W_t

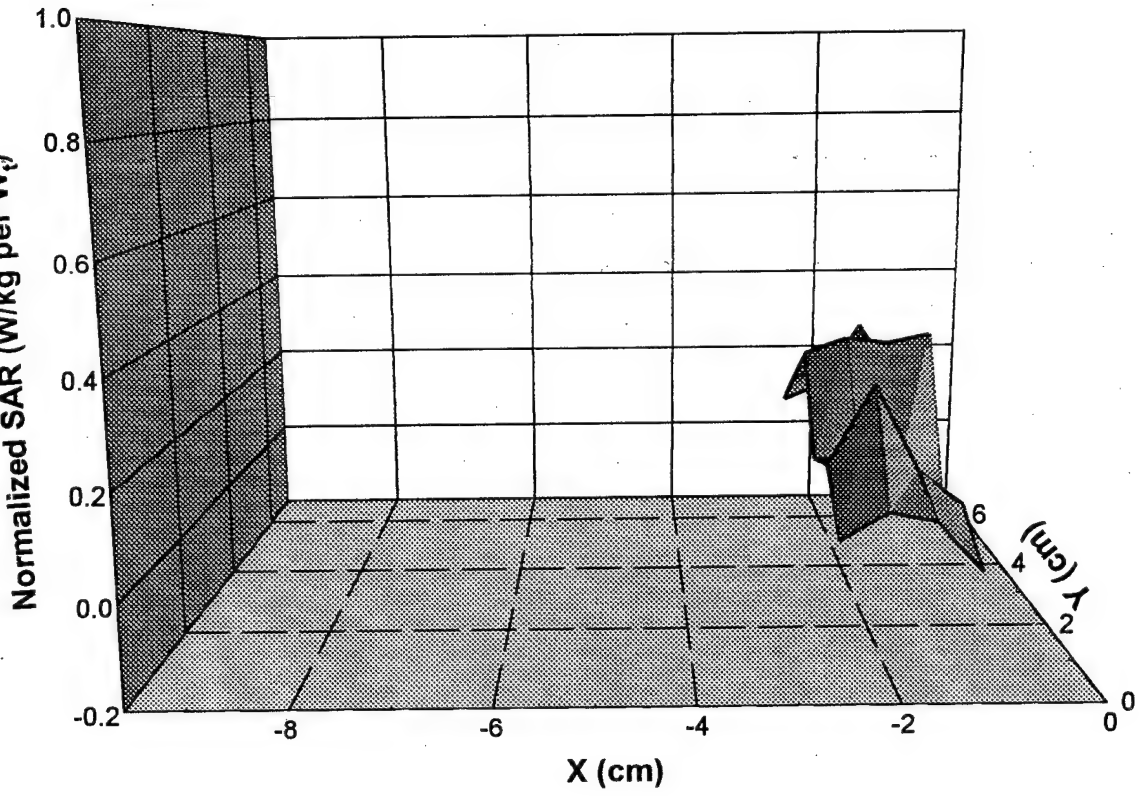

Figure 17: Normalized SAR Distribution : 70 MHz

Number of data points (N) = 24
Net Input Power (W_t)(mean +/- sd) = 23.44 +/- 0.579 W
Max. Norm. SAR = 0.244 W/kg per W_t @ (-1,4)
Norm. SAR (mean +/- sd) = 0.076 +/- 0.134 W/kg per W_t

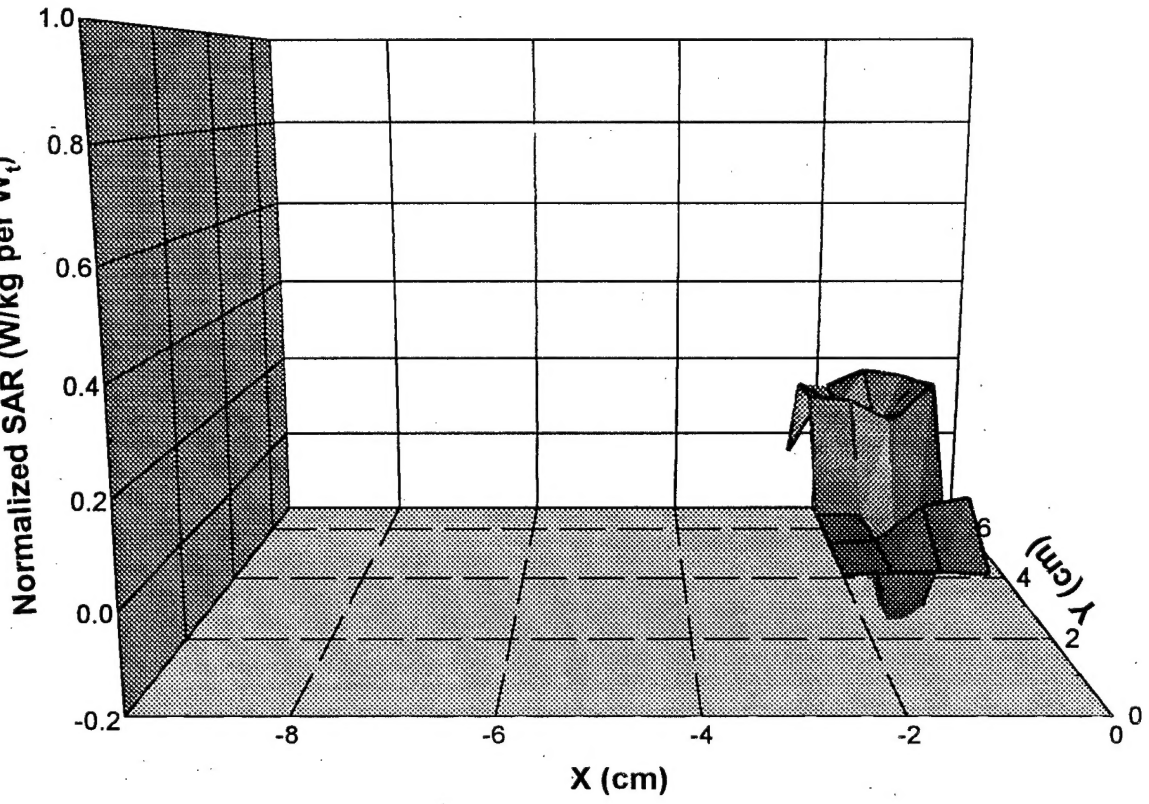

Figure 18: Normalized SAR Distribuiton : 80 MHz

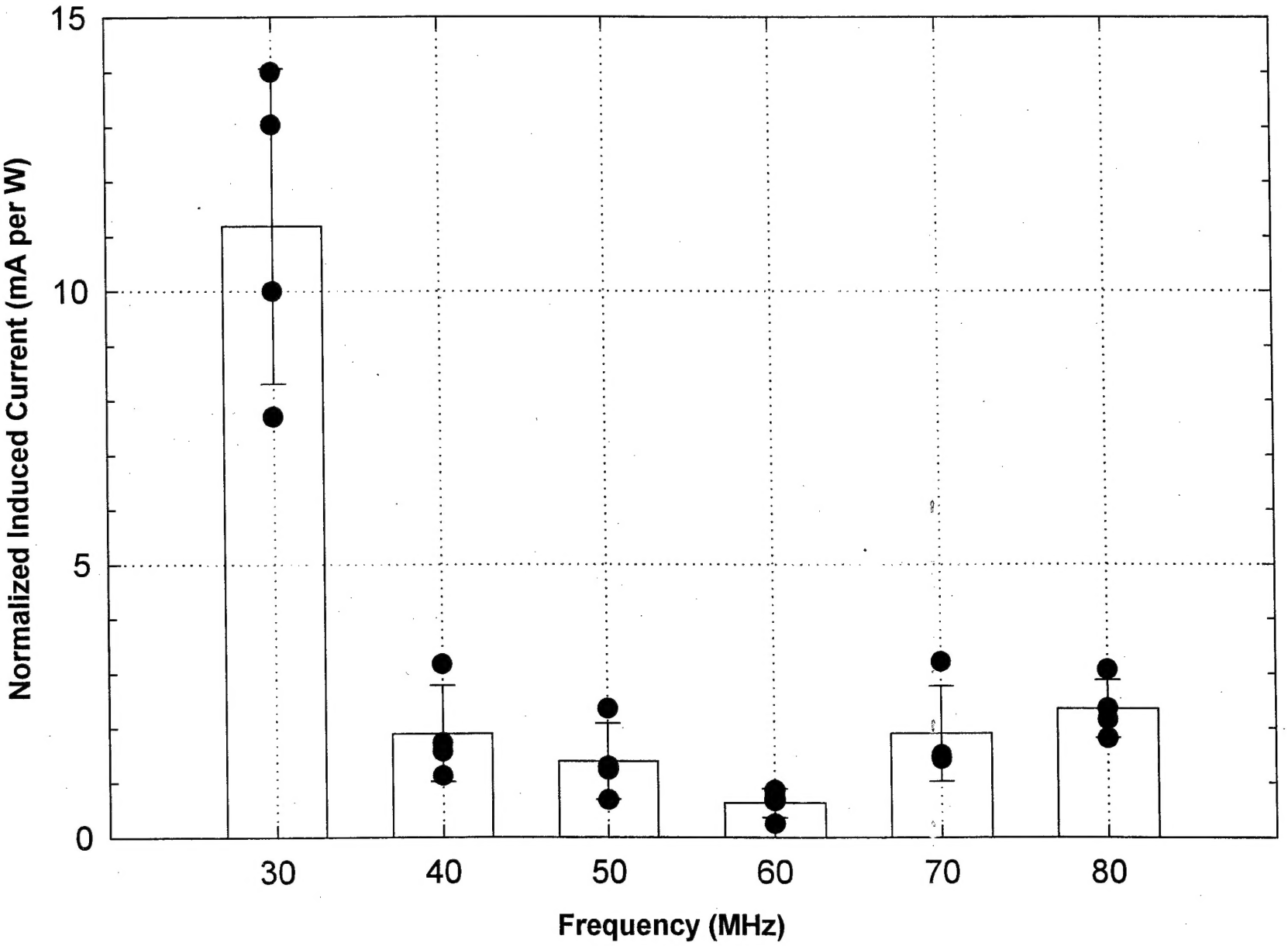

Figure 19: Mean Induced Ankle Current

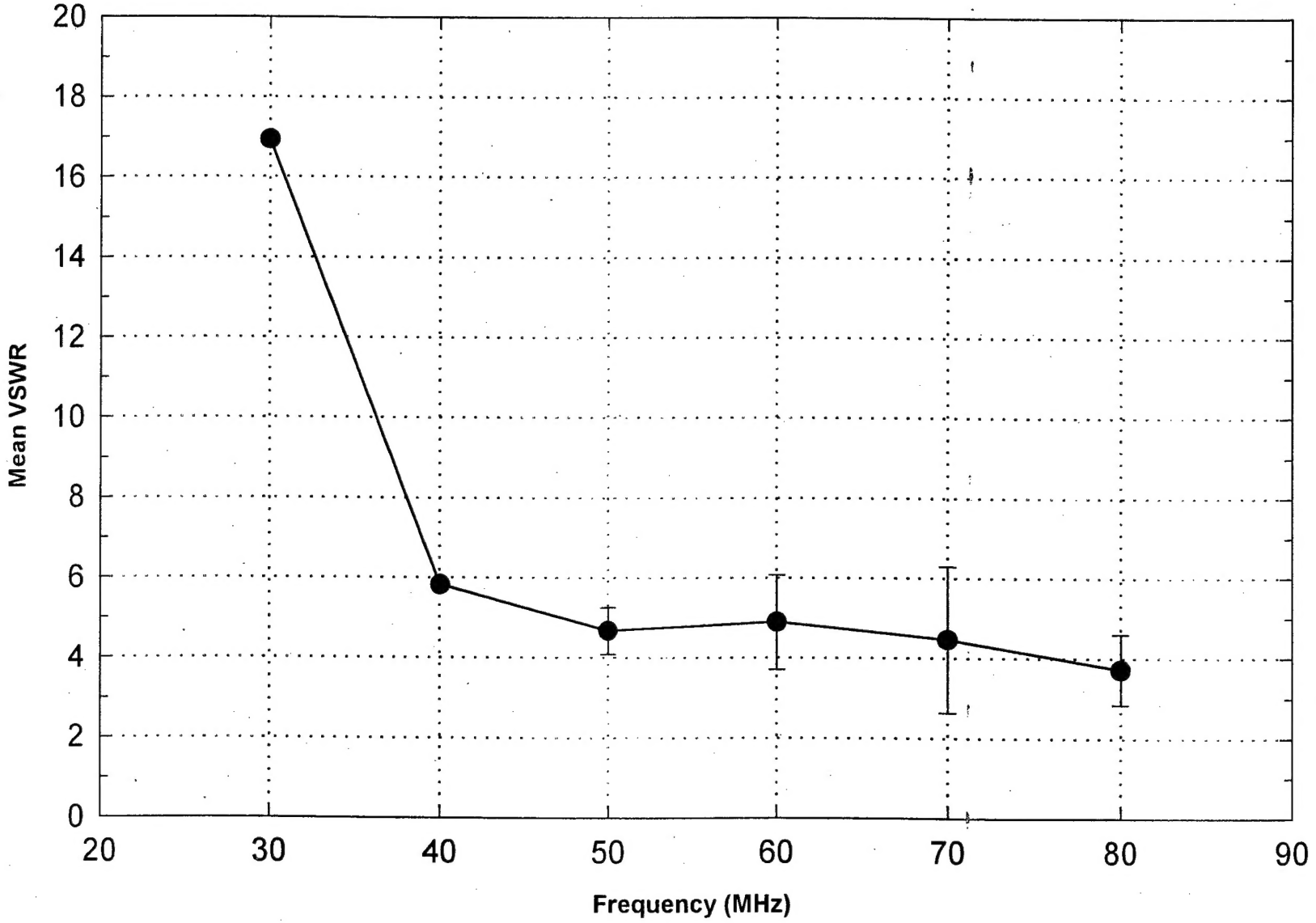

Figure 20: Mean VSWR vs Frequency

Appendix I

List of Equipment

1. Advanced Membrane Transducer Antenna, Model # Px-AMT-2-28XD-LIGHT EPPM, S/N 050497-USArmy-X1-1
2. Synthesized RF Generator, Fluke Model # 6062A, S/N 452405.
3. RF Amplifier, Amplifier Research, Model 50W1000, S/N 5163.
4. Thruline Power Meter, Bird Electronic Corporation, Model 43 S/N 267389.
5. Power Sensors 100 W(25 - 60 MHZ) and (50 - 100 MHZ), Bird Electronics Corporation, Model # 100A and 100B.
6. Broadband Exposure Meter, Holaday Industries, Model HI 3003, S/N 39453.
7. Electric Field Probe, Holaday Industries, Model IME, S/N 013.
8. Amber Thermograsphic Camera System, Model # Radiance -1.
9. Flurooptic Thermometer, Model Luxtron 3000, S/N 30225.
10. Luxtron probes (2 nos.), Model # MAM-05.
11. Ankle Current Coil Meter and Coil, Holaday Industries, Model # HI-4416.
12. AMT Antenna Stand and Positioner, designed and fabricated in- house.
13. Styrofoam Template for Planar Field Measurements, fabricated in-house.
14. Muscle Equivalent Phantom Model of Human Torso at 70 MHZ, fabricatediIn-house.